METEOR-BERICHTE

No. 94-4

NORDATLANTIK 1993

Cruise No. 26

24 August - 26 November 1993

Edited by:

Erwin Suess, Klaus Kremling, and Jürgen Mienert

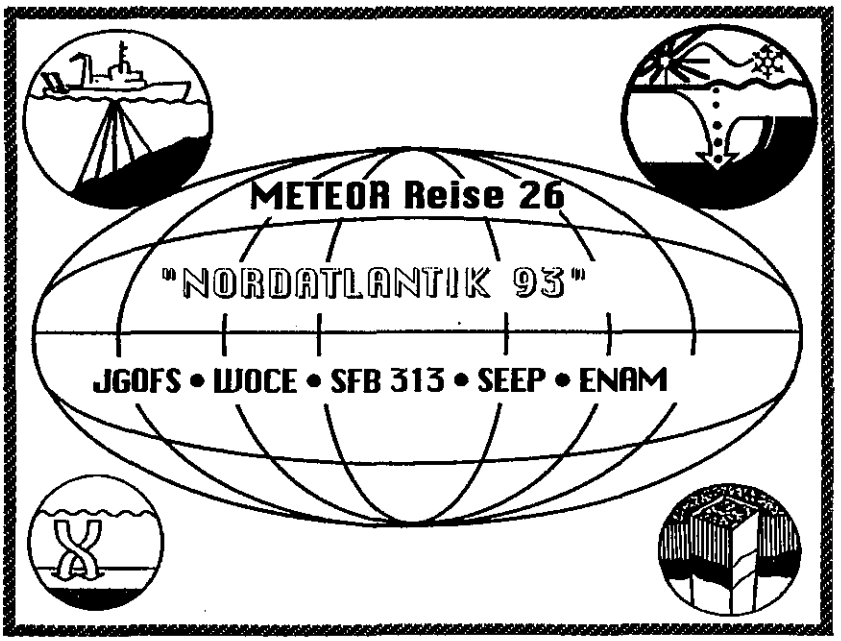

Editorial Assistance:

Ingrid Rogge, Keiko D. Kähler-Mähl

Institut für Meereskunde an der Universität Kiel

Leitstelle METEOR

Institut für Meereskunde der Universität Hamburg

1994

Table of Contents

Abstract

The 26th voyage of RV METEOR to the North Atlantic, the Skagerrak, the Norwegian, East Greenland and Barents Seas consisted of three legs whose research programs served several large integrated, and multi-disciplinary projects. During the first leg, M 26/1, the programs were related to WOCE (World Ocean Circulation Experiment), specifically the North Atlantic overturning rate determination and to the JGOFS project (Joint Global Ocean Flux Study).

Of seven WOCE moorings three (M2, E1 and E2) had to be dredged because of release problems and/or possible loss of buoyancy. Two of them (F2 and W2) released and surfaced as planned; another two moorings (D2 and A2) could not be located for different reasons. Hydrographic parameters for characterization of water masses were also obtained at all sites as well as at those of the JGOFS moorings (L1, L2, L3). All three of these were successfully redeployed during M 26/1 after they had been recovered in early summer of 1993 by the deep submersibles MIR. Throughout most of M 26/1, a continuous and contamination-free pumping system was deployed and a composite transect of chemical parameters measured. Among them are the nutrients, organic acids, biomarkers and trace elements. They are important basic data for several of the JGOFS subprojects which examine the interaction of dissolved and particulate trace constituents in relation to seasonal and meridional particle production and flux.

During the second and third legs, M 26/2 and M 26/3, the research programs served the Sonderforschungsbereich 313 (Environmental Change in the northern North Atlantic) as well as those of two European Community projects SEEP (Gas and Water Seepage on the European Continental Margin) and ENAM (European North Atlantic Margin). Other projects, addressing the well-known cold water carbonates of the Norwegian Sea (Boreale Flachwasserkarbonate) and the history of post-glacial rebound of the Scandinavian shield (Hebungsgeschichte Skandinaviens), were also part of M 26.

The SFB-work concerned two long-term sediment trap moorings in the Norwegian and Greenland Basins, the first of them was successfully recovered and redeployed, the second one failed to surface. Work on the Norwegian, East Greenland, and Barents Sea margins yielded many miles of shallow subsurface acoustic images, sufficient core material, surface samples, hydrographic, plankton and benthos samples to serve the needs of five of the eight SFB-subprojects. The micropaleontological and planktological assemblages of these samples were further characterized by environmental parameters like nutrients, salinity and temperature, from throughout the water column. The objectives concerned reconstruction of Late Pleistocene temperatures, rates and controls of production of benthic and pelagic biogenic carbonates and formation and imprinting of geophysical signals.

The Skagerrak, the Faeroe-Shetland Channel, and slope and shelf of the Barents Sea were the areas of work during M 26/2 related to the SEEP project. In the Skagerrak a 6-m long core with abundant *pogonophorans* and high CH_4, NH_4-, and ΣCO_2-concentrations was taken from an active seep. Widespread anomalies in the bottom water indicated seep activity. Suspected seep localities in the Faeroe-Shetland Channel were shown to be sedimentary drift bodies. Sampling on the Barents Sea slope yielded *pogonophorans* as well as slightly elevated methane contents, but no evidence for vigorous venting. Deep-tow-boomer, hydrochemical, and video-surveys in the Barents Sea showed structural control of a large crater field, varying intensities of "gas saturation" at depths, chaotic morphology which supports the idea that these craters are the result of violent gas hydrate explosions, and a distinct pattern of dissolved methane with strongly increasing gradients in the bottom water towards the northern end of the crater field.

The relationship between stability and gas contents of Storegga slide sediments was the main objective of the ENAM project. Hydrosweep, Parasound and deep-tow-boomer systems were successfully used. Geotechnical properties were measured *in situ*, as well as pore pressure gradients, and the propagation velocities of compressional sound waves. With this approach numerous subsurface features related to gassy sediments were identified when comparing disturbed and undisturbed parts of the northern edge of the Storegga Slide.

Vibro-coring yielded several cores of sandy sediment from the Norwegian shelf for the objectives of the Norwegian-German cooperative program. Equally successful was a transect of grab samples of shallow water carbonates from across the Spitsbergen Bank to serve the objectives of the DFG-Projekt: Boreale Flachwasserkarbonate.

The science program during M 26, with the exception of the Mediterranean transit and work south of 50°N, was adversely affected by unfavorable weather throughout the cruise. Extra steaming due to high winds and seas, clean-up and repair of equipment after major storms hit the vessel, icy conditions on deck, sea-ice, weathering high seas or seeking shelter on numerous occasions, used up about the same time as the total station-time. In spite of this, sampling and surveys were sufficiently completed to address all objectives in reasonable detail. The overall success was in large part due to the dedication and professionalism of the vessel's master and crew.

Zusammenfassung

Die 26. Reise des FS METEOR führte in den Nordatlantik, das Skagerrak, die Norwegen-, Ostgrönland- und Barentssee und setzte sich aus drei Fahrtabschnitten zusammen, die verschiedenen großen, integrierten und multidisziplinären Projekten dienten. Während des ersten Fahrtabschnittes, M 26/1 waren die Programme mit WOCE-NORD (World Ocean

Circulation Experiment - Northatlantic Overturning Rate Determination) und dem JGOFS-Projekt (Joint Global Ocean Flux Study) assoziiert.

Von sieben WOCE-Verankerungen mußten drei (M2, E1 und E2) aufgrund von Auslöserproblemen und/oder einem möglichen Verlust von Auftrieb gedredged werden. Zwei weitere (F2 und W2) lösten aus und kamen wie geplant zur Oberfläche; zwei Verankerungen (D2 und A2) konnten aus unbekannten Gründen nicht gefunden werden. Es wurden hydrographische Parameter zur Charakterisierung der Wassermassen an allen diesen Stationen und denen der JGOFS-Verankerungen (L1, L2, L3) gewonnen. Alle wurden während M 26/1 erfolgreich wiederverankert und mit entsprechenden Sinkstoffallen bestückt, nachdem sie im Frühsommer 1993 mit den Tieftauchbooten MIR geborgen worden waren. Während des überwiegenden Teils von M 26/1 wurde ein kontinuierlich arbeitendes und kontaminationsfreies Pumpsystem eingesetzt und ein zusammengesetzter Schnitt von chemischen Parametern gemessen, u.a. Nährstoffe, organische Säuren, Biomarker und Spurenelemente. Dies sind wichtige Grunddaten für verschiedene JGOFS-Teilprojekte, welche die Wechselbeziehungen von gelösten und partikulären Spurenstoffen im Verhältnis zur saisonalen und meridionalen Partikelproduktion und Gesamtstoffffluß untersuchen.

Während des 2. und 3. Fahrtabschnittes, M 26/2 und M 26/3, dienten die Forschungsprogramme dem Sonderforschungsbereich 313 (Veränderungen der Umwelt: Der nördliche Nordatlantik) wie auch den zwei europäischen Projekten SEEP (Gas and Water Seepage on the Continental Margin) und ENAM (European North Atlantic Margin). Zwei weitere Projekte, welche die bekannten Kaltwasserkarbonate (Boreale Flachwasserkarbonate) und die Geschichte des postglazialen Aufstiegs des skandinavischen Schildes (Hebungsgeschichte Skandinaviens) zum Ziel hatten, waren ebenfalls Teil von M 26/2.

Die SFB-Arbeiten befaßten sich mit zwei Langzeitverankerungen in dem Norwegischen und den Grönländischen Becken, von denen die erste erfolgreich geborgen wurde, die zweite aber nicht zurück zur Oberfläche kam. Die Arbeiten an den Kontinentalrändern der Norwegen-, Ostgrönland- und Barentssee erbrachten viele Meilen von flachseismischen Aufzeichnungen, ausreichend Kernmaterial, Oberflächenproben, hydrographische, Plankton- und Benthosproben, welche den Ansprüchen von 5 der 8 SFB-Teilprojekte dienen. Die mikropaläontologischen und planktologischen Probennahmen wurden durch die Umweltparameter Nährstoffe, Salinität und Temperatur der Wassersäule ergänzt. Ihre Zielsetzung war mit der Rekonstruktion der Temperaturen des späten Pleistozäns, Raten und Steuerungsfaktoren der Produktion benthischen und pelagischen biogenen Karbonats und der Bildung und Prägung geophysikalischer Signale befaßt.

Das Skagerrak, der Färöer-Shetland Kanal, der Hang und der Schelf der Barentssee waren die Arbeitsgebiete des SEEP-Projektes während M 26/2. Im Skagerrak wurde ein 6 m langer Kern mit zahlreichen *Pogonophoren* und hohen CH_4, NH_4 und ΣCO_2-Konzentrationen an einem aktiven Seep gewonnen. Ausgeprägte Anomalien im Bodenwasser sprachen für einen

aktiven Fluidaustritt. Erwartete Seep-Lokationen im Färöer-Shetland Kanal erwiesen sich als sedimentäre Driftkörper. Die Beprobung am Barentssee Hang erbrachte *Pogonophoren* und leicht erhöhte Methankonzentrationen, jedoch keinen Hinweis auf einen ausgeprägten Fluidausstrom. Deep-tow Boomer-, Hydrochemie- und Video-Vermessungen in der Barentssee zeigten die Struktur eines großen Kraterfeldes, variierende Intensitäten von Gassättigung mit der Tiefe, chaotische Morphologien, welche die Vorstellung der Entstehung der Krater durch eine massive Gashydratexplosion unterstützen, sowie ein ausgeprägtes Muster gelösten Methans mit stark ansteigenden Gradienten im Bodenwasser zum nördlichen Ende des Kraterfeldes.

Die Beziehung zwischen Hangstabilität und Gasinhalt der Sedimente der Storegga Rutschmasse aufzuzeigen war die Hauptzielsetzung des ENAM-Projektes. Hydrosweep, Parasound und das Deep-tow Boomer System wurden erfolgreich eingesetzt. Geotechnische Eigenschaften wurden *in situ* gemessen, wie auch Porendruckgradienten und die Ausbreitungsgeschwindigkeit von Kompressionswellen in oberflächennahen Sedimenten. Mit diesem Ansatz konnten zahlreiche akustische Anomalien auf gashaltige Sedimente zurückgeführt werden, nachdem gestörte und ungestörte Teile des nördlichen Randes der Storegga Rutschmasse verglichen worden waren.

Mit Hilfe des Vibro-corers konnten Kerne mit sandigen Sedimenten und vorwiegend grober Textur vom norwegischen Schelf für die Zielsetzungen des Norwegisch-Deutschen Kooperativprogramms gewonnen werden. Hierdurch wird eine hochauflösende Rekonstruktion der Hebungsgeschichte des norwegischen Schildes ermöglicht. Ebenso erfolgreich war ein Schnitt von Greiferproben aus Flachwasserkarbonaten über die Spitzbergenbank (Boreale Flachwasserkarbonate), um die Besiedlungsgeschichte im Zuge der postglazialen Entwicklung besser verstehen zu können.

Das wissenschaftliche Programm war während der gesamten Reise M 26, mit Ausnahme des Mittelmeertransits und den Arbeiten südlich 50°N, durch widrige Witterung beeinträchtigt. Zusätzliche Dampfzeiten durch starke Winde und hohe See, Zeitverlust durch Aufräumungs- und Reparaturarbeiten nach den schweren Stürmen, Eis an Deck, Bildung von Meereis, Abwettern und Schutzsuchen vor herannahenden Sturmtiefs, beanspruchte ebensoviel Zeit wie die gesamte Stationszeit. Trotz dieser Widrigkeiten konnten alle Beprobungen und Vermessungen abgeschlossen werden, um die wissenschaftlichen Ziele aller beteiligten Projekte in vertretbarem Rahmen erfüllen zu können. Dieser Erfolg ist in großem Maße dem Einsatz des Kapitäns und der Schiffsbesatzung zu verdanken.

1 Research Objectives

1.1 Introduction

The 26th voyage of RV METEOR to the North Atlantic, the Skagerrak, the Norwegian, East Greenland and Barents Seas comprised three legs (Fig. 1), which were organized to achieve the objectives of several large, integrated and multidisciplinary projects. During the first leg, M 26/1, the projects were related to the German contributions to the international programs JGOFS (Joint Global Ocean Flux Study) and WOCE (World Ocean Circulation Experiment, specifically the North Atlantic Overturning Rate Determination). During the second and third legs, M 26/2 and M 26/3, the projects addressed the goals of the Sonderforschungsbereich 313 ("Environmental Change in the northern North Atlantic") were continued as well as those of the European Community projects "SEEP" (Gas and Water Seepage on the Continental Margin) and "ENAM" (European North Atlantic Margin). Two other projects, one addressing the well-known cold water carbonates of the Norwegian Sea (Boreale Flachwasserkarbonate) and the other the history of post-glacial rebound of the Skandinavian shield (Hebungsgeschichte Skandinaviens) were also incorporated into the cruise plan of M 26. These projects are financed by the Deutsche Forschungsgemeinschaft (DFG) and the Norwegian-German cooperative program, respectively.

1.2 Projects

JGOFS is a long-term, international program investigating the fate of carbon in the ocean, atmosphere, and sediments of the most recent past. The central aim of JGOFS is the deployment of sediment traps in key areas of the world's ocean. The German contribution to this project is on the long-term variability of particle fluxes in the North Atlantic along a profile from about 30°N to 60°N at 25°W. The aim is to determine and understand the processes controlling the short-term seasonal and interannual fluxes of carbon and associated biogenic trace and nutrient elements under climatic and oceanic conditions as encountered along this transect. During M 26/1 six individually funded JGOFS-subprojects were carried out; their respective programs are discussed in detail later on.

WOCE is an international program to understand the circulation of the global ocean well enough to be able to predict ocean response and feed back to long-term changes in the atmosphere. WOCE comprises three tasks: (1) the velocity field of the ocean, (2) the atmosphere-ocean exchange and (3) the water masses, their exchange, and turnover. The German involvement with WOCE during this cruise concerns the North Atlantic turnover rate determinations and water mass exchange.

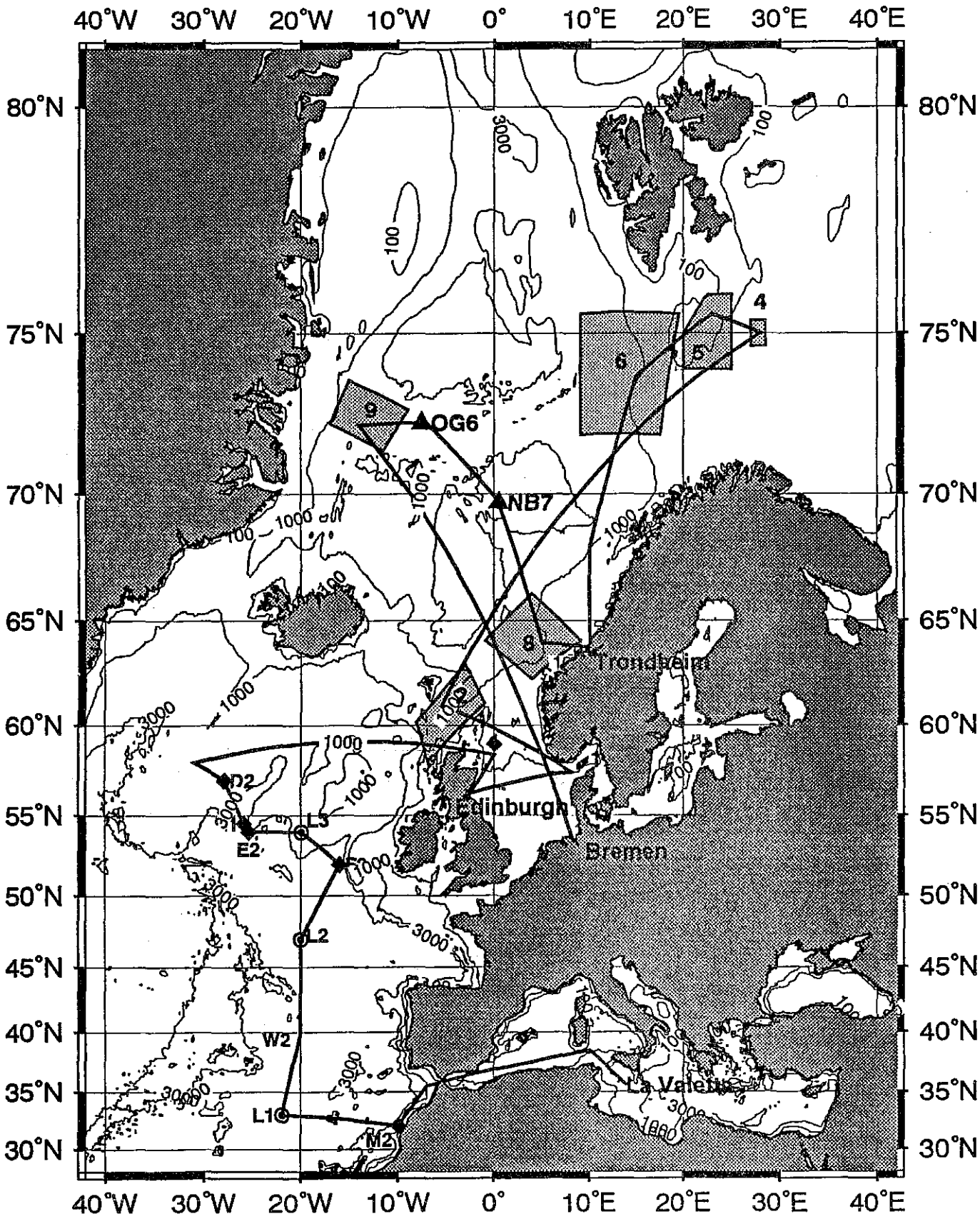

Fig. 1: Cruise Track and working areas of METEOR cruise no. 26.

The SFB 313 is an interdisciplinary research project at the University of Kiel devoted to document, understand, hindcast, and predict the environmental changes in the northern North Atlantic. The SFB 313 has been active for more than 6 years and is organized into 8 subprojects, four of which address the "Production, accumulation and transformation of sediments constituents". Four other subprojects address the "Evolution of Quaternary climate and ocean circulation". The main area of investigation has been the North Atlantic, the East Greenland, Norwegian and Barents Seas.

Two topics developed from past and current research of the SFB 313 have lead to joint projects within the European Community program MAST-II, SEEP and ENAM. Integration of these topics, feed-back into the SFB 313, and collaboration with scientists from neighbouring European countries were essential elements in planning of cruise M 26. The project SEEP addresses the gas and water seepage on the continental margin, whereas ENAM deals with pathways, processes and fluxes of sedimentation of the European North Atlantic Margin.

Cold water carbonates and *Lophelia*- reef communities are peculiar occurrences in Subarctic and Arctic waters. At present it is unclear what influence the hydrography has on the development of these communities. Two hypotheses, either that they are nourished by seeps or by specific oceanographic boundaries forming turbulent internal waves which supply extra food, were at the center of the objectives of the high-latitude shallow-water carbonate program.

The history of the Negogene uplift of the Norwegian mainland is broadly known but lacks a high-resolution chronostratigraphic framework. The objective of this program, under the German-Norwegian cooperative agreement, was therefore a high-resolution analysis of a characteristic coarse-grained shelf sequence off central Norway. Such sediments normally are difficult to sample because of their lithology but lend themselves to vibro-coring, a sampling technique attempted during M 26.

Tab. 1: Legs and Chief Scientist of METEOR cruise No. 26

Leg M 26/1

24 August-25 September 1993, La Valetta/Malta - Edinburgh/Great Britain

Chief scientist: Dr. K. Kremling

Leg M 26/2

28 September-25 October 1993, Edinburgh - Trondheim/Norway

Chief scientist: Prof. Dr. E. Suess

Leg M 26/3

28 October-26 November 1993, Trondheim - Bremen/Germany

Chief scientist: Dr. J. Mienert

Coodination:

Prof. Dr. E. Suess

Master:

Captain H. Bruns

2 Participants

Tab. 2: Participants of METEOR cruise no. 26

Leg M 26/1

Name	Speciality	Institute
Kremling, Klaus, Dr. (Chief ccientist)	Marine Chemistry	IfMK
Deckers, Monika, Dipl.-Biol.	Planktology	IfMK
Heise, Susanne, Dipl.-Biol.	Geochemistry	GEOMAR
Heuermann, Rüdiger, Dipl.-Phys.	Physics	UOL
Klein, Holger, Dipl.-Oz.	Oceanography	BSH
Kreutz, Mattias, Dipl.-Chem.	Geochemistry	GEOMAR
Link, Rudolf, Technician	Marine Chemistry	IfMK
Lippert, Gabi, Technician	Marine Chemistry	IfMK
Loquay, Klaus-Dieter, Technician	Physics	UOL
Lundgreen, Ulrich, Dipl.-Chem.	Marine Chemistry	IfMK
Osterroht, Christoph, Dr.	Marine Chemistry	IfMK
Petersen, Johannes, Technician	Marine Chemistry	IfMK
Rudat, Ute, Technician	Marine Chemistry	IfMK
Schiebel, Ralf, Dr.	Palaeontology	GPIT
Schüßler, Uwe, Dr.	Marine Chemistry	IfMK
Streu, Peter, Technician	Marine Chemistry	IfMK
Ulbricht, Hellmuth, Dipl.-Meteor.	Meteorology	SWA
Wehner, Frank, Dipl.-Oz.	Oceanography	IfMH
Wüllner, Helmut, Technician	Oceanography	IfMH

Leg M 26/2

Name	Speciality	Institute
Suess, Erwin, Prof. Dr. (Chief scientist)	Geochemistry	SFB 313/GEOMAR
Andruleit, Harald, Dipl.-Geol.	Geology	SFB 313
Bassek, Dieter, Technician	Meteorology	SWA
Brierly, Andrew, Dipl.-Biol.	Geophysics	BGS
Dando, Paul R., Dr.	Geochemie	MBA
Derrick, John F., Technician	Geophysics	BGS
Domeyer, Bettina, Technician	Geology	SFB 313/GEOMAR
Freiwald, André, Dr.	Sedimentology	GEOMAR
Gamenick, Inez, Dipl.-Biol.	Biology	ZIUH
Körner, Thomas, Technician	Marine Chemistry	SFB 313/IfMK
Lammers, Stephan, Dipl.-Geol.	Geochemistry	SFB 313/GEOMAR
Lie, Hans Erik, Dipl.-Geol.	Geology	GDO
Linke, Peter, Dr.	Biogeochemistry	SFB 313/GEOMAR
Long, David, Dr.	Geophysics	BGS
Maaßen, Jörg, Dipl.-Chem.	Marine Chemistry	SFB 313/IfMK
Marx, Stefan, Student	Marine Physics	GKSS
Meggers, Helge, Student	Sedimentbiology	GPIC/GEOMAR
Niven, Stewart J., Dr.	Microbiology	MBA
Pheasant, John, Technician	Geophysics	BGS
Röpstorf, Peter, Dr.	Biology	FUB
Schott, Thorsten, Technician	Electronics	GECON
Schumann, Marcus, Technician	Geology	SFB 313/GEOMAR
Smith, David, Technician	Geophysics	BGS
Sörensen, Poul, Technician	Geochemistry	RISö
Tselepides, Anastassios, Dr.	Biology	IMBC
Ulbricht, Hellmuth, Dipl.-Meteor.	Meteorology	SWA
Viergutz, Thomas,Technician	Oceanography	SFB 313
Wernecke, Gerhard, Dipl.-Phys.	Marine Physics	GKSS
Willamowski, Claudia, Dipl.-Chem.	Marine Chemistry	SFB 313/IfMK
Windoffer, Reinhard, Dr.	Biology	ZIUH
Winckler, Gisela, Dipl.-Phys.	Tracer Oceanography	IfUH
Zeller, Ute, Dipl.-Biol.	Planktology	SFB 313

Leg M 26/3

Name	Speciality	Institute
Mienert, Jürgen, Dr. (Chief scientist)	Geophysics	SFB 313/GEOMAR
Auffret, Gerald A., Dipl.-Geol.	Sedimentphysics	IFREMER
Baas, Jaco, Dr.	Sedimentology	GEOMAR
Bassek, Dieter, Technician	Meteorology	SWA
Bauerfeind, Eduard, Dr.	Planktology	SFB 313/IfMK
Baumgärtner, Carolin, Dipl.-Geol.	Sedimentology	GEOMAR
Beese, Helmut, Technician	Electronics	SFB 313
Bobsien, Michael, Dipl.-Geophys.	Geophysics	SFB 313
Brett, Colin P, Technician	Geophysics	BGS
Darlington, Eric, Technician	Geophysics	GEOTEK
Evans, Dan, Dr.	Geophysics	BGS
Floc'h, Gilbert, Technician	Geotechnics	IFREMER
Franke, Christoph, Student	Geology	GPIK
Hamich, Andreas, Dipl.-Geol.	Sedimentology	GEOMAR
Hensch, Heidrun, Technician	Micropaleontology	GPIK
Hiller, Birgit, Dipl.-Biol.	Planktology	GPIT
Hollender, Franz-Josef, Dipl.-Geophys.	Geophysics	SFB 313
Kenyon, Neil, Dipl.-Geol.	Geophysics	IOSDL
Landure, J. Y., Technician	Geophysics	IFREMER
Langseth, Markus, Prof. Dr.	Geophysics	LDEO
Mellenthin, Katja, Student	Planktology	SFB 313/IfMK
Pflaumann, Uwe, Dr.	Mikropaleontology	SFB 313/GPIK
Rehder, Wilma, Technician	Geology	GPIK
Roekoengen, Kare, Dr.	Sedimentology	NTH
Schultheiss, Peter, Dr.	Sedimentphysics	GEOTEK
Steen, Eric, Technician	Geology	SFB 313
Toularastal, Claude, Technician	Geophysics	IFREMER
Ulbricht, Hellmuth, Dipl.-Meteor.	Meteorology	SWA
Wallis, David Gray, Technician	Geophysics	BGS
Weinelt, Martin, Dr.	Sedimentology	GEOMAR

Tab. 3: Participating Institutions

BGS	British Geological Survey Murchison House West Mains Road Edinburgh EH9 3LA Scotland, United Kingdom
BSH	Bundesamt für Seeschiffahrt und Hydrographie Bernhard-Nocht-Straße 78 20359 Hamburg, Germany
DGS	Geological Survey of Denmark Thoravej 8 2400-Copenhagen NV, Denmark
FUB	Freie Universität Berlin Malteser Straße 74-100 12249 Berlin, Germany
GDB	Geological Institut, University of Bergen Department of Geology, Sec. B, Allegaten 41, 5007 Bergen, Norway
GDO	Geology Department University of Oslo PB 1047, Blindern 0316 Oslo 3, Norway
GECON	Geophysik Consulting GmbH Wildrosenweg 3 24119 Kronshagen/Kiel, Germany
GEOMAR	Forschungszentrum für Marine Geowissenschaften Wischhofstraße 1-3, 24148 Kiel, Germany
GEOTEK	Fern Cottage Marley Lane, Haslemere Surrey GU27 3RF, United Kingdom
GKSS	Forschungszentrum Geesthacht GmbH Max-Planck-Straße Postfach 1160 21494 Geesthacht, Germany

Tab. 3: continued

GPIK	Geologisch-Paläontologisches Institut der Universität Kiel Olshausenstraße 40/60 24118 Kiel, Germany
GPIT	Geologisch-Paläontologisches Institut der Universität Tübingen, Sigwartstr. 10 72076 Tübingen, Germany
IfUH	Institut für Umweltphysik der Universität Heidelberg Im Neuenheimer Feld 366 69120 Heidelberg, Germany
IKU	Institutt for Kontinentalsokkelundersökelse Trondheim, Postboks 1883 Hakon Magnussons Gate 1B 7001 Trondheim, Norway
IMBC	Institute of Marine Biology Crete P. O. Box 2214, 71003 Iraklion-Crete, Greece
IfMH	Institut für Meereskunde der Universität Hamburg Troplowitzstraße 7 22529 Hamburg, Germany
IfMK	Institut für Meereskunde der Universität Kiel Düsternbrooker Weg 20 24105 Kiel, Germany
IFREMER	Centre de Brest Department Geosciences Marines B. P. 70 29280 Plouzane CEDEX, France
IOSDL	Institute of Oceanographic Sciences Deacon Laboratory Brook Road Wormley, Godalming, Surrey, GU 5 UB, United Kingdom
LDEO	Lamont-Doherty Earth Observatory of Columbia University Palisades New York 10964, U.S.A.

Tab. 3: continued

MBA	Marine Biological Association of the United Kingdom Citadel Hill Plymouth, PL1 2PB, United Kingdom
NGI	Norwegian Geotechnical Institut, Oslo P.O. Box 40 Taasen, 0316 Oslo, Norway
NTH	Norges Tekniske Högskole (Norwegian Technical University) Institutt for Geologi og Bergteknikk Högskoleringen 6 7034 Trondheim, Norway
RISö	Risö National Laboratory Environmental Science and Technology Department P.O. Box 49, 4000 Roskilde, Denmark
SFB 313	Sonderforschungsbereich 313 der Universität Kiel Heinrich-Hecht Platz 10 24118 Kiel, Germany
SWA	Seewetteramt Hamburg German Weather Service Bernhard-Nocht-Straße 76 20359 Hamburg, Germany
UEA	University of East Anglia Norwich NR4 7TJ, United Kingdom
UOL	Universität Oldenburg Fachbereich Physik Postfach 2503 26111 Oldenburg, Germany
ZIUH	Zoologisches Institut und Museum der Universität Hamburg Martin-Luther-King-Platz 3 20146 Hamburg, Germany

3 Research Programme

3.1 Joint Global Ocean Flux Study (JGOFS)

The main objective of Leg 1 was to continue research activities within the framework of the German JGOFS-projects entitled "Long-term studies on the variability of particle flux in the North Atlantic". Hence the primary objective of M 26/1 was on sediment trap studies, specifically to redeploy five of the key long-term moorings which had previously failed to return, but were recovered earlier in the summer of 1993 by submersibles. Material from these traps has been successfully used in conjunction with hydrographic studies to elucidate the fate of sorbed trace elements and the partitioning between dissolved and particulate carriers of trace elements. Natural and anthropogenic biomarkers are another group of trace constituents which interact with sinking particulate matter. The vertical distribution of ketones and PCBs, among others, in the water column and their respective concentrations in particulate matter, are used as tracers for fast carbon cycling processes. The tracer studies were supplemented by planktological studies and investigations on the fate of algal pigments during settling of particles. Other objectives of the JGOFS experiments were concerned with (1) the seasonal and interannual fluxes of carbonate from planktonic organisms as a function of forminiferal ecology, (2) optical characterization of dissolved and particulate organic substances, and (3) the recycling of nutrient elements from the sediment-water interface.

3.1.1 Tracer Chemistry

A fundamental problem of chemical oceanography are the strikingly low concentrations of dissolved trace elements in seawater. Currently, they can only be explained by sorption on and sedimentation with biogenic particles. During Leg M 26/1 the vertical flux of trace elements and its variability in relation to biological processes in the surface layer was investigated in the JGOFS latitudinal transect. The main research aims were studies of the chemical composition of surface particulates (in relation to particle size, time, space and physical-biological events), the seasonal variations of trace element fluxes (using sediment traps) and the compositional differences between suspended particulate matter (SPM) and sedimenting particles in the water column.

3.1.2 Organic Tracer Chemistry

Information about the biological influence on chemical composition and on the degradation and transformation processes of sinking organic particles was the main objective of the organic tracer chemistry program. Investigations were carried out as part of long-term studies along a latitudinal transect on the formation and transport of naturally occuring organic particles using biomakers and on transport of particle bound hydrocarbons using

anthropogenic tracers. It is assumed that the North Atlantic Ocean may act as a major sink for stable anthropogenic compounds which resist biological and chemical degradation.

Of special interest on this cruise were the questions concerning the changes in the composition of sinking organic matter (related to time, space, particle size, and physical or biological events in the surface layer), the identification of "biomakers" in the particulate material, that may yield information about biological composition in the pelagic ocean and the explanation of a tentative relationship between organic compounds and the behaviour of trace elements.

Additionally the distribution and composition of dissolved amino acids dissolved in the surface layer was investigated in a horizontal profile using a continuous pumping system.

3.1.3 Planktology

The planktological project of the JGOFS long-term study on the variability of particle fluxes is concerned with the production, turnover and sedimentation of biogenic particles in the North Atlantic. Within this subproject planktological process studies repeatedly in different seasons are conducted with a regional focus on the BIOTRANS area between 47°N and 20°W to determine the region's seasonal variability.

Beside the deployment of sediment traps at 500 m depth, jointly with moorings of the chemical groups, the phytoplankton stock, its vertical distribution and composition at the mooring stations and the modification of algal pigments through mesozooplankton organisms by means of gut-fluorescence" experiments were investigated on this leg.

3.1.4 Planktonic Foraminifera and Lunar Phase Cycle

Most calcareous zooplankton reproduction (e.g. planktonic foraminifers) is dependent on the lunar phase (population dynamics). As a result the particle flux is also phase-controlled. Therefore, the characteristic cycles (e.g. Ca-cycle) as well as the processes that mark or mask these cycles should be investigated. Processes which mask the cycles include seasonal primary production and the change of particle transport with water depth.

On this leg the emphasis on sampling was on the upper and central water column. Process studies and long time-scale surveys were intended to clarify the carbon and calcium cycle in the water column. They will increase our understanding of climate change during the Late Pleistocene and early Holocene. An attempt will be made to convert the process studies into computer models. Earlier METEOR cruises (M 6, M 10, M 11/1, M 12/3, M 17/2 and M 21) are used as a reference for the long-time surveys.

3.1.5 Marine Optics

Dissolved and particulate organic substances were investigated by optical methods. With fluorescence spectroscopy certain organic compounds that belong to the marine carbon cycle can be measured with high sensitivity and in some cases their chemical identity can be recognized. Well-known examples are chlorophyll and other algal pigments, marine "gelbstoff", and some aromatic amino acids and their derivatives.

In addition to measurements made with a laboratory luminescence spectrometer on discrete water samples, a newly developed *in situ* fluorometer was used for the first time. This instrument allows a continuous analysis of these substances with depth, and measurements are integrated into the continuous "Kiel Pumping System". This data yield near surface maps along the ship track.

To support and verify the optical data, plankton analyses will be made including taxonomy and measurements of chlorophyll and other algal pigments following to standard methods.

3.1.6 Pore Water Geochemistry

The burial flux of organic carbon in sediments initiates complex biological decomposition and physicochemical dissolution and precipitation processes. They are reflected in concentration gradients of the species involved in the pore water. Based on these concentration gradients the vertical flux of dissolved components from the sediments to the water column can be calculated.

The immediate goal of this JGOFS project is the estimation of the flux of dissolved components through the sediment-water-interface for key regions" of the Atlantic Ocean. Initially, total dissolved inorganic carbonate and the nutrients nitrate, nitrite, ammonia and silicate and subsequently trace metals will be studied. From this regional distribution pattern, characterizing the chemical environment and the chemical processes of the sediment / pore water-system, it is planned to deduce a distribution pattern of nutrient fluxes for the North Atlantic.

3.2 World Ocean Circulation Experiment (WOCE)

The Atlantic Ocean has the most intensive meridional circulation of all oceans. Water masses of tropical and subtropical origin are carried northwards near the surface and deep water of artic and subarctic origin southwards towards the equator. The transformation and sinking of water masses at high latitudes are important processes for the overturning" of the ocean. The

overturning rates and the intensity of the meridional transports of mass, heat and material are forcing parameters for the modelling of the ocean's role in the climate system.

This leg is part of a five-year field-effort within WOCE-NORD (World Ocean Circulation Experiment - North Atlantic Overturning Rate Determination). This program started in 1991 along a line connecting Cape Farvel (S-Greenland) with Porcupine Bank (SW Ireland) by using seasonally repeated hydrographic sections in combination with current measurements from moored arrays. The long-term current series, in combination with repeated hydrographic sections, will be used to estimate the rates of meridional water mass exchange in the northern North Atlantic. In this context, the cruise is part of the German WOCE program, and international project contributing to a modern description of the world's ocean.

During leg M 26/1 four current meter moorings (positions A2, D2, E2 and F2, see Fig. 2) were to be exchanged after a one-year deployment and at the same time, CTD-casts were to be taken on these positions. In addition, an attempt was made to recover the moorings E1 by dredging, which could not be released in 1992. The same was attempted for the mooring M2, which previously could not be recovered within the WOCE project "Eastern Boundary Current" (BSH).

3.3 Sonderforschungsbereich 313 (SFB 313)

The objectives of the SFB 313 during M 26 included: (1) sediment trap studies in the Norwegian and East Greenland Basins; (2) seasonality in hydrographic faunal and floral characteristics of the Norwegian Current; (3) biomarker and inorganic tracer studies in order to characterize particulate organic matter sources and early diagenetic modifications; (4) distribution patterns of isoprenoides, alkanes, alkenones and PCB's in the water column and the particulate load; (5) vertical and horizontal faunal and floral distribution in the Norwegian Current to completed an annual sampling cycle which was begun earlier; the planktonic organisms of interest were coccolithophores (*Emiliania huxley*, for biometric studies), diatoms and radiolarians; (6) the formation of geophysical signals in sedimentary sequences and the structural relationship of facies units; (7) the reconstruction of surface and bottom water mass properties in the boundary region between the East Greenland and the Irminger Currents; (8) to obtain data on the CO_2-system and its stable isotope characteristics from the Greenland and the Norwegian seas in order to model their role in the glacial-interglacial CO_2-exchange between the ocean and the atmosphere.

The interdisciplinary research project SFB 313 is organized into eight subprojects which address water column processes, benthic turnover, and the formation of the sediment record. During M 26 sampling and shipboard work was conducted by five of these subprojects as follows.

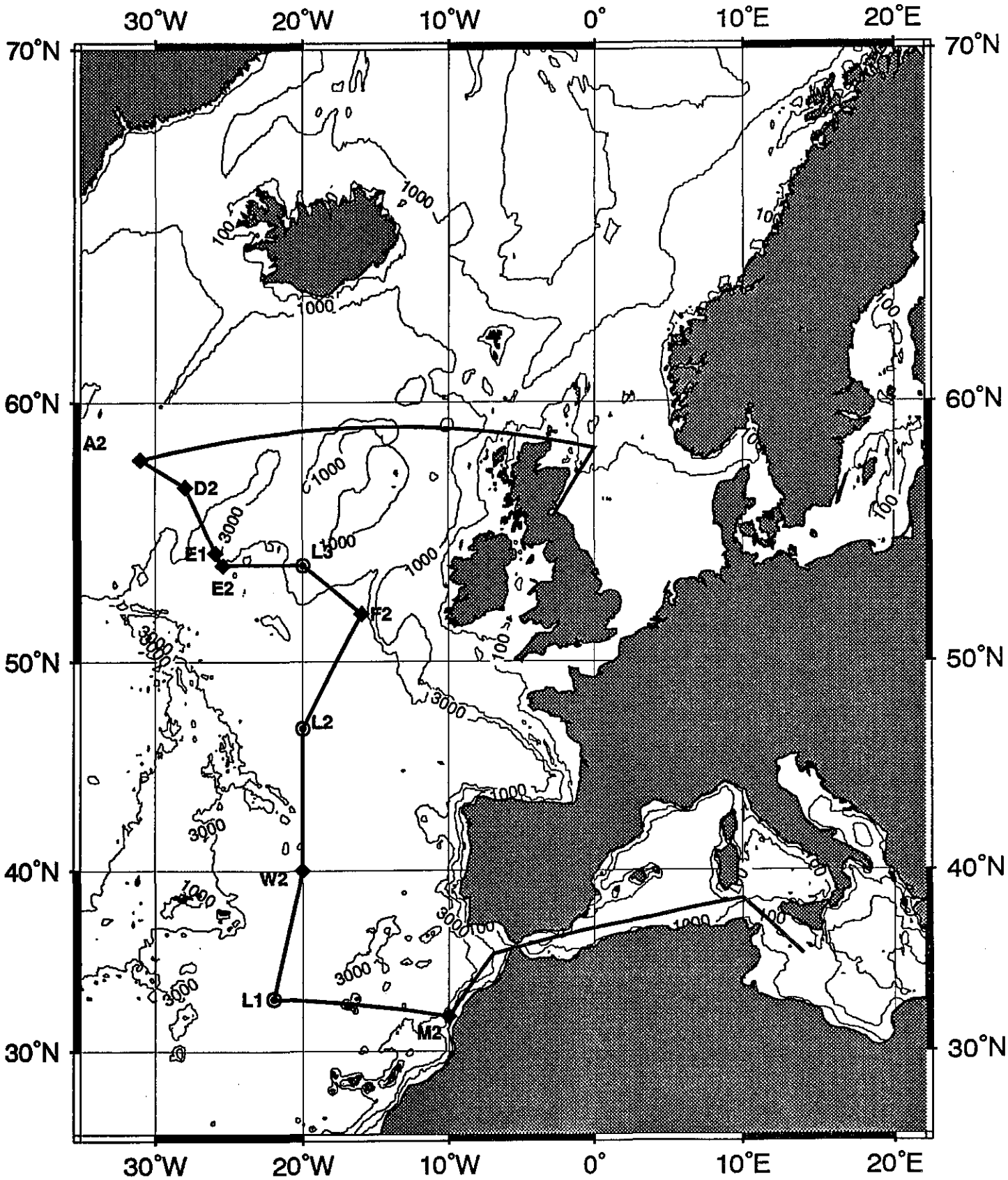

Fig. 2: Cruise track and working area of METEOR cruise no. 26, leg 1

Vertical particle flux (A1)

Long-term sediment trap studies in the Norwegian Sea and East Greenland Sea Basins have shown large interannual variations in total mass flux so far. Interestingly, the flux at the site in the East Greenland Sea is less affected by grazing pressure than that in the Norwegian Sea Basin. In order to continue the long-term flux record and verify the differences between these basins, two sediment trap moorings in each of the basins, with traps at three depth levels, were recovered.

Benthic turnover

Benthic material turnover as exemplified by chemical components of the organic carbon reservoir (biomarker) have been used to diagnose the source of sedimentary carbon and to partition mineralization in the water column, at the sediment-water interface and within the upper sediment layers. The latter includes early diagenetic modifications of biomarkers and the effects of seep input in certain areas to supplement the vertical flux. Accordingly, during M 26 the complex processes of benthic turnover were addressed through pore water and biomarker studies, as well as sediment microbiological investigations.

Evolution of geophysical signals in sediments (B1)

The overall objective of project B1 "Geophysical signals in sediments" was to determine the variety of large-scale seafloor-back scattering and to deduce from it seafloor processes to improve our understanding of the interaction between ice sheets, current regimes, and sedimentary processes on the East Greenland Margin. For subseafloor studies the (p-wave) sound propagation was measured on sediment cores taken from the various sedimentary environments. Acoustic measurements on these cores are used for the interpretation of the sediment subbottom-profiler records.

Reconstruction of surface and bottom water mass properties (B2/B3)

The area of the Norwegian-Greenland Seas is a key region for the understanding of the relationship between planktonic foraminiferal assemblages deposited at the sediment surface and the major water mass properties, salinity and temperature, in which they dwell. Water mass properties can be reconstructed along depth-transects and based on the sediment's microfossil contents. The relationship is then used, after calibrating the properties by means of a set of transfer equations involving todays properties, to reconstruct paleoconditions. This approach yields important parameters for climate and ocean reconstructions. The current data base is incomplete along the water mass boundaries of the East Greenland and Irminger Currents. This area is characterized by very strong regional gradients in sea surface temperature and salinity. The sampling transects during M 26/3 were designed to fill these gaps.

CO_2-modelling

The work of the SFB 313 has resulted in an air-sea exchange model for CO_2 as a function of sea surface temperature and wind stress. The model indicates that the glacial ocean, assuming

an enlarged area of low temperature surface waters and increased wind stress, may generate the very same atmospheric CO_2 contents and $\delta^{13}C$ signal of ΣCO_2 as have been found in Greenland and Antarctic ice cores. The sea surface temperature and wind stress of the East Greenland and the Norwegian Seas play a major role in this scenario. Hence it was attempted to collect additional data on the CO_2-system and its stable isotope characteristics.

3.4 Gas and Water Seepage on the Continental Margin (SEEP)

The input of submarine gas and fluids from cold seeps and their influence on material turnover and faunal adaptations at the sediment-water interface are among the major research objectives of the SEEP project. Cold seeps are ubiquitous along the European continental margin in a variety of tectonic settings but their role in nutrient, carbon dioxide and methane input is completely unknown. Most frequently seeps are related to subsurface hydrocarbon reservoirs and gas hydrate accumulations but also Holocene organic-rich sediments may generate enough methane by fermentative processes that gas escape has been documented. Tasks of this interdisciplinary investigation of fluid and water seepage are to determine in the dissolved mass and water transport, subsurface structure at seep sites, methane utilization, benthic material turnover, and faunal adaptation. During M 26/2 areas of known gas seep sites in the Skagerrak, a suspected site in the Faeroe-Shetland Channel, the Barents Sea slope and a crater field on the Barents Sea shelf were investigated.

The multi-disciplinary approach of SEEP is focussed on: (1) determining the subsurface structure at seep sites; (2) quantifying the fluid and geochemical mass fluxes using an *in situ* device deployed from a surface vessel via a lander system; (3) measuring the rates of sulphate reduction, methane oxidation and methanogenesis at different horizons in sediment cores from seep and non-seep sites; (4) comparing the species composition, density and distribution of benthic fauna at seep sites with that in the surrounding sediments unaffected by seepage; and (5) examining the structural and ecological adaptations of organisms living in seep areas with reference to the physical and chemical environment of the seeps.

3.5 European North Atlantic Margin - Sediment Pathways, Processes and Fluxes (ENAM)

The way margin processes change in space and time to form facies units, the relationship between the architecture of these units, and images on seismic profiles need to be understood. In order to interpret the seismic records of this margin with confidence we need to know the full range of lateral and vertical variability of sedimentary facies and their geometry. During M 26-3 cruise we studied the Quaternary, glacially influenced, margin off Norway. In the Storegga Slide area we used existing sediment core and seismic data for planning our investigations. Based on this information we planned to do seismics, coring and other *in situ*

operations to define in detail the surface and subsurface morphology, and to investigate sediment dynamics at the sea floor. Analysis of high resolution seismic profiling (boomer), multibeam and parametric echo sounding records (Parasound), together with the analysis of cores and *in situ* geotechnical measurements should provide information on recent and currently active sediment mass-wasting processes and on the likelihood of sediment slope failures.

In situ measurements in the target areas of the northern rim of Storegga Slide, using four stations deploying the Pop Up Pore Pressure Instrument (PUPPI), one station for the Module Geotechnique and one station for the Ocean-Bottom Hydrophone (OBH), provided pertinent data on sediment stability that cannot be obtained by sampling and laboratory analysis. In particular the pore pressure and the compressional-wave velocity /shear-wave velocity will allow us to estimate the *in situ* stress state. This will enable us to differentiate between normally consolidated and overconsolidated sediments and any underconsolidated sediments, which are considered to be less stable .

It is presently unclear whether sediments that are liable to fail in the future currently exhibit *in situ* properties that predict future failure. We are certainly well aware of extensive studies that have been made to evaluate sediment stability in the North Sea, especially for engineering structures. So far, much of the continental slope of northern Europe has not been investigated in detail nor has the potential and the relationship between the occurrence of gas hydrates and the failure of sediments been studied. The great environmental importance of slide processes is clearly demonstrated by the Storegga Slide, which is one of the largest known slope failures.

3.6 High-latitude Shallow Water Carbonates

Calcareous communities of bivalve-balanids and bivalve-bryozoans were previously found to inhabit the eastern area of the Spitsbergen Bank. At present it is unclear what influence the Arctic water masses have on the development of these communities. A special sampling program was carried out for comparative studies of these communities. These communities off Spitsbergen are the largest cold-water carbonate deposits beyound the Arctic Circle. It is thought that they have developed in response to changing sealevel and oceanographic frontal systems during postglacial environmental conditions.

3.7 Neogene Uplift of Norwegian Mainland

The history of the Neogene uplift of the Norwegian mainland may be preserved in a typical sedimentary sequence which can be traced along the Norwegian shelf. In seismic profiles this sequence is expressed as a succession of oblique-sigmoid reflectors which offlap from a late

Pliocene regional unconformity. This unconformity is generally covered by glacial-marine material of Pleistocene age and locally varying thickness of up to 300 m. The sequence itself, which reaches thicknesses of more than 1500 m in places, is of Pliocene age. The lower sequence boundary transgresses from lower to upper Pliocene from the central North Sea to the area off northern Norway. The rapid sedimentation represented by this sequence is caused by a high input of terrigenous detritus as a result of enhanced erosion of the mainland in the course of the Neogene uplift of the Scandinavian Shield. Information about the conditions of input and deposition of this strata and their chronostratigraphic framework is still insufficient due to lack of suitable sampling devices. The deployment of a vibro-corer, necessary to penetrate the sandy parts of the strata, in an area with thin Quaternary cover was the objective of this cruise.

4 Narrative of the Cruise

4.1 Leg M 26/1 (K. Kremling)

On 8th August, METEOR left La Valetta, Malta, at 08:30 pm as scheduled, and started the first part of the cruise. Objectives of the leg were mooring recovery and deployments and station work in the North Atlantic. The stations are part of the German contribution to the international projects JGOFS and WOCE.

Several working groups completed a surface profile through the western Mediterranean on transit to the first mooring position, a distance of more than 1300 nautical miles. At sea, the continuous pumping system ("Kiel Pumping System") was installed to enable a continuous and low-contamination sampling of the surface layer (from about 7 m water depth). Pumping water at (1.2 m^3/h) samples are distributed via a pipe-system and are available to all working groups in the laboratories. The samples used to study the horizontal distribution or variabilities of physical, chemical, or biological parameters. Beside hydrographic and hydrochemical standard parameter, trace elements and organic trace substances were measured or sampled.

Also, a fast-spinning centrifuge was connected to the system which enabled an accumulation of suspended particulate matter for subsequent chemical analysis. Apart from a short technical problem of the pumping system during the first week, all equipment worked well during the entire leg.

After passing the Strait of Gibraltar in the night of 28 August, we reached station M2 off the coast of Marocco (32°34, 3'N/10°03, 0'W) on 30 August. We attempted to recover the mooring that did not surface in 1992 as part of the WOCE project "Eastern Boundary Current". A wire loop ca. 6000 m long weighted down with anchors was lowered from deck

to the ocean floor at the mooring's position (depth ca. 2000 m). It was intented to snag the mooring by a slow motion of heaving and lowering the loop. Unfortunately, two attempts failed which had been carefully planned and conducted by master Bruns and his crew. Thus, we had to assume that the mooring had been severed above the acoustic release - presumably due to intensive offshore fishing. A loss that oceanographers have to deal with.

During the following days work was more successful: No problems occurred when we lowered the first JGOFS mooring (L1 with four sediment traps at 500, 1000, 2000 and 4000 m at 33°08,5'N/21°58,5'W at 5300 m) in the northern Canary Basin, west of Madeira on 3 September. The position was in the immediate vicinity of a current meter mooring which had been recording for more than 13 years for the Department of Marine Physics of the Institute for Oceanography at IfM, Kiel. The water column was sampled intensively prior to work on the mooring. Station work was completed with a successful deployment of a multicorer. After this we headed north, where METEOR could recover an acoustic mooring (W2) in the Iberian Basin on 5 September in only 2.5 hours. This mooring had been deployed by a German-French group collaborating on physical oceanographic problems.

The third week of our cruise started off quite rough with an airflow related to a low pressure cell. Wind force of Bft 9 to 10 from the NW hampered the approach to the JGOFS station considerably. Thus, after delay of one day we reached the station L2 on 8 September. There we started CTD/rosette section work at wind force Bft 7. Thanks to the continuously decreasing wind after midday, we could deploy successfully the various phyto- and zooplankton nets. Only the multicorer caused severe problems, we were unable to recover any sediment. The causes for malfunctioning are still unknown.

On the next morning at 06:00 am we started - wind force Bft 5 to 6 - to lower the most important JGOFS-mooring at L2 with four sediment traps, one ADCP-device and two current meters at 47°48,0'N/19°47,6'W at 4562 m. Deployment worked well and took only 3.5 hrs. including lowering of the head buoy.

On 10 September, we reached station F2 SW of Ireland. This is the first mooring along the line between Cape Farvel and Porcupine Bank for the project WOCE-NORD. The release at 03:30 pm, locating at 03:40 pm, and recovery at 05:55 pm of the current meter mooring was routinely done in good weather conditions. The next morning, we re-deployed the current meters (6) in less than three hours at 52°24,1'N/16°22,2'W at 3500 m.

Between the stations the continuous surface section was sampled by a pumping system. Owing to complicated analyses, most parameters can only be analyzed on land. However, strong gradients of dissolved carbonate and chlorophyll a-contents were clearly observed, while between 38° and 40°N chlorophyll a-doubled in concentration reaching a value of about 1 mg/m^3. On the other hand, the nutrient values phosphate, nitrate, silicate remained low, within the range of the analytical detection limits.

On 13 September, 08:00 am, we worked on the last JGOFS mooring at station L3, successfully lowering the array with 3 sediment traps and 3 current meters at 54°39,8'N/21°13,6'W at 3050 m. Several hydrocasts, net tows and multicorer deployments were carried out during the night at this station. The wind from an easterly direction had decreased in the meantime such METEOR arrived at the next WOCE station.

There, on 14 September, the mooring E2 was to be replaced. However, after triggering the acoustic release, the mooring failed to surface. We decided to use the dredging method already described above and were very pleased when it worked successfully. After 12 hours of work the vessel's master and his crew managed to hieve the entire and complete undamaged mooring, inclusive of anchor weights on deck. Also, very important, we recovered the damaged release and are now able to search for the technical failure. In the morning of 15 September, we re-deployed the new mooring (E3) at 54°24,8'N/25°,7'W; the work was completed in 2 hours.

Thus, we headed for WOCE station D2 in fine weather and accompanied by schools of curious whales. However, we were most disappointed that this mooring did not surface, too. Unfortunately, due to increasingly stronger winds (Bft 6-7) and rough seas during the next few hours, we were unable to locate and retrieve the mooring by dredging as done previously. Following this unsuccessful attempt we lowered the new mooring D3 at 57°33.3'N/28°10.4'W at 2300 m.

In the meantime, severe storm, which had been forecasted for several days by the meteorologist onboard eventually arrived with wind force Bft 11 and above. Friday, 17 September and all day long we attempted to ride out the storm. In view of the distance of more than 1000 nautical miles to be covered to Edinburgh and a strong easterly current expected to develop, we decided to abandon the last WOCE station (A2) SE of Greenland and headed home at first with 2 to 3 knts.

During this transit on 18 September, we could take up work again on the surface section with the continuous pumping system. The section was completed - through the Hebrides Islands and Pentland Firth - to the northern North Sea. In the morning of 23 September, METEOR arrived in Edinburgh (Leith) and the first leg ended after more than 5000 nautical miles.

4.2 **Leg M 26/2** (E. Suess)

The RV METEOR departed Leith/Scotland at noon, 28 September, and sailed for the Skagerrak (Fig. 3) where she arrived on station in the morning of 1 October. The search for previously known seeps begun using a TV-fitted multicorer system (TV-MUC) and a series of hydrocasts. The latter yielded the distribution of methane anomalies in the near bottom water

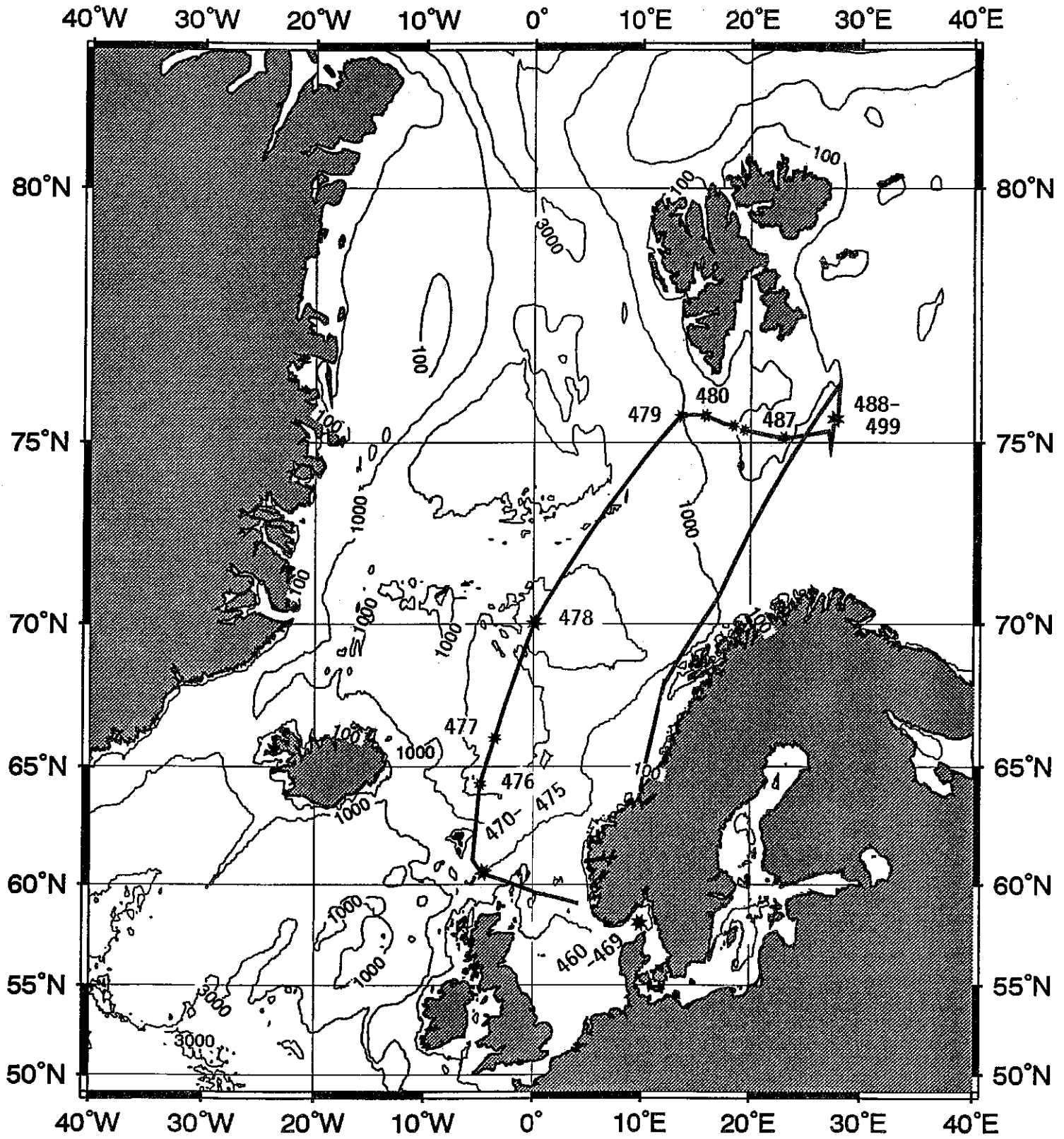

Fig. 3: Cruise track and stations during METEOR cruise M 26/2; SEEP-objectives were pursued at stations 460-469 (Skagerrak), 470-475 (Faeroe-Shetland Channel), 480 (Barents Sea Slope), and 488-499 (Barents Sea crater field).

and identified one point source with concentrations >1500 nl/L of CH_4 in the lower water column. Due to low visibility, the survey with the TV-MUC was unable to image any actively seeping sites; neither was the side-scan-sonar survey successful in doing so. It appears that the usual benthic symbiotic communities found at active seep sites are not flourishing here due to rapidly shifting sediments. The MEDUSA system for *in situ* profiling of methane also failed soon after it was launched for the first time.
Conventional gravity coring yielded a 6 m long core with abundant *pogonophorans* and high CH_4, NH_4-, and ΣCO_2-concentrations in the pore fluids, giving evidence that it came from an active seep. In addition, two large box cores (GKGs) were collected from the same area which contained the amount of biomass than the surrounding sediment several times, indicating the seep activity. Because of the very time-consuming search for active seep sites, the VEnt SPider (VESP) for *in situ* flow measurements was not deployed and METEOR departed the Skagerrak at noon on 2 October with course for the Faeroe-Shetland Channel.
We reached the area on 4 October at about 01:00 am after crossing the North Sea with relatively calm weather conditions. During the next 24 hours >100 nm of combined side-scan-sonar and deep-tow-boomer surveys, perpendicular the axis of the Faeroe-Shetland Channel, were carried out in order to ascertain the near-surface structure of potential seep localities at around 900-1000 m water depth. These had been postulated from multi-channel seismic surveys by the British Petroleum Co. The deep-tow-boomer survey, yielding excellent penetration and high depth resolution, however, showed that these features were most likely sediment drift bodies shaped by the swift bottom current through the channel. At the Faeroe side of the channel a depression similar to the craters of the Barents Sea, was observed but no methane anomaly detected in the water column nor the bottom water immediately above.

Work on deck and sampling over the side of the vessel were restricted during most of the day on 5 October due to high seas, 6-7 m, and strong winds, Bft 8-10 and completely halted during the evening. In the night METEOR headed for Torshavn, Faeroe Islands, since the weather forecast did not indicate any change, and we abandoned plans entirely to sample Lousy Bank. This decision was a major setback for the "cold water carbonate project". We reached Torshavn in the morning of 6 October.

During the day and the following morning in Torshavn spare parts for equipment (TV, gas chromatograph etc.), replacement of a grab sampler, kindly provided by the Faeroe marine biological station BIOFAR, and exchange of two scientists took place. Repairs of the *in situ* methane system MEDUSA progressed well during the sheltered stay at Torshavn. On 7 October at 11:00 am local time METEOR departed and took a northerly course towards the Barents Sea. Along this more than 1200 nm transect, three stations in the Norwegian Current were extensively sampled for hyrdrographic, planktonic and benthic biological parameters. The first station was situated at the northern slope of the Island-Faeroe Ridge, the second above the Aegir Ridge, and the third in the center of the Norwegian Basin. Here the SFB 313 has maintained a sediment trap mooring fore more than 5 years. Sampling was completed on 10 October around 02:00 pm and the Barents Sea slope at 74°N was reached on 11 October.

Meanwhile winds had increased again, snow flurries as well as air temperatures around freezing, slowed down work on deck, and the vessel's speed had to be reduced to below 6 kts. Around 08:00 am on 12 October a parasound survey was begun to locate potential seep sites within the well-know high-accumulation area on the Barents Sea slope, SW of Spitsbergen. Hydrochemical, biological and geological sampling at suspected seep sites, characterized by acoustically turbulent sediments, and along a drainage canyon (Kveitehola) yielded pogonophorans as well as slightly elevated methane contents in the water column, evidence for vigorously venting seeps was not found.

Sampling continued during the following days (13/14 October) across the Spitsbergen Bank, where biogenic carbonates were collected. During the early evening of 14 October the weather deteriorated rapidly and a major storm developed during the night and the following day. An extreme low pressure system (< 958 hPa) located over northern Norway moved towards the Kara Sea and METEOR was caught in a very strong cold northeasterly flow of air that reached velocities of >70 kts. (>12 Bft) which were sustained over several hours during the night. Wave heights of >15 m were recorded. During 16 October the winds died down and the air temperature dropped to -6°C which hampered clean-up and repairs after the storm on deck considerably. We reached the main area of investigation, the Barents Sea crater field, on 17 October and carried out a shortened deep-tow-boomer survey across several of the most prominent features. It became clear that two preferred directions of alignment of the craters existed, presumably structurally determined, and that the subsurface showed varying intensities of "gas saturation". Based on these features several coring, hydrographic, biological, and video-surveys were carried out during the remaining time. The air and water temperatures kept dropping and increasingly affected our work schedule.

During a period of calm but cold weather on 18 October the *in situ* benthic chamber system VESP was deployed inside three of the craters. The video images showed disrupted strata and chaotic debris deposited along well-defined and steep slopes. The boulders and thrown fragments were up to 1-2 m in diameter, supporting the idea, expressed earlier by Norwegian scientists, that these craters are the result of violent gas hydrate explosions. Geological sampling should help determine the age of the eruption. No evidence for present vigorous seep activity was found, even though the bottom water around the craters showed very significantly increased dissolved methane contents. The CTD-work and sampling for methane showed a distinct pattern with strongly increasing gradients in the bottom water towards the northern end of the crater field.
Daily snow flurries and low air temperatures (-10.2 °C) continued throughout the week and made it impracticable to further deploy heavy equipment. This affected the deep-tow-boomer system as well as the MEDUSA. The latter system had been repaired successfully but regrettably could not be used without endangering personnel. In the morning of 20 October fresh "pancake ice" and few drifting ice growlers were sighted at 75°51N/27°30E. The sea was calm, air temperature -12.7 °C, and only 7 nm distant lay a field of pocks marks, suspected to be the source of the high bottom water methane content. However, the coverage

of "pancake ice" increased during the next few hours and northerly winds carried more extensive accumulations of ice towards the vessel, hence we decided to turn back and instead of completing another station within the Norwegian Current at about 72°N/13°E. During the following transit the weather forecast again predicted a major SW-storm approaching the vessel around 22 October.
Based on the previous experience, it seemed prudent to abandon the sampling of the Norwegian Current station and seek shelter. Accordingly, around noon on 21 October the vessel's position was south at 70°30N and 17°0E and we steamed towards Vestfjorden on the norgwegian coast and later on around the outer Lofoten Islands towards Trondheim. On 23 October METEOR took shelter at Forhavet in the northern part of Trondheim Fjord and awaited the passing of the storm, Bft 8-10, which lasted for about 24 hours. In the morning of 25 October she tied up at Trondheim harbor and the 2nd leg of the 26th voyage ended as scheduled.

In summary, the science program during the leg M 26/2 was adversely affected by unfavorable weather conditions throughout. Extra steaming time due to high winds and seas, time for clean-up and repair of equipment after a major storm hit the vessel on 14-15 October, icy conditions aboard, sea-ice, and weathering high seas on three different occasions, used up more time than the entire station-time combined. In spite of this, sampling and surveys were sufficiently completed to address all objectives in reasonable detail.

4.3 **Leg M 26/3** (J. Mienert)

The third leg of the 26th cruise of R.V. METEOR was a joint expedition of several institutes to carry out four main research programs on the Norwegian shelf and Margin, the East Greenland margin and adjacent basins (Fig. 4). The research programs included "Environmental Change in the northern North Atlantic" (SFB 313, University of Kiel), European Commission funded MAST II project "ENAM" (European North Atlantic Margin: Sediment pathways, processes and fluxes), the German-Norwegian cooperation project of the Norwegian continental shelf (University of Bergen and Kiel), and the Geologisches- METEOR left Trondheim at 11:00 am on Thursday 28 October 1993. We began the vibrocoring program on the Norwegian shelf on 29 October 1993. The sea was relatively calm, Bft 2, with a swell of up to 2-3 m making handling of the 6 m high vibrocorer relatively easy. During darkness we profiled the area with Parasound and Hydrosweep to get an overview of the distribution of Pliocene sedimentary sequences. Knowledge of these sequences is important for reconstructing the subsidence history of the margin.

Sea state Bft 8-9 on 30 October 1993 made the remaining vibrocorer work impossible because of the ship's rolling. Only Parasound profiling was accomplished. We left the shelf at 10:00 am and reached Fröya Island at 03:30 pm where a fishing boat picked up three

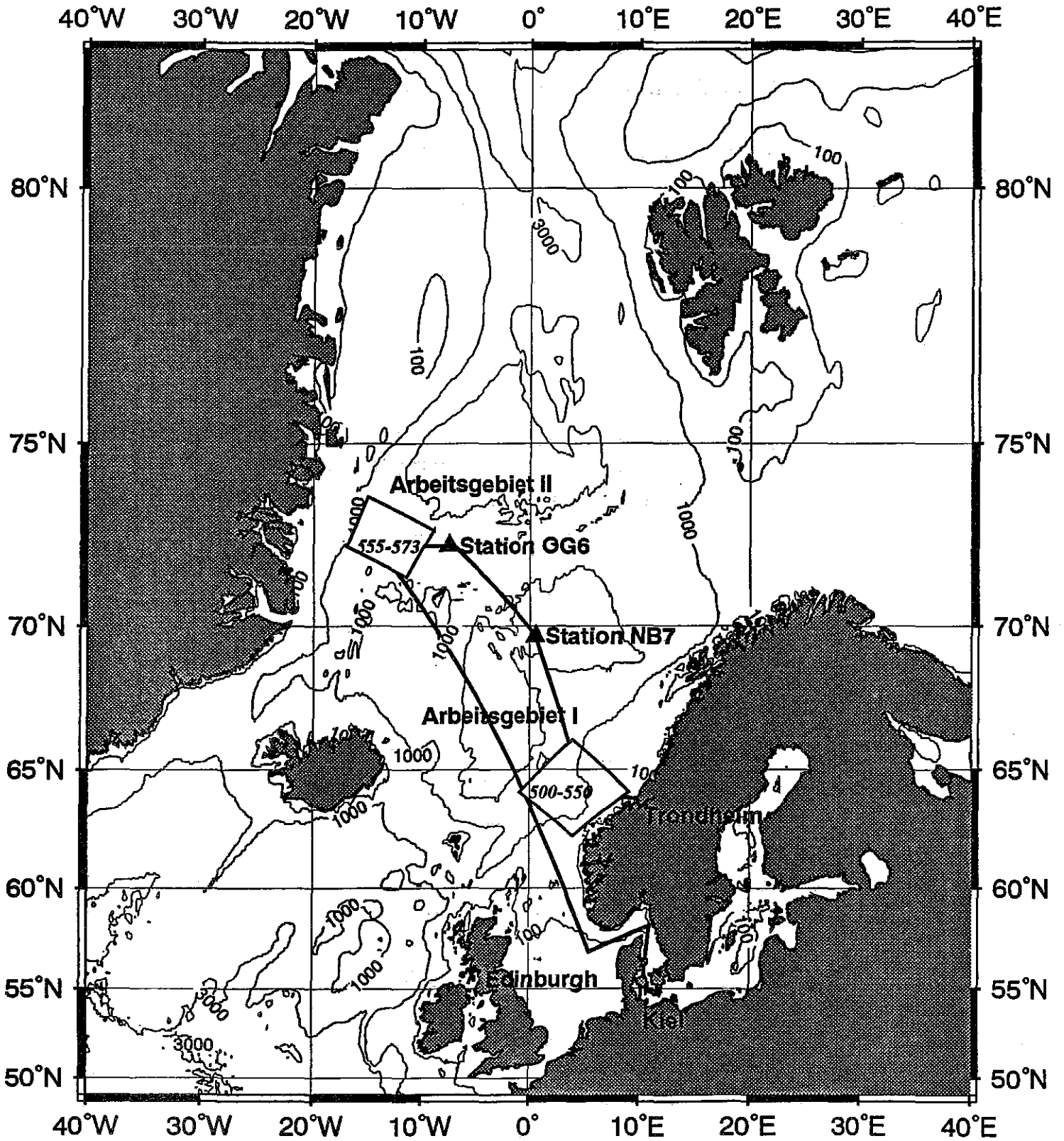

Fig. 4: Cruise track and working areas of METEOR cruise no. 26, leg 3.
Paläontologisches Institut der Universität Tübingen (GPIT) project "Lunar phases of zooplankton".

scientists from METEOR. Afterwards we sailed out of the Fjord and awaited the passing of the storm under the protection of the island.

On 31 October 1993 we left Fröya Island at 02:00 pm heading west towards the working area on the Norwegian Margin. The first short Parasound profile (12 km long) provided information about the site location, i.e. the sea floor and its subbottom, where a Pop Up Pore Pressure Instrument (PUPPI) test and deployment were performed successfully on 1 November 1993. The retrieval of two sediment cores from 1000 m water depth will allow comparison of the pore water pressure data with the physical properties of the sediment. The first deep-tow-boomer profile was done for about 15 h on a 125 km long track. The fish was towed at a depth of about 600 m below the sea surface at a speed of 4.5 knts. Across an area about 30 km northward from the rim of the Storegga Slide. The record showed a penetration of about 200 ms, several pock marks in water depths of 800 to 1000 m, and wipe-out of acoustic features which indicated the presence of gassy sediments well below the sediment surface.

The first boomer profile ended on 2 November at 01:00 pm at 1400 m water depth. IFREMER's Module Geotechnique was rigged for its first test at 1400 m water depth. The test on the sea floor included the penetration of three sensors into the sediment. The test was carried out at three locations that were about 500 m apart. Between these stations the ship travelled at a speed of 2.5 knts. With the module about 150 m above the sea floor. The module was recovered at 06:00 pm and immediately showed that the automatic coring device had not returned to its initial position within the frame of the module. No geotechnical data were collected during this deployment because of a bad cable connection. We continued our program with the deployment of the 12 m gravity corer, the second PUPPI deployment and a CTD test. The second boomer profile started at 09:00 pm from deep (1400 m) to shallow (500 m) water. All profiles were run parallel to the first boomer profile in order to determine the 3-D architecture of the sea bottom along the northern rim of the Storegga Slide. Recent faulting was noted on the profiles.

Calm sea allowed two 12 m gravity cores to be taken on 3 November 1993. The first at 1400 m and the second at 800 m water depth. Afterwards the Ocean Bottom Hydrophone (OBH) - Pinger test and a second PUPPI wire test were made before launching the equipment on the sea floor for *in situ* measurements of changes in compressional wave velocities (OBH) and pore water pressures (PUPPI). The third boomer profile started from shallow to deep water at around 09:00 pm. This profile showed similar structural features related to gas accumulation as noted on the other profiles.

The boomer survey ended in the morning of 4 November 1993 and the Ocean Bottom Hydrophone - Pinger experiment started. On our first profile we lowered the 3.5 kHz deep-tow pinger together with the OBH to a depth of 50 m above the sea floor. An acoustic release

disconnected the OBH from the pinger and subsequently the pinger was towed away from the OBH at a speed of 2 knts. This allowed us to carry out a wide angle reflection experiment. We stopped profiling at a distance of about 1 nm from the OBH and got the pinger back on board. On our second profile we lowered the deep-tow-boomer into the water and ran a 2 nm boomer line across the OBH position. After finishing the profile the boomer was brought back on deck and the OBH was released from the sea floor by an acoustic signal.

The wind force and sea state increased to Bft 5-6 and the visibility decreased on 5 November 1993. In the morning the acoustic signal to release PUPPI was sent. However, the release sytem did not function and a cable on the deck's hydrophone was replaced. The hydrophone transmitted clearly and PUPPI's position was seen on a computer screen. Despite the fact that the acoustic release system was now working properly, the mechanical release system malfunctioned. PUPPI 1 remained at its position on the sea floor. After several attempts we abandoned the PUPPI station and took a core at our next station, an area of gassy sediments. The sediments of the core showed intense formation of hydrotroilite indicating the presence of methane, not surprising in an area of extensive mud volcanoes where gas is seeping through the sea floor. A Module Geotechnique station at about 1000 m water depth was partly successful because only one sensor (shear strength) worked. PUPPI 2 was released and recovered without problems at 07:40 pm. Afterwards we started Parasound and Hydrosweep profiling.

On 6 November 1993 we carried out work at three stations, with CTD and Multinet deployments, a gravity coring station and a PUPPI launching at 1300 m water depth. All stations were successfully completed. Boomer profiling started at approx. 10:00 pm and ended in the morning of 7 November 1993. A low pressure cell moving from Iceland towards the NE entered our working area and the sea state rose. The boomer fish was recovered and brought on deck at 01:00 pm. Afterwards we had three hours of steaming time to the next two coring stations located at about 870 m water depth. The cores were successfully retrieved. Afterwards the boomer fish was launched into the water and profiling started at 07:00 pm.

On 8 November 1993 the low pressure front caused an increase of wind speed to Bft 6-8 during which the deep-tow-boomer winch failed and the fish had to be hauled in with another winch. PUPPI 3 was recovered earlier than planned because the automatic clock release was set for 03:00 am on 10 November 1993 when the storm was expected to hit us. The subsequent launching of a new PUPPI 4 was the most exciting one because it was positioned directly above a 400 m wide and 3-5 m deep mud volcano at 873 m water depth. At this location we also launched a CTD and a Multinet. In order to reach shelter from the upcoming storm which was forecast to reach Bft >11 we left the area at 04:00 pm and sailed to Fröya Island. We reached the island at 04:00 am in the morning of 9 November 1993, returned at our working area on the Norwegian margin on 10 November 1993 at 11:30 pm and started Parasound/Hydrosweep profiling.

During the morning of 11 November 1993 we recovered PUPPI 4, the instrument which was launched into a mud volcano. The first data playback showed that one channel (upper port) had malfunctioned and had not obtained a complete data set. However, the lower-port channel had recorded the complete 68.5 hour record. At 11:00 am we left the working area on the Norwegian margin and sailed towards the first sediment trap station. We arrived there on 12 November 1993 at 12:00 am and the sediment trap mooring was successfully released, surfaced, recovered and brought on deck. The traps had worked well and collected relatively high amounts of biogenic material. Afterwards a CTD, a Multinet, and a box corer station were completed in 3300 m of water. We left the mooring station at 00:00 and sailed northwestward towards the second sediment trap station.

Here the water temperature was 0°C and the air temperature -2.3°C. We started with a water sampler and completed a CTD station. The release of the sediment trap mooring started on 14 November 1993. The release worked well and a range measurement showed that the mooring was coming up. However, after about 30 minutes it remained at a constant water depth of 1375 m. Range measurements from different directions showed unquestionably that the mooring did not move any more. With two transciever systems located on board but we tried again without success. Both showed the same distance to the mooring without any indication of further movements of the sediment traps. Our initial finding is, that some of the floats at the top part of the mooring had collapsed and had settled on the sea floor. After releasing the mooring, the acoustic release came up to 1375 m. It remained there because the top of the mooring was anchored to the sea floor and as a result, the mooring was apparently up-side down. After several more attempts to release the mooring we put the acoustic system to sleep and left the site.

On 15 November 1993 air temperatures dropped to - 10°C and water temperatures varied between -0.5 and -1.0 °C. Ice and snow covered the ship on our transit to the next working area, located NW of Vesteris Banken on the East Greenland Margin. Twenty-one Parasound/Hydrosweep profiles, two box cores and one CTD station added to the information of parts of a 500 km long channel system that runs from the shelf edge in the southern part of the Greenland Basin to the deepest part of the basin in the northeast. The profiles show a less than 10 km wide and less than 100 m deep channel system. The channel is believed to have been formed by turbidity currents and may be presently inactive. This latter hypothesis is based on undisturbed and Holocene (?) sediments recovered from the channel floor. No anomalous bottom water masses were recorded in the channel during a short time interval (10 min) of CTD measurements. We left the area and sailed on a course of 270° towards the sea-ice margin off East Greenland.

A further drop in temperature on 17 November 1993 caused an increase in ice buildup on the vessel. Finally, winds of Bft >10 made it impossible to continue station work. We were forced to interrupt the work and everybody and all systems went on stand by. On 18

November 1993, a decreasing wind allowed us to commence the station work. A CTD, Multinet and box core were successfully deployed within 20 miles of the ice margin.

On 19 November 1993, a rapidly moving low pressure cell caused extremely strong winds (Bft > 12, maximum wind speeds of 93 knts, average wind speed 76 knts) and all station work was halted. During the morning of 20 November 1993 the storm had passed. Despite the still rough sea conditions we attempted to take a box core. The corer came back on deck slightly bent and empty. Parasound and Hydrosweep profiling were carried out next.

We sailed south attempted under still stormy weather conditions passing the second mooring station where we determined acoustically that the mooring had not moved. On 25 November we entered the Kiel Fjord and docked inside the Schwentine River in front of GEOMAR at 05:30 pm.

5 Preliminary Results

5.1 Physical Oceanography

5.1.1 The WOCE Moorings (H. Klein, H. Wüllner)

Beside the attempt to recover the mooring M2 off Marocco (32°24.2'N, 10°03.1'W) the main objective was the recovery and redeployment of four current meter moorings along the transect ACM-8, between Cape Farvel and northwestern Ireland (Position A, D, E, and F in Table 4). Due to release problems and/or the possible loss of buoyancy due to corrosion or fishery activity, moorings M2, E1, and E2 had to be dredged. We were not successful in finding M2 and E1, but E2 could be recovered completely. Because of stormy weather we were unable to steam to position A. Since completion of the METEOR cruise, we succeeded in recovering this mooring with the help of FFS WALTHER HERWIG". Some preliminary results obtained from mooring E2 and F2 data will be discussed in the following:

Tab. 4: Mooring positions WOCE section ACM-8

I.D.	Position		Depth [m]	Time	Institution
A2	59° 8.1'N	34° 4.4'W	2630	9/05/ -	IFMH
D2	57°24.7'N	28°13.5'W	2587	9/03/92-	IFMH
E2	54°17.3'N	25°51.4'W	3003	9/02/92 - 9/14/93	BSH
F2	52°22.7'N	16°21.7'W	3481	8/30/92 - 9/10/93	BSH
D3	57°33.3'N	28°10.4'W	2294	9/16/93 -	IFMH
E3	54°24.8'N	25°51.7'W	3299	9/15/93 -	BSH
F3	52°24.1'N	16°22.2'W	3501	9/11/93 -	BSH

I.D.: Mooring identifier
IFMH: Institut für Meereskunde Hamburg
BSH: Bundesamt für Seeschiffahrt und Hydrographie

Table 5 summarizes some statistics of the low-frequency currents. Periods shorter than 48 hours have been removed using a Gaussian low-pass filter. At mooring site F2 all instruments worked properly. The mooring was placed in the Rockall Trough close to the western slope of the Porcupine Bank. As in the year before, the currents were weak and variable. A progressive vector diagram is given in Figure 5, based upon the original unfiltered data. Time marks (+) are given every 30 days. At all instrument depths the mean transport is directed towards the SW. Generally, the eddy kinetic energy kE exceeds the mean kinetic energy kM (1) by more than an order of magnitude. The mean vector speed v is about 3 cm/s or less, the

maximum scalar speeds vmax range between 15 and 20 cm/s. Only at 481 m depth vmax amounts to 33 cm/s. Between 180 and 480 m depth there is a northward transport during the first 4-5 month (September-January), then the currents turn to the WSW.

At mooring E2, southwestwards off the Rockall Plateau, there is a steady southeastward transport at about 200 m above the bottom (see Fig. 6). In 175 m depth the transport goes in a northward direction and is much weaker, although the mean scalar speed vs is higher than in the near-bottom layer (see Table 5).

For the determination of meridional transports and the detection of seasonal signals in these currents we need the records of the missing moorings and the time series of further deployments. Having time series of a few years duration, such analysis will be done at the end of the field program in 1995.

Tab. 5: Summary statistics of low-frequency currents

Depth	u	u'u'	v	v'v'	v	v_s	SF	Dir.	K_E	K_M
[m]	(cm/s)	(cm^2/s^2)	(cm/s)	(cm^2/s^2)	(cm/s)		%	deg	cm^2/s^2	
Mooring F2										
181	-2.5	80.6	-1.4	73.0	2.8	13.9	20	240	76.8	4.0
481	-1.1	46.0	-2.9	82.0	3.1	8.8	35	201	64.0	4.8
781	-1.2	50.5	-1.1	47.7	1.6	10.5	16	228	49.1	1.3
1981	-2.2	24.5	-0.2	18.1	2.2	6.8	33	264	21.3	2.5
2981	-0.2	7.4	-0.8	5.5	0.9	5.0	17	195	6.4	0.4
3431	-0.7	20.0	-0.5	13.5	0.9	6.9	12	233	16.8	0.4
Mooring E2										
175	-0.2	3.3	0.6	3.5	0.6	11.0	5	339	3.4	0.2
2825	-1.1	16.8	-2.2	21.5	2.4	7.0	35	206	19.1	3.0

u,v = Means of the zonal and meridional component of the current vector; u'u',
v'v' = zonal and meridional variances;
v = Mean vector speed; vs = mean scalar speed:
SF = Stability factor: (v/vs)*100;
dir = Mean direction; KE, KM = eddy and mean kinetic energy

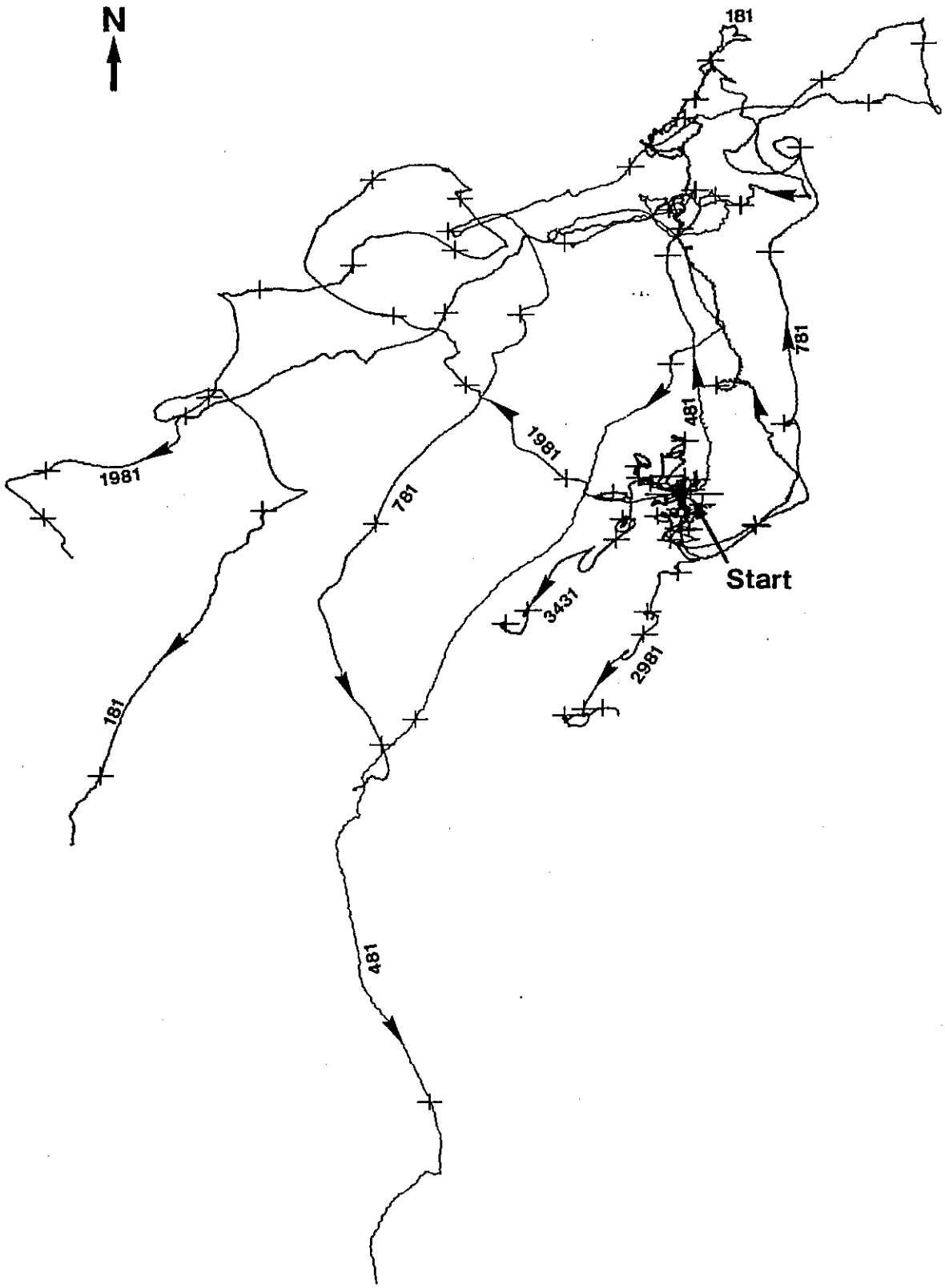

Fig. 5: Progressive vector diagram of mooring F2: Time marks (+) are given every 30 days, the numbers give the instrument depths.

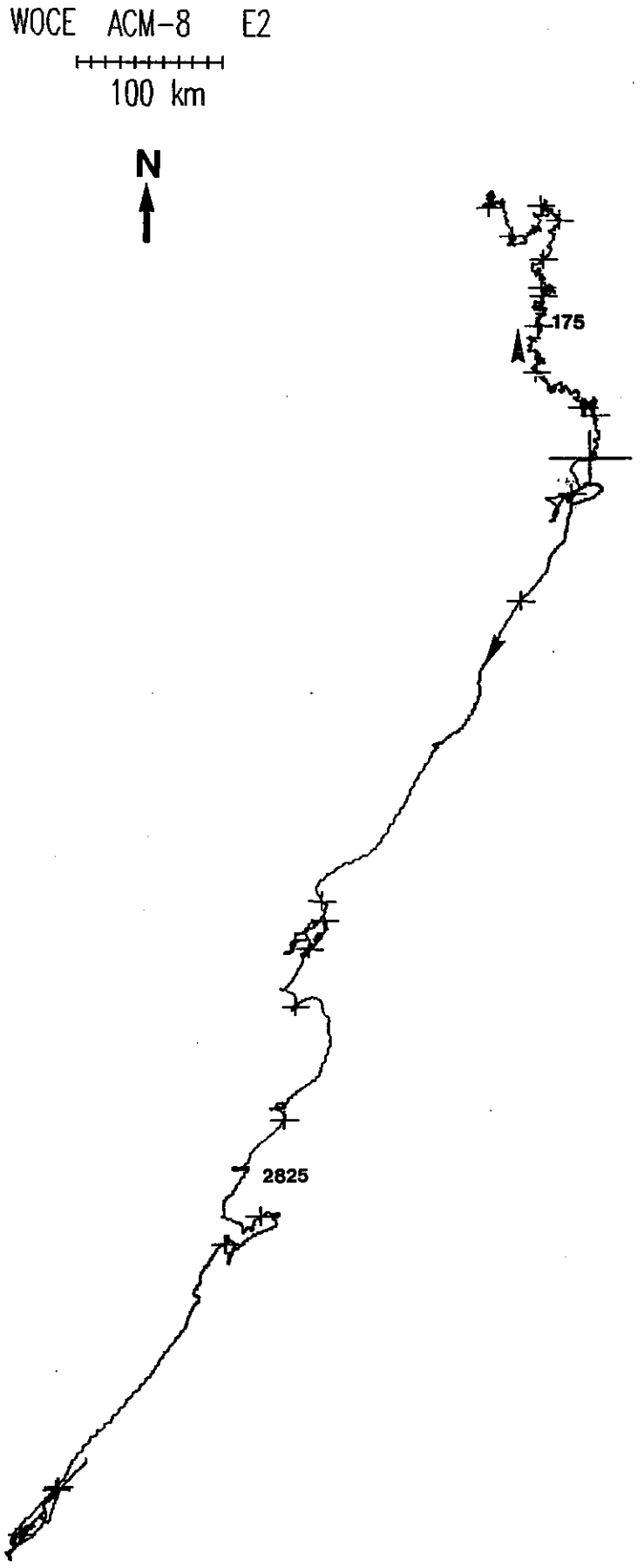

Fig. 6: Progressive vector diagram of mooring F2: Time marks (+) are given every 30 days, the numbers give the instrument depths.

5.1.2 Hydrographic Parameters in the JGOFS area (F. Wehner)

During METEOR M 26/1 CTD-profiles to the bottom were taken at the following mooring positions M2 at the North African continental slope, L1 in the Madeira Basin, L2 in the West European Basin, F2 at the Pocupine Bank and L3, E1/E2, D2 at the northern continental slope of the North Atlantic deep-sea basins (see also Figure 2). For CTD-measurements an EG&G MarkV-CTD was used, equipped with pressure- , temperature-, conductivity- and oxygen sensors integrated in a 12*10 l rosette system of General Oceanic. In addition, a backscattering fluorometer was installed at profiles to about 1000 m to resolve the vertical distribution of phytoplankton within the photic zone. For the calibration of the CTD-instrument reversing thermometers were used and bottle samples were taken for salinity measurements with an Autosal-salinometer.

The temperature and salinity profiles are presented in Figures 11 to 16 simultaneously with the nutrient and oxygen profiles (see Chapter 5.2.1). For the Atlantic stations L1 to D2, the recorded temperature and salinity profiles exhibit a strong seasonal stratification above the main thermocline as expected for the late summer season.

The mixed layer depth was less than 20 m at station L1 in the Madeira Basin and about 50 m at L2. The temperature of the mixed layer decreased from about 24 to 17.5°C in conjunction with a decrease in salinity of about 1.5 psu between these two stations, indicating the transition zone between the subtropic and subarctic circulation. At station L1 the influence of Mediteranean Water (MW) at a depth of 1000 to 1200 m became apparent by increasing salinity and temperatures. At station L2 the signal of MW was detectable but less pronounced than at station L1.

Stations F2, L3, E1 and D2 further to the north showed decreasing temperature and salinity values within the mixed layer, indicating that the profiles were taken in the subarctic regime of the North Atlantic circulation. The salinity minima within the surface layer represent the input of fresh water due to melting ice during the summer season in these regions, which is advected with the general circulation.

5.1.3. Hydrographical Parameters in the Northern North Atlantic (M 26/2) (G. Winckler, T. Viergutz)

Vertical profiles in the water column of temperature, conductivity and pressure were taken on 17 stations. On 12 of these stations, oxygen profiles were recorded. For these measurements a Neil Brown Mark V CTD equipped with the relevant sensors was used. These data provide essential background information for several projects. This concerns the characterization of water masses, of environmental parameters for planktological studies, of evidence for venting of fluids in near-bottom waters, and the calibration of temperature functions based on

foraminiferal assemblages. A typical vertical profil (Sta. 466-1) of the working area in the Skagerrak is shown in Figure 7. A very distinct discontinuity layer exists. The boundary between the Baltic outflow and the North Sea inflow lies between 40 and 60 m.

Three water masses were identified flowing through the Faeroe-Shetland Channel. The deepest one, between about 600-1100 m. An intermediate layer with increasing temperature and salinity between 600-1000 m, showing a salinity maximum, and a well-mixed surface layer.

Four stations were sampled along the Norwegian Current to determine salinity and temperature as environmental parameters. The Norwegian Sea deep water mass with constant S and T was characterized, an Atlantic water mass with pronounced salinity and temperature maxima and a surface layer of variable thickness with seasonally low temperature and salinity from meltwater were observed.

During our work in the Barent Sea we attempted to use the CTD and the water bottle rosette for near-bottom sampling in the pockmarks. For this purpose the altimeter on the probe proved to be an excellent feature. By permanently monitoring the distance to the sea floor it was possible to obtain water samples from inside single pockmarks in the crater field.

5.1.4 Hydrographical Parameters in the Norwegian Current

(E. Bauerfeind, H. Beese)

Vertical profiles of temperature and salinity were measured at 12 stations with a CTD (Neill Brown Mark V) during METEOR cruise M 26/3. Casts were carried out at every station at which samples with the multiple opening and closing net were taken. In Figure 8, a typical profile (raw data) for the study area 1 (Storegga Slide) and the profile obtained at the mooring position in the Norwegian Basin are given. In the Storegga Slide area, a thin layer of isothermal and low saline water, most probably influenced by the Norwegian Coastal current, was present above water of Atlantic origin, charaterized by a high salinity. This water extends down to 400 m. From this layer down to the sea floor there is the influence by Norwegian Sea Deep water. At the mooring position NB 7, the warm Atlantic water extends down to 800 m. In deeper water the temperature continuously decreases to -0.843°C indicating the presence of Norwegian Sea Deep water. At the surface, a warm isothermal and highly saline layer extends down to 170 m (Fig. 9).

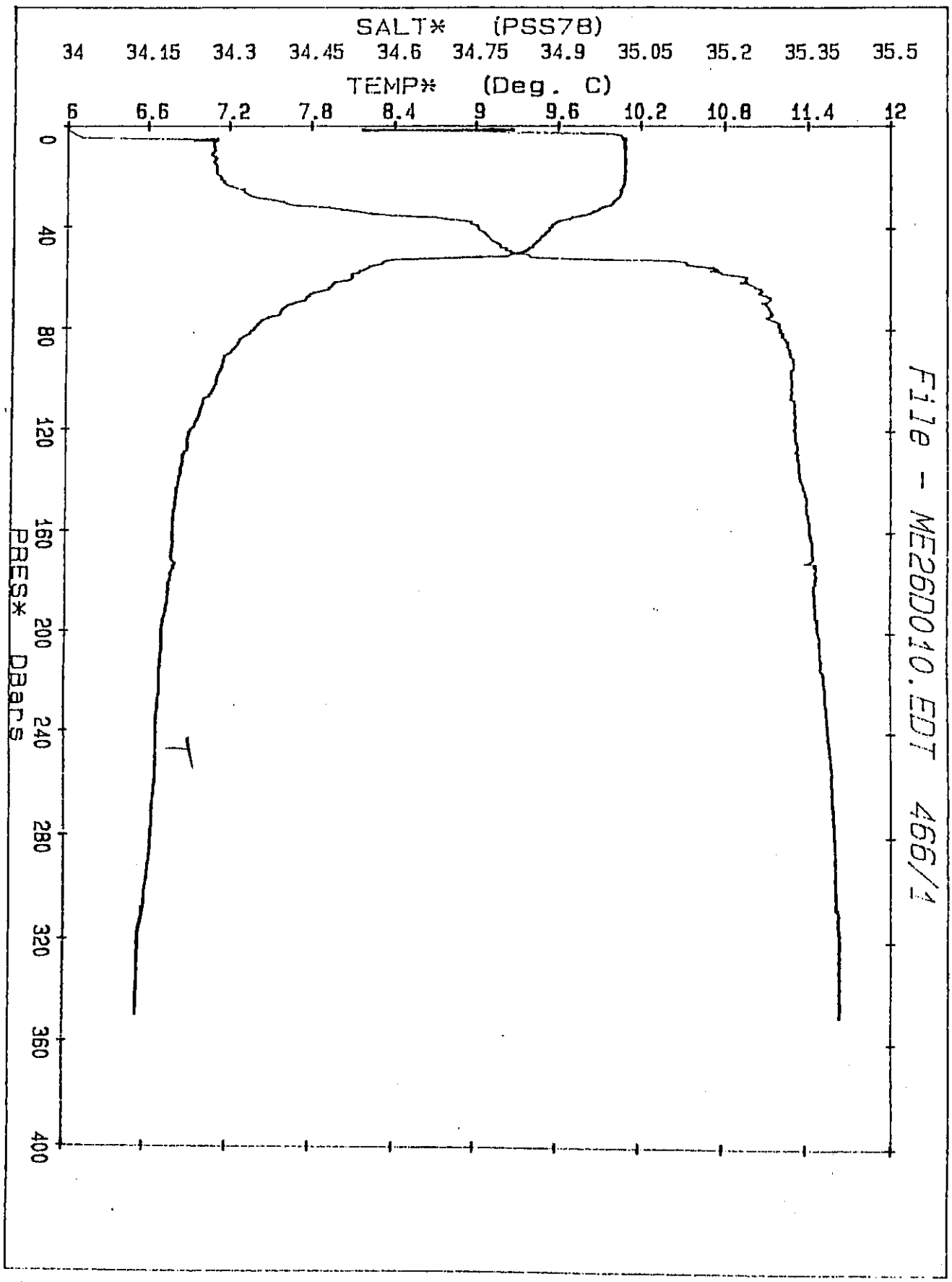

Fig. 7: A typical vertical profile (Sta. 466-1) of salinity and temperature (raw data) in the Skagerrak with a very distinct discontinuity layer, which indicates the boundary between the Baltic outflow and the North Sea inflow between 40 and 60 m.

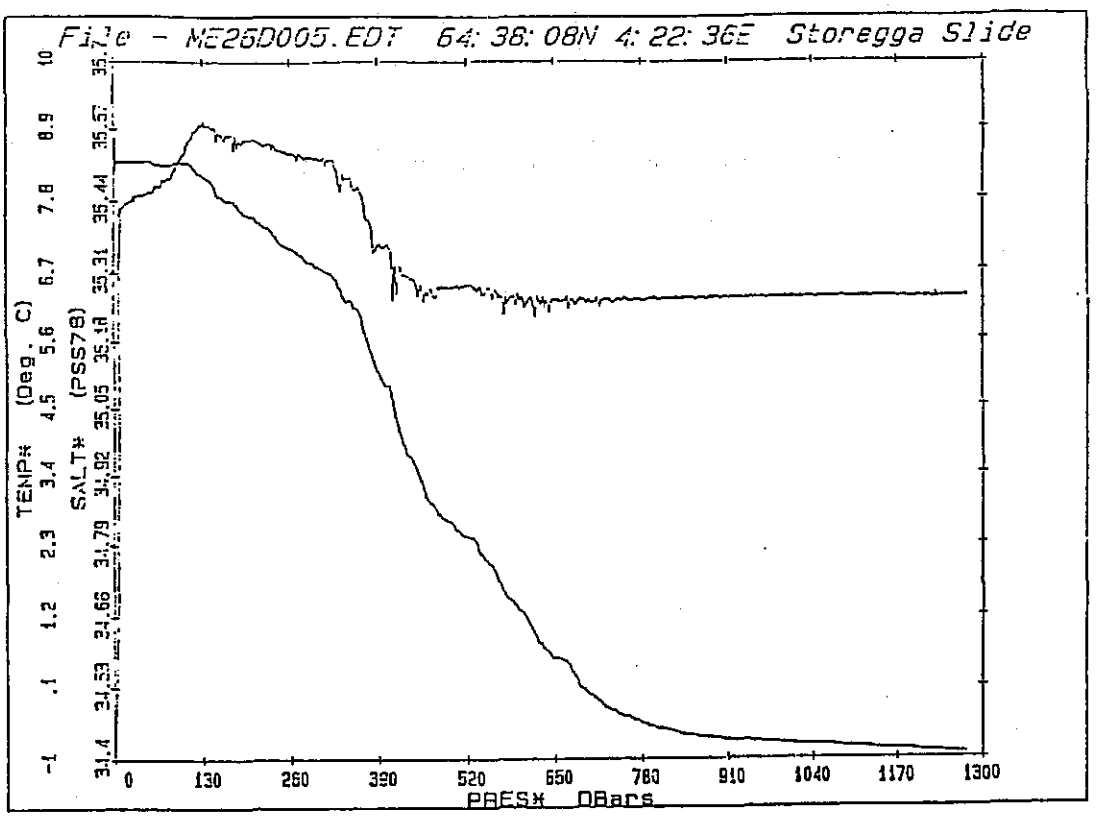

Fig. 8: Vertical distribution of salinity and temperature (raw data) at the Storegga Slide area.

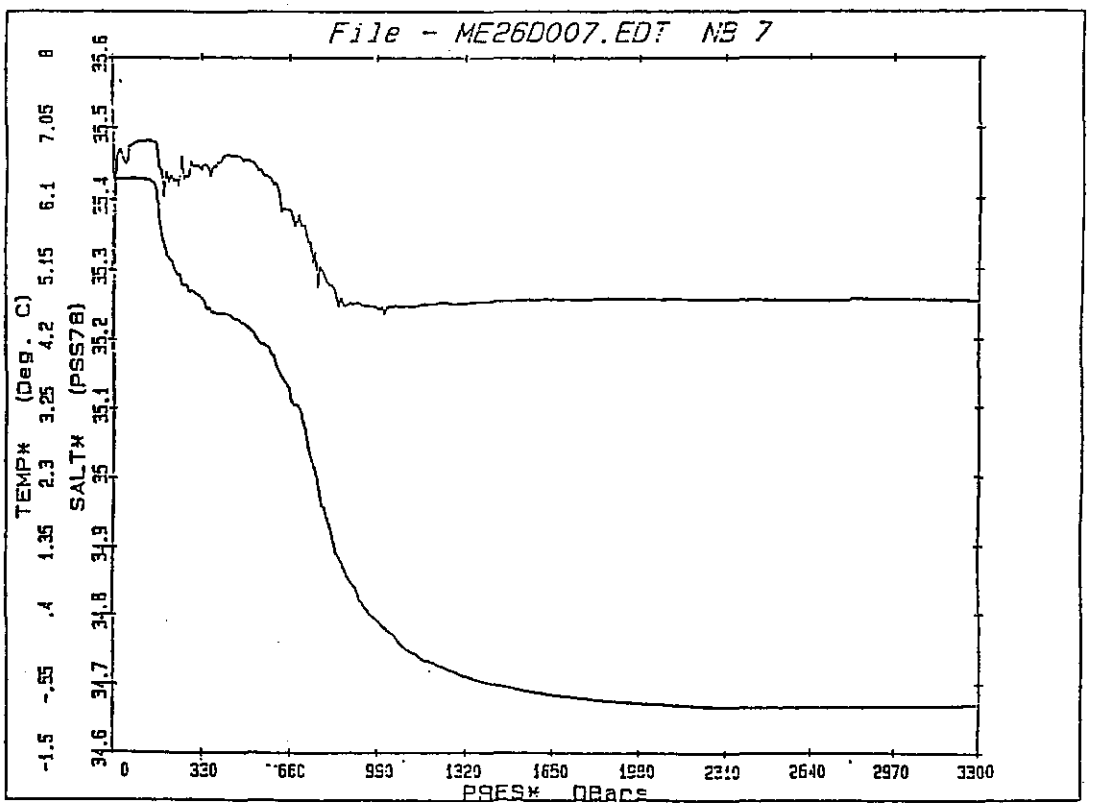

Fig. 9: Vertical distribution of salinity and temperature (raw data)at the mooring position in the Norwegian Basin

5.1.5 Hydrographical Parameters in the East Greenland Current

(H. Beese, E. Bauerfeind)

The vertical profiles of temperature and salinity in the Greenland Basin are charaterized by a shallow thermocline and a low-salinity layer (Fig. 10) influenced by waters of the East-Greenland Current. This layer extends to 80-100 m depth, where a steep gradient in temperature and salinity is present. Below this, a warm layer (1.01°C - 0°C) extends to 300 m, indicating the influence of some warm Atlantic water. Temperature continuously decreases to -1.015 °C down to the sea floor, whereas salinity shows a slight increase. Clearly, the influence of Atlantic water is much less here than in the Norwegian Current and the cold deep water mass better developed.

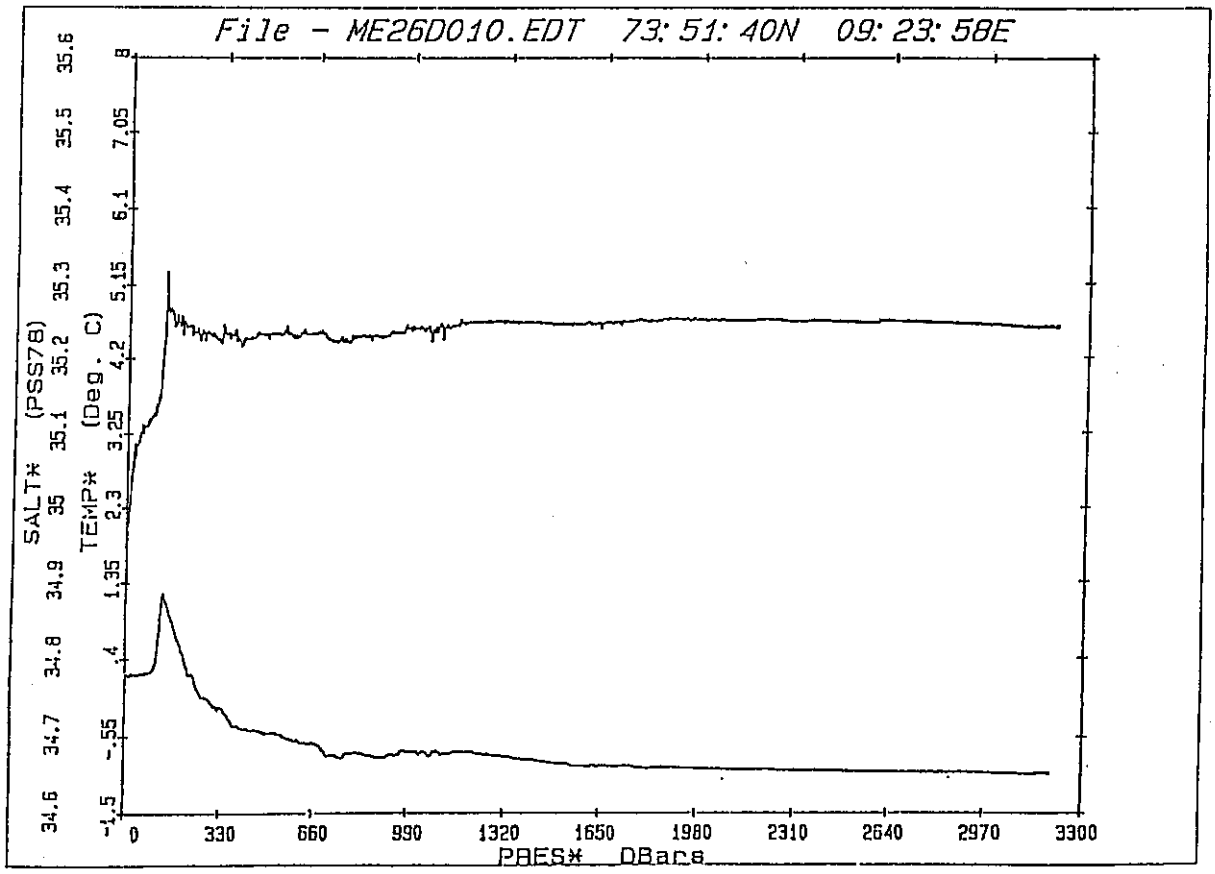

Fig. 10: Vertical distribution of salinity and temperature (raw data) in the Greenland Basin.

5.2 Chemical Oceanography

5.2.1 Nutrients and Dissolved Oxygen in the JGOFS Area (U. Rudat)

Samples for nutrient and oxygen analyses were taken at all stations of M 26/1 throughout the water column from CTD casts. The measurements were restricted to nitrite, nitrate, phosphate and silicate and are performed on board by means of an autoanalyser system. Oxygen was determined by the Winkler titration method. Nutrients were also determined in all surface water samples taken from the continuous pumping system along the transects from Malta to Edinburgh. The preliminary data are shown in the following Figures 11-18 along with the CTD data.

5.2.2 Nutrients and Dissolved Oxygen in the Northern North Atlantic (E. Suess)

Nutrient and oxygen analyses were performed on about 200 samples from 18 stations during M 26/2. These data, in conjunction with the salinity and temperature recordings, provide essential background information for several of the projects. This concerns the characterization of water masses, of environmental parameters for planktological studies, of evidence for venting of fluids in near-bottom waters, and the calibration of temperature functions based on foraminiferal assemblages. The data were generated by the nutrient group of the Institut für Meereskunde at Kiel utilizing an autoanlyzer system with flow injection for the nutrients and a manual Winkler titration method for oxygen.

In the Skagerrak the upper water column was low in salinity down to a depth of 40 m, probably indicating the outflowing Baltic Sea water. Below that a stable water mass of almost constant salinities and temperatures was found. The nutrient patterns showed corresponding variations. Characteristic of this pattern was the strong nutricline between the upper and the lower water mass exemplified by nitrate and silicate; i.e. 2-6 μM NO_3 in the surface and > 10 μM NO_3 at depth and 0.2 μM PO_4 in the surface and > 0.6 μM PO_4 at depth. A prominent NO_2-maximum was found at two stations believed to be influenced by venting of fluid from the seafloor. In one case, Sta. 463, NO_3 and PO_4 decreased correspondingly in the near-bottom layer as did the oxygen content. At the same depth level, about 10 m above the sea floor, very high CH_4 concentrations were found (>1500 nl/L). It is interesting to speculate whether these patterns reflect increased benthic consumption, i.e. denitrification triggered by the CH_4-supply or dilution by exiting fluids.

Three water masses were identified flowing through the Faeroe- Shetland Channel. The deepest one, between about 600-1100 m, showed constant salinity and temperatures. However, in the prominent depression at the channel floor the nutrient structure did not correspond to that of the adjacent water mass. Silica and nitrate decreased significantly inside

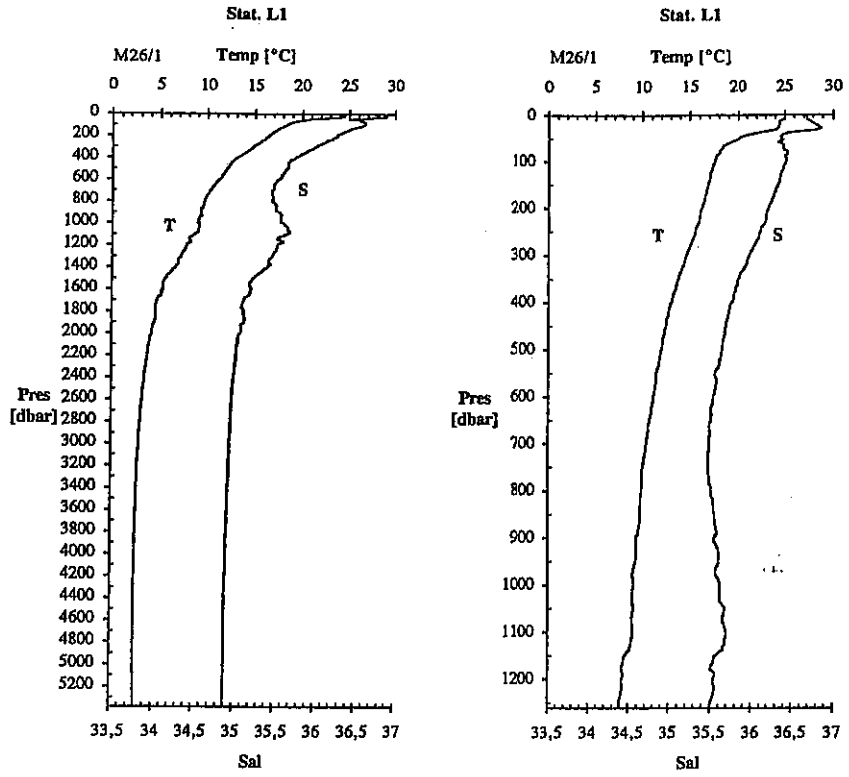

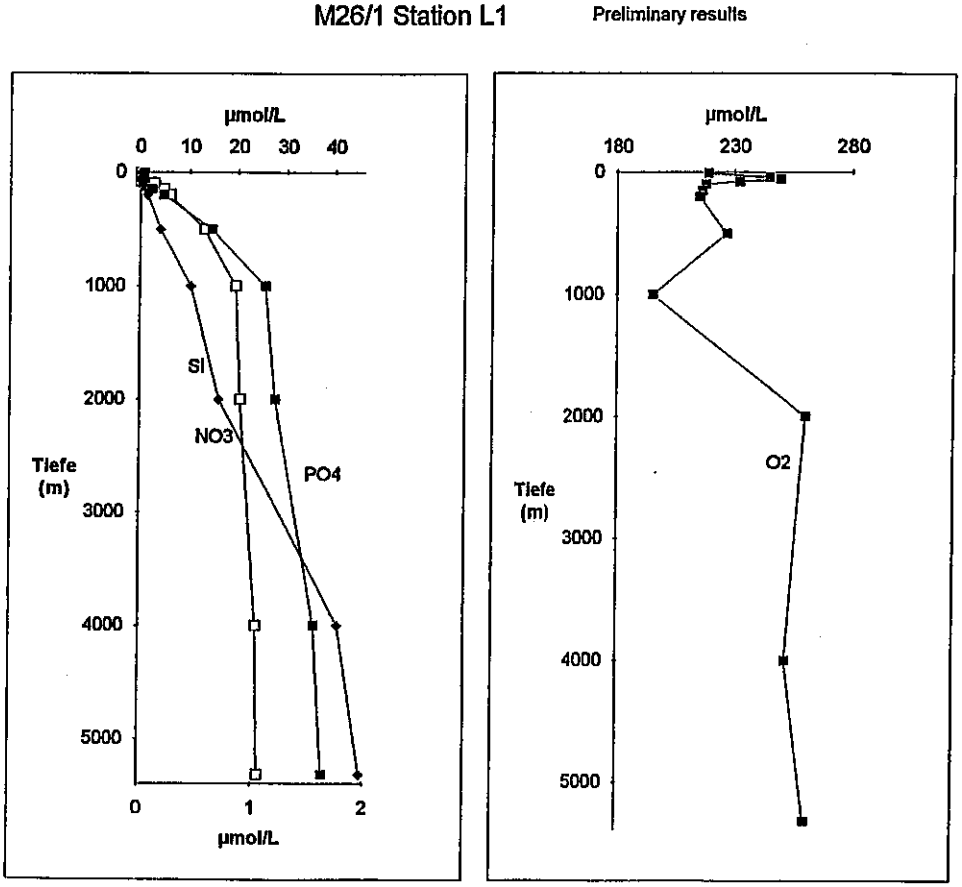

Fig. 11: Vertical profile of salinity and temperature, nutrients and dissolved oxygen (raw data) at station L1.

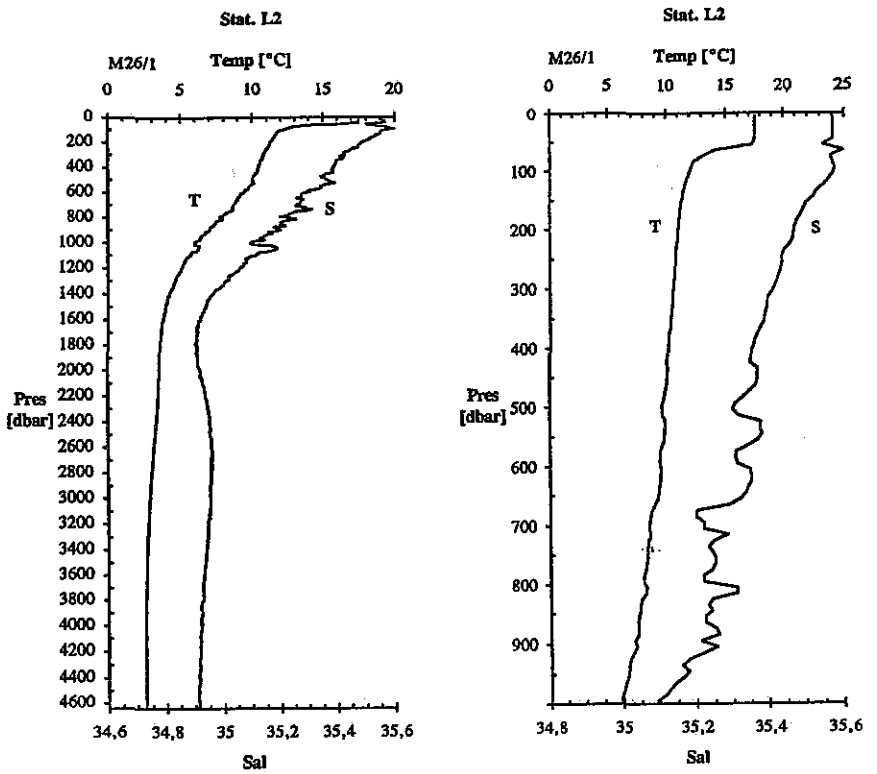

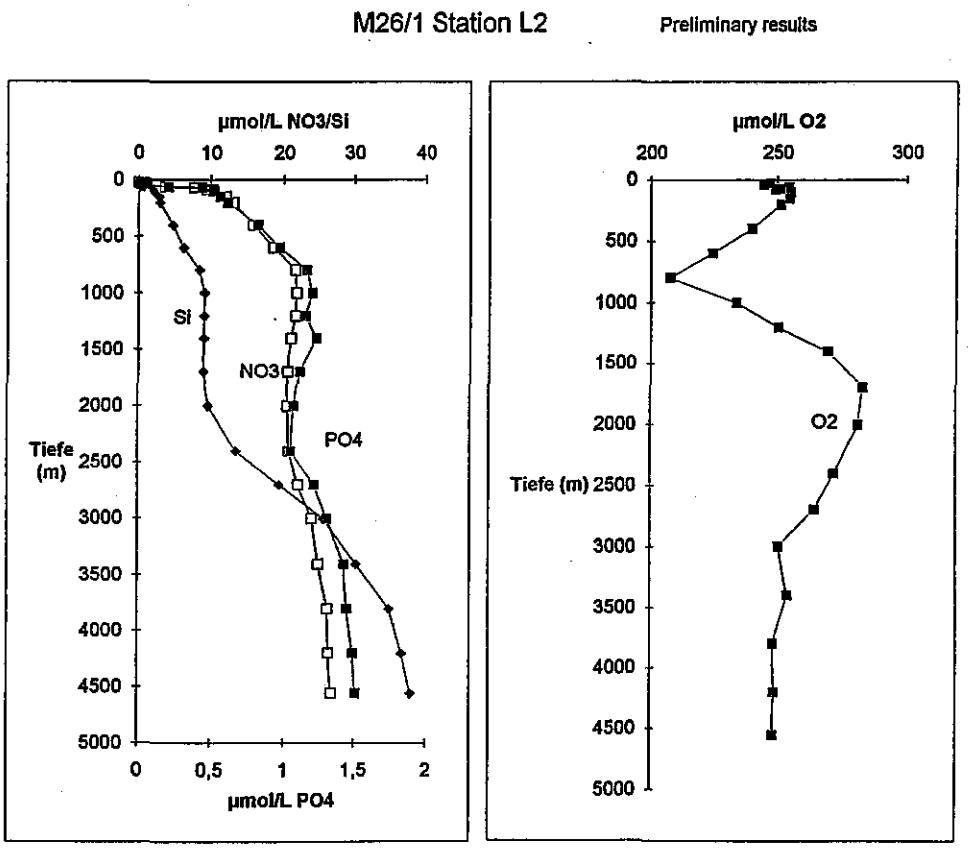

Fig. 12: Vertical profile of salinity and temperature, nutrients and dissolved oxygen (raw data) at station L2.

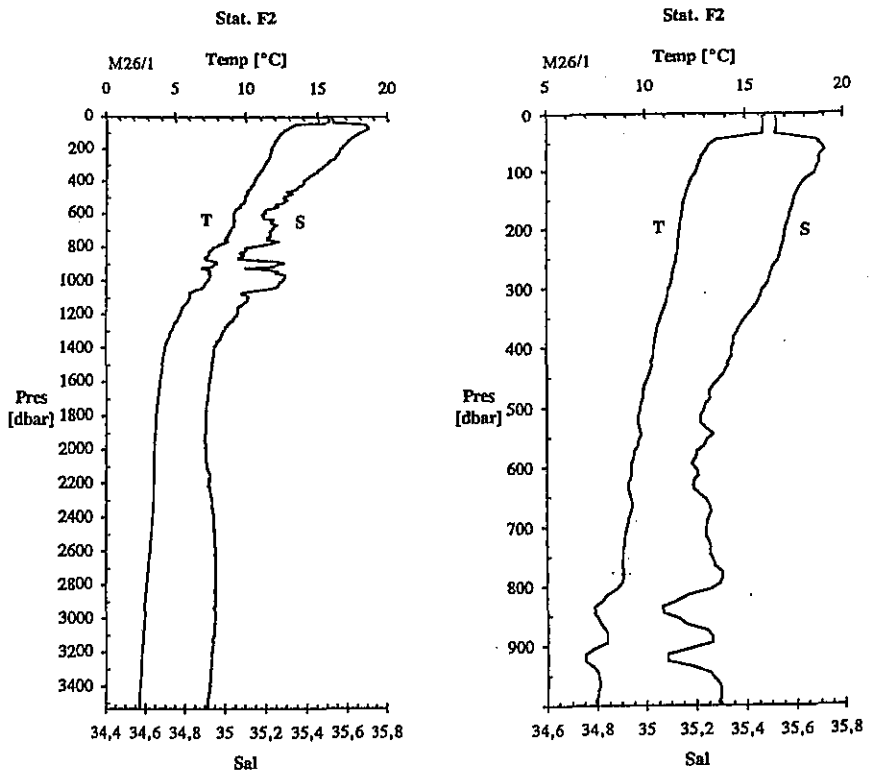

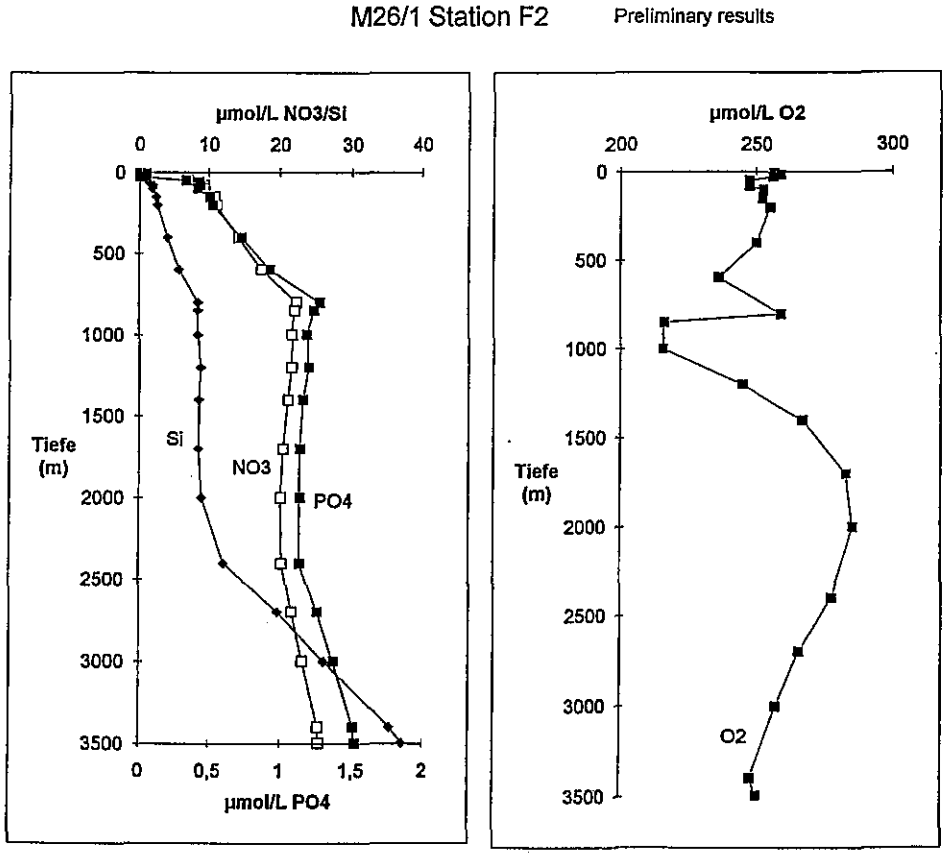

Fig. 13: Vertical profile of salinity and temperature, nutrients and dissolved oxygen (raw data) at station F2.

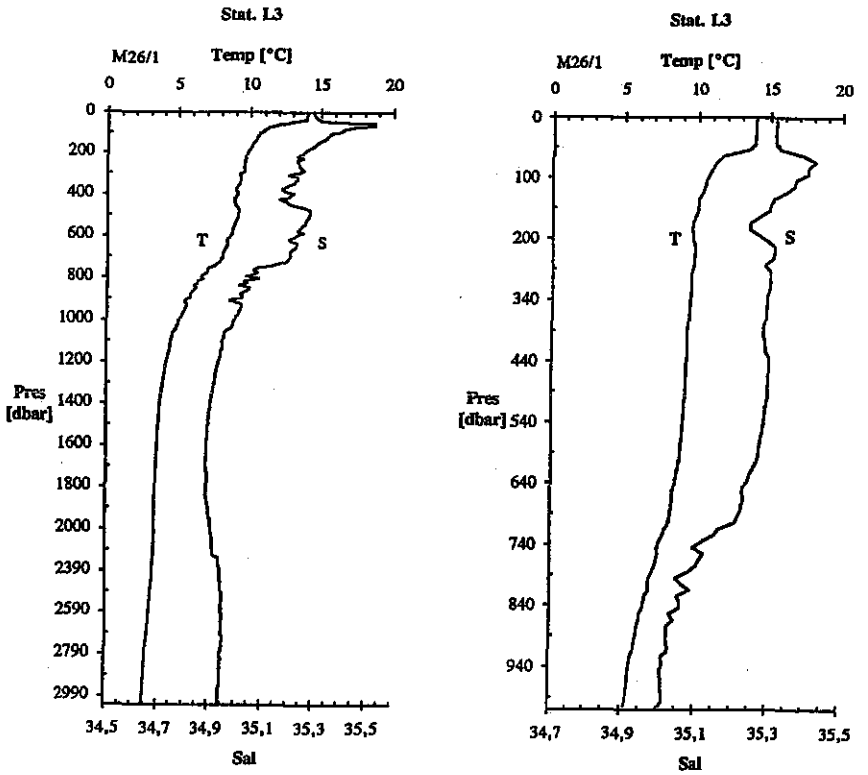

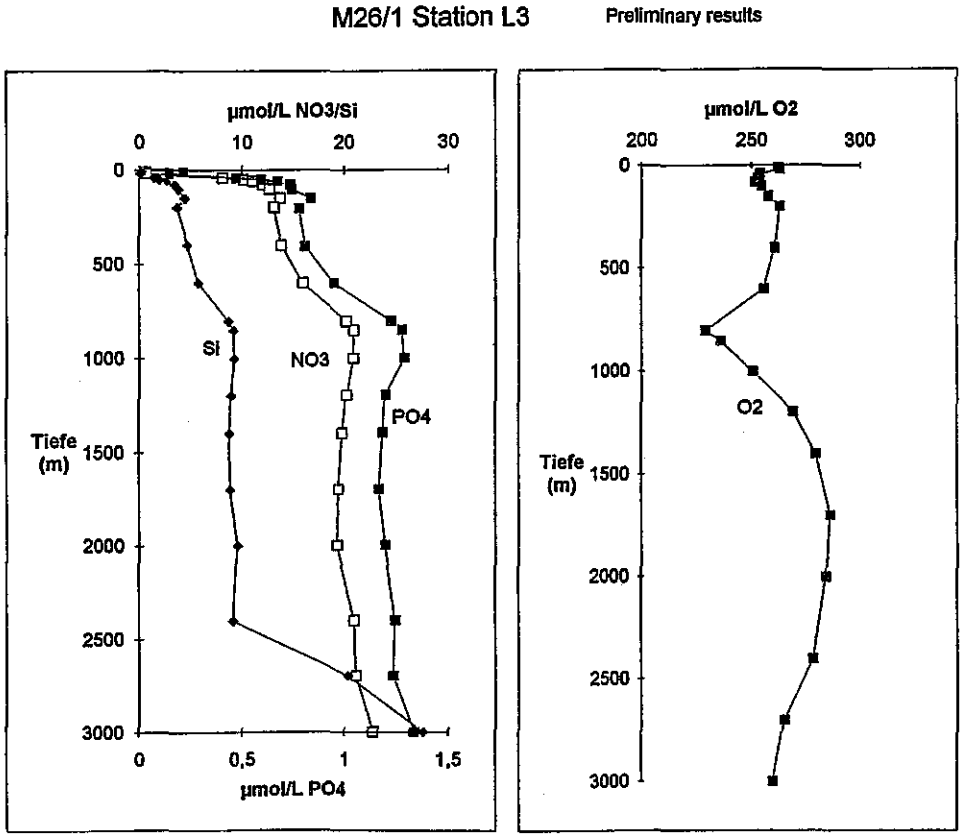

Fig. 14: Vertical profile of salinity and temperature, nutrients and dissolved oxygen (raw data) at station L3.

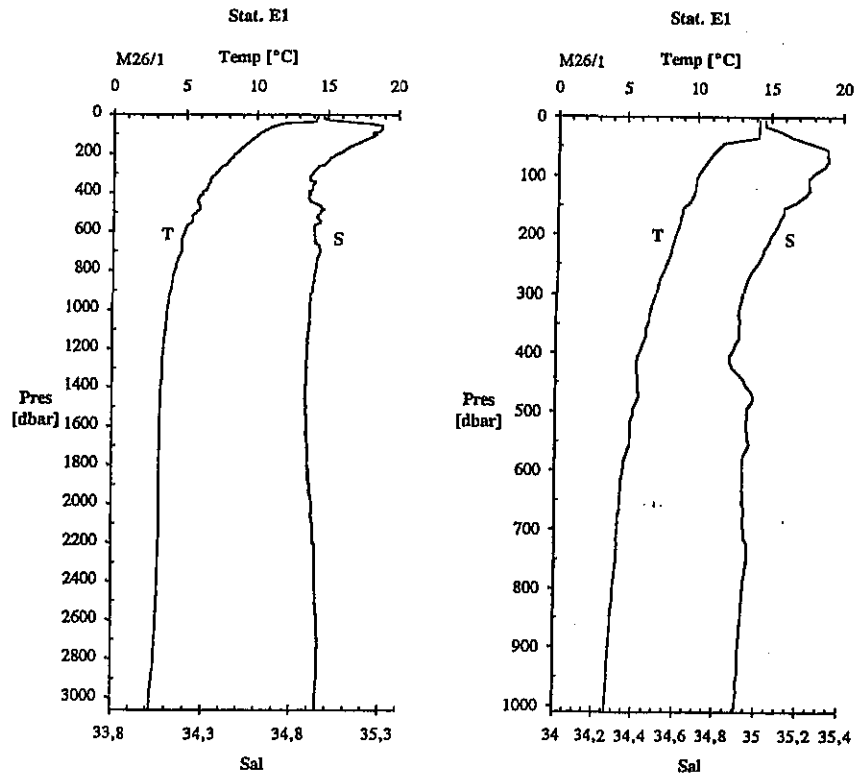

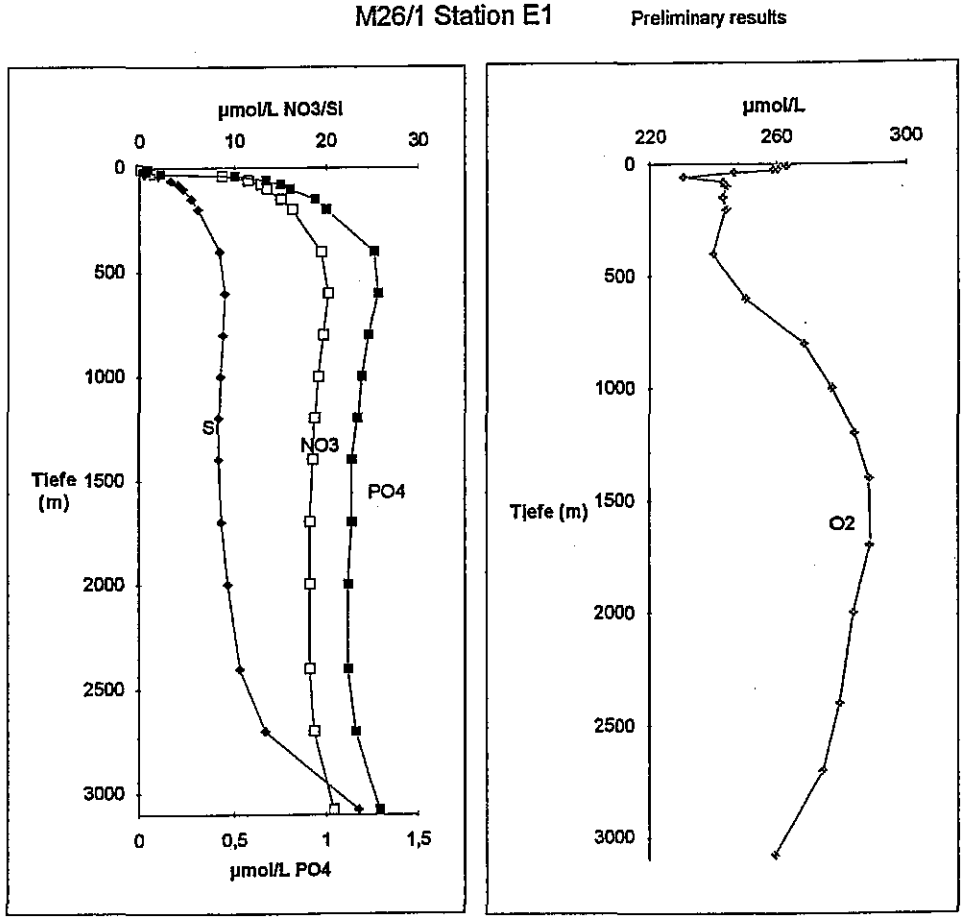

Fig. 15: Vertical profile of salinity and temperature, nutrients and dissolved oxygen (raw data) at station E1.

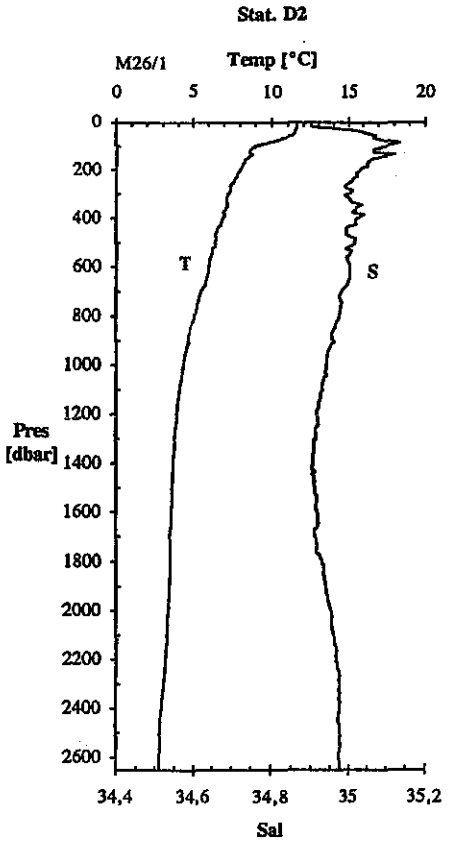

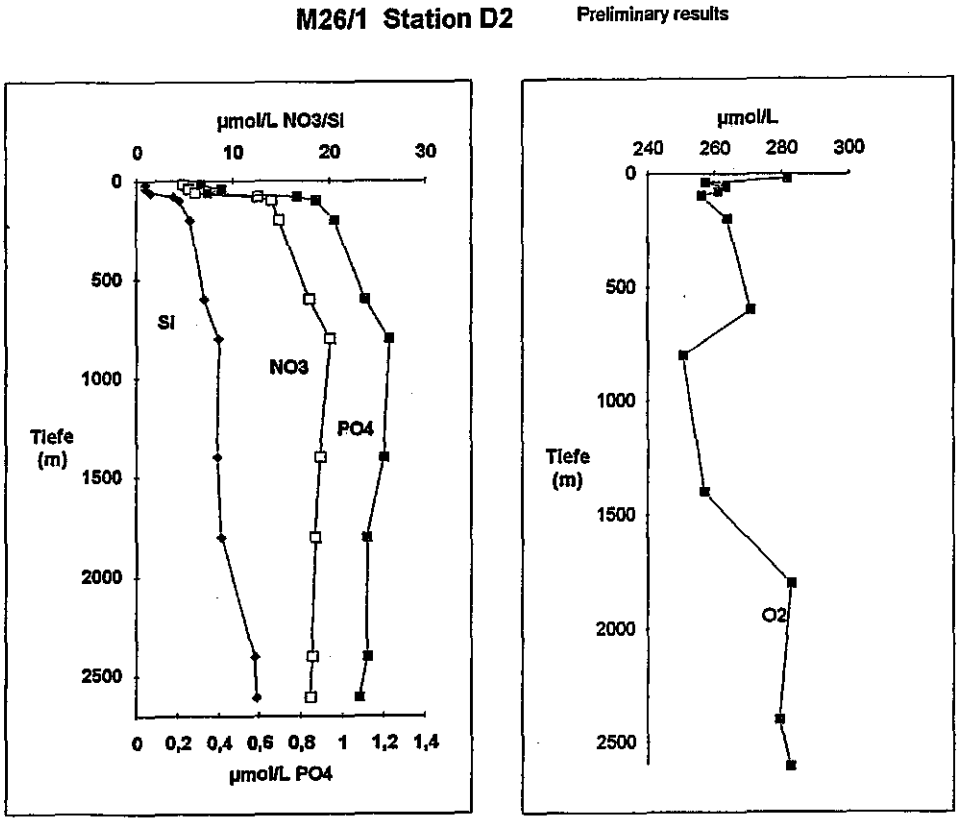

Fig. 16: Vertical profile of salinity and temperature, nutrients and dissolved oxygen (raw data) at station D2.

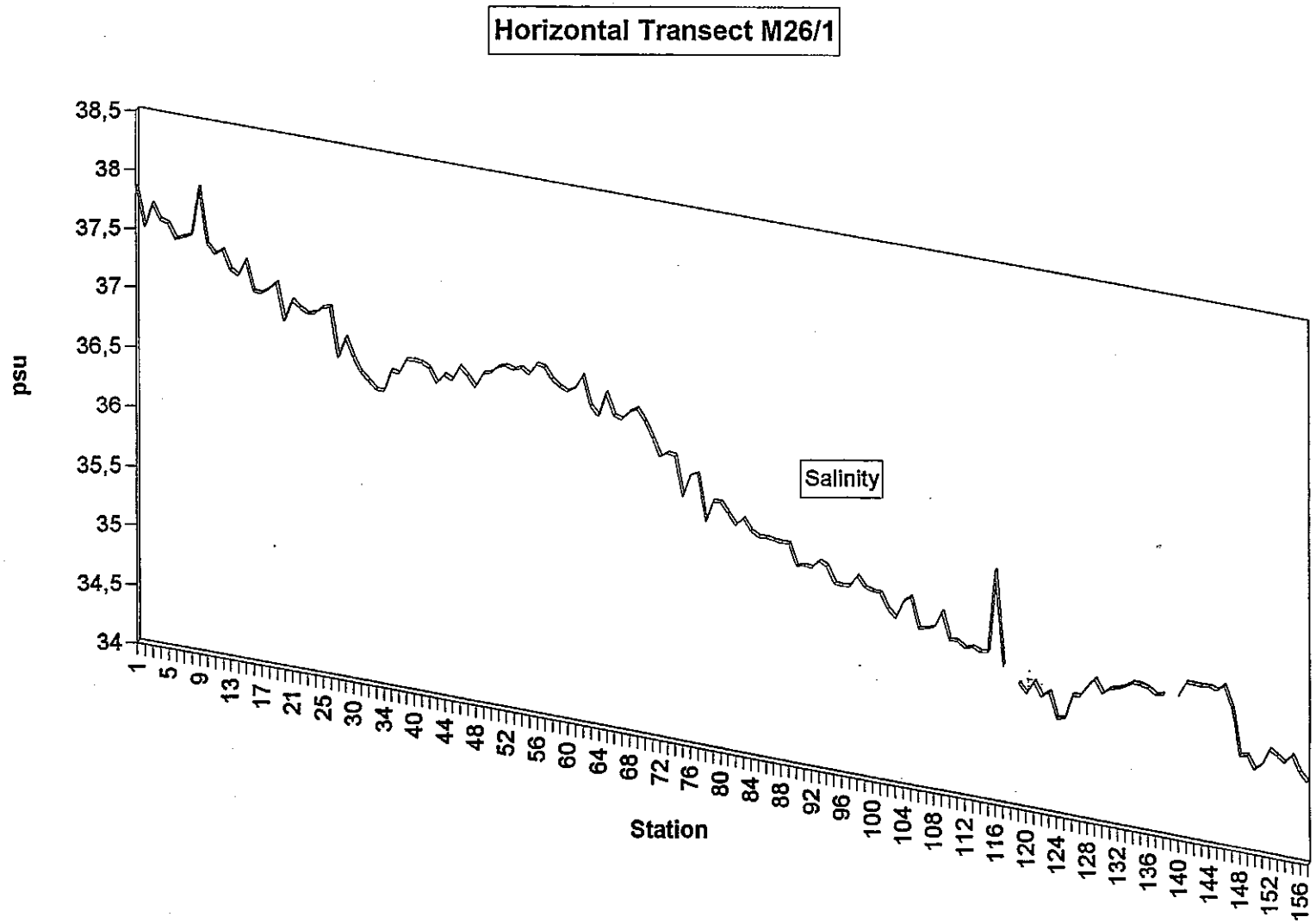

Fig. 17: Horizontal profile of salinity from surface water samples taken from the continuous pumping system along the transects from Malta to Edinburgh (for geographical positions of the stations see 7.1.2).

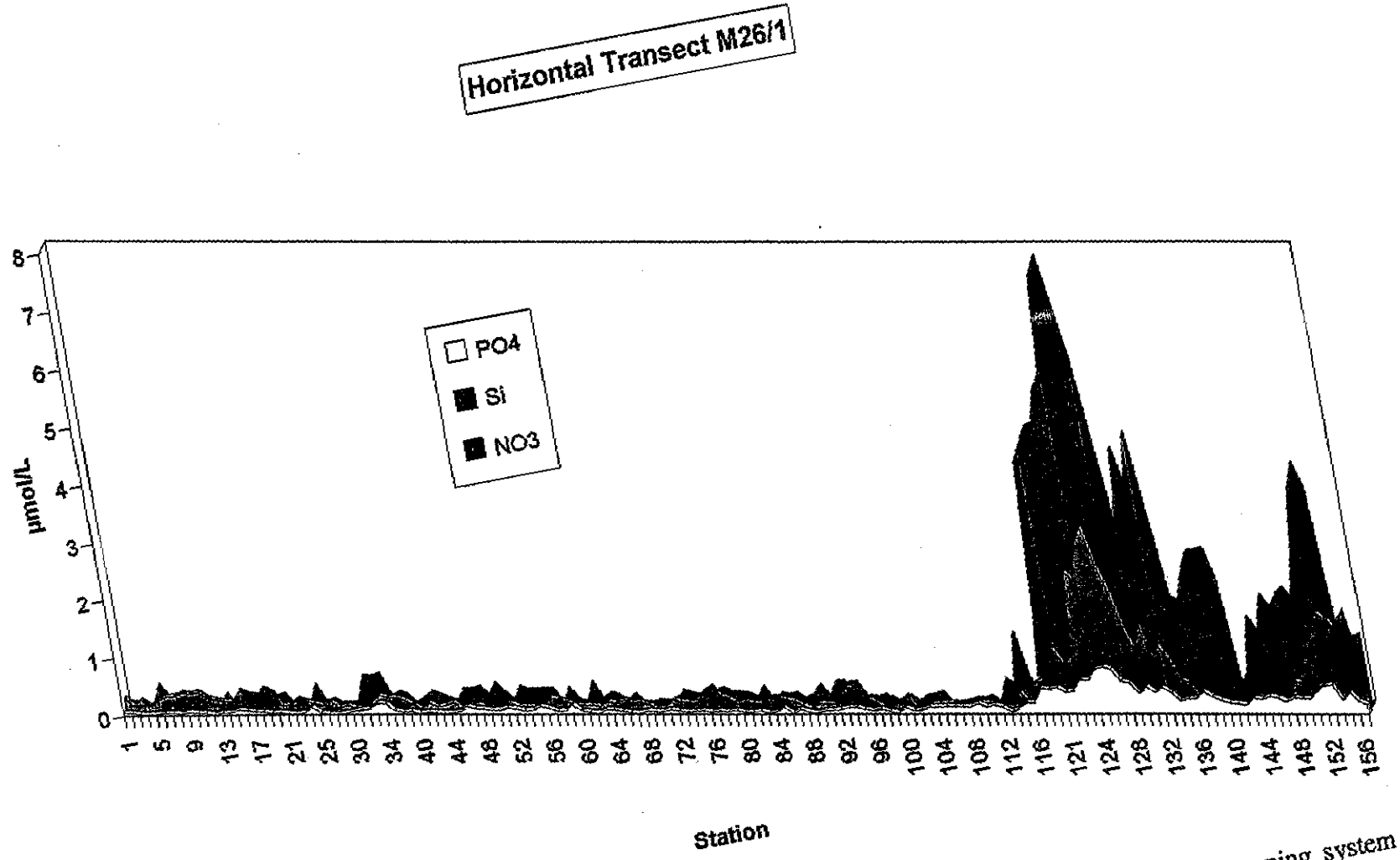

Fig. 18: Horizontal profile of nutrients from surface water samples taken from the continuous pumping system along the transects from Malta to Edinburgh (for geographical positions of the stations see 7.1.2).

the depression whereas outside they were high. Since no methane anomaly was detected anywhere near this area, which would indicate an active seep, the reason for the nutrient distribution remains unclear.

Four deep stations were sampled across the Norwegian Current to determine O_2, S, T, and nutrients as environmental parameters in conjunction with plankton net sampling, sediment trap fluxes and benthic and pelagic microfauna. The stations combine for a meridional transect spanning 1200 nm from 63°N to 75°N. The stations are located on the eastern flank of the Island-Faeroe Ridge, the Aegir Ridge, the deepest part of the Norwegian Basin and the Barents Sea slope. High nutrient and oxygen contents characterized the deep water with silica accumulating from N to S. The Barents Sea slope station was located above suspected methane seepage and showed, as in the shallow waters of the Skagerrak, significant NO_2 increase and concomitant decrease of NO_3 and PO_4 just above the sea floor. It remains to be seen, whether or not these patterns are in any way related to venting activities.

Six shelf stations in and around the Barents Sea crater field showed a coherent nutrients pattern identifying a well-mixed surface layer (80 m), a transitional water mass (80-300 m) and a bottom layer (> 300 m). The entire water column is well oxygenated. The surface layer at the northernmost site (M 499) is influenced by melt water which dilutes the nutrient and salt contents. The intermediate and bottom layers are well-defined high salinity waters separated by a strong nutricline. The bottom water shows high and constant silica contents and is enriched in methane.

5.2.3 Trace Elements in the JGOFS Area (U. Schüßler, P. Streu, G. Lippert)

The formation of particulate trace elements in the surface layer is an important process controlling cycling in the ocean. Particles in the euphotic zone are the major source for vertical transport of matter within the water column. These particles are derived predominantly from biological activity. Suspended particulate material (SPM) may eventually be transformed to sinking particles. A large number of chemical elements is adsorbed onto this particulate material, either by passive adsorption or by active biological uptake. The low trace element concentrations in ocean waters are mainly due to removal via sinking particles. The chemical composition of surface SPM has, therefore, a major impact on vertical fluxes of particulate trace elements.

Trace element investigations during M 26/1 focused on the qualitative and quantitative chemical composition of SPM in the surface layers as well as in sinking material. In addition, an intensive sampling schedule on dissolved trace elements in near-surface waters was done. These studies were performed as part of the entitled German JGOFS program "Long-term study on the variability of particulate fluxes in the North Atlantic". This project is a joint

study by three IFMK departments (Planktology, Organic Trace Compound Chemistry, Trace Element Chemistry).

Previous field activities related to particulate fluxes in the water column were extended by depolyments of three sediment trap moorings in different latitudinal zones of the NE Atlantic Ocean (ca. 33°N/22°W, 47°N/20°W, 54°N/21°W). The moorings are equipped with 11 sediment traps and additional current meters, both with mechanic and acoustic detection. Instruments were deployed at depths ranging from 300-4000 m. Prior to deployment, the trap cups were filled with preservative-added seawater under low-contamination conditions. Sampling intervals were 13-29 days each, providing a high temporal resolution. The moorings are to be recovered and replaced in 1994, extending the investigations started in 1992 still further.

In addition to studying vertical trace element fluxes, it is attempted to investigate temporal variabilities in the chemical composition of sinking particles at different depths. These investigations will be carried out in close co-operation with the "Organic Trace Compound" group within the joint JGOFS project.

Surface SPM can be regarded as direct precursor of sinking material. Comparing the elemental composition of SPM with that of sinking material will thus allow conclusions about the processes governing trace element distributions, in particular near the ocean surface. A total of 14 SPM samples from surface waters was obtained by large volume centrifugation using the "Kiel Pumping System" while the ship was underway. The SPM samples were extracted from each 12-25 m^3 of seawater (sampling depth ca. 7 m), resulting in relatively large amounts of material; thus enabling different chemical analyses to be made on identical samples. The M 26/1 cruise extends our seasonal coverage to include early autumn samples.

Throughout the cruise, samples for dissolved trace elements were collected also using the "Kiel Pumping System" (a total of 157 samples at about 30 nm intervals). These samples will give more detailed insight into the regional distributions of some poorly studied dissolved trace elements (e.g. cobalt and lead). In combination with particulate trace element data, it will be possible to determine trace element distribution coefficients in surface waters, relying on samples obtained under identical and low-contamination conditions. Trace elements of particulate and dissolved matter were sampled throughout this leg, giving rise to a approx. 5000 nm of surface section along the entire track. All trace element samples will be processed onshore in an clean laboratory environment. Other parameters were sampled at the same frequency (nutrients, salinity, chlorophyll, POC/PON) to supplement this data set. Analyses and data interpretation will be performed in co-operation with the hydrographic and the planktological groups.

5.2.4 Organic Tracers

5.2.4.1 Organic Acids in the JGOFS Area (Ch. Osterroht)

Dissolved organic acids were extracted from sea water by a proven and previously used method. Sea water pumped aboard by the continuous "Kiel Pumping System" (KPS) is acidified to pH 2,5 with HCl. By this step all acidic substances are rendered to their protonated form and made more hydrophobic. The acidified sea water is filtered through glass fiber filter and then drawn through adsorption columns filled with silanised silica gel. The sorbed material is reextracted with acetonitrile and methanol/0.2N molar ammonia solution. The combined organic extracts are stored deep frozen and worked up in the laboratory. The samples taken while the ship is under way were integrated over a known distance depending on pump rate and exhaustion of the adsorption columns. The following samples were taken: Two on the way through the western Mediterranean (165 l and 236 l), one along the Moroccan coast on the way to station M2 (256L), one on the way west to the Madeira Rise, to about 20°W (283 l), two on the way north along longitude 20°W over the Madeira Rise and the Iberian Abyssal Plain (245 l and 213 l), two on the further way north over the Porcupine Abyssal Plain to the Celtic shelf (187 l and 265 l), four on the way NW to about 58°N/ 31°W (215 l, 243 l, 268 l and 154 l), and the last two on the way east over the Island Basin to the Hebrides shelf (213 l and 233 l). By that approach 14 samples were taken extracting 3176 l of sea water. Compared to the Baltic Sea, the content of particulate and dissolved organic material is considerable lower in the Mediterranean Sea and the Atlantic Ocean, so that exhaustion or overloading, of the columns as well as a clogging of the filter never occured. The extract yields will be worked up in the laboratory.

5.2.4.2 Amino Acids in the JGOFS Area (U. Lundgreen)

Samples were collected for data on the variability of amino acid concentration and composition with respect to different latitudinal zones of the Atlantic. With the simultaneous analysis of sediment and overlying water samples, information on transport processes across the sediment-water boundary layer should be attainable.

The Kiel-sediment-traps are suitable for chemical analysis of constituents and organic trace the particulate matter. For this purpose, the sediment traps were cleaned thoroughly before the cruise. On board, the trap's sampling bottles were filled with *in situ* water in a cleanbench and fitted to the rotatory sample holder immediately after filling and only a few hours before deployment, thus avoiding sample-contamination from the ship's deck. Every technical device to deploy was equipped with new batteries and finally checked before deployment.

In parallel to the mooring deployment, water samples were taken for analysis of the amino acid composition. Water was sampled from the upper ocean mixed layer (about 7 m depth)

with the "Kiel Pumping System" (KPS), which provides continuous clean sampling during ship's movement. The distance between two sampling sites was about 60 nautical miles, a total of 78 water samples were taken in this manner. In addition, the water column was sampled vertically with a CTD-rosette on 7 locations and water and sediment samples were obtained from multicorer sampling tubes on 3 of these locations.

Each water sample was filtered through a 0.4 m polycarbonate membrane filter under light pressure (300 mbar) of nitrogen gas. The filter and one part of the filtrate were stored deep-frozen at -20°C, the other part of the filtrate was hydrolyzed with 0.1 molar HCl at 110°C for 24 hours and then stored at room temperature. The samples will be analyzed at the shore-based laboratory by a HPLC-technique following a standard procedure previously described by MINTROP (1990) and WENCK et al., 1991. In this way, dissolved free amino acids, dissolved combined amino acids and particulate amino acids can be determined.

5.2.5 **Biomarker in the Northern North Atlantic** (J. Maaßen, C. Willamowski)

The chemical composition of particulate organic matter (POM) in the water column and the organic material in the surface sediments are important for the determination of the transport rates, alteration processes, possible sources and transport processes. Biomarkers are good tools for monitoring the composition and the processes, as they keep structural information about their possible sources. These markers might be a key for an understanding the complex system at the water/sediment interface. Besides vertical input through the water column, which is correlated to biogenic particles of different size and composition, lateral advection and resuspension processes play a mayor role in the near bottom water column.

In order to charaterize these processes, special classes of biomarkers (i.e. alkanes, isoprenoids) were analyzed on board and samples were collected for the analysis on land of anthropogenic tracers. During leg M 26/2 five stations were sampled for suspended matter in the water column with two deep sea *in situ* pumps or, alternativly, with a 400-l stainless steel water sampler or the CTD-rosette samplers. POM was obtained by filtering the water through GF/F glas/fiber/filters *in situ* or on board. Sediment samples from the upper 10 cm were obtained from the multicorer or the boxcorer on five stations. After cutting the cores into 1-2 cm slides, water was removed from the sediment by ultra-centrifugation.

In order to complete the investigations of transport processes in the water column at the high accumulation area at the Barents Sea slope, stations 480 and 481 were sampled close to the bottom and in the surface waters. The samples will be used for the analysis of biogenic compounds of different sources. Additionally, surface water samples of the upper 10 m to 200 m were obtained at the Sta. 467-2 in the Skagerrak, Sta. 473-1 in the Faeroe-Shetland Channel and at Sta. 478-5 at the Lofoten Basin for intercomparison. The station in the

Lofoten Basin is the site of a long-term sediment trap mooring of the SFB 313. It will be continued through 1996.

Surface sediment samples of the upper 10 cm were obtained at the same stations except at Sta. 481, where no cores were recovered. Instead one sediment sample was obtained from the Barents Sea shelf at Sta. 492-8 from within a crater. The labile organic material, the biomarker samples were processed direct after recovery for chemical analysis. After extraction with organic solvents different classes of compounds were separated by column chromatography. These classes were identified and quantified by gaschromatography using a flame ionisation detector (GC-FID). Further processing and other analysis using GC-MS and Multi-GC)will be done at the SFB 313/IfMK.

The chromatograms of the alkane/isoprenoid fraction of the suspended material in the different working areas show a broad variety of compounds according to different sources. The alkane concentrations decrease sharply with depth within the first 200 m and change their composition. The alkane-distributions at the high accumulation area at the Barents Sea slope both in the water column and the surface sediments compare well with those obtained from the sediment trap mooring BI-2 in 1991 and the underlying sediments. In the bottom water we found signs a for strong lateral advection of old resuspended sedimentary material. Several compounds showed with strong concentration gradients near the bottom, which may be good biological indicators for this advection process. The mass-spectrometric analysis of this markers will be done at the SFB 313/IfMK. Further processing of the data and comparison with the informations of previous cruises to this working area may give informations about possible sources of the transported material.

5.2.6 Marine Optics on Dissolved Organic Matter in the JGOFS Area

(R. Heuermann, K.D. Loquay)

Optical measurements were performed on dissolved and particular organic substances by using fluorescence techniques. Prominent examples for this substances are yellow (humic) substances as a major compound of the marine DOM, chlorophyll and other phytoplankton pigments like phycoerythrin, fucoxanthin and phycocyanin, and the aromatic amino acid tryptophan bound to proteins. For these measurements a newly developed multiwavelength *in situ* fluorometer was used (Table 8). Connected to the "Kieler Pumping System", a continuous recording of the surface layer was thus obtained for the whole cruise. To verify the data collected with this new device, samples were also taken every 30 sm and analyzed with a standard laboratory spectrofluorometer. Samples taken with the rosette sampler at depths were processed with this instrument as well. From the large number of excitation and emission spectra (Tables 6 and 7) obtained with the laboratory fluorometer only the chlorophyll fluorescence data have been processed so far. Near-surface profiles of

Tab. 6: Excitation spectra measured with the laboratory fluorometer

excitation spectra measured with the laboratory fluorometer			
emission / nm	excitation / nm	identificable substances	peak wavelength of identificable substance
340	210 - 320	tryptophan	230, 270
420	210 - 400	yellow substance	
590	400 - 560	phycoerythrin	
630	400 - 600	phycocyanin	
680	400 - 670	chlorophyll	400..460

Tab. 7: Emission spectra measured with the laboratory fluorometer

emission spectra measured with the laboratory fluorometer			
excitation / nm	emission / nm	identificable substances	peak wavelength of identificable substance
230	240 - 420	tyrosin tryptophan yellow substance	290..300 325..350 410..460
270	280 - 500	tryptophan yellow substance	325..350 410..460
308	315 - 500 450 - 730	yellow substance chlorophyll	410..460 685
355	370 - 500 450 - 730	yellow substance chlorophyll	410..460 685
420	440 - 750	yellow substance phycoerythrin chlorophyll	520..560 580..600 685
530	570 - 750	phycocyanin xantophylle (fucoxanthin, ..)	620..640 680

Tab. 8: Excitation/emission wavelengths of the *in situ* fluorometer

excitation / emission wavelengths of the in situ fluorometer			
excitation / nm	emission / nm	identificable substances	(-) not yet available during M26/1
270	300 340 450	water Raman scatter tryptophan yellow substance	
420	490 550 590 680	water Raman scatter yellow substance phycoerythrin chlorophyll	- -
530	630 680	phycocyanin xantophylle	- -

chlorophyll, yellow substance and tryptophan measured with the *in situ* fluorometer in the Strait of Gibraltar are presented as well.

Fluorescence close to the surface

In the "blue" Mediterranean water the fluorescence signals of chlorophyll are close to zero for recordings with both instruments. Near the Straits of Gibraltar the signals increase markedly. The gradients of chlorophyll in this region are clearly recognizable in the profile measured with the *in situ* instrument. They are given here as averaged values with a horizontal resolution of 400 m (Fig. 19). The same structure is only poorly resolved in the data of regular surface sampling made at singular stations (Fig. 20). Two maxima are remarkable in both data sets, which seem to be a typical feature in the mixing region of Atlantic and Mediteranean water, as it is also shown in a CZCS image taken in May 1980 (Fig. 19). Yellow substances and tryptophan signals are high in Mediterranean waters (eastern section in Fig. 19). Compared to chlorophyll these signals show a locally similar but on larger scales independent structure in the Straits of Gibraltar.

Chlorophyll fluorescence measured on samples with the laboratory fluorometer are shown in Figure 21 for the S-N transect which includes the JGOFS stations at 20°W longitude. Starting at 40°N the chlorophyll fluorescence increases by a factor of nearly 20 and shows high patchiness. Figure 22 displays the E-W-profile of chlorophyll fluorescence on latitude 59°N with maximum values in the transition region from the deep-sea basin to the shelf.

Depth profiles of chlorophyll fluorescence

Chlorophyll fluorescence and extracted chlorophyll a measured at the main JGOFS stations L1, L2 and L3 are shown in Figure 23 to 25. At the other stations the two methods show similar results. Measurable chlorophyll concentrations are found down to depths of 90 m. The reason for the deviations of both profiles at station L3 between 40 and 90m depth is not clear yet.

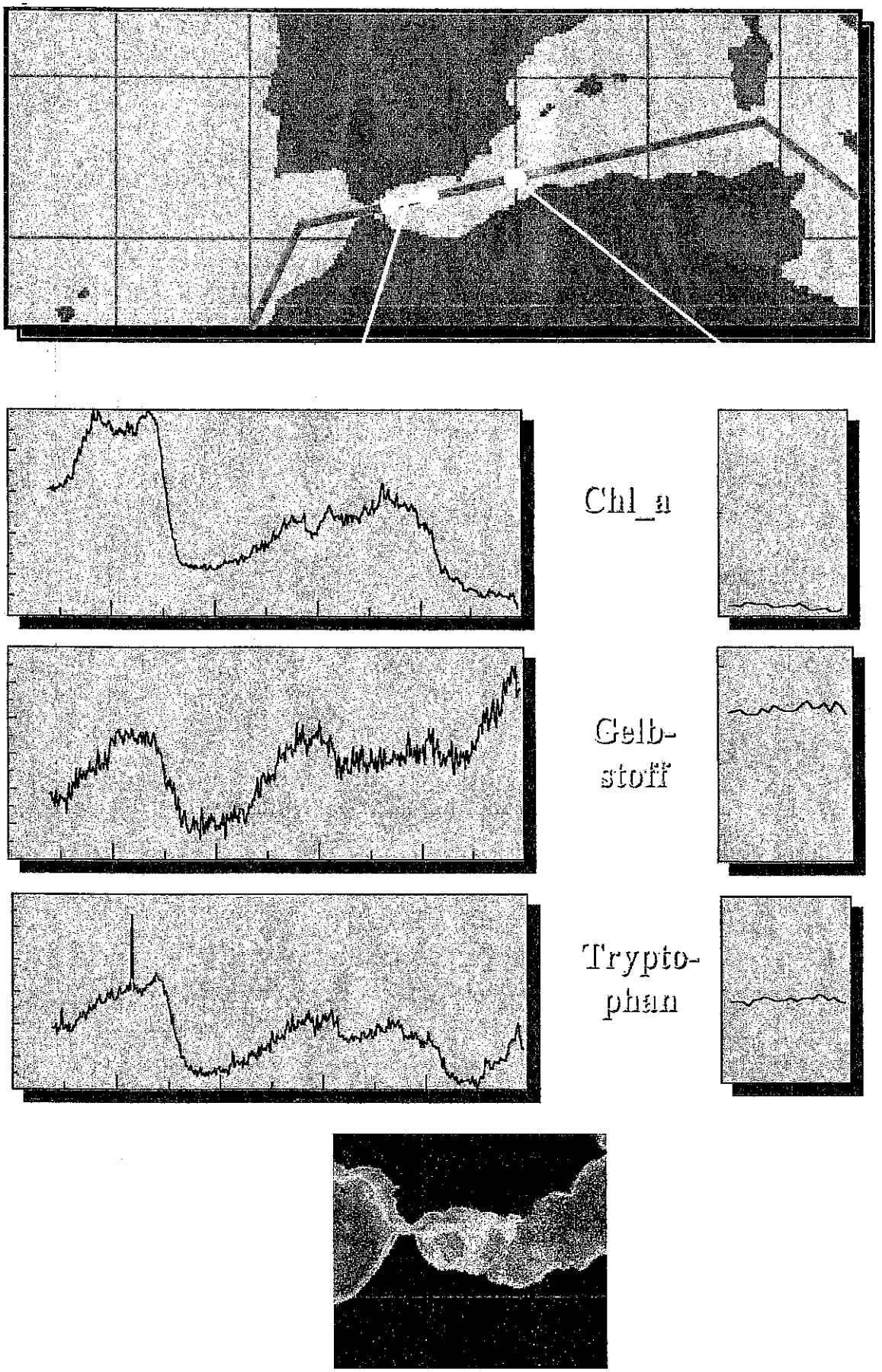

Fig. 19: Chlorophyll, Gelbstoff and Tryptophan distribution in the Strait of Gibraltar.

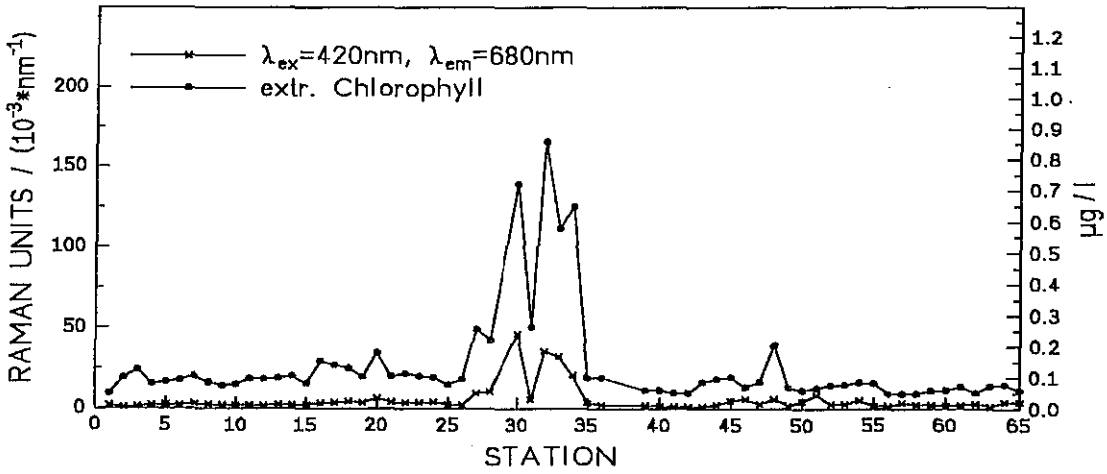

Fig. 20: Chlorophyll distribution on the E-W transect

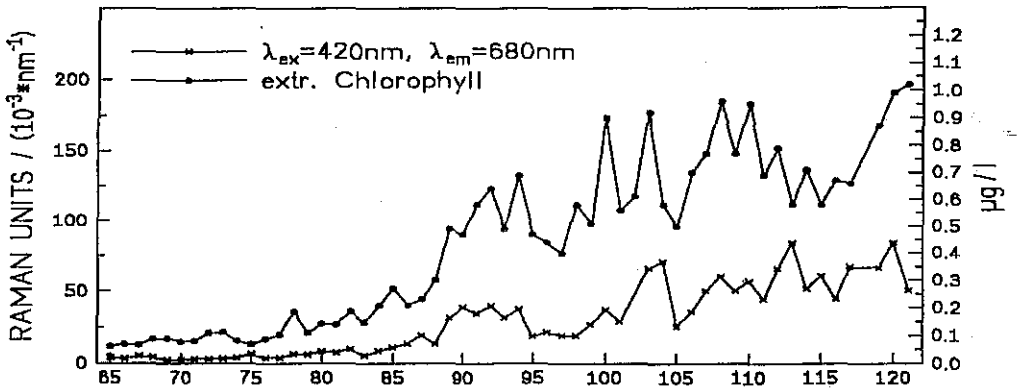

Fig. 21: Chlorophyll distribution on the S-N transect

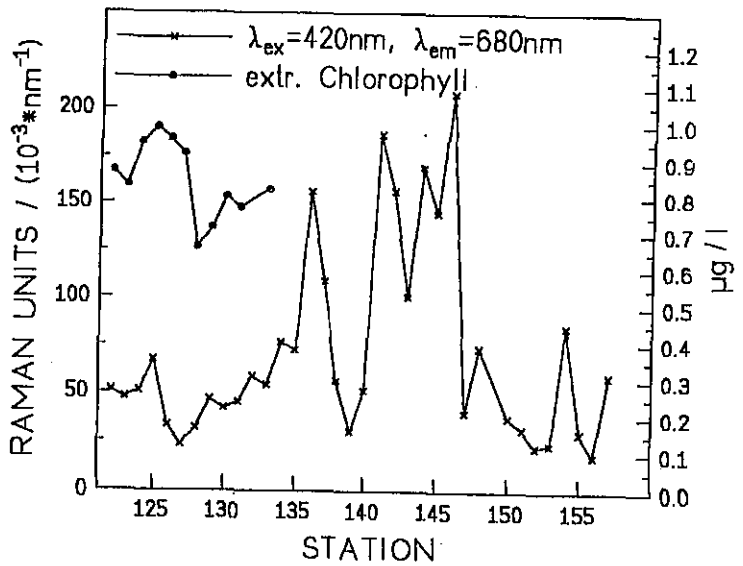

Fig. 22: Chlorophyll distribution on the W-E transect

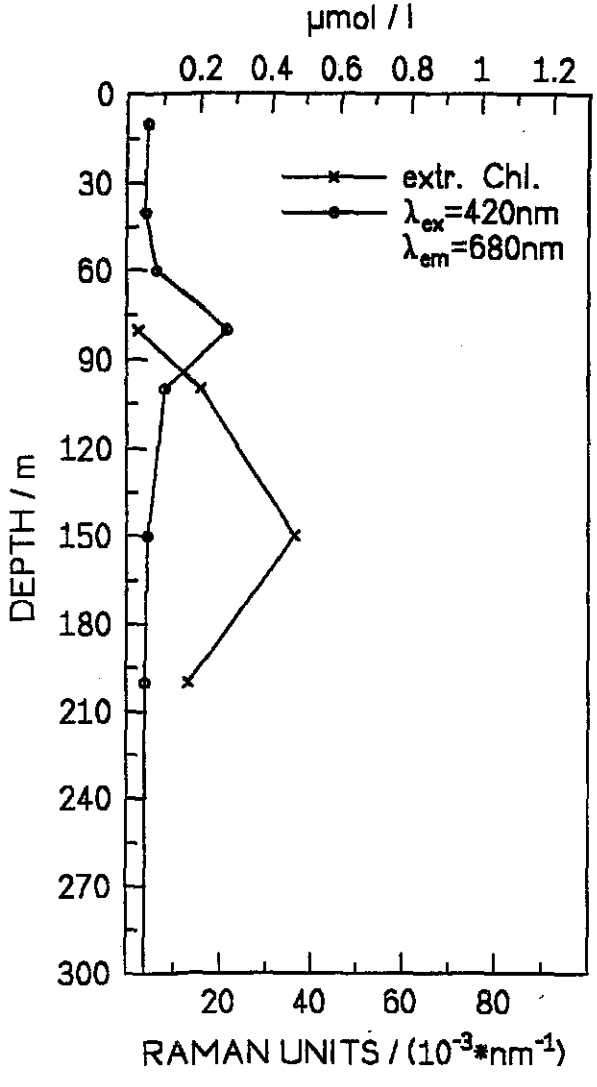

Fig. 23: Depth profile of extracted chlorophyll fluorescence at 680 nm at Sta. L1

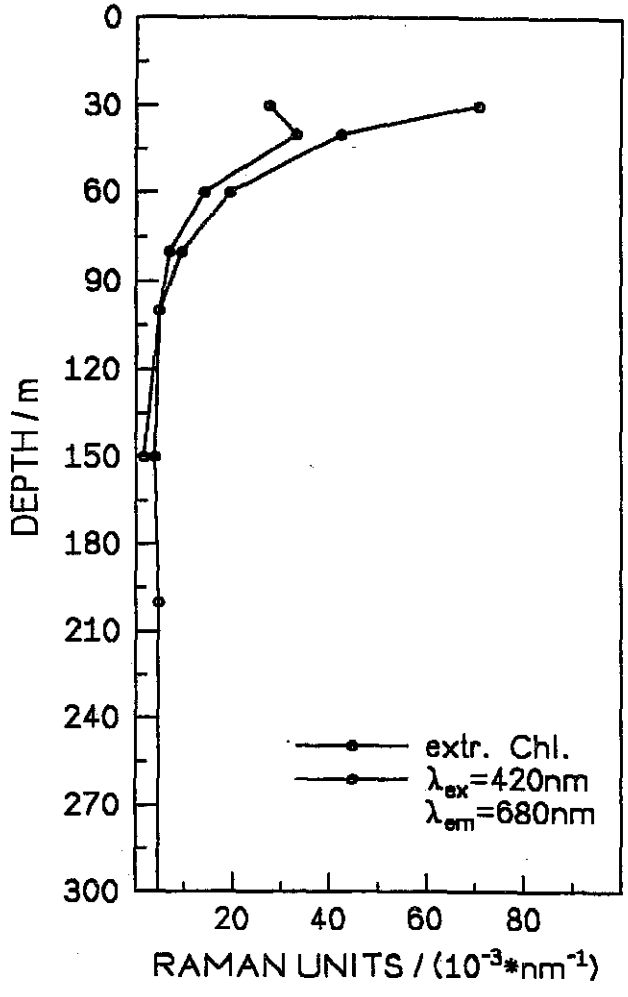

Fig. 24: Depth profile of extracted chlorophyll fluorescence at 680 nm at Sta. L2

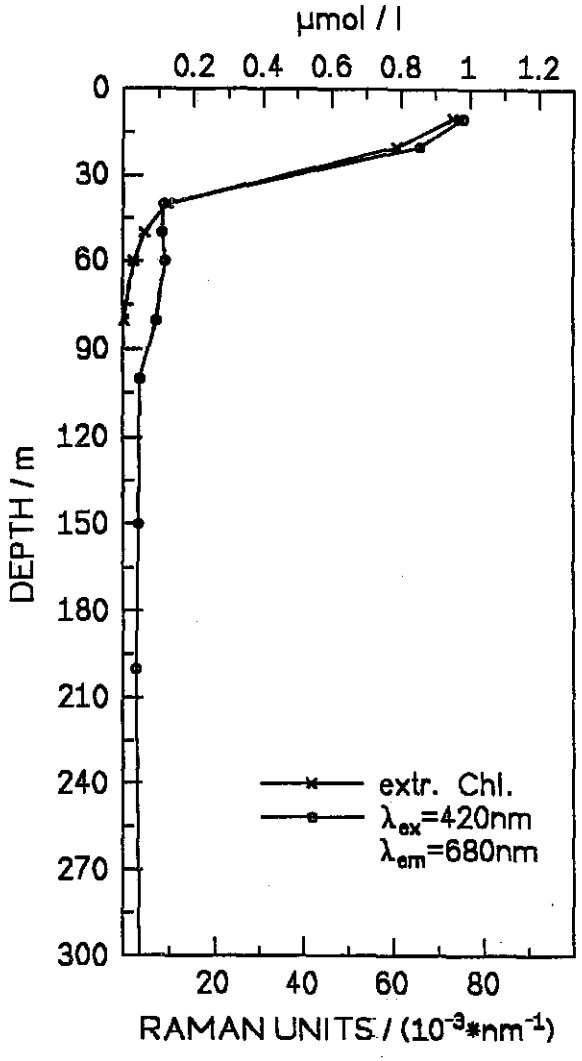

Fig. 25: Depth profile of extracted chlorophyll fluorescence at 680 nm at Sta. L3

5.3 Biological Oceanography

5.3.1 Planktology in the JGOFS Area (M. Deckers)

Planktological investigations were carried out along the transect from Malta to Edinburgh. Activities can be separated into four subjects as follows. (1) Continuous sampling was done in cooperation with the chemical and optical working groups on bord. Surface samples were collected by the "Kiel Pumping System" every 30 nm to determine chlorophyll a content and for C/N analysis. (2) Between 33°N and 54°N along about 20°W the above sampling procedure was extended. Additional samples were taken for particulate silicate, high performance liquid chromatography of plant pigments, and microscopical analysis. This allows a detailed description of phytoplankton stock and composition during fall in the eastern North Atlantic. While chlorophyll a was analyzed on board and PPC subsequently ashore, all other parameters await later analysis. (3) At the three JGOFS long-term mooring stations (L1:33°N/22°W, L2:47°N/19°W, L3:54°N/21°W) sediment traps were deployed in 500 m depth in cooperation with the chemical working groups to quantify the vertical particle flux out of the upper ocean. These traps are deployed for a period of one year with biweekly to monthly sampling intervalls depending on the season. Vertical sampling took place in the upper 200 m of the water column by CTD-rosette with the same planktological parameters as described above. (4) Zooplankton net hauls were taken in the upper 250 m at the three JGOFS mooring stations and additionally at the WOCE station F2 (52°N/16°W) with multiple opening and closing nets (200 µm mesh size) in 50 m steps for microscopical and HPLC-gut content investigations. Further net hauls were made with a 200 µm-ring net for gut fluorescence experiments. Samples from these experiments will be further investigated by HPLC-analysis. With this attempt the influence of the zooplankton feeding pressure on the vertical carbon flux will be determined.

Results

Both the chlorophyll a (Fig. 26, 27) and the nutrient values (see 5.2.1) were low in the Mediterranean Sea and southern North Atlantic. Only northward from 40°N (Sta. 78) higher chlorophyll a values were detected although the nutrient values were as low as before. A steady increase of the chlorophyll values was recorded towards the North with a high fluctuation between the stations. This will be compared with the hydrodynamic conditions and available sea surface temperatures. However, these do not suggest a simple explanation.
Throughout the whole transect dinoflagellates dominated the share of the biomass. Only at 54°N, the diatoms contributed more than 20% of the plant biomass. Periodical nutrient input from below the nutricline can be expected to be directly transformed into phytoplankton biomass, providing the base for high phytoplankton stocks in the absence of measurable nutrient concentrations at the surface. An increase in the nutrient values occured at 54°N and continued along the eastward part of the transect and accordingly, the chlorophyll values also show a small increase. It is expected, that the contribution of diatoms to the total phytoplankton biomass did also rise, as can be seen at the 54°N station.

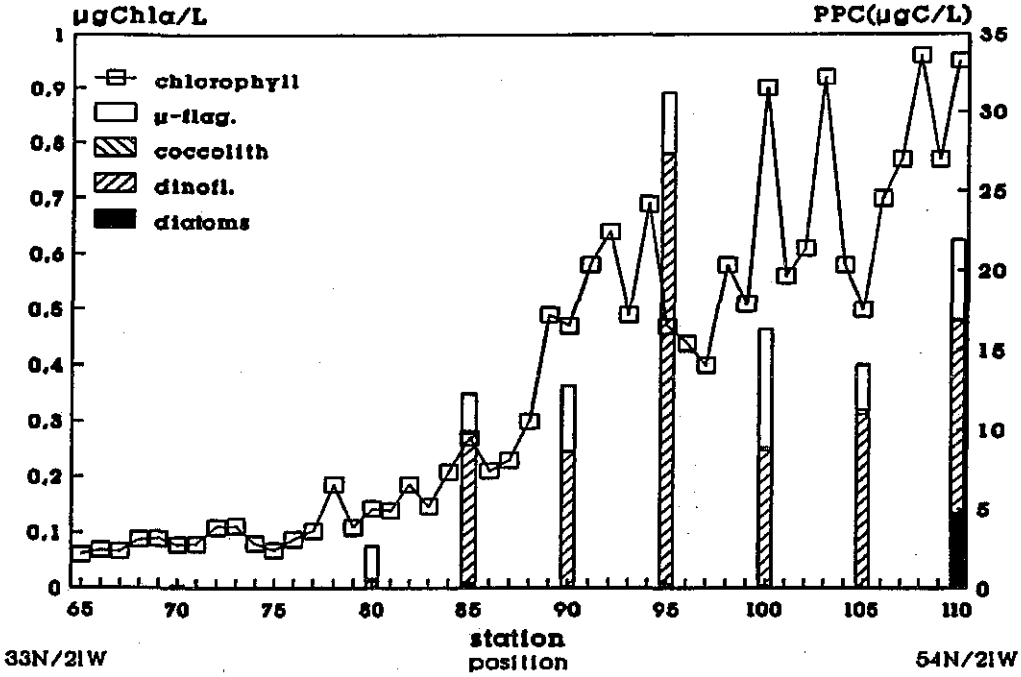

Fig. 26: Chlorophyll a and phytoplankton carbon (microscopical analysis) along the transect between JGOFS mooring stations 33°N/22°W, 47°N/19°W and 54°N/21°W (the chlorophyll values of the whole transect are shown in chapter 5.2.6, compared with the *in situ* fluorescence).

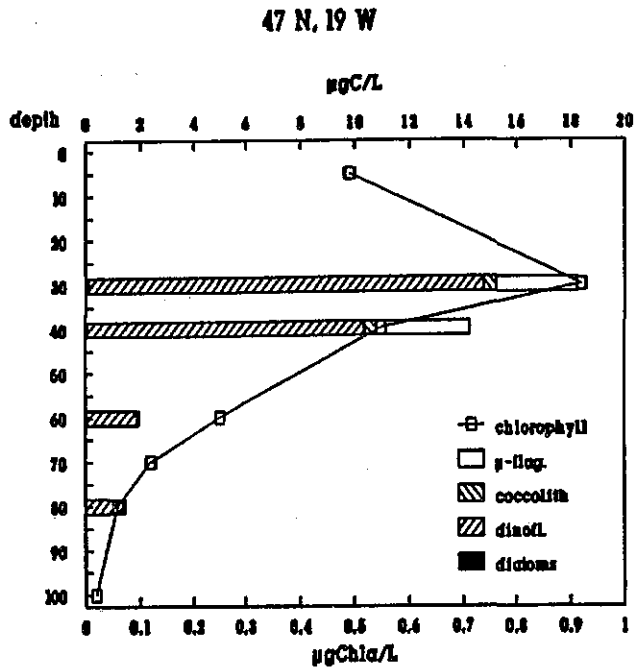

Fig. 27: Chlorophyll and phytoplankton carbon at the main JGOFS investigation area (no values above 30 m due to bad weather conditions; chlorophyll value in 5 m originates from the nearest surface station).

5.3.2 Population Dynamics of Planktonic Foraminifera (R. Schiebel)

Multiple opening-closing net samples (MCN samples) were taken to investigate planktonic foraminifers at the JGOFS stations complementing the Tübingen stock of sample series from METEOR M 6, M 10, M 11/1, M 12/3; M 17/2 and M 21 cruises. These samples offer the possibility of comparing spatial and seasonal distribution patterns of planktonic foraminifers in the NE-Atlantic. Additional samples from WOCE-stations improve our knowledge of the spatial foraminiferal distribution. CTD- and fluorometer-data as well as plankton investigations parallel to MCN sampling allow investigation of oceanographic environmental parameters that influence the planktic foraminiferal fauna. Multicorer (MC) sediment samples for comparisons of recent versus fossil coenoses reflect the paleoceanographic conditions and the climatic record of the sampled time interval.

At each sampled JGOFS station L1, L2, and L3 three vertical hauls (100 mm mesh size) from 100, 700, and 2500 m water depth were carried out. Each haul included five consecutive depth intervals (0-20-40-60-80-100 m / 100-200-300-500-700 m / 700-1000-1500-2000-2500 m). This offers a practicale and detailed record of the planktic foraminiferal fauna. At WOCE station F2 also three hauls (down to 2500 m water depth), at WOCE station E1 two hauls (700 m) and at WOCE station D2 one haul (100 m) were taken.

Multicorer (MC) samples were collected at stations L1, L2, L3, E1, and D2. Due to the limited amount of sediments cored at station L2 and L3, only the surface sediment was sampled to observe living benthic deep-sea foraminifers. These sediment samples were preserved with the appropriate bottom water of 2°C for further observations in our laboratory at Tübingen. From MC L1, E1, and D2 also the upper five sediment centimeters were sampled in 1 cm intervals. Sediment was stained with methanol/rose bengal solution. Maximal sampling depth was 26 cm below core top.

Results

At station L1 (33°09'N/20°00'W) the fauna was rich in species but poor in specimens and consisted of *Globigerina bulloides*, *Globigerinella siphonifera*, *Globigerinita glutinata*, *Globorotalia inflata*, *G. scitula*, *G. truncatulinoides*, and *Neogloboquadrina incompta* in the upper 100 m of the water column. Empty tests were relatively small probably juvenile tests. The amount of aggregates in the water column was low. Copepods and ostracods were frequent in the upper 100 m, between 100 and 2500 m many empty tests of pteropods were found. Below 100 m depth in addition to the above mentioned species *Globorotalia menardii* tests were present. While in the upper 700 m the foraminiferal fauna was poor in specimens, at 700 to 1000 m water depth many small *G. bulloides*, *G. inflata* and *Globigerinoides ruber* tests were present. This points towards pulses in production of planktic foraminiferal tests into the deep-sea.

The foraminiferal fauna at station L2 (47°47'N/19°45'W) showed *G. bulloides*, *G. inflata*, *N. incompta*, *Turborotalita quinqueloba* and *Orbulina universa* in the upper 100 m. The fauna was poor in species and as poor in specimens as at station L1. Aggregates and metazoan were abundant, at 100 to 700 m mainly pteropods and copepods were observed. Empty *Globigerinita uvula* and *N. incompta* tests were frequent. The assemblage at 700 to 2500 m water depth was dominated by *G. bulloides*. At both stations (L1 and L2) CTD profiles showed a well stratified water column. Thermohaline discontinuities were observed at 35 m and 45 m, respectively. This indicates a low level of mixing and nutrients.

In contrast to stations L1 and L2 at station L3 (54°39'N/21°16'W) many living *G. bulloides*, *G. inflata*, and *T. quinqueloba* were found. In addition, below 700 m *N. incompta* as well as many small sized, empty tests were present. Many aggregates and metazoan, mainly pteropods, copepods and ostracods, were found at the depth interval from 0 to 2500 m. South of station L3 at WOCE station F2 (52°23'N/16°21'W) only small sized, empty foraminiferal tests were found. The fauna was dominated by *T. quinqueloba*. Aggregates, pteropods and copepods were rare. West of station L3 at WOCE station E1 (54°21'N/25°53'W) the foraminiferal fauna was strictly stratified within the water column. At 0 to 20 m depth only few foraminifers were found, at 20 to 40 m interval the fauna was rich in living specimens. The association of empty tests at 40 to 700 m depth consits of *N. incompta* as well as *G. bulloides*, *G. inflata*, and *T. quinqueloba*. At this depth interval and at 0 to 20 m depth pteropods (*Limacina* spp.) are frequent. At WOCE station D2 at 57°25'N/28°14'W, in addition to the living fauna, the thanatocoenosis contains *N. pachyderma* (sinistral), *G. uvula*, *G. bulloides* and *T. quinqueloba*. Between 40 to 60 m no foraminiferal tests were found which might be due to the sampling method. Living pteropods were frequent between 20 and 40 m depth. At the northern stations (F2, L3, E1 and D2) a higher degree of surface water mixing compared to the southern stations (L1 and L2) can be inferred from CTD-profiles. This indicates higher nutrient contents which may cause larger amounts of organic material.

The planktonic foraminiferal species distribution is in agreement with the result of OTTENS (1991) from the NE-Atlantic (August/September, upper 5 m of the water column). According to this author, the fauna at station L1, with large amounts of *G. glutinata*, *G. scitula* as well as *G. menardii* and *G. ruber* corresponds to an association typical for the Azores Current (AC). These species are missing in northern water masses. At stations L2, L3, F2, and E1 *G. bulloides*, *G. incompta*, *T. quinqueloba*, and *G. inflata* are dominating the fauna, typical for the North Atlantic Current (NAC). *Neogloboquadrina pachyderma* (sinistral) was found exclusively at the northernmost station D2, indicating cooler, subpolar and polar, water masses.

5.3.3 Seasonal Changes in the Living Assemblage and Sedimentation of Planktonic Foraminifera (B. Hiller)

Recent planktonic foraminifera constitute a major percentage of the total living zooplankton. Their empty shells on the ocean floor contribute substantially to the sediment and form the so-called "Globigerina ooze". Biomass production, including production of calcareous shells, is influenced by seasonal changes in the living assemblage. As a result, the amount of $CaCO_3$ deposited varies throughout the year. The main goal is to study regional and seasonal variations in the living planktonic foraminiferal assemblage, and in the sedimentation rate of their shells. It is the first time that winter conditions this late in the year could be investigated. The investigation follows former work done in this area on cruises M 10/3, M 17/2 and M 21/4+5. This work is part of a long-term survey which intends to elucidate the carbon and calcium cycle in the water column. It constitutes part of the German JGOFS program.

Samples were collected from the upper 2500 m of the water column. The photic zone was sampled at standard depth intervals (100 m, 700 m, 2500 m) with a multiple opening and closing net (MSN). CTD-data taken at the same stations allow to link our results to the hydrographic conditions. In addition 6 large box cores (GKG) were taken at the sediment trap positions and at the East Greenland Margin.

Results

Foraminiferal assemblages at the Norwegian Margin are influenced by the North Atlantic Current and showed transitional features. The samples are poor in species as well as in individuals, and are dominated by *Turborotalita quinqueloba* and *Neogloboquadrina incompta*. The northernmost station at 64°46,2'N, 04°30,2'E showed a subpolar influence with the occurrence of *Globigerinita uvula*. Species composition at all stations does not vary between live assemblage and sinking shells caught in deeper water. The live assemblage is concentrated in the upper 20 m. Noteworthy is the high abundance of living *Limacina* sp., a pteropod which is transported by the North Atlantic Current to the area of sampling. There are no characteristic differences between the foraminiferal assemblages at the sediment trap position NB7 (69°41,4'N; 00°28,9'E) in the Norwegian Basin and at the Norwegian Margin. *Turborotalita quinqueloba* and *N. incompta* are still dominant. Only a few shells of the subpolar distributed species *G. uvula* were found.

5.3.4 Vertical Distribution and Lipid Content of the Mesozooplankton in the Northern North Atlantic (U. Zeller)

Ecological studies in zooplankton have often been conducted in order to obtain information about the life history; growth and development, feeding and seasonal vertical migration behaviour. High latitude marine environments are characterized by a few species, which dominate the zooplankton community. For the present study of carbon budgets related to

zooplankton in the northern North Atlantic the spatial and vertical distribution of these organisms was studied on cruises in February, May and July 1991. These studies were supplemented by investigation of the biochemical compounds like lipid, carbon and nitrogen content. During this cruise, the data set should be complemented by "winter values" of the different organisms.

Metazooplankton was collected in vertical hauls (from 1000 m to the sea surface in steps of 100 and 500 m) using a multiple opening and closing multinet. Animals were immediately sorted by species, and aliquots were deep-frozen in liquid nitrogen for lipid analysis. Remains of the sample were preserved with borax-buffered formaldehyde (4% end concentration) and stored for later microscopical counting.

The first results indicate that the most abundant and therefore the most relevant copepodits in the pelagic ocean of the investigation area is *Calanus finmarchicus*. The vertical distribution of this species looks similar to the observed results during July 1991. Most of these animals were located in the depth between 500-1000 m, which seems to be their overwintering depth. Detailed analyses of the lipid content of *C. finmarchicus* copepodit stage V, show even during the measuring time, that animals which are located at different depths, have changing lipid contents. Animals, which are located at the surface have less amounts of lipid, while the copepods from the overwintering depth build up to 40% lipid of their dry weight. The amount of total lipid in this depth is comparable with the July data of 1991, which emphasizes that the metabolic requirements of this species are completed as early in the year as August. This result shows, that the greatest energy transfer is between spring and late summer, where copepodits obtain their main energy supply from grazing on phytoplankton.

5.3.5 Vertical Particle Flux in the Northern North Atlantic

(E. Bauerfeind, K. Mellenthin)

Sediment trap moorings

Long-term measurements of the vertical flux of particulate matter have been conducted, at two locations in the northern North Atlantic for several years. The traps are located in areas that are influenced by different hydrographic regimes. The position in the Norwegian Basin is influenced by the warm waters of the North Atlantic Current and remains ice-free year round. The mooring located in the Greenland Sea is influenced by waters of Arctic origin at the surface, and exhibits a strong seasonal variation in ice coverage. It was planned to recover the moorings NB 7 (69°41.35'N, 00°28.85'E, water depth of 3285 m), in the Norwegian Basin, and OG 6 (72°21.57'N, 07°36.14'W, water depth 2621 m), in the Jan Mayen Current. Both moorings were deployed in July 1992, and each is equipped with sediment traps at 500 m, 1000 m and 2000 m depth (NB 7).

The mooring NB 7 was successfully recovered on 12 November. Each of three traps had collected material at the 20 pre-programd time intervals. Initial macroscopic inspections of the trap samples revealed a seasonal signal in vertical particle flux showing high flux rates after the deployment in July/August 1992, decreasing rates in the period September-December 1992, and consistently low sedimentation in the subsequent months until June 1993. A distinct increase to a maximum in sedimentation is noticed in the second half of June with decreasing but still high values in July/August of 1993.

A comparison of the amount of material in the collector cups in the 3 different depths horizons showed a consistently higher amount of material in the cups of the 1000 m trap throughout the deployment period. This points to a considerable lateral advection of particulate matter at this depth level. More detailed information about the amount and composition of the collected material will be available after chemical, biochemical and microscopic analysis of the samples. On 14 November the site of mooring OG 6 was reached. The mooring was located and successfully released. However, the acoustic release stopped after having risen to a depth of 1380 m and did not move any farther. Most probably the mooring lost buoyancy and parts of it had sunk to the sea floor, thus preventing the mooring from reaching the surface. As it was not possible to dredge for the mooring during this cruise it was to abandoned.

Water samples

Bottle casts were made in order to gain further insights in the concentrations of inorganic dissolved nutrients during winter and in their vertical distribution which largely determines the amount of phytoplankton biomass formed during spring. This was done at the two trap positions with a rosette water sampler deployed throughout the entire water column. Subsamples were collected, conserved and stored in a refrigerator for further analysis at the shorebased laboratory.

Zooplankton

Overwintering zooplankton populations within the upper water layers are crucial for the onset of vernal phytoplankton growth and the build-up of phytoplankton biomass. Therefore, vertical tows with a multiple opening and closing net (mesh size 0.100 mm) were conducted at different depth horizons in the Norwegian Basin and in the East Greenland Sea. This work was done in co-operation with B. Hiller, University of Tübingen (see chapters 5.3.2 and 5.3.3). First examinations of samples revealed a maximum abundance of copepods at depths between 500 and 700 m. Nevertheless, a considerable amount of copepods and other zooplankton organisms were present in depths shallower than 500 m as well. Besides zooplankton, relatively high numbers of phytoplankton organisms were present in the upper 80 m of the water column. These were dominated by the dinoflagellates *Ceratium furca* and *C. fusus* in the Norwegian Basin, and *C. arcticum* in the East Greenland Sea. Besides dinoflagellates, several diatom species, mainly belonging to the genus *Chaetoceros* , were observed in the East Greenland Sea.

5.4. Marine Geosciences

5.4.1 Pore Water Geochemistry in the JGOFS Area (M. Kreutz)

The recycling of dissolved mineralization products and nutrients from sediments of the Atlantic Ocean to the bottom water is one important aspect of the German JGOFS-program. The burial flux of organic carbon in sediments initiates complex biological decomposition and physicochemical dissolution- and precipitation-processes. They are reflected in concentration gradients of the dissolved species in the pore water. Based on these concentration gradients, the vertical flux of dissolved components in the sediments can be calculated. The immediate goal of this JGOFS sponsored effort is the regionalisation of the flux of dissolved components through the sediment/water interface for "key regions" of the Atlantic Ocean. A close cooperation exists with the Sonderforschungsbereich 261 (SFB 261) (University of Bremen, Alfred-Wegener-Institut, Bremerhaven), in which the GEOMAR effort is concentrated on data collected from the North Atlantic and that of the SFB 261 on data from the South Atlantic.
Initially, total dissolved inorganic carbonate and the nutrients nitrate, nitrite, ammonia, phosphate and silicate are of interest. Subsequently the distribution and flux of trace metals will be studied as well. From these regional data an Atlantic-wide estimate of dissolved material transport will be deduced from the chemical and sedimentary environment and the processes at the sediment/pore water system, the relation between sediment facies and organic carbon burial flux and the modeling of early diagenesis. The modeling of the early diagenetic processes and the chemical environment requires the quantification and combination of transport processes like bioturbation and of microbiological metabolic processes (BERNER, 1980; JAHNKE et al., 1982a,b; EMERSON, 1985; BOUDREAU, 1987). The modeling also requires knowledge of important control mechanisms from the water column, such as primary production and sediment accumulation, which are major goals of other JGOFS-programs. The modeling relies on a considerable body of existing data supplemented by a limited amount of additional measurements from "key regions" from the Atlantic Ocean.

Sediment samples were taken at the mooring sites L1, E2 and D2 by the multicorer (MUC) and prepared for pore water analysis. Because of bad weather conditions, it was not possible, unfortunately, to take samples at the other sites.
The pore water samples were extracted from slices of 0.5 - 1.0 cm in thickness, using a polycarbonate squeezer with 0.2 mm filters at *in situ* temperature (2°C). Nutrient concentrations were analyzed on board using an autoanalyzer. High resolution profiles of the formation factor and oxygen distribution were also measured by microelectrodes. Additionally, sediment was sampled for subsequent measurements of the fine scale distribution of organic carbon.

Results

As an example total carbonate, nutrients, and oxygen rmeasurements from site D2 are presented in Figures 28/29 and listed in Table 9. The nitrate profile (NO_3) shows a rapid increase of nitrate in the upper 3 cm below sediment/water interface and reflects oxygen respiration coupled with intensive nitrification (BENDER et al., 1977; FROELICH et al., 1979; EMERSON et al., 1980). From 3 cm below the sediment surface, nitrate concentrations become nearly constant. There are no signs of denitrification, which suggests carbon limitation and the presence of oxygen in the observed interval. The nitrite profile (NO_2) shows a maximum 1 cm below sediment surface, in the area of most intensive nitrification. The slow decrease of nitrite to 12.5 cm suggest a slow-down nitrification. Below 12.5 cm, the nitrification becomes too slow to permit a measurable build-up of this intermediate, because nitrite is quickly oxydized to nitrate (JAHNKE et al., 1982b).

The ammonia profile (NH_4) shows a slight increase of ammonia down to 12.5 cm below sediment surface. The bacterial deammination of organic matter produces ammonia as intermediate product, which is oxidized quickly to nitrite and to the final product nitrate respectively (BERNER, 1980). Below 12.5 cm ammonia increases rapidly. This is unusual for oxic conditions, but the reason may be, that the bacterial oxidation of ammonia to nitrite becomes very slow or is inhibited completely. The result would be an enrichment of the intermediate nitrification product ammonia.

The phosphate profile (PO_4) increase with depth, however while it may be approaching a constant value at depth, this was not observed due to the short coring depths. The PO_4-concentrations are relative low; conspicuous is, that the phosphate concentration in bottom water is higher than in the pore water immediately below the sediment surface. Very likely, phosphate is extracted from the pore water by fixation. The result is a diffusive flux of bottom water phosphate into the surface sediment (BALZER, 1989; JAHNKE et al., 1989; ZABEL et al., 1993).

The silicate profile (SiO_2) shows a rapid increase of silicate in the upper 7 cm of the sediment. A constant value seems to be reached at the end of the core. Silicate concentrations are generally low and point to low biogenic input of opal-A to the sediment (SPENCER, 1983).

The total carbondioxide profile (ΣCO_2) suggests increasing dissolution of calcite and biological activity in the upper 4 cm of the sediment (ARCHER et al., 1989). Except for the maximum at depth of 13 cm, no further increase of ΣCO_2 is detected; below 23 cm the ΣCO_2 concentration seems to increase again.

The oxygen profile (O_2) was calculated from the nitrate data, using the Redfield-ratio (REDFIELD, 1958; FROELICH et al., 1979). In the upper 3.5 cm a steep gradient exists where oxygen decreases from 280 to 190 µmol/l. Below, that oxygen decreases very slow; the chemical environment of the entire core is oxic.

Tab. 9: Pore water nutrients and oxygen data from station D2.

Site: D2 (M458/93)
Position: 57°25.286'N/28°13.331'W
Water depth: 2568 m

Depth [cm]	NO_3- [µmol/l]	NO_2- [µmol/l]	NH_4 [µmol/l]	PO_4 [µmol/l]	SiO_4 [µmol/l]	t-CO_2 [µmol/l]	O_2 [µmol/l]
0.00	18.22	0.00	1.02	1.14	13.13	6.00	280.24
0.25	29.40	0.68	1.02	0.72	40.08	6.14	231.81
0.75	31.40	0.84	1.37	0.72	64.88	6.14	223.19
1.50	34.00	0.60	1.48	1.28	89.64	6.33	215.60
2.50	36.68	0.56	1.48	1.40	115.72	6.33	204.04
3.50	40.00	0.36	1.48	1.20	134.00	6.51	189.72
6.50	41.44	0.20	2.15	1.84	153.40	6.51	183.51
9.50	41.56	0.12	2.49	2.16	161.88	6.51	182.99
12.50	41.96	0.00	2.89	1.96	170.40	6.69	181.27
17.50	43.16	0.00	6.56	2.24	182.80	6.51	176.10
22.50	43.36	0.00	11.04	2.56	191.16	6.51	175.24
27.50	41.88	0.00	33.72	2.68	193.68	6.69	168.86

Oxic respiration is the dominant process affecting the pore water nutrients, ΣCO2 and oxygen distribution in the core presented here. The nutrient concentrations are generally low and suggest a low burial flux of organic carbon. This compares well with the primary production maps (BERGER et al., 1987; BERGER, 1989) and the empirically determined control of organic matter, (SARNTHEIN et al., 1988) and the resulting fluxes.

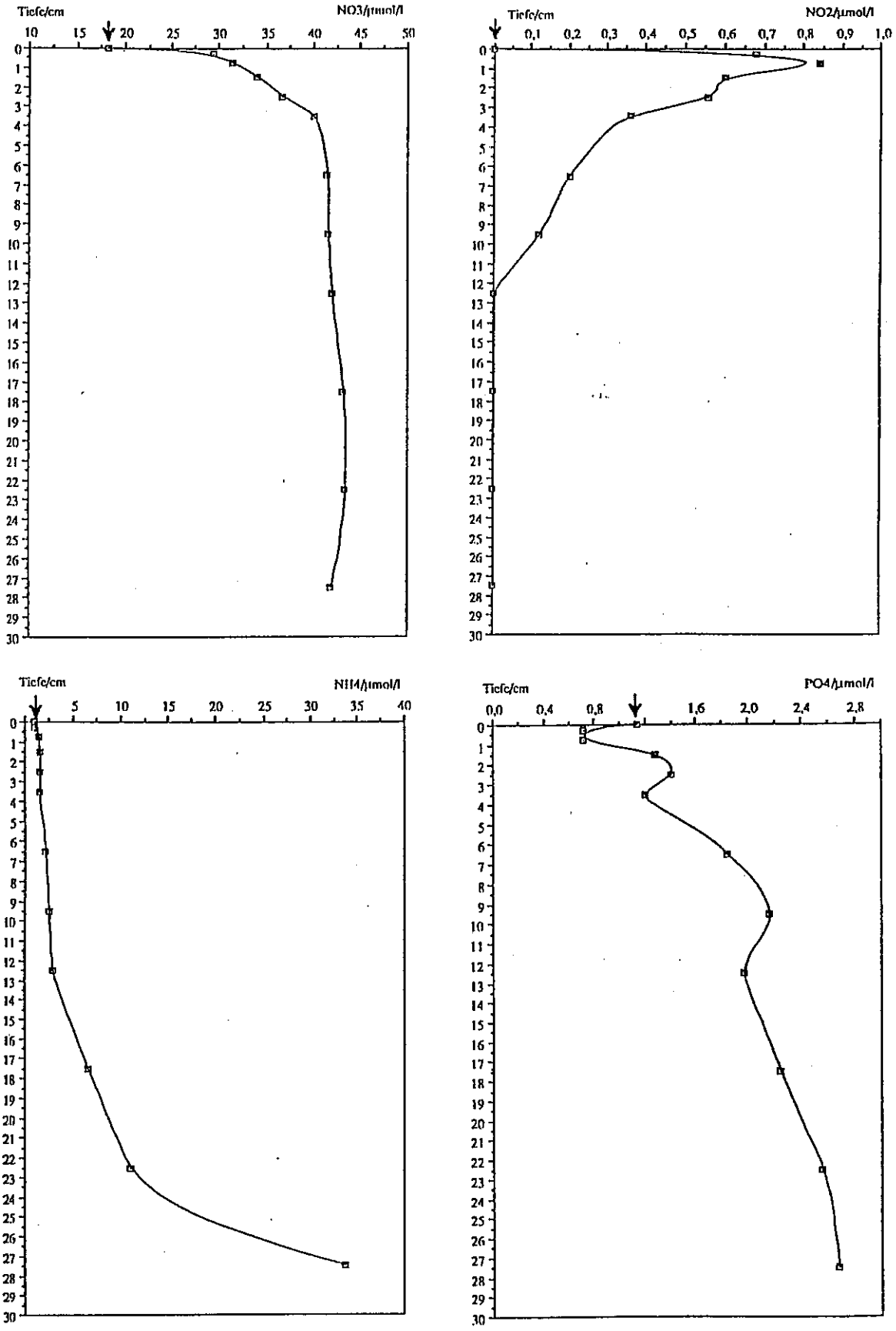

Fig. 28: Pore water results from site D2

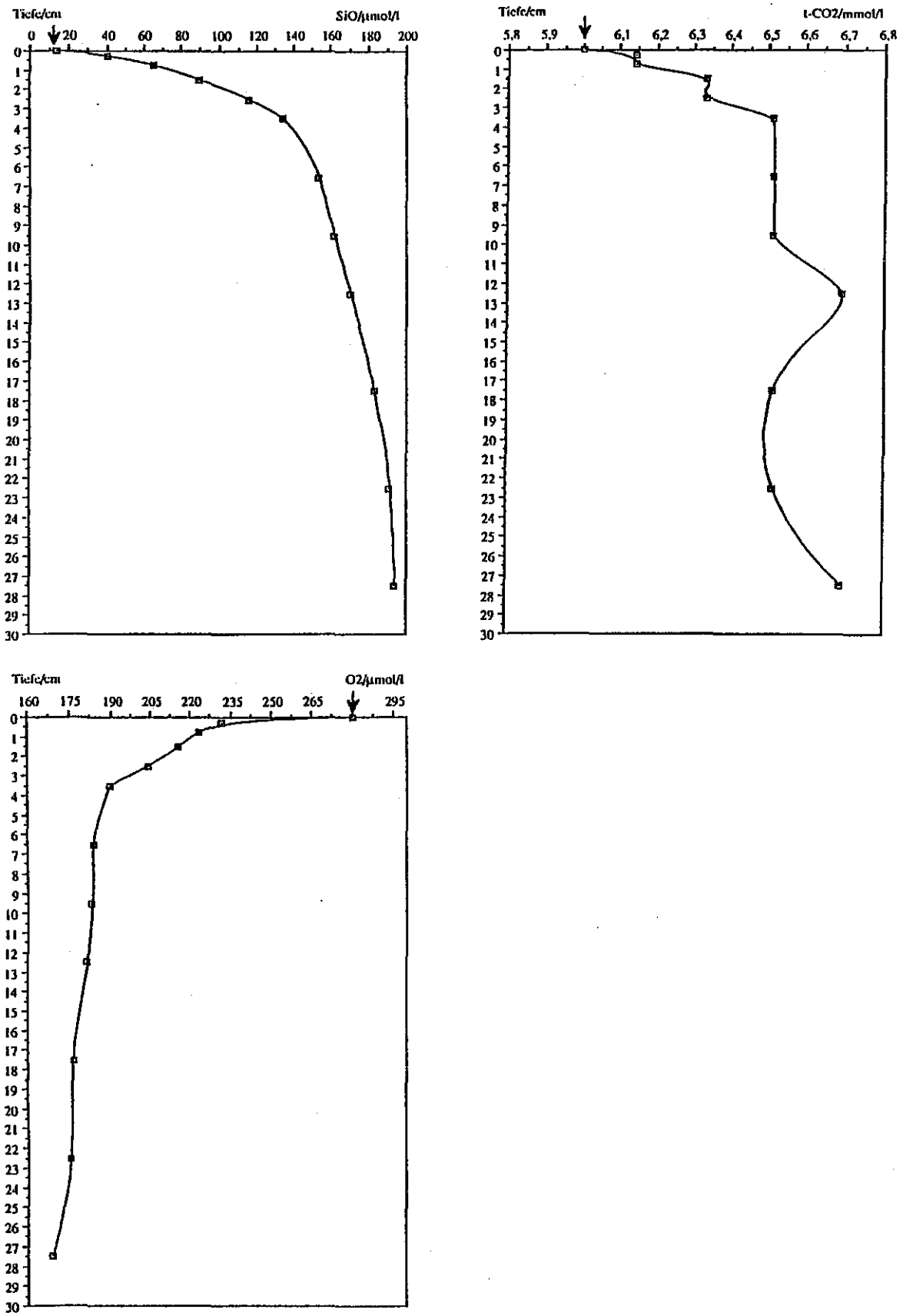

Fig. 29: Pore water results from site D2 (continued)

5.4.2 Paleoecology of the Pelagic Ocean (SYNPAL) (SFB 313)

(H. Andruleit, H. Meggers)

The goal of the SYNPAL projekt is the synoptic study of the temporal and spatial development of plankton communities by looking at the four planktonic groups coccolithophorids, diatoms, radiolarians and dinoflagellate-cysts. The remains of these groups in the sediments form the scattered survivors of planktonic life of much higher diversity in the upper water column. We attempt to link these remnants with the actual living communities to reconstruct, on the one hand, paleoecology and evolution of planktonic life and, on the other hand, to use this knowledge to obtain detailed information of the paleoceanographic and climatic development. Therefore, we attempt to evaluate the processes which are taking place in the photic zone, the water column and the sediment. The basis for this study is the synoptical examination of plankton, sediment trap, and sediment samples.

On this cruise the focus of research was on the horizontal and vertical sampling of the Norwegian Current to complete our data set on the late fall communities in this region. Additionally some samples from the Skagerrak area were taken. At a total of 6 Stations water samples (1 to 2 l) were taken at several depth intervals for coccolithophorid and diatom investigations with a rosette sampler, based on previous CTD profiling. For each sample the salinity and temperature was recorded. To investigate the radiolarian fauna, especially the deep living ones, a ring net (46 µm mesh size) was deployed at three depth intervals from 1000 to 500 m, 500 to 100 m and from 100 m to the surface. Additionally, surface samples from box cores were taken of the underlying sediments (see sample list, Table 10). The water samples were filtered immediately through cellulose nitrate filters (45 mm diameter, 0.45 µm pore size) by means of a vacuum pump on board. The filters were dried at 50°C for some hours and stored with silica gel in plastic petri-dishes without further washing or conservation. The net samples were poisend with formol and stored at low temperatures.

Due to very limited possibilites to examine the samples on board there are only few results obtained so far.

- Microscopic analysis of water samples from the Skagerrak show remarkably high amounts of dinoflagellate cysts. Their numbers exceed more than 1000 individuals per litre in the shallowest samples. Lower in the water column the amount of cysts decreases to zero. In no other regions of the cruise were comparable amounts found.

- There is no direct means to evaluate the number coccolithophorids because of their small size; a scanning electron microscope is needed for that. At least an indication that sufficient individuals are present can be gleanded from staining of the filters. All filters from the surface samples show a high abundance, whereas the deeper samples often seem barren.

- In all net samples high amounts of copepods, foraminifers and radiolarians were found. The foraminifers are dominated in all samples by subpolar forms with high frequencies of *Globigerina quinqueloba.* Other taxa like *Neogloboquadrina pachyderma* sin., *Globigerinata glutinata* and *Globigerina bulloides* are of minor importance. In contrast to the copepods the foraminifers show decreasing amounts with greater depth.

Tab. 10: Sample list M 26/2

station	device	depth [m]	date	location	sample depth (l) [m]	temp.	sal.	remarks
460-7	CTD	304	30.09.93	58°02,61N/9°39,79E	0 (1)	11,3	nv	CTD out
					25 (1)	nv	nv	of order
					50 (1)	nv	nv	
		Skagerrak			100 (1)	nv	nv	
					150 (1)	nv	nv	
					288 (1)	nv	nv	
463-2	CTD	329	1.10.93	58°02,78N/9°39,18E	0 (0,75)	10,1	33,48	CTD okay
					25 (0,75)	10,13	34,33	>1000 Dinocysts
					50 (0,75)	8,16	35,17	per litre
		Skagerrak			75 (0,75)	7,28	35,28	
					200 (0,75)	6,95	35,38	
					300 (0,75)	6,58	35,38	
472-1	CTD	993	5.10.93	60°25,91N/4°54,25W	0 (1,5)	9,6	34,2	
					41 (1,5)	9,61	35,39	
					77 (1,5)	9,53	35,39	
		Faeroe-Shetland Channel			531 (1)	0,86	35,17	
					827 (2)	-0,54	35,19	
					952 (2)	-0,76	35,19	
476-1	CTD	2901	8.10.93	63°45,07N/5°00,04W	0 (1,5)	7,8	34,25	
					16 (1,5)	7,82	35,22	
					51 (1,5)	7,82	35,22	
					77 (1)	6,98	35,28	
		Island-Faeroe Ridge			101 (1,5)	6,75	35,34	
					159 (1,5)	5,12	35,3	
					1017 (2)	-0,55	35,2	
					2891 (1,5)	-0,88	35,2	

Tab. 10: continued

station	device	depth [m]	date	location	sample depth (l) [m]	temp.	sal.	remarks
477-1	CTD	2291	8.10.93	65°49,4N/3°16,42W	0 (1,5)	7,4	33,66	
					16 (1,5)	7,42	35,17	
					26 (1,5)	7,43	35,17	
					49 (1,5)	6,87	35,13	
					83 (2)	3,33	35,26	
		Aegir-Ridge			107 (2)	3,3	35,3	
					158 (1)	3,33	35,32	
					604 (2)	0,0	35,19	
					2016 (2)	-0,94	35,21	
477-2	RN	2326	8.10.93	65°49,77N/3°18,83W	1000-500	(see st.477-1) 10cm rip!		
477-4					500-100			
477-5			9.10.93		100-0			
477-6	GKG	2275	9.10.93	65°49,39N/3°16,13W			surface sample	
478-1	CTD	3297	10.10.93	70°00,00N/0°00,01W	0 (2)	7,9	34,08	
					23 (2)	7,94	35,4	
					33 (2)	7,9	35,4	
					58 (2)	7,9	35,42	
		Lofoten-Basin (central station)			158 (2)	4,98	35,38	
					209 (2)	4,81	35,4	
					511 (2)	4,26	35,41	
					1016 (2)	0,0	35,19	
					3291 (2)	-0,84	35,21	
478-2	RN	3297	10.10.93	70°00,01N/0°00,12W	1000-500	(see st. 478-1) rip repaired		
478-3					500-100			
478-4					100-0			
478-6	GKG	3296	10.10.93	70°00,34N/0°03,79W			surface sample	
480-1	CTD	1589	12.10.93	74°59,11N/14°22,53E	0 (2)	6,3	34,13	
					56 (2)	6,43	35,34	
					104 (2)	6,63	35,46	
		Barents Sea slope			506 (2)	3,33	35,37	
					1014 (2)	-0,4	35,21	
					1583 (2)	-0,94	35,22	

5.4.3 Paleoceanography of the Norwegian Margin: Temperature Transfer Functions (U. Pflaumann, H. Hensch)

More detailed knowledge on the paleoceanographic history of the Norwegian shelf paleotemperature estimates can be obtained from sediment cores with a high time resolution. Proxy data for paleotemperatures can be estimated by analysing quantitatively the faunal assemblages of the planktonic foraminifera. Using the "Modern Analogue Transfer Technique" estimates of the sea surface temperatures for winter and summer can be derived (PFLAUMANN et al., 1994). Our data base contains the modern assemblages of more than 750 sediment surface samples from the Atlantic and 232 samples from latitudes > 50°N. In order to improve the resolution of this data set for the region along the Norwegian margin, and to enable first approximations of the influence of the Norwegian Coastal Current on the fauna of the sediment surface, samples from 6 box cores of the Norwegian Margin were studied. Their content of planktonic foraminifera (> 0.150 mm) was analyzed quantitatively. The fauna is dominated by *Neogloboquadrina pachyderma* right coiling var. Other species are *N. pachyderma* left, *Globigerina bulloides and G. quinqueloba* (Table 11).

Tab. 11: Percentages of planktonic foraminifera in surface sediment samples from the Norwegian Basin.

Surface sample no.	23490-2	23492-3	23498-1	23500-1	23502-1	23503-1	23505-1
Globigerina							
bulloides	15.93	11.65	8.14	9.21	3.49	9.59	1.53
quinqueloba l.	1.55	0.00	1.63	1.63	0.00	4.08	14.22
quinqueloba r.	2.65	0.00	0.98	2.71	0.53	2.24	12.58
Globigerinella							
aequilateralis	0.00	0.00	0.00	0.00	0.00	0.20	0.00
Orbulina							
universa	0.00	0.00	0.00	0.00	0.21	0.00	0.00
Globorotalia (Turborotalia)							
inflata	0.88	0.00	2.93	2.17	1.06	1.84	0.00
Neogloboquadrina							
pachyderma l.	5.53	5.34	38.76	23.04	36.05	26.94	57.44
pachyderma r.	72.35	81.07	45.93	58.27	58.67	53.67	13.89
Globigerinita							
glutinata	1.11	1.94	1.63	2.98	0.00	1.43	0.33
Sum counted	452	107	307	369	454	490	914

The distribution map (Fig. 30a-f) of the main species indicates that the species percentages of the new samples are consistent with the previous data set.

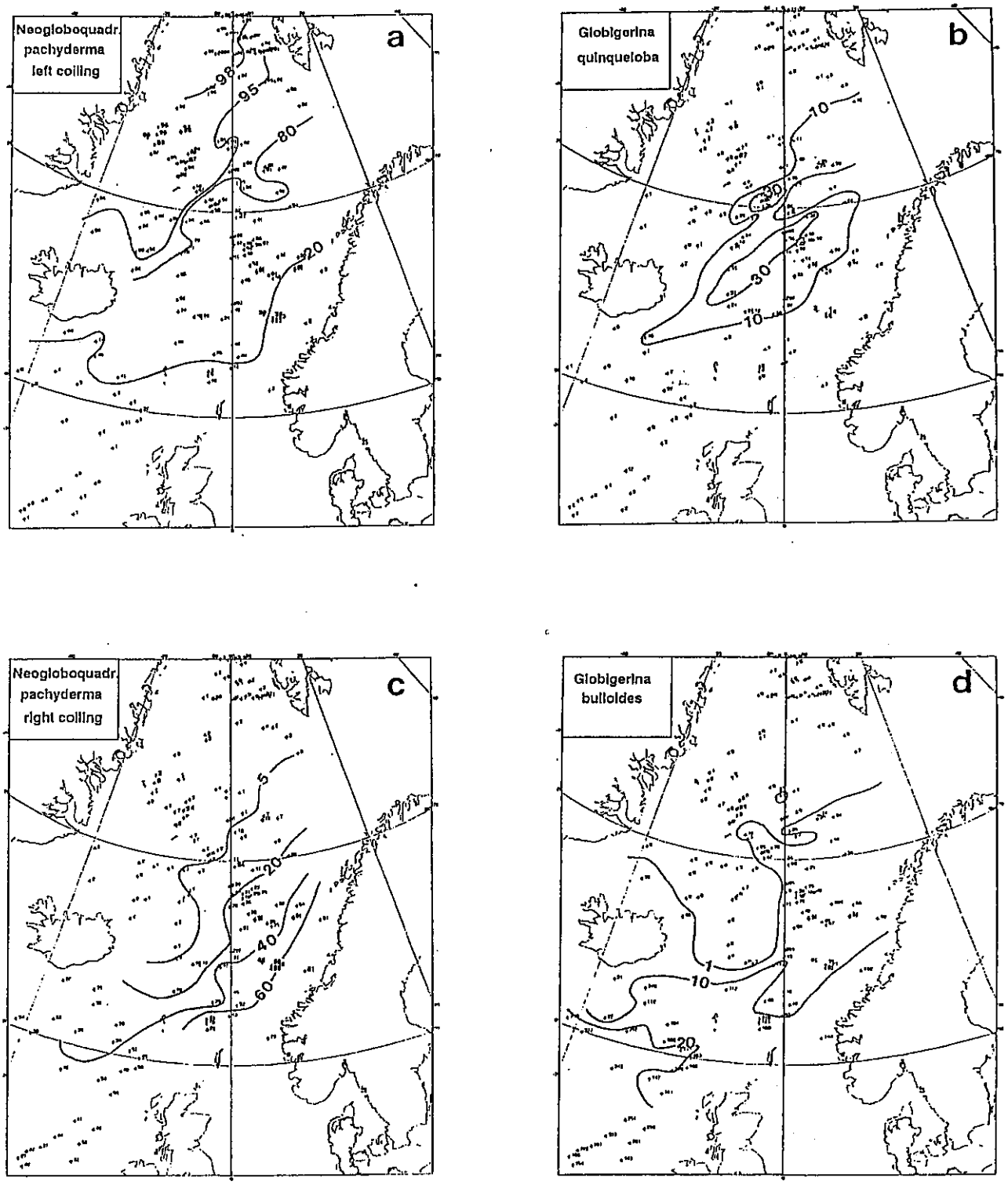

Fig. 30a-d: Distribution patterns of planktonic foraminifer species dominant in the Greenland-Iceland-Norwegian Sea. Numbers indicate percentages of planktonic foraminifera. Data set acc. PFLAUMANN et al., including the new data of M 26/3. a) *Neogloboquadrina pachyderma* var. sinistra, b) *Globigerina quinqueloba*, c) *Neogloboquadrina pachyderma* var. dextra, d) *Globigerina bulloides* (x10).

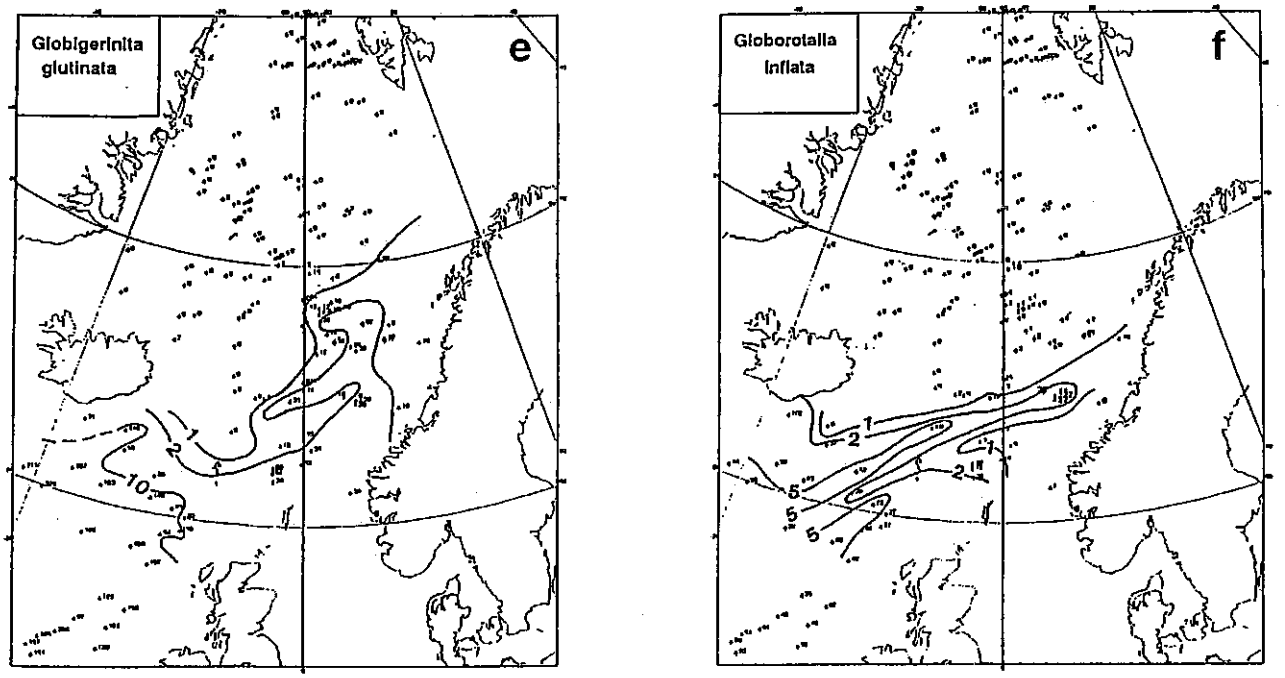

Fig. 30e,f: Distribution patterns of planktonic foraminifer species dominant in the Greenland-Iceland-Norwegian Sea. Numbers indicate percentages of planktonic foraminifera. Data set acc. PFLAUMANN et al., including the new data of M 26/3. e) *Globigerinita glutinata* (x10), f) *Globorotalia inflata* (x10)

Off Norway, *N. pachyderma* right var. shows high values along the margin. A new pattern is observed for the distribution of *Globorotalia inflata*, showing a narrow tongue of relatively high frequencies running from its main distribution area in the intermediate to subtropical latitudes to the NE off Norway. The new sample set helps to explain isolated occurrences of this species in the Norwegian Sea. Applying the combined Dietrich/Levitus set as a temperature database (SEIDOV, in prep.), the new samples off Norway fit well into the data set of summer and winter temperatures (Fig. 31a-b, Tables 12 and 13).

Tab. 12: Sea surface temperatures interpolated from the combined Dietrich-Levitus data set of SEIDOV (in prep.) for the Norwegian Margin samples. For legend see Table 13.

Station	Latitude	Longitude	w1	s1	w5	s5
23490-2	64°20.73'N	08°23.66'E	5.60	12.33	6.14	10.66
23492-3	64°18.10'N	08°09.70'E	5.58	11.20	6.54	9.76
23500-1	64°43.40'N	04°55.00'E	6.41	11.54	6.60	0.04
23501-1	64°43.04'N	04°27.25'E	6.45	11.34	6.56	9.88
23502-1	64°37.00'N	04°27.10'E	6.42	11.40	6.57	9.93
23503-1	64°46.00'N	04°30.10'E	6.43	11.51	6.61	10.02
23505-1	69°41.40'N	00°28.80'E	4.40	8.46	4.25	6.85

Tab. 13: Sea surface temperature estimates for Leg M 26/3 samples. Estimates by SIMMAX24, 232 samples from North of 50°N, Dietrich-Levitus data model. sim = similarity index. w1dw = winter, 0 m, geogr. distance weighted. w1 = winter, 0 m, not geogr. distance weighted. s1dw = summer, 0 m, geogr. distance weighted. s1 = summer, 0 m, not geogr. distance weighted. std = standard deviation of the 10 most similar modern analogue samples. lat. and long. in degrees and minutes x 100.

Station	Latitude	Longitude	nn	sim	w1dw	w1	std	s1dw	s1	std
23490-2	64°20.73'N	08°23.66'E	10	0.984	6.8	7.8	2.1	11.7	12.2	1.8
23492-3	64°18.10'N	08°09.70'E	10	0.981	6.9	7.8	2.1	11.7	12.3	1.8
23498-1	64°57.00'N	03°31.00'E	10	0.979	6.6	6.8	0.7	10.6	10.8	0.6
23500-1	64°43.40'N	04°55.00'E	10	0.974	6.6	6.7	0.8	10.8	10.9	0.6
23501-1	64°43.04'N	04°27.25'E	10	0.974	6.6	6.7	0.8	10.7	10.9	0.6
23502-1	64°37.00'N	04°27.10'E	10	0.969	6.5	6.7	0.9	10.6	10.8	0.7
23503-1	64°46.00'N	04°30.10'E	10	0.972	6.6	6.8	0.9	10.8	10.9	0.6
23505-1	69°41.40'N	00°28.80'E	10	0.988	4.0	4.0	1.2	8.1	8.2	1.2
23506-1	72°23.57'N	07°36.14'W	10	1.000	0.4	0.5	1.3	4.3	3.7	2.5
23507-1	73°49.80'N	09°15.10'W	10	1.000	0.3	0.2	0.9	3.9	3.3	2.1
23508-1	73°51.60'N	09°23.70'W	10	1.000	0.4	0.6	0.8	3.8	3.7	1.3
23509-1	73°50.00'N	13°30.10'W	10	1.000	0.2	0.0	0.9	3.6	2.7	2.4
23510-1	73°27.20'N	13°25.90'W	10	1.000	0.3	0.3	1.1	4.1	3.7	2.0
23511-2	73°12.90'N	15°00.10'W	10	1.000	0.4	0.5	0.8	4.3	4.1	1.5
23512-1	72°56.50'N	13°25.40'W	10	1.000	0.3	0.4	0.9	4.3	4.1	1.7

a Dietrich-Levitus Winter Surface Water Temperatures

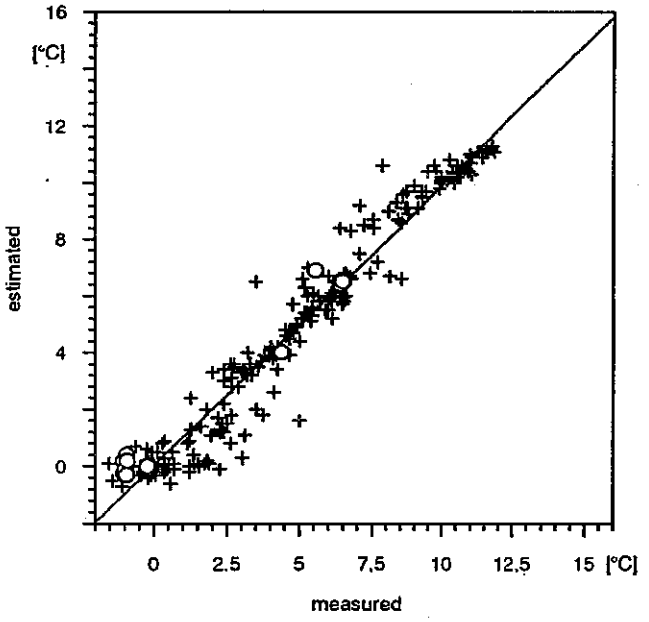

Polynom - Regression: (N = 245)
$y = a + bx + cx^2 + dx^3 ...$
a = 0.0306809608
b = 0.9881441794
Varianz der Residuen = 0.6863708459
Stdabw. der Residuen = 0.8284750122
Korrelationskoeffizient = 0.9764959492
df = 243
p <= 0.001 %

b Dietrich-Levitus Summer Surface Water Temperatures

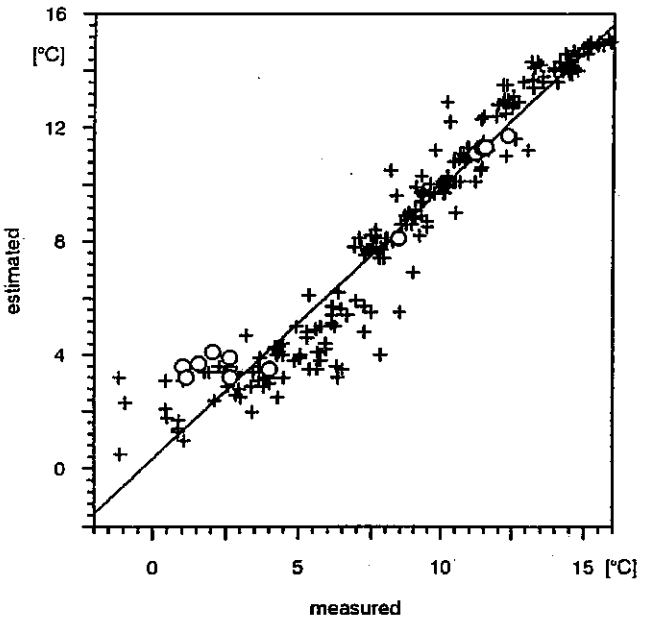

Polynom - Regression: (N = 245)
$y = a + bx + cx^2 + dx^3 ...$
a = 0.3547636102
b = 0.9542600167
Varianz der Residuen = 1.040673725
Stdabw. der Residuen = 1.0201341701
Korrelationskoeffizient = 0.9686384432
df = 243
p <= 0.001 %

Fig. 31: Comparison between SIMMAX estimated and measured sea surface temperatures: a) winter, b) summer. + = data from PFLAUMANN et al., 1994, o = data from cruise M 26/3.

Two gravity cores (SL 23501 and SL 23503) were studied onboard to obtain preliminary information on the paleotemperature record of the topmost 1 to 2 m. The coarse grain analysis (Fig. 32, Tables 14 and 15) accompanying the foraminiferal faunal analyses (Tables 16 and 17), showed stable sedimentation conditions in core 23501 down to 100 cm and in core 23503 down to 145 cm (Fig. 33). Below that core depth, a layer of high abundances of radiolarians and other siliceous microfossils was encountered, while the number of planktonic foraminifera was strongly reduced. The samples further downcore contained larger amounts of inorganic particles. The paleotemperatures were estimated by the Modern Analogue Technique using the EPOCH transfer formula SIMMAX24 with the Levitus temperature data set of 754 sediment-surface samples from the Atlantic Ocean.

Tab. 14: Sea surface temperature estimates for Leg M 26/3 samples. Estimates by SIMMAX24, 232 samples from North of 50°N, Dietrich-Levitus data model. sim = similarity index. w1dw = winter, 0 m, geogr. distance weighted. w1 = winter, 0 m, not geogr. distance weighted. s1dw = summer, 0 m, geogr. distance weighted. s1 = summer, 0 m, not geogr. distance weighted. std = standard deviation of the 10 most similar modern analogue samples. lat. and long. in degrees and minutes x 100.

Station	cm	w1dw	w1	std	s1dw	s1	std
23501-1	10	6.9	7.6	1.9 1	1.0	11.9	2.9
23501-1	20	6.7	7.4	2.0	11.2	12.1	2.9
23501-1	30	9.4	9.6	2.0	12.6	13.1	3.1
23501-1	40	8.1	8.0	1.6	11.5	11.5	1.5
23501-1	50	10.5	10.7	1.0	14.1	14.6	2.0
23501-1	60	9.7	10.0	2.4	13.5	14.1	3.4
23501-1	70	8.1	8.4	2.6	11.7	12.3	3.3
23501-1	80	9.5	9.8	1.9	13.0	13.5	3.0
23501-1	90	7.4	8.3	2.3	11.0	11.7	3.2
23501-1	98	9.7	9.8	1.1	13.0	13.2	1.6

Tab. 15: Sea surface temperature estimates for the Norwegian shelf core SL 23503-1. For legend see Table 13.

Station	cm	w1dw	w1	std	s1dw	s1	std
23503-1	0	6.8	7.4	1.9	10.9	11.8	3.0
23503-1	5	6.8	7.7	2.4	11.6	13.1	3.8
23503-1	15	7.1	8.7	2.9	12.3	14.4	3.9
23503-1	25	6.9	8.2	2.6	11.8	13.5	3.5
23503-1	35	6.5	7.0	1.9	11.2	12.0	2.9
23503-1	45	6.7	7.1	1.9	11.4	12.1	2.9
23503-1	55	6.5	7.0	1.9	11.2	12.0	2.9
23503-1	65	6.8	7.4	1.9	10.9	11.8	3.0
23503-1	75	6.7	7.1	1.9	11.3	12.1	2.9
23503-1	85	6.8	7.4	1.9	10.9	11.8	3.0
23503-1	95	6.4	6.3	1.3	10.3	10.2	1.1
23503-1	105	6.5	6.6	0.8	10.5	10.6	0.5
23503-1	115	6.0	5.8	0.9	9.9	9.3	1.1
23503-1	125	6.8	7.6	2.0	11.0	11.9	2.9
23503-1	135	6.1	6.0	1.0	10.0	9.8	0.9
23503-1	145	6.0	5.8	0.9	10.0	9.5	1.1
23503-1	155	6.1	5.9	0.9	10.0	9.6	1.1
23503-1	165	6.3	6.4	0.9	10.1	9.9	1.0
23503-1	175	6.6	7.2	1.9	10.7	11.6	3.0
23503-1	185	6.7	7.1	2.4	10.7	11.0	3.6
23503-1	195	6.1	6.3	0.9	10.0	9.8	1.0

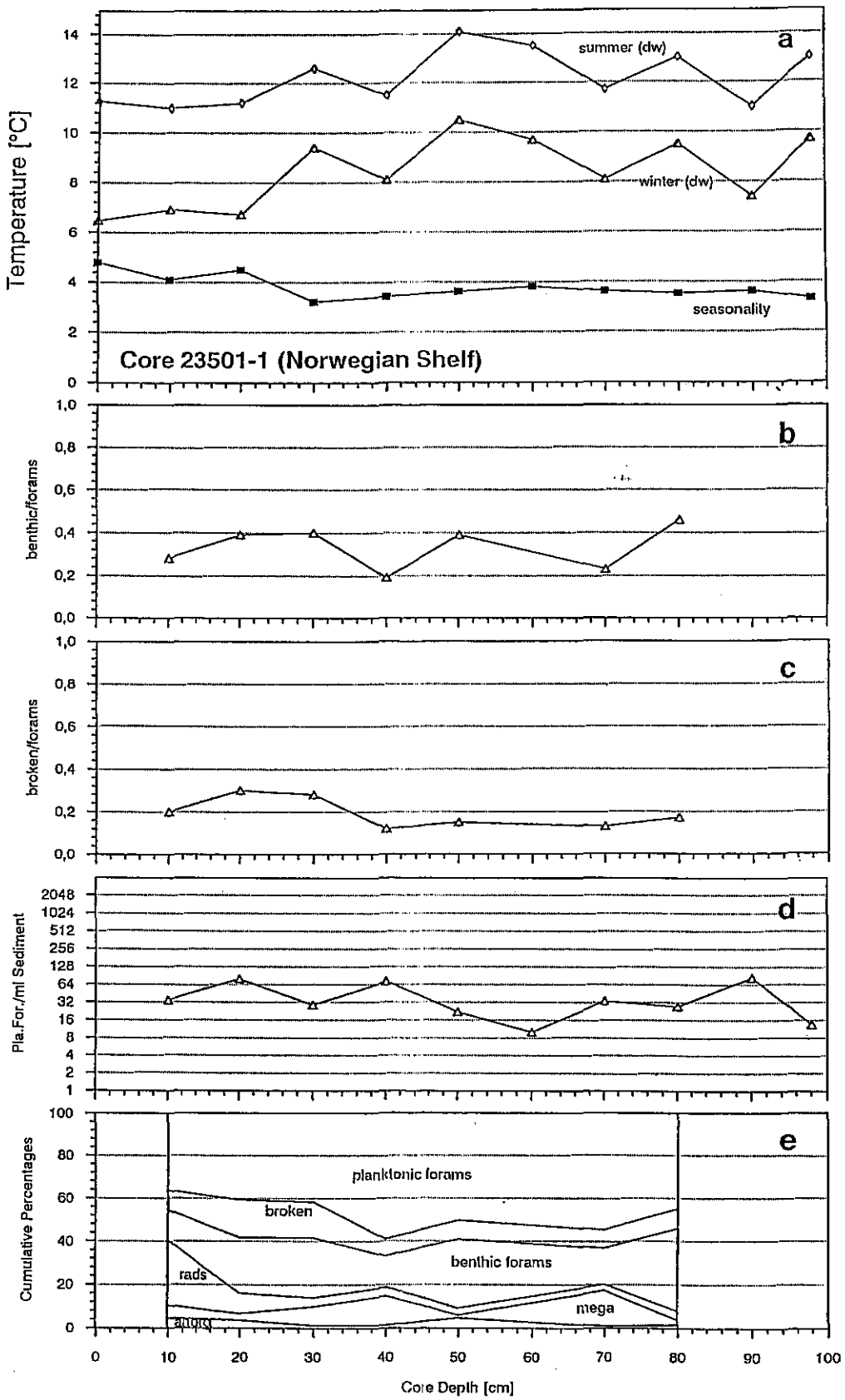

Fig. 32: Coarse grain analysis and paleotemperature estimates of the topmost metres of gravity core SL 23501-1 from the Norwegian shelf. Diagrams denote from top to bottom: Estimates of seasurface temperatures by the SIMMAX24 transfer formula; Portion of benthonic foraminifera > 0.150 mm; Portion of broken specimens of the planktonic foraminifera; Number of planktonic foraminifera > 0.150 mm per ml sediment; Cumulative percentages of the main components > 0.150 mm.

Both cores show only small variations in temperature. The estimates of the lowermost samples of core 23503 are based on a too small number of specimens, therefore the values are not very meaningful. However, Pleistocene conditions were not reached. This points to high sedimentation rates in this area, more than 10 cm/1000 years for 23501 and more than 20 cm/1000 years in 23503 and promises good time resolution for shorebased investigations on the paleoceanographic record of the Norwegian Coastal Current.

Tab. 16: Coarse grain analysis data for the Norwegian shelf core SL 23503-1. Values in percentages of all particles > 0.150 mm. sed = inorganic particles, mega = megafossils, rads = siliceous microfossils, pell = fecal pellets, bent = benthonic foraminifera, brok = broken planktonic foraminifera, plaf = whole planktonic foraminifera.

Station	cm	sed	mega	rads	pell	bent	brok	plaf	count
23501-1	10	4.7	5.7	30.0	0.0	14.0	9.3	36.4	473
23501-1	20	3.6	3.1	9.3	0.0	25.8	17.5	40.7	194
23501-1	30	1.2	8.7	4.1	0.0	27.6	16.6	41.9	344
23501-1	40	1.2	13.5	4.1	0.0	14.3	7.8	59.2	245
23501-1	50	4.6	1.4	3.2	0.0	31.7	8.7	50.5	218
23501-1	60	0.0	0.0	0.0	0.0	0.0	0.0	100	1
23501-1	70	1.0	16.2	2.9	0.0	16.6	8.4	54.9	308
23501-1	80	1.6	2.3	4.0	0.0	37.9	9.2	44.9	303

Tab. 17: Coarse grain analysis data for the Norwegian shelf core SL 23503-1. For legend see Table 16.

Station	cm	sed	mega	rads	pell	bent	brok	plaf	count
23503-1	0	7.1	1.8	2.0	0.0	37.9	8.0	43.3	1132
23503-1	5	4.2	1.0	1.0	0.0	29.3	10.4	54.1	499
23503-1	15	1.3	2.4	3.0	0.0	31.1	15.4	46.7	832
23503-1	25	2.0	1.6	2.5	0.0	20.1	15.0	58.8	687
23503-1	35	0.4	0.4	0.2	0.0	25.0	19.2	54.8	480
23503-1	45	1.7	0.1	2.5	0.0	25.3	26.2	44.2	764
23503-1	55	1.3	0.7	1.1	0.0	20.3	22.3	54.3	622
23503-1	65	2.1	1.3	2.5	0.0	23.1	21.2	49.7	791
23503-1	75	4.9	2.2	3.8	0.0	20.5	18.3	50.3	366
23503-1	85	5.0	0.4	1.0	0.0	21.8	19.7	52.1	482
23503-1	95	4.4	0.4	1.0	0.0	29.6	17.7	46.9	733
23503-1	105	6.2	1.5	0.9	0.0	29.1	13.6	48.7	337
23503-1	115	7.4	1.1	2.6	0.0	27.8	21.8	39.3	611
23503-1	125	5.7	1.0	2.0	0.0	30.0	25.2	36.2	600
23503-1	135	2.7	6.1	2.8	0.0	30.3	24.2	33.9	819
23503-1	145	0.7	13.9	2.0	0.0	13.9	14.6	55.0	151
23503-1	155	2.9	14.4	38.6	0.0	8.6	5.6	29.8	409
23503-1	165	22.2	7.2	3.2	0.0	14.0	5.9	47.5	221
23503-1	175	2.5	4.0	2.7	0.0	29.7	18.6	42.5	630
23503-1	185	0.0	11.1	18.5	0.0	27.8	3.7	38.9	54
23503-1	195	4.2	14.6	31.2	0.0	4.2	4.2	41.7	48

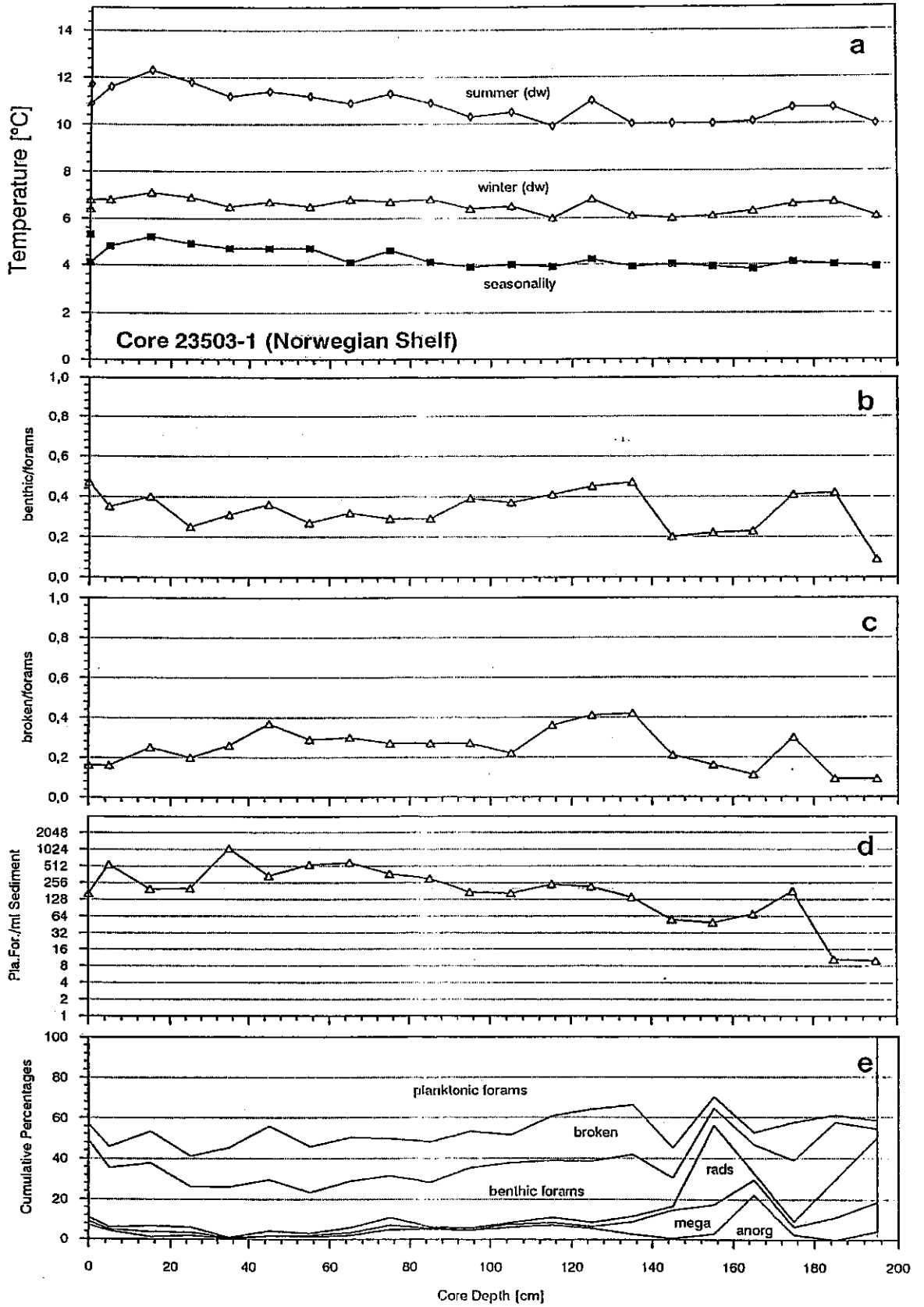

Fig. 33: Coarse grain analysis and paleotemperature estimates of the topmost two metres of gravity core SL 23503-1 from the Norwegian shelf. Diagrams denote from top to bottom: Estimates of seasurface temperatures by the SIMMAX24 transfer formula; Portion of benthonic foraminifera > 0.150 mm; Portion of broken specimens of the planktonic foraminifera; Number of planktonic foraminifera > 0.150 mm per ml sediment; Cumulative percentages of the main components > 0.150 mm.

5.4.4 Paleoceanography of the East Greenland Margin: Temperature Transfer Functions (U. Pflaumann, H. Hensch)

Important insight into the oceanographic and climate history of the last 300.000 years has been gained thanks to sedimentary, isotopic, and micropaleontological investigations of cores from the Greenland-Iceland-Norwegian Sea. We now focus to obtain a high time resolution of the climatic conditions and evolution for the past 30.000 years. The aim is to study the impact of the various abrupt climatic changes on the record of former surface- and deep-water circulation by means of various proxy data. It was planned to collect many sediment cores in the hemipelagic environment off Greenland in water depths between 1200 and 3500 m. This goal was only partially achieved due to the bad weather and sea conditions. However, we gained six box cores with sediment recovery of 30-40 cm. The initial investigations show that more detailed shorebased studies will provide a good time resolution for the Holocene paleoclimatic history.

The sediment surfaces were slightly damaged but, as expected, the planktonic faunal composition predominantly consists of left coiling *Neogloboquadrina pachyderma* small amounts of right coiling forms of the same species and of *Globigerina quinqueloba* and *G. bulloides*. accompany this species (Table 18). Using the combined Dietrich/Levitus set (SEIDOV, in prep.; Table 19) as temperature data base, the new samples off Greenland yielded winter temperatures falling within the previous scatter. However, the summer estimates are anomalously warm by more than 2°C (Fig. 34 to 39). This trend was also observed in the previous data set and may indicate a non-linear mode of the transfer function. Another explanation of the deviation may be the crude grid of the present temperature data base available, which may not sufficiceto resolve the strong gradients along the Greenland Margin.

Tab. 18: Percentages of planktonic foraminifera in sediment surface samples from the East Greenland Margin.

Surface sample no.	23506-1	23507-1	23508-1	23509-1	23510-1	23511-2	23512-1
Globigerina							
bulloides	0.08	0.00	0.07	0.00	0.00	0.55	0.17
quinqueloba l.	0.40	0.60	1.68	0.50	0.17	0.76	0.50
quinqueloba r.	0.00	0.20	0.56	0.00	0.33	0.42	0.39
Globigerinella							
aequilateralis	0.00	0.00	0.00	0.00	0.00	0.00	0.00
Orbulina							
universa	0.00	0.00	0.00	0.00	0.00	0.00	0.00
Globorotalia (Turborotalia)							
inflata	0.00	0.00	0.00	0.00	0.00	0.00	0.00
Neogloboquadrina							
pachyderma l.	98.40	98.20	95.97	99.34	98.50	97.51	98.38
pachyderma r.	1.12	1.00	1.72	0.17	1.00	0.76	0.56
Globigerinita							
glutinata	0.00	0.00	0.00	0.00	0.00	0.00	0.00
Sum counted	882	501	744	786	601	1444	1791

Tab. 19: Sea surface temperatures interpolated from the combined Dietrich-Levitus data set of Seidov (in prep.) for the East Greenland Margin samples. For legend see Table 13.

Station	latitude	longitude	w1	s1	w5	s5
23506-1	72°23.57'N	07°36.14'W	-0.20	4.03	-0.13	2.06
23507-1	73°49.80'N	09°15.10'W	-0.92	2.67	-0.72	1.19
23508-1	73°51.60'N	09°23.70'W	-0.92	2.65	-0.73	1.18
23509-1	73°50.00'N	13°30.10'W	-1.04	1.06	-1.01	0.40
23510-1	73°27.20'N	13°25.90'W	-0.97	1.60	-0.91	0.66
23511-2	73°12.90'N	15°00.10'W	-1.01	1.17	-1.00	0.39
23512-1	72°56.50'N	13°25.40'W	-0.90	2.07	-0.84	0.88

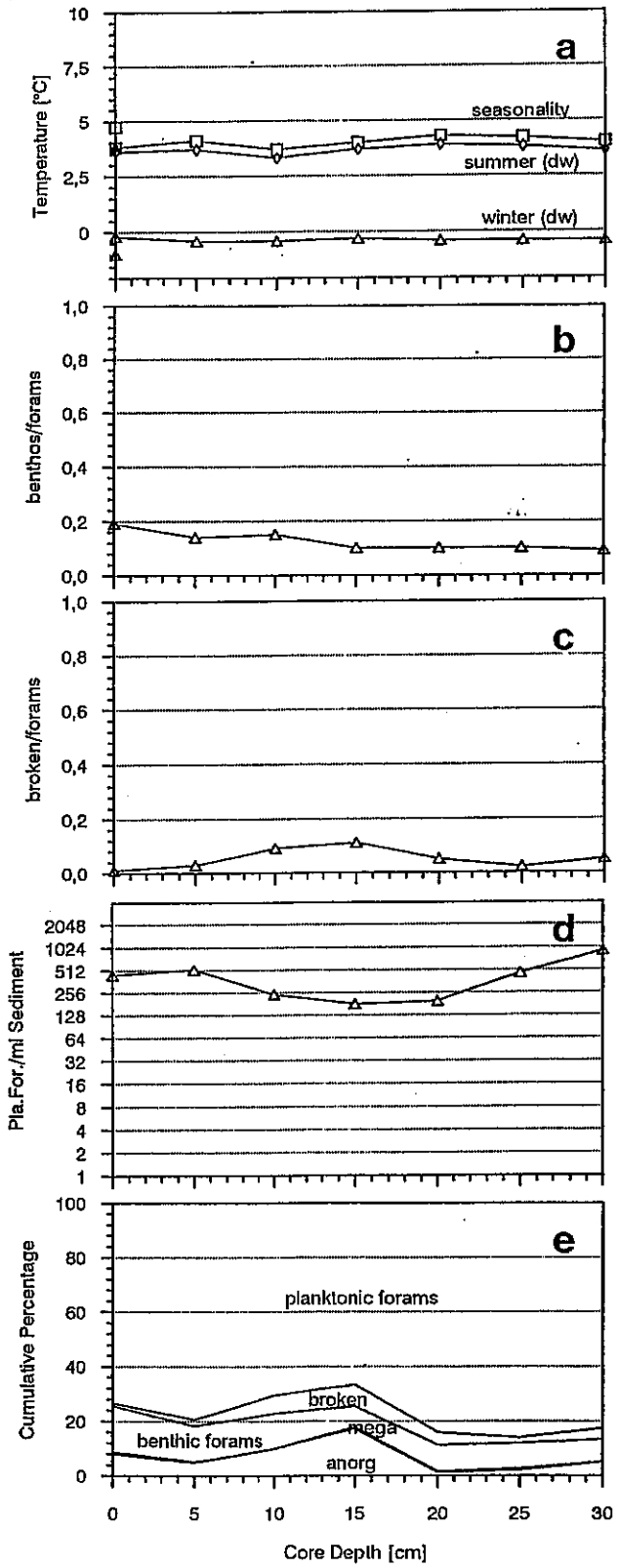

Fig. 34: Coarse grain analysis and paleotemperature estimates of the large boxcore samples GKG 23506 Eastern Greenland Margin. Diagrams denote from top to bottom: Estimates of seasurface temperatures by the SIMMAX24 transfer formula; Portion of benthonic foraminifera > 0.150 mm; Portion of broken specimens of the planktonic foraminifera; Number of planktonic foraminifera > 0.150 mm per ml sediment; Cumulative percentages of the main components > 0.150 mm.

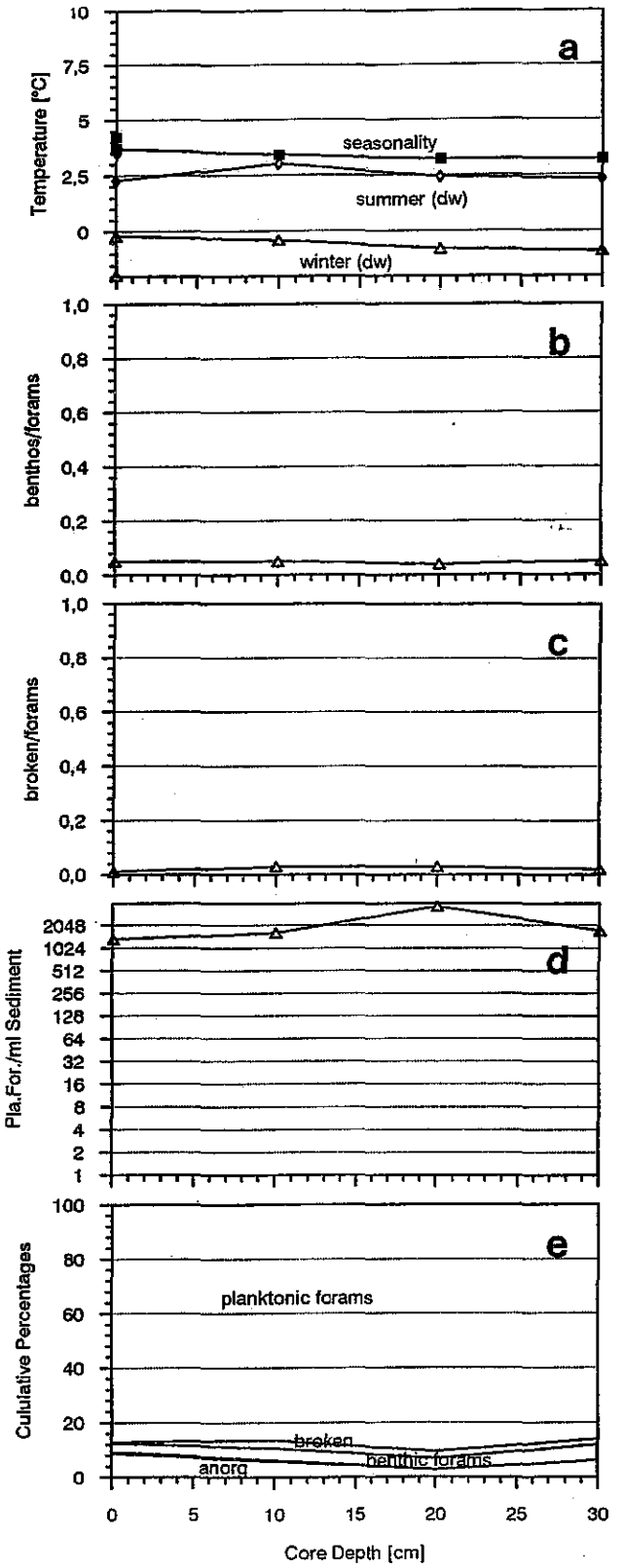

Fig. 35: Coarse grain analysis and paleotemperature estimates of the large box core samples GKG 23507 E-Greenland Margin. Diagrams denote from top to bottom: Estimates of seasurface temperatures by the SIMMAX24 transfer formula; Portion of benthonic foraminifera > 0.150 mm; Portion of broken specimens of the planktonic foraminifera; Number of planktonic foraminifera > 0.150 mm per ml sediment; Cumulative percentages of the main components > 0.150 mm.

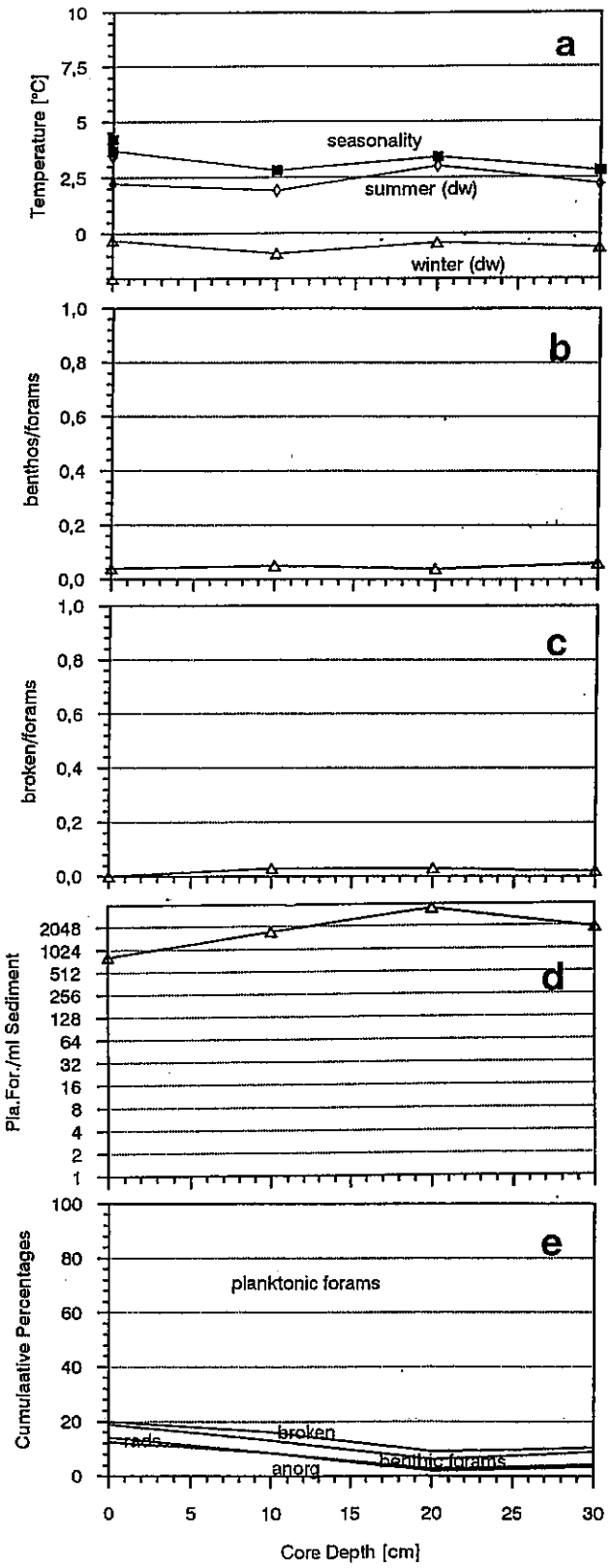

Fig. 36: Coarse grain analysis and paleotemperature estimates of the large boxcore samples GKG 23508 E-Greenland Margin. Diagrams denote from top to bottom: Estimates of seasurface temperatures by the SIMMAX24 transfer formula; Portion of benthonic foraminifera > 0.150 mm; Portion of broken specimens of the planktonic foraminifera; Number of planktonic foraminifera > 0.150 mm per ml sediment; Cumulative percentages of the main components > 0.150 mm.

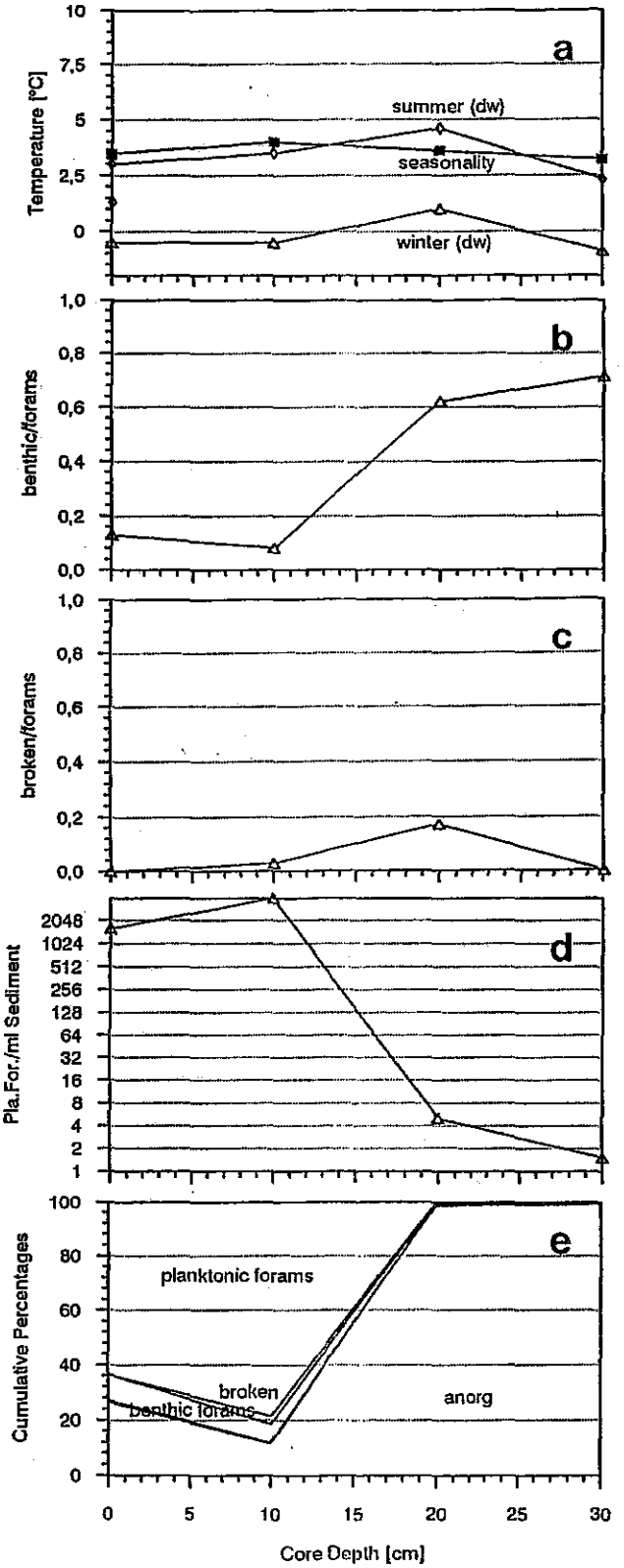

Fig. 37: Coarse grain analysis and paleotemperature estimates of the large boxcore samples GKG 23509 E-Greenland Margin. Diagrams denote from top to bottom: Estimates of seasurface temperatures by the SIMMAX24 transfer formula; Portion of benthonic foraminifera > 0.150 mm; Portion of broken specimens of the planktonic foraminifera; Number of planktonic foraminifera > 0.150 mm per ml sediment; Cumulative percentages of the main components > 0.150 mm.

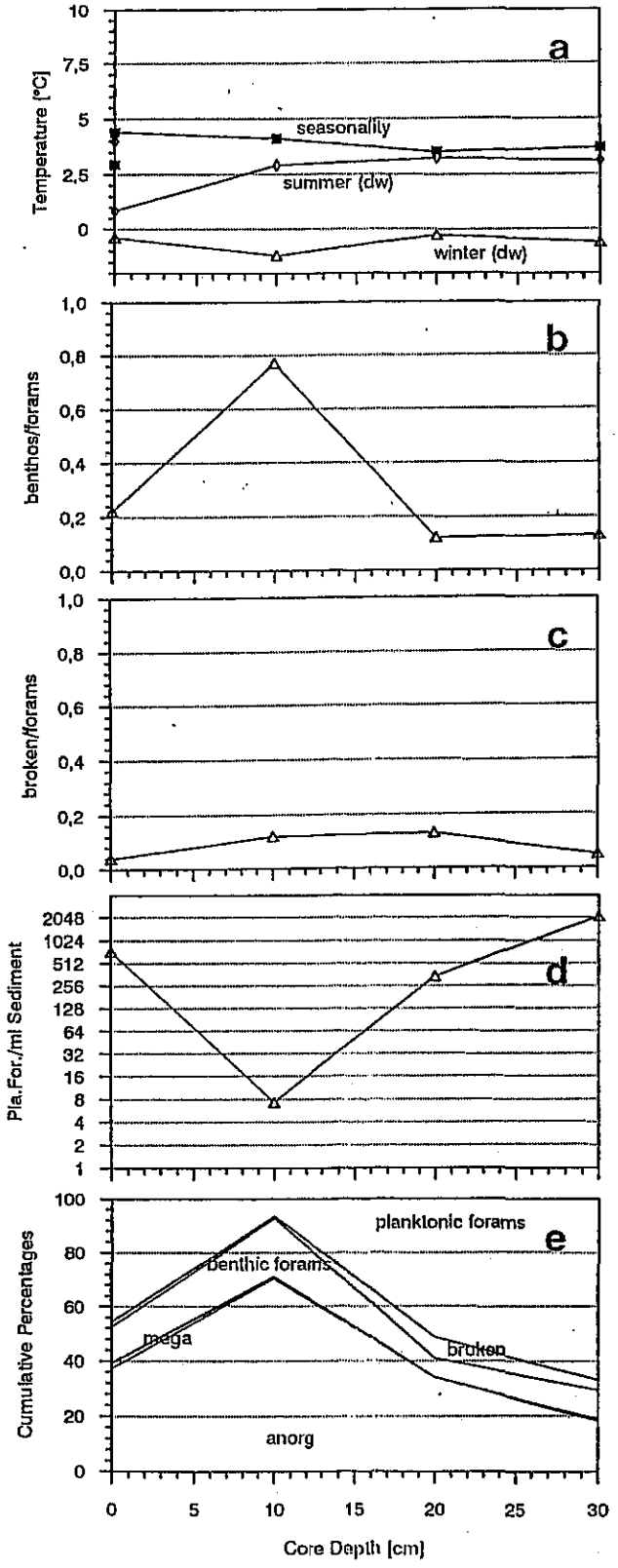

Fig. 38: Coarse grain analysis and paleotemperature estimates of the large boxcore samples GKG 23511 E-Greenland Margin. Diagrams denote from top to bottom: Estimates of seasurface temperatures by the SIMMAX24 transfer formula; Portion of benthonic foraminifera > 0.150 mm; Portion of broken specimens of the planktonic foraminifera; Number of planktonic foraminifera > 0.150 mm per ml sediment; Cumulative percentages of the main components > 0.150 mm.

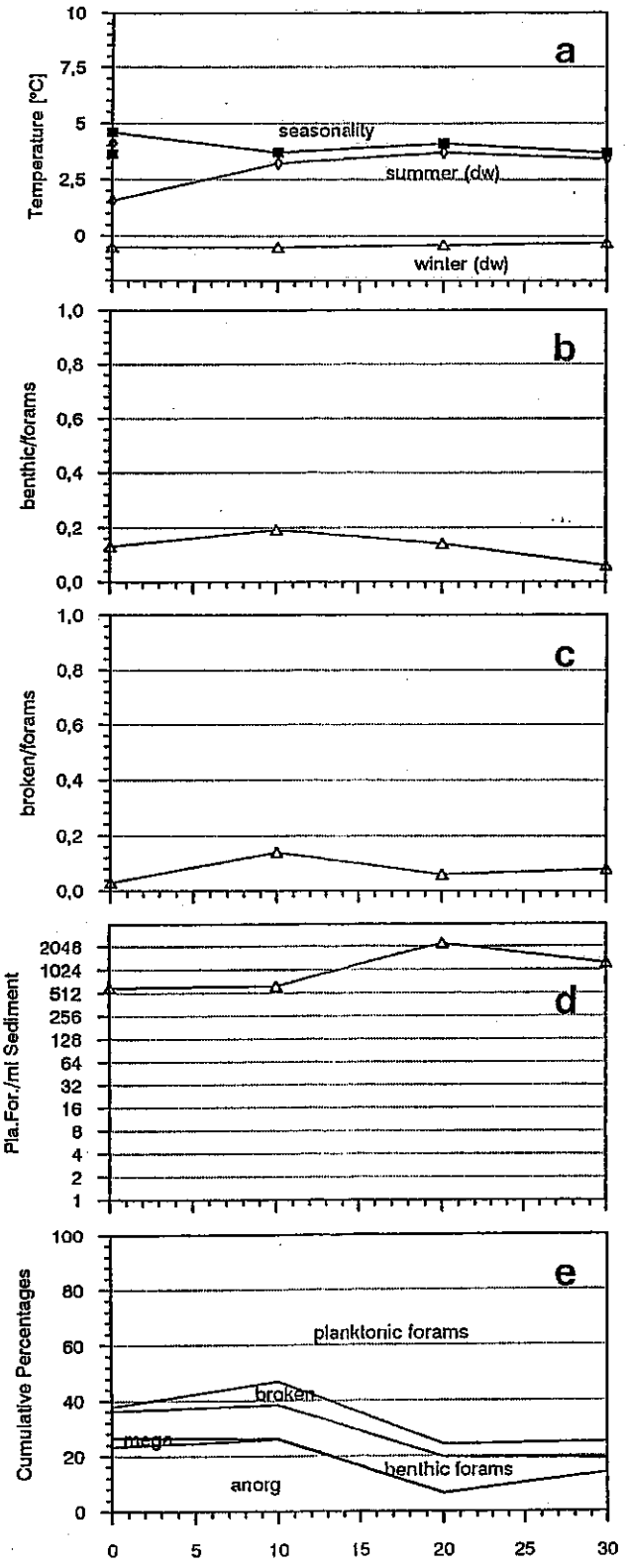

Fig. 39: Coarse grain analysis and paleotemperature estimates of the large boxcore samples GKG 23512 E-Greenland Margin. Diagrams denote from top to bottom: Estimates of seasurface temperatures by the SIMMAX24 transfer formula; Portion of benthonic foraminifera > 0.150 mm; Portion of broken specimens of the planktonic foraminifera; Number of planktonic foraminifera > 0.150 mm per ml sediment; Cumulative percentages of the main components > 0.150 mm.

5.4.5 Parasound and Hydrosweep Profiling: Greenland Basin

(F.-J. Hollender, J. Baas, M. Bobsien, C. Baumgärtner)

In 1992 the IOS long range side-scan sonar GLORIA, was used on a cruise of the RV LIVONIA to map large-scale changes in sedimentary processes along the East Greenland continental-margin (MIENERT et al., 1993). The research area encompassed, from North to South, the Boreas Basin, the Greenland Basin, and a small basin north of Jan Mayen. One of the aims of the present cruise was to collect detailed information about the surface and subsurface geology of the Greenland Basin in order to correlate various back-scattering characteristics of the GLORIA data with the sea bed topography and the physical properties of the sediment. Therefore, Parasound and Hydrosweep profiles were run and box cores and gravity cores taken. In this chapter the preliminary results of the Parasound and Hydrosweep data are presented. For a description of the Parasound and Hydrosweep systems the reader is referred to chapter 5.4.11.4 of this report.

Results

The Parasound records are of good quality. The quality of the Hydrosweep records is highly variable due to bad weather conditions. The preliminary results are based on the analogue data. Details will become available after the post-processing of the digital data. Profiles of various length and direction (554, 555, 558, 561, 563, 565, 567, 569, 571, 572, 573 and 574) were run in the Greenland Basin (see 7.3 for positions). The seismic sequence dominantly consists of regularly stratified reflectors. Some characteristic features that diverge from this pattern are as follows:

Submarine channels

Profile 555 comprised ten traverses across a sinuous channel. The channel has a W-E orientation at approximately 73°30'N and 9°-10°W. It gradually changes into a downstream direction from V-shaped into U-shaped (Fig. 40), with characteristic steep slopes at the outer bank of the bend and more gradual slopes at the inner bank of the bend. Concurrently, the channel depth increases from approx. 50 m to approx. 90 m. In all cross-sections, terraces are present, probably signifying multiple stages of incision. Smaller channels were observed in the profiles 563 and 565. They make up an area with numerous features as opposed to the single meandering channel described above. Their average depth is approx. 10 m.

Sediment waves

Sediment waves were observed in profile 569 (Fig. 41). They measure several metres in height and several kilometres in wavelength. Their geometry is continuous downward into the sedimentary sequence. By analogy with other features of this kind, there is the implication of current flow over a long period of time in the direction of the side with the lower rate of sedimentation, i.e. towards the right in Figure 41. Having a steep angle of climb, the sediment waves could be classified as "in-phase" climbing bedforms. This suggests that bedform migration is of minor importance relative to the rate of sedimentation from suspension.

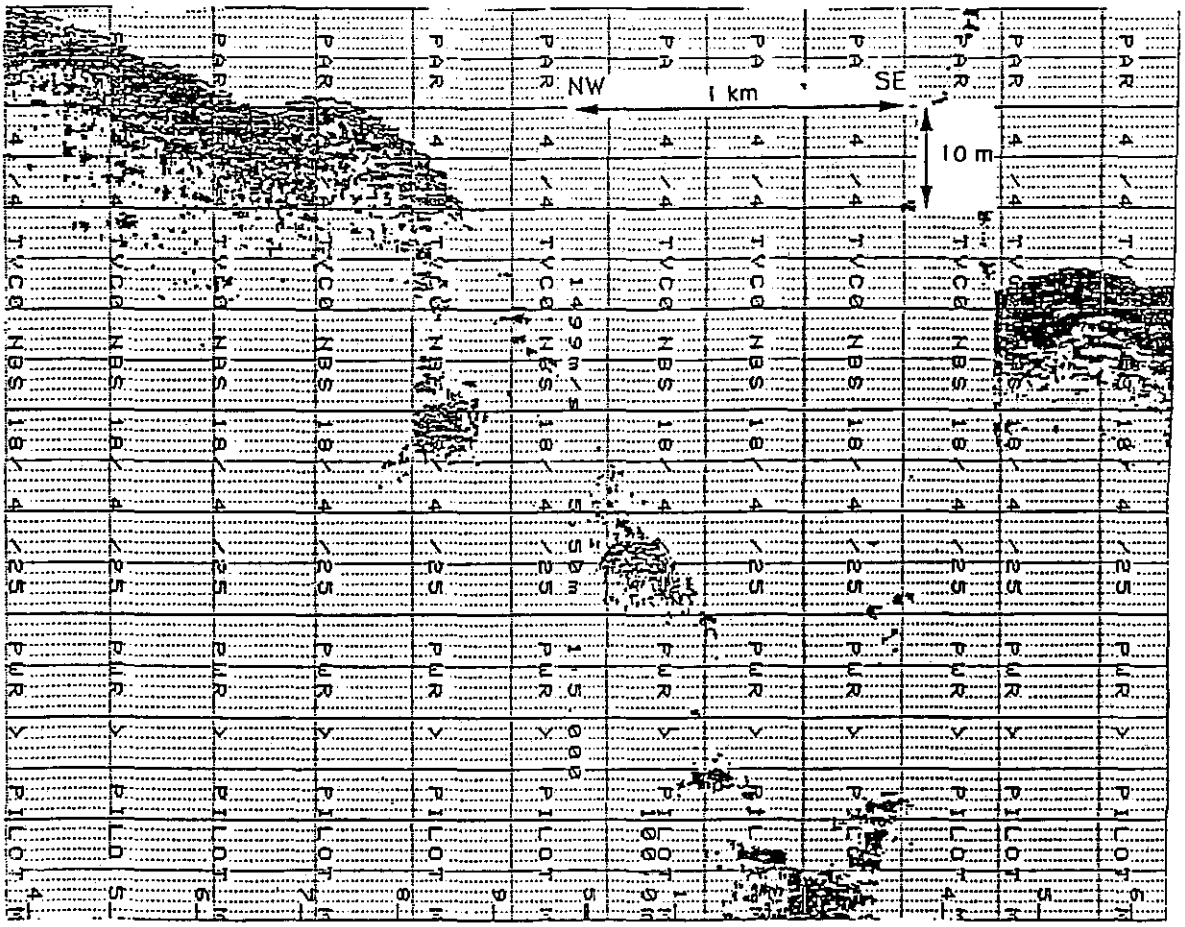

Fig. 40: Submarine channel. Note slightly U-shaped channel floor, steep outer bend and gradual inner bend. Profile 555. Water depth: 3040 m. Location: 73°34.021 N 10°03.541'W.

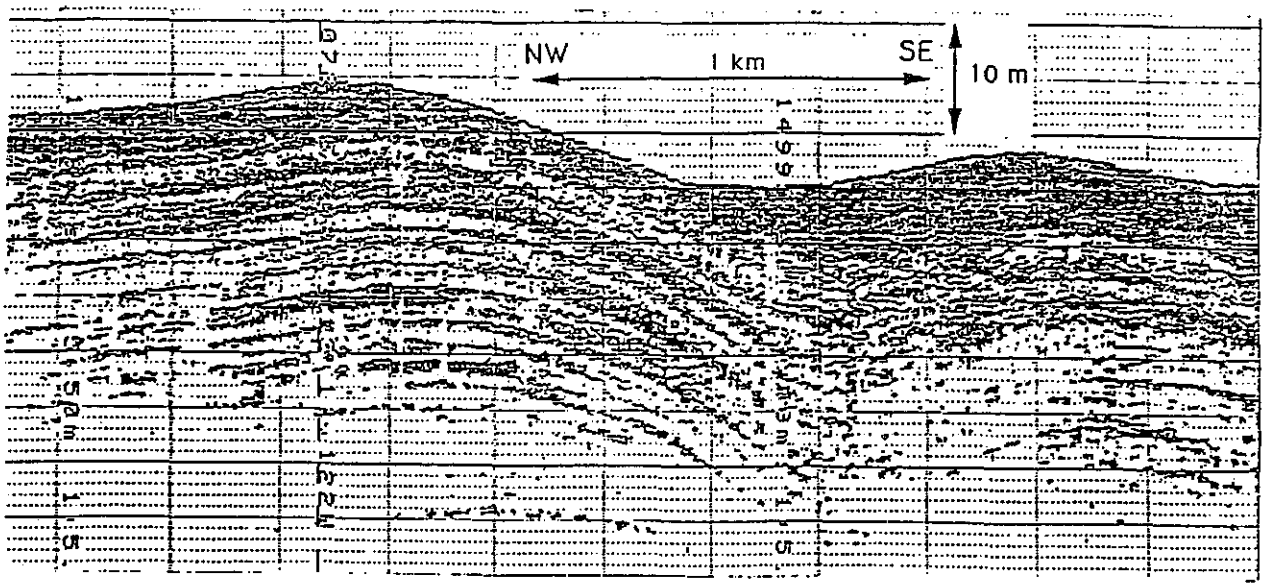

Fig. 41: Sediment waves. Profile 569. Water depth: 2580 m. Location: 72°53.911'N 13°11.134'W.

Gravity flow deposits

Several profiles show chaotic seismic units, which are interpreted as gravity flow deposits (e.g. 554, 561 and 574). They have a variety of forms; some are only a few hundreds of metres long whereas others extend for tens of km (Fig. 42).

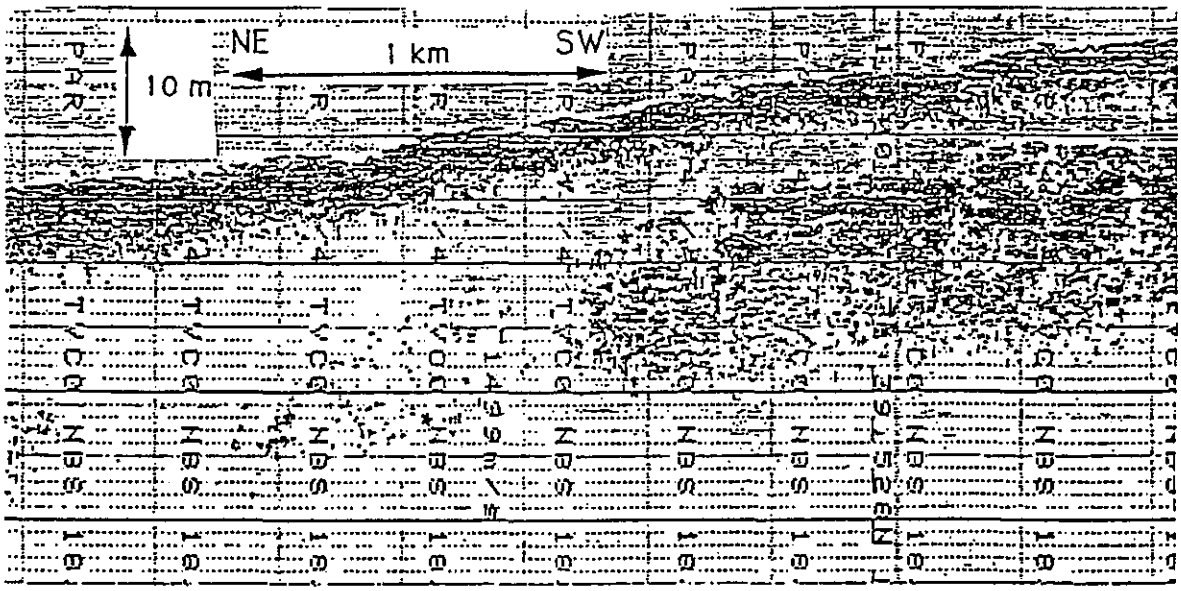

Fig. 42: Gravity flow deposits. Profile 561. Water depth: 2860 m.
Location: 73°39.526'N 12°03.376'W.

5.4.6 Sedimentary Processes: East Greenland Margin

(J. Mienert, N.H. Kenyon, F.-J. Hollender)

The working area extends from 72°N to 74°N and from 9°W to 15°W, ranging in water depth from 2200 to 3300 m. The following two major processes act on the sea floor. (1) Downslope processes have formed a turbidity current channel system, which has several tributary channels in the upper slope region that are up to 10 m deep and 10 km wide. Farther downslope it develops into a V-shaped, 80 m-deep, and 10 km-wide channel and it broadens into a U-shaped channel just north of Vesteris Banken. Two 50 cm long box cores retrieved hemipelagic sediments that are probably of Holocene age. One is located within the channel and the other comes from the levee of the channel. At the base of the cores there are ash layers and also sandy sediments. One of the ash layers may be the Vedde ash which has an age of about 10.000 years. Our preliminary results lead to the conclusion that this approx. 500 km long channel system in the Greenland Basin is presently inactive. The last turbidity flows most likely took place during the transition from the last glacial to interglacial time. A second downslope process is observed on Parasound records, which show debris flows on the slope in water depths of about 2200 m. Below this water depth, no debris flows were recorded. (2) The along-slope transport of sediments is shown by sediment waves which are thought for the most part to be due to contour current activity. In a few cases also turbidity current activity on the levees of the channel forms sediment waves. The current-controlled bedforms have amplitudes of up to 10 m and wavelengths of up to 2 km. The wave crests strike in an approximately E-W direction, indicating along-slope transport near the oceanic ridge of Jan Mayen where the currents are deflected from a southerly to a more southeastern direction. Another type of sediment waves is found on the slope off East Greenland. These waves have lower wavelength but similar amplitudes, and are believed to be due to flow stripping of the upper part of turbidity currents. We do not know whether the various contour-current and turbidity-current controlled wave fields are presently active.

5.4.7 Visual Descriptions of Margin Sediments

(U. Pflaumann, W. Rehder)

East Greenland Margin

Six large box cores (GKG) were successfully taken on the eastern margin of Greenland and two in the adjacent basins. The sediments were visually described onboard immediately after their retrieval (Table 20). The sediment surface was washed out from the heavy sea conditions. It damaged at least the uppermost 5 to 10 mm of the soft sediment as it was stirred up and partly lost, with the water runoff. The uppermost centimetres of sediment are monotonous silty clays containing at the surface, big tests of *Pyrgo*, tubes of agglutinated foraminifera, and/or worms. In many cases sponges in a life position were observed. The sediments below the surface were investigated later when the sides of the box cores were opened. In most cases the sediment was stiff enough to enable a quick visual inspection,

despite the strong movements of the ship. For further studies the sediment core was sampled according to the following general scheme:

1) Sediment surface, 10 x 10 cm, 0-1 cm deep, conserved by Rose Bengal
2) " , 10 ml syringe, 0-1 cm, for plankton foram studies
3) " , 10 ml syringe, 0-1 cm, for stable isotope studies
4) " , polyethylene bag, 0-1 cm, bulk sample
5) Sediment column: 2 archive tubes for Kiel and Tübingen core repository
6) " : 2 tubes to be cut in the ship board lab into 1 cm slices and packed into bags, for Kiel and Tübingen repository
7) " : X-ray slice, to be prepared onboard
8) " : 10 ml syringes at 5 cm intervals for shorelab plankton foram analysis
9) " : ditto, for stable isotope studies
10) " : 10 ml syringes for shipboard initial research of the plankton foraminiferal species content.

Further information became available in the course of the preparation of the X-ray slices in the onboard laboratory under better conditions and without the time restrictions.

Tab. 20: Coarse grain analysis data for the large boxcore sediments from Station OG6 (23505-1 and 23506-1) and from the Eastern Greenland Margin. For legend see Table 16.

Station	cm	sed	mega	rads	pell	bent	brok	plaf	count
23505-1	0	0.0	0.3	0.2	0.0	2.3	3.2	94.0	972
23505-1	5	1.8	0.3	0.3	0.0	5.7	5.4	86.3	871
23505-1	10	2.6	0.3	0.0	0.0	11.0	11.8	74.3	762
23505-1	15	22.4	2.0	0.0	0.0	44.9	16.3	14.3	49
23506-1	0	7.8	0.8	0.1	0.0	16.8	1.1	73.4	1248
23506-1	5	4.8	0.3	0.0	0.0	13.2	2.3	79.3	1307
23506-1	10	9.9	0.0	0.0	0.0	12.9	6.7	70.5	685
23506-1	15	17.1	0.6	0.0	0.0	7.6	8.0	66.7	537
23506-1	20	1.3	0.2	0.0	0.0	9.7	4.7	84.1	465
23506-1	25	2.1	0.6	0.0	0.0	9.2	2.0	86.2	1070
23506-1	30	5.2	0.0	0.0	0.0	8.1	4.1	82.6	2190
23507-1	0	8.7	0.5	0.0	0.0	3.3	0.2	87.3	574

Tab. 20: continued

Station	cm	sed	mega	rads	pell	bent	brok	plaf	count
23507-1	10	5.8	0.3	0.0	0.0	4.5	2.8	86.5	706
23507-1	20	2.7	0.1	0.0	0.0	4.0	2.5	90.7	1019
23507-1	30	6.2	0.0	0.0	0.0	5.7	2.1	86.1	761
23508-1	0	12.5	1.6	0.4	0.0	4.4	1.0	80.1	1010
23508-1	10	8.5	0.1	0.0	0.0	4.6	2.9	84.0	1293
23508-1	20	1.9	0.8	0.0	0.0	3.5	2.9	90.9	485
23508-1	30	3.4	0.8	0.0	0.0	4.6	1.6	89.6	1085
23509-1	0	26.3	0.8	0.1	0.0	9.4	0.0	63.5	1507
23509-1	10	11.4	0.3	0.0	0.0	6.7	2.8	78.8	632
23509-1	20	98.6	0.0	0.1	0.0	0.8	0.1	0.5	1923
23509-1	30	99.2	0.1	0.1	0.0	0.5	0.0	0.2	1442
23510-1	0	23.9	1.5	0.0	0.0	8.9	2.4	63.3	949
23511-2	0	37.3	1.8	0.2	0.0	13.1	1.9	45.8	3150
23511-2	10	70.3	0.7	0.0	0.0	21.6	0.9	6.4	559
23511-2	20	34.0	0.0	0.0	0.0	7.0	7.7	51.3	1429
23511-2	30	18.3	0.7	0.0	0.0	10.4	3.7	66.9	586
23512-1	0	23.3	3.1	0.1	0.0	9.7	1.6	62.2	2878
23512-1	10	25.9	0.3	0.0	0.0	12.2	8.5	53.1	588
23512-1	20	6.3	0.4	0.0	0.0	12.8	4.7	75.8	554
23512-1	30	14.0	0.0	0.0	0.0	5.0	6.1	74.9	622

Microscopic studies

For initial information about the coarse grain content, a known volume of the sediment samples was washed through a 63 µm sieve, and the size fraction > 0.150 mm was evaluated quantitatively. The particles were grouped into: a) inorganic particles, including dropstones, b) megafossils, c) siliceous microfossils (mainly radiolarians), d) benthic foraminifera (including broken remains), e) broken parts of planktonic foraminifera; and f) complete planktonic foraminifera. The last group was further subdivided into species and variants.

Remarks on the box core sediments

GKG 23506 (72°23.6'N, 7°36.2'W, 2670 m)

The brownish-grey silty to sandy clay showed that the tests of the benthonic foraminifer *Pyrgo* are slightly more abundant between 20 and 28 cm, and some stronger bioturbation occurs between 20 and 22 cm. Seven samples looked at microscopically indicate the presence

of a unit with reduced number of planktonic foraminifera/ml sediment. The account for the reduced abundace of foraminifera between 10 and 20 cm only partly higher amount of broken specimens. The benthic portion of the forams is relatively low (20%) with diminishing portions downcore. No significant changes in paleoenvironment were observed.

GKG 23507 (73° 49.8'N, 9° 15.1 W, 3150 m)
Brownish grey sandy and silty clay, 38 cm thick and fairly homogenous. The preservation of the foraminifera is excellent, with only small numbers of broken specimens. At the base of the core, two layers of volcanic ash are separated by a silty clay.

GKG 23508 (73°51,6'N, 9°23.7'W, 3202 m)
The sediment surface and the uppermost 32 cm are similar to the top unit of GKG 23507. Between 32 and 37 cm we recovered a fine sandy layer, deposited on a yellowish brown clay. This core was taken from the meandering valley of a deep-sea channel. The similarity of the topmost sedimentary record inside and outside the channel reflects current by low activity of this submarine flow system.

GKG 23509 (73°50.6'N, 13°30.1'W, 2534 m water depth)
The core contains normal hemipelagic sediments between 0 and 15 cm. At the sediment surface, small dropstones were encountered. At 20-30 cm subbottom, the amount of planktonic foraminifera is very low, indicating an additional admixture of silty or clayey material.

GKG 23511 (73°13.0'N, 15°01'W, 2230 m water depth)
This is the westernmost core of the cruise, thus representing the coldest environment. The vicinity of the steepest slope is indicated by relatively reduced numbers of foraminifera near the surface, partly caused by an admixture of inorganic components with the sand fraction. Farther downcore, the planktonic foraminiferal numbers indicated normal environmental conditions.

GKG 23512 (72°56.5'N, 13°25.4'W, 2610 m water depth)
In this core *Lamellibranchiata* were observed at the sediment surface. The number of planktonic forams is similar to that of neighbouring sites. At the base of the core (below 34 cm), reddish colours were noted.

In summary this part of the Greenland continental margin is covered by a homogenous layer of hemipelagic sediments about 20 cm thick. Below that, a more varied sedimentary record is encountered.

Norwegian margin and Basin
GKG 23505 (69°41.4'N, 0°28.8'E, 3291 m)
The uppermost sedimentary unit, a yellowish grey, foram-bearing, silty, bioturbated clay, reaches down to 12 cm core depth. The number of planktonic foraminifera is 200 specimens/ml of sediment, a more-or-less constant number not consistent with the other components of the size fraction > 0.150 mm. The lowermost sample (15 cm) investigated on the ship contains higher amounts of inorganic sediment particles. The samples at 20 cm subbottom, as well as these from the clay below 36 cm, are barren of microfossils. Shorebased studies will examine the character of the lamination between 12 and 35 cm core depth. Coarse grain analysis and paleotemperature estimates are shown in Figure 43.

The coarse grain analyses data of the gravity core 23503-1 from the Norwegian Shelf is listed in Table 10.

5.4.8 Gas and Water Seepage on the Continental Margin (SEEP)

5.4.8.1 Seep Geophysics (D. Long, J. Pheasant, D. Smith, J. Derrick,)

Various pieces of seismic surveying equipment were available to look for geophysical evidence of shallow gas at the seabed and in near seabed sediments and therefore to suggest possible sites for sampling. The equipment included deep towed side-scan sonar, deep-towed-boomer, Parasound, echo sounder and Hydrosweep. Due to deployment configurations the deep towed side-scan sonar and the deep towed boomer could not be deployed simultaneously. The success of some of the equipment was weather and sea dependent, particularly so with the Hydrosweep, where cavitation beneath the ship would cause serious distortion to the signals. During station keeping while sampling, the echosounder and the Parasound, with its gain turned to maximum, proved useful in tracking equipment to the seabed.

Skagerrak
A small grid of side scan survey lines (Lines 461-1 to 461-7) were run over the area of interest with the aim of locating features of potential gas escape (Fig. 44). Although no pockmarks had been previously reported from this area of the Skagerrak, it was hoped that bubble trains in the water column might be recorded. No such features were located. A shipwreck was identified, confirming that the survey was in the same area as the Challenger 1991 cruise when the wreck was also located. Simultaneous to the running of the side scan sonar, parasound and hydrosweep systems were operated and recorded (Parasound settings: 5 kHz, pulse length 4, gain 6.0). The results suggested that there were low amplitude (< 5 m) ridges or mounds, sub parallelling the strike of the seabed slope, although the accuracy of the hydrosweep display was uncertain. The parasound revealed acoustic penetration to approx 5 m with indistinct discontinuous subseabed reflectors. Locally some of these reflectors were

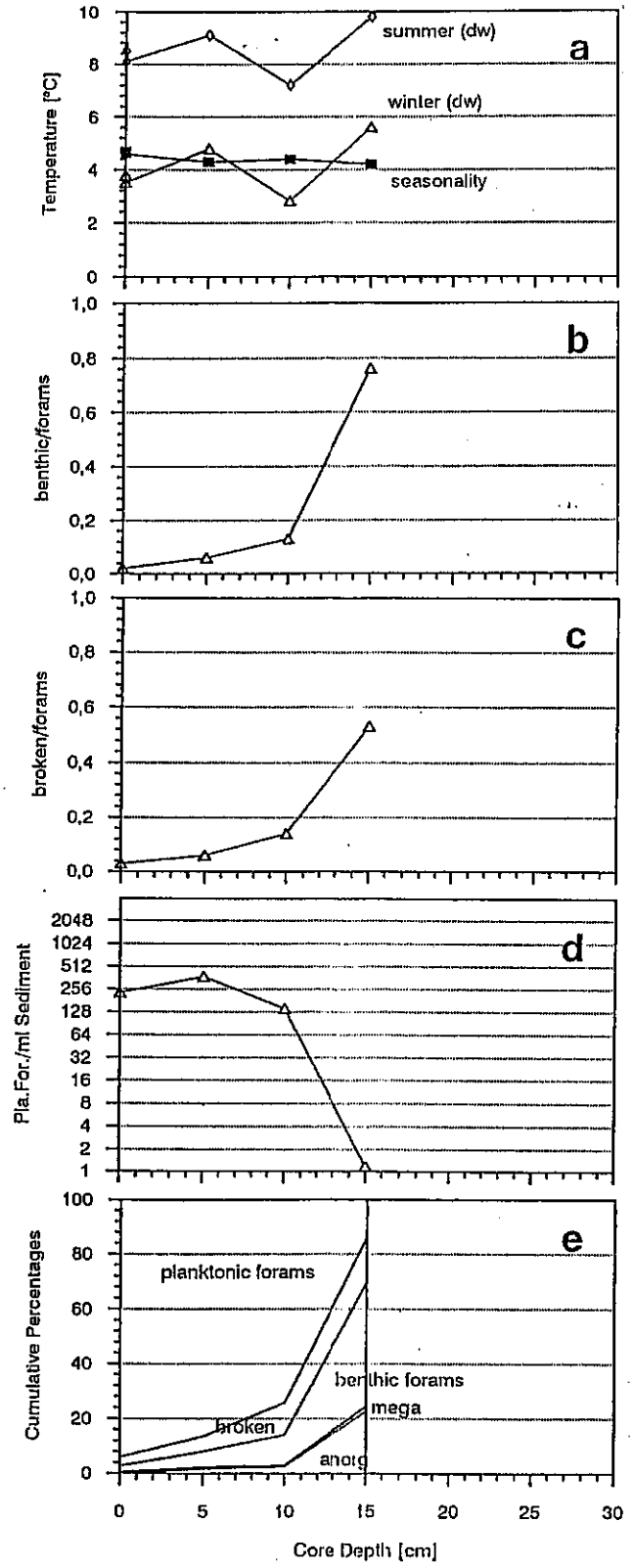

Fig. 43: Coarse grain analysis and paleotemperature estimates of the large boxcore samples GKG 23505 Norwegian Basin. Diagrams denote from top to bottom: Estimates of seasurface temperatures by the SIMMAX24 transfer formula; Portion of benthonic foraminifera > 0.150 mm; Portion of broken specimens of the planktonic foraminifera; Number of planktonic foraminifera > 0.150 mm per ml sediment; Cumulative percentages of the main components > 0.150 mm.

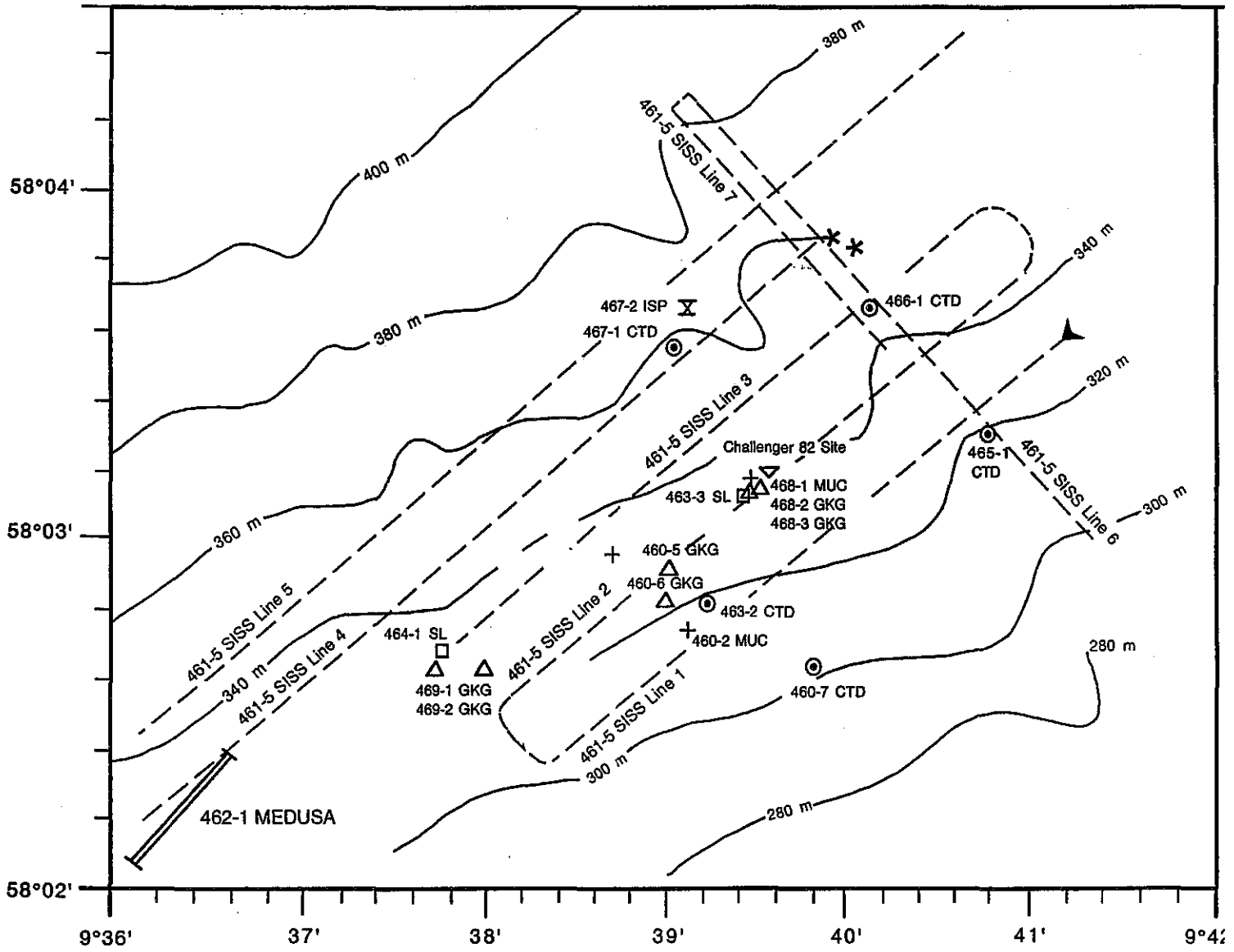

Fig. 44: Skagerrak sampling sites and survey lines; SISS = Side scan sonar, CTD = hydrographic station, GKG = Box core sites, MUC = Multicorer sites, ISP = *in situ* pump, SL = Gravity corer site, MEDUSA = *in situ* methane detection survey; *ship wreck site located 1991 and 1993 (METEOR); RV CHALLENGER seep site.

enhanced, and elsewhere, apparent acoustic blanking occured. The survey lines were positioned such that the parasound signature of the successful cores of 1991 could be determined. Initial plottings suggested that an area of acoustic blanking existed in the vicinity of the successful 1991 cores and that this might be a diagnostic parasound signature. It occured at the peak of a mound or ridge with enhanced reflectors beneath the slope on either side of the mound. A single core (Sta. 463-3) placed in this area was not successful in locating a seep. A second site chosen in an area of enhanced reflectors beneath a ridge or a mound (Fig. 45) proved more successful in locating a methane seep (Sta. 464-1).

The 1991 cruise proved that the distribution of seeps was extremely localized, so no inference is drawn on the absence of a seep from the area of apparent gas blanking. It was noted that whilst the ship was stooging about a site during the deployment of equipment, the Parasound reflectors, particularly the enhanced reflectors were discontinuous indicating the limited spatial extent of the physical features which cause them.

Faeroe - Shetland Channel

Based on a single line of processed, 3 min (1.5 min subseabed), deep seismic exploration data kindly supplied by British Petroleum illustrating suspected gas chimneys and enhanced reflectors, a deep towed side scan sonar traverse (Line 470-1) down the west Shetland slope, across the floor of the Faeroe - Shetland Channel and up the Faeroese side to approx. 800 m water depth was conducted (Fig. 46). Parasound and Hydrosweep were also run along this traverse. Not obvious, gas related features were noted at the sites suggested by British Petroleum.

On the floor of the channel, close to the foot of the Faeroese slope, a large depression with steep walls was noted (approx 1 km x 2 km x 40 m) on the Hydrosweep (Fig. 10) and side scan sonar records. The Parasound revealed little acoustic penetration of the floor of the depression suggesting the absence of a soft sediment infill. A CTD was collected from this site (Sta. 470-2) but no physical sampling. Several deep depressions attributed to current scouring have been noted previously from the centre of the channel, just east of this site (STOKER, 1989) and the depression located by this survey may have a similar origin. Initial thoughts that this crater may be due to hydrate blow-out were reduced when no CH_4 anomaly was found in the bottom water of the CTD (Sta. 470.2) although due to the low bottom water temperature and high hydrostatic pressure, methane would not be stable as a free gas in water but would occur as a hydrate.

The boomer was run along a profile (Line 471-2, Fig. 47) through all the sites suggested by BP and along a short cross profile (Line 471-1) parallel to the channel thalweg through the site considered to have the greatest potential for shallow gas. No obvious evidence of shallow gas was seen on either profile. The boomer profiles suggest that the floor of the Faeroe - Shetland Channel comprises lensoid bodies locally separated by fine layered reflectors. Box cores were taken at several localities to reveal an extremely coarse bottom sediment, e.g. site

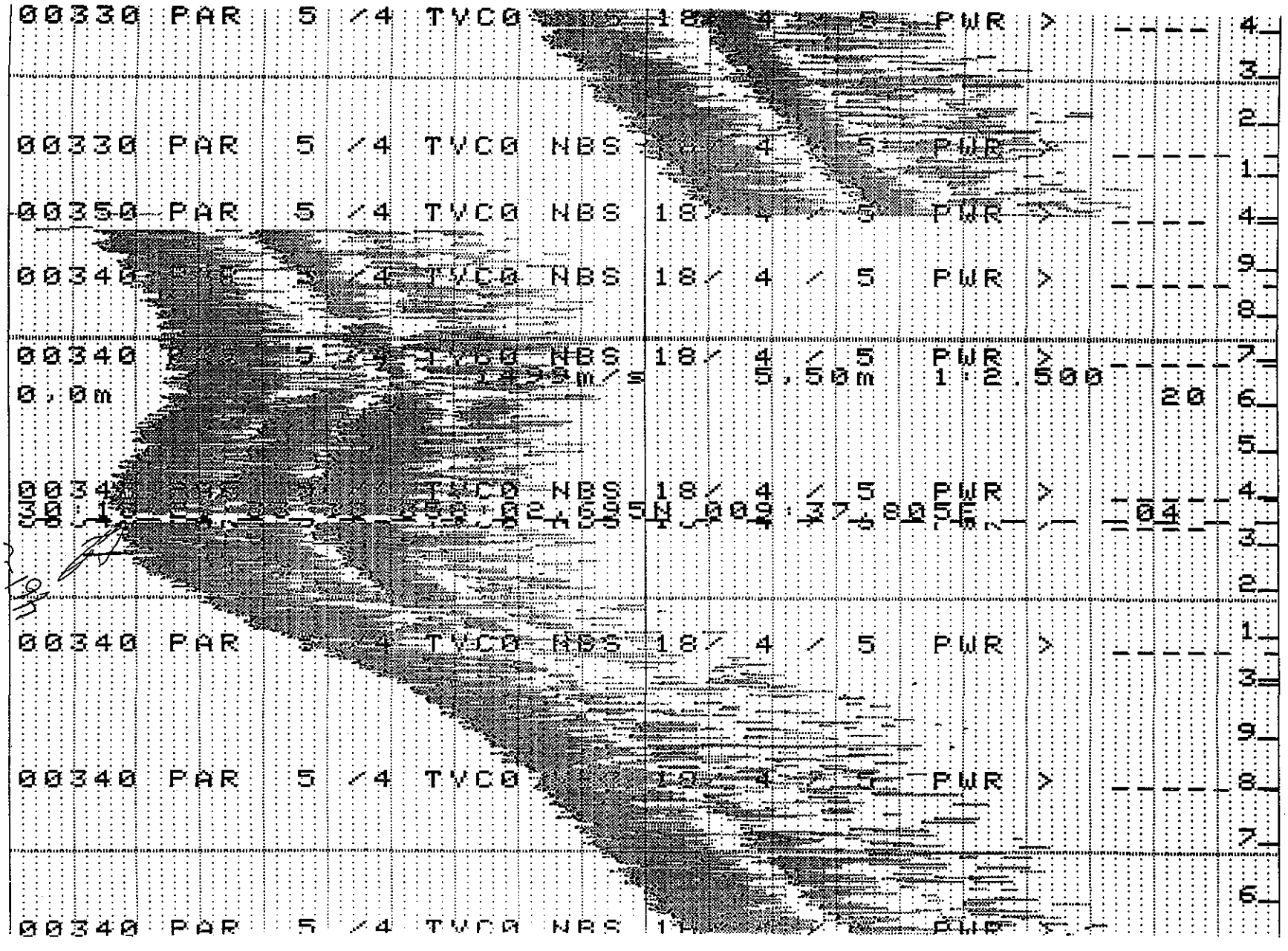

Fig. 45: Parasound record 461-3 through site of subsequent core 463-1 taken in ridge with enhanced reflectors. Vertical range of profile is 20 m.

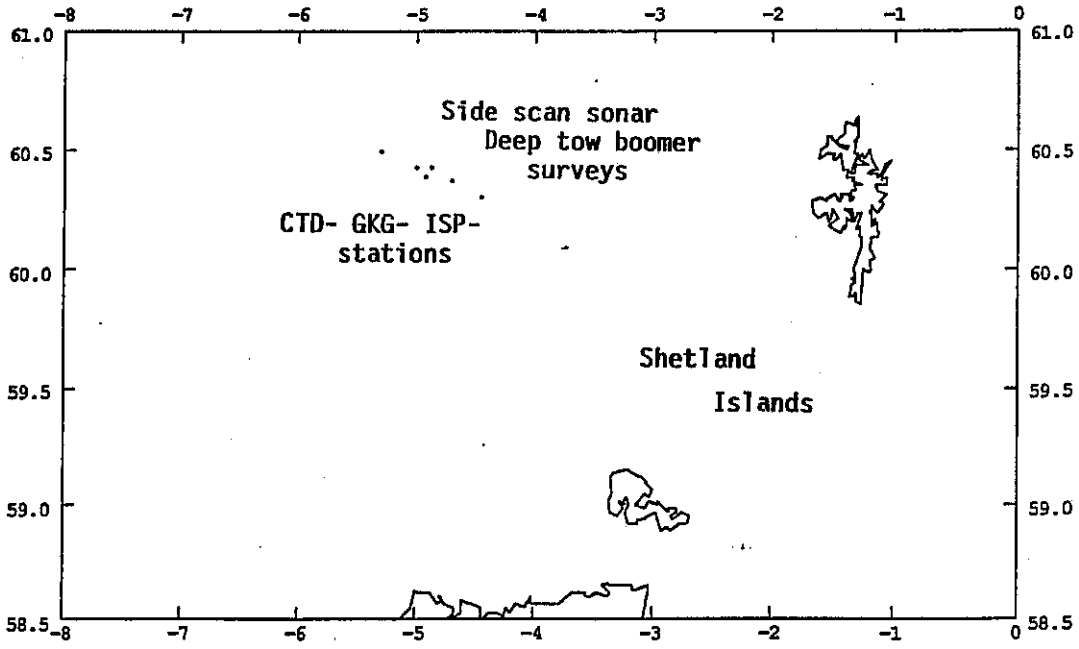

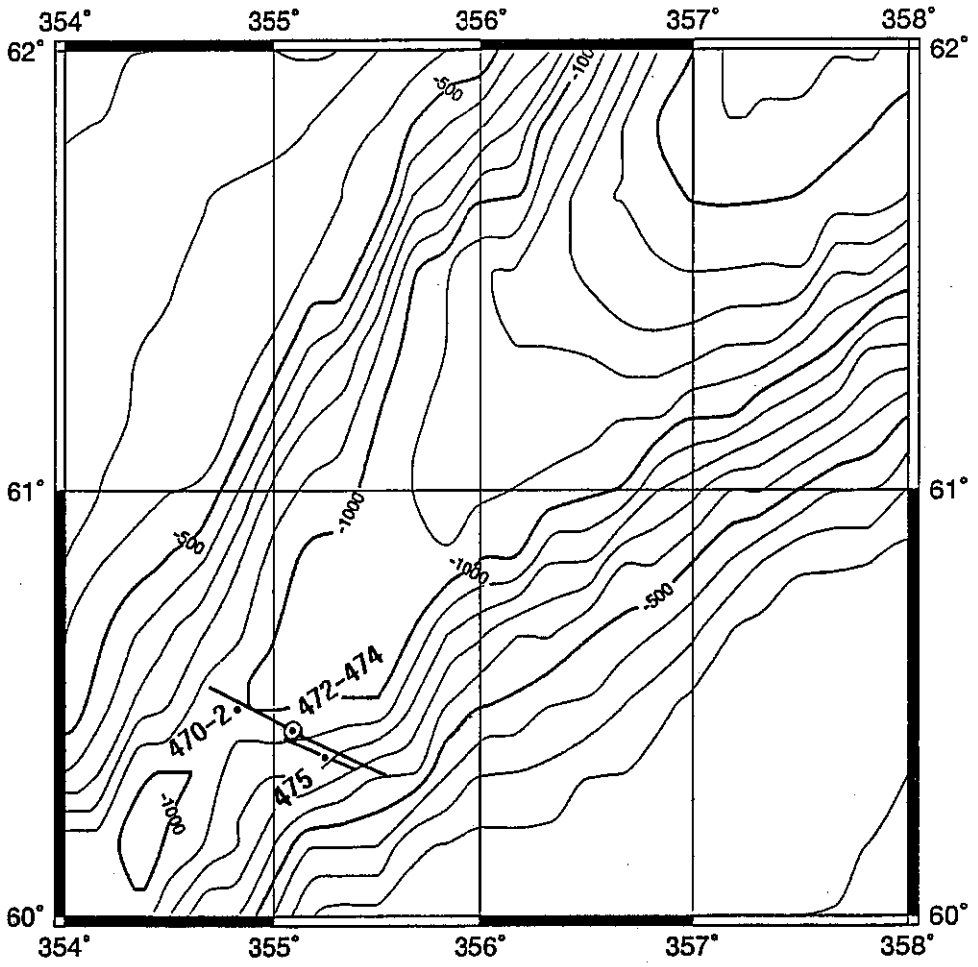

Fig. 46: Faeroe-Shetland Channel sampling and survey area; the long line = SISS survey, the short line = DTBS (deep-tow-boomer system); Station 470-2 = CTD and CH_4 cast; 475 = GKG box core sampling site; 472-474 = geological sampling of sediment drift body.

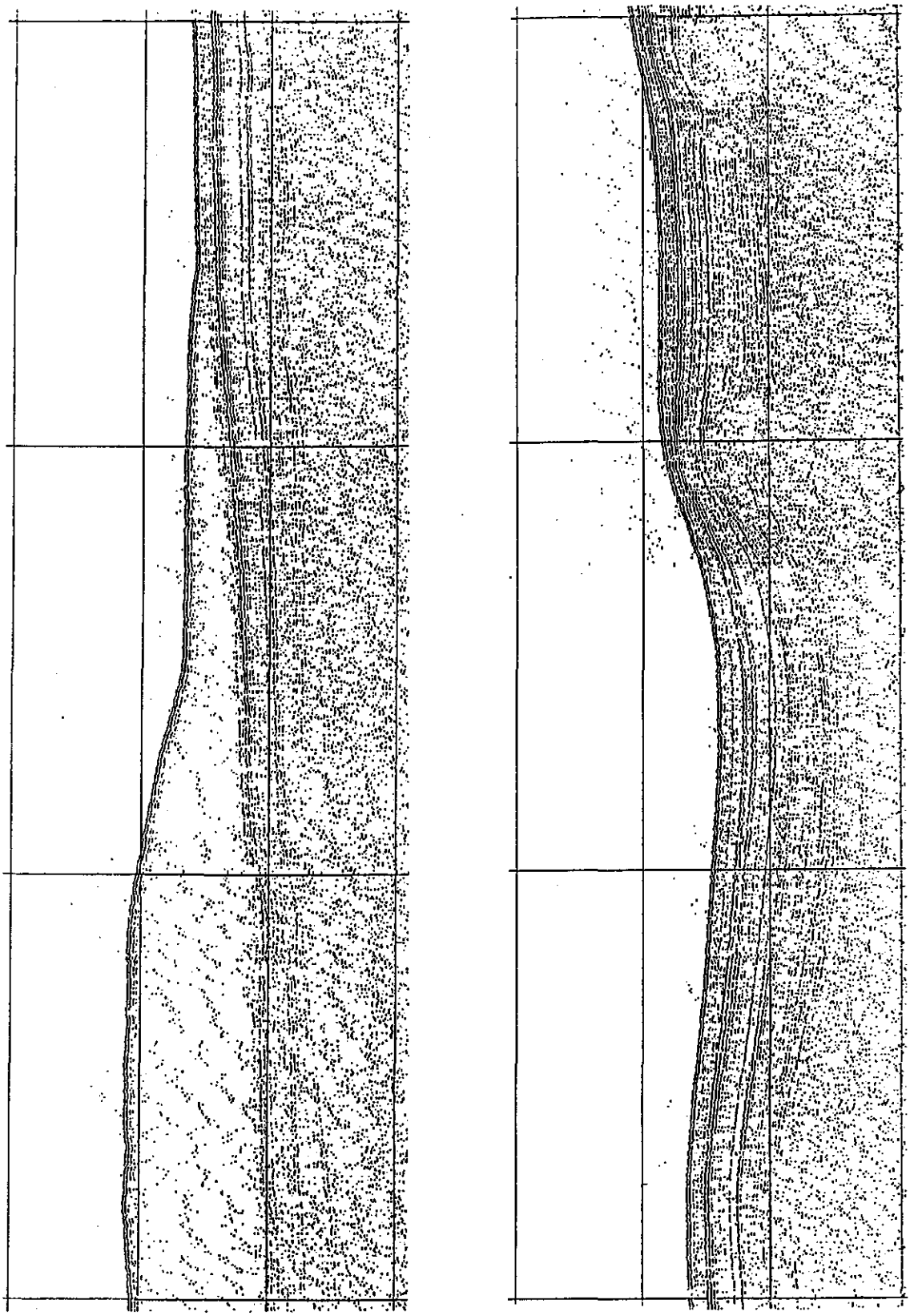

Fig. 47: Deep-tow-boomer record on the SE-flank and bottom of the Faeroe-Shetland Channel showing a sediment drift body thinning down slope and reduced sediment accumulation at the channel floor; the two sections shown are continuous and cover about the distance from Sta. 475 to the NW-end of the DTBS-line shown in Fig. 46; vertical scale 30 ms, horizontal scale approx. 650 m.

474 contained subrounded to angular multilithic clasts up to 20 cm diameter within a light olive brown matrix of muddy sand to sandy mud, evidence of winnowing occured at the seabed. The lensoid bodies are probably cross-sections of sediment drifts. The side scan sonar indicated an along channel orientation to features close to the foot of the slope.

Barents Sea slope

Hydrosweep and Parasound were run upslope from more than 2000 m water depth in the Norwegian Sea (Fig. 48), west of the Barents Sea across an area of maximum recent deposition northwest of Bear Island (Line 479-1). Due to the weather conditions the Hydrosweep did not give meaningful results because of cavitation beneath the ship. Good results were obtained with the Parasound (settings 4 kHz, pulse length 4 and gain 6.0). Initial penetration of approximately 20 m increased upslope to in excess of 40 m and locally reached 50 m at the end of the profile in 1200 m of water. Near the base of the slope small ridges with amplitudes <1 m were observed in the uppermost sediments, possibly sedimentary bodies formed by contouritic currents. Further upslope several lensoid bodies, up to 3 m amplitude, were seen with well layered sequences, these were attributed to slump material. At approximately 1600 m water depth acoustic blanking (obliterating all reflectors below the seabed) and a hummocky seabed suggested fluid expulsion may be present. Above this site the subsurface reflectors were multilayered but locally the slope was too steep that the parasound didn't lock on (instrument limit is a slope angle of 4°). Acoustic blanking was also present at the end of the profile about 7 m below seabed. Returning back downslope to the site at 1600 m water depth revealed a similar sequence as on the first traverse, though the acoustic blanking was not as apparent. As the survey direction was changed, the Hydrosweep system worked revealing a topographic feature 500 m to starboard of the ship and this was believed to be the intended target. A third approach successfully traversed the feature which was sampled (Sta. 480-6) and contained some CH_4.

Barents Sea crater field

Three deep towed boomer profiles (Lines 488-1 to 488-3, Fig. 49) were run through several of the craters identified in the 1991 METEOR cruise (No. M 17/2) confirmed the presence of pinnacles within some of the craters, particularly near the centre of the craterfield. They gave a hard acoustic response for the upper surface of the pinnacles with the crater floor recorded eneath, the side slopes of these features were too steep to be resolved on the boomer records. Parasound, echosounder and Hydrosweep were also run on these profiles, but with only limited success with the Hydrosweep. The gain on the echosounder was turned up high to detect interference (possible gas plumes) in the water column.

A grid of Hydrosweep lines (Lines 491-1 to 491-13) oriented at right angles to the swell mapped the bathymetry west of the existing data set with the aim of extending the area of known craters. Only a few more were identified. However, it confirmed that almost all the topographic highs recorded in 1991 outside the craters were erroneous, probably caused by "cross-talk". The distribution of craters exhibited a strong linear pattern representing two

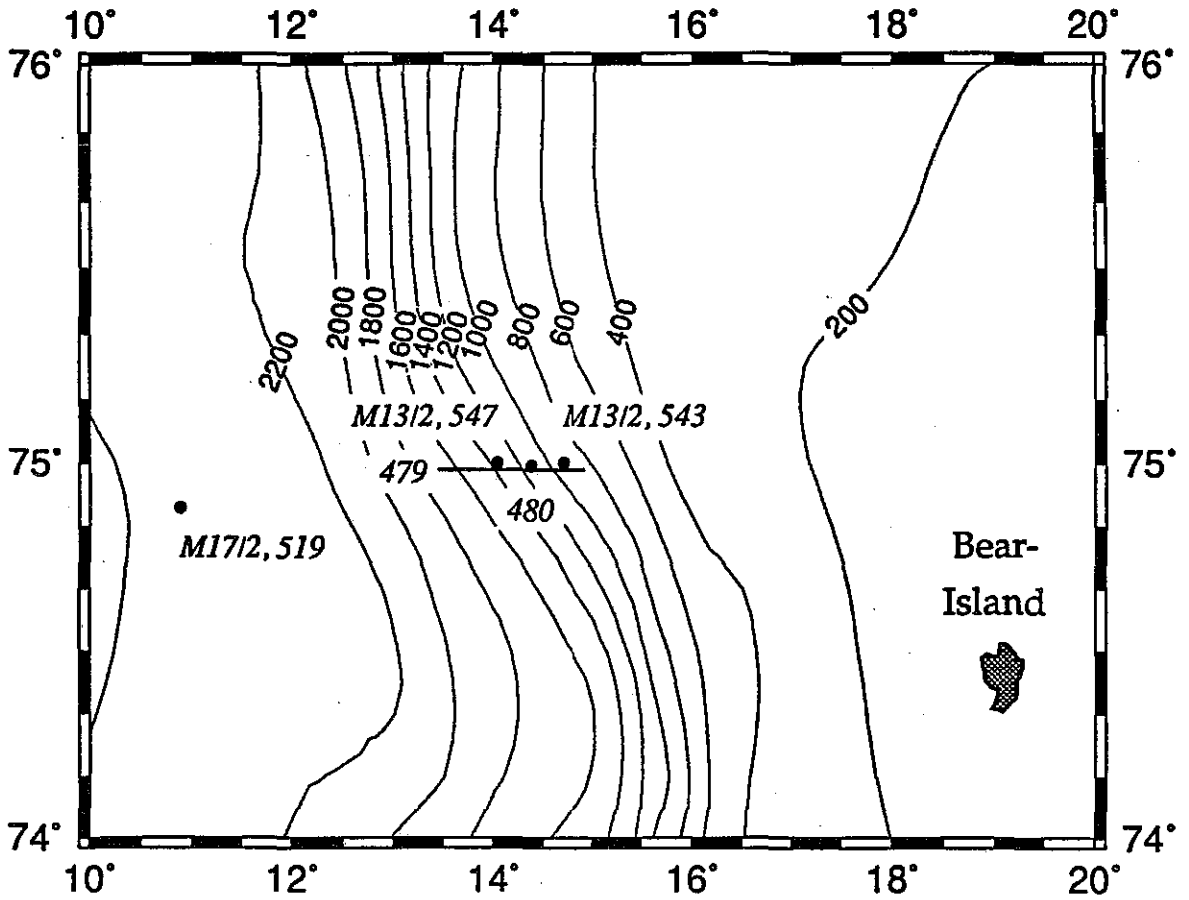

Fig. 48: Barents Sea slope site; stations 479-480 = Parasound survey line; 480 = coring station; also shown are coring and hydrocast stations from previous cruises (M 13, 1990 and M 17, 1991).

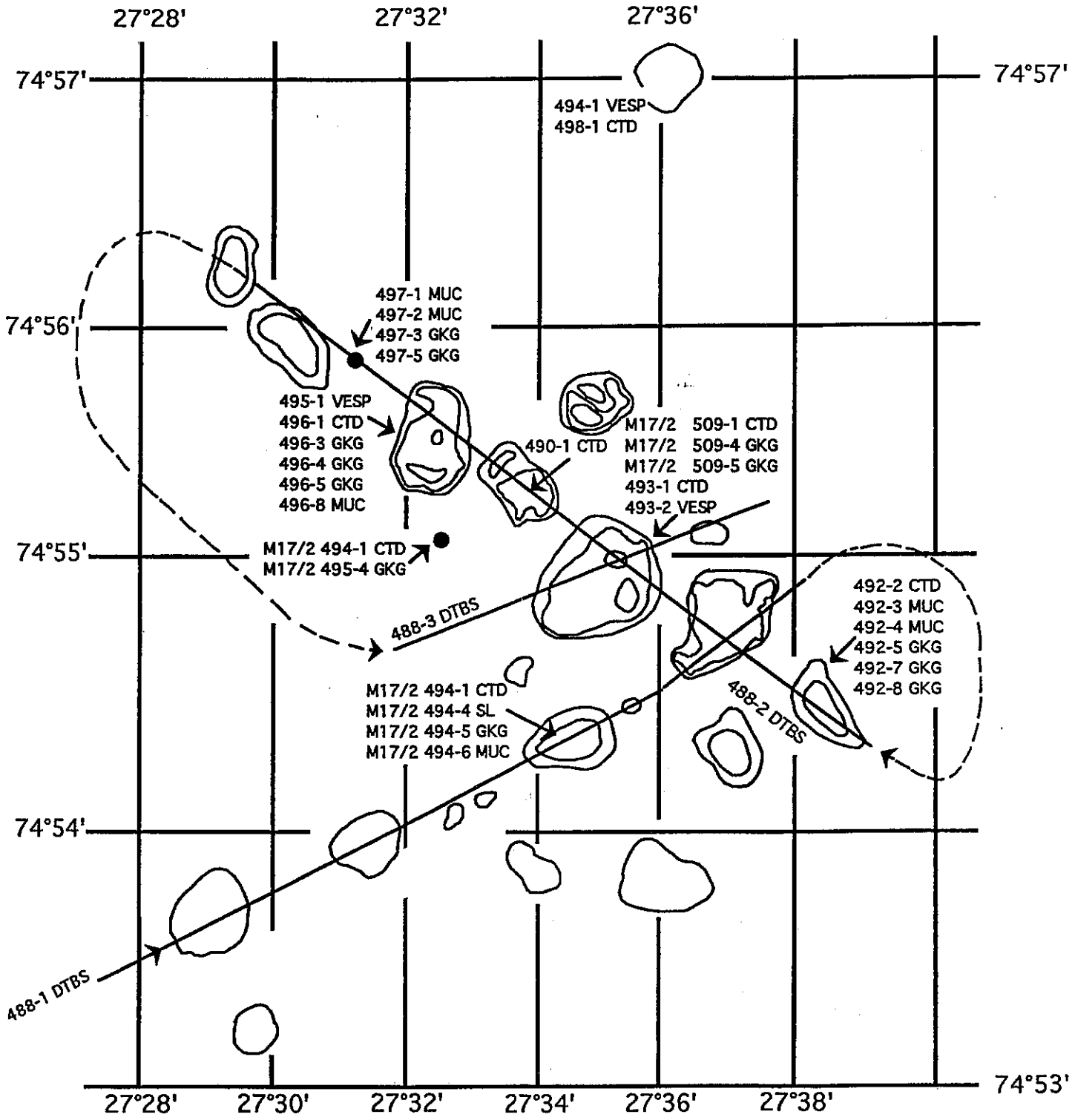

Fig. 49: Sampling and surveying the Barents Sea crater field; DTBS = deep-tow-boomer lines; several craters were extensively sampled (492, 493 and 496), others were sampled during a previous cruise (M 17/2, 494 and M 17/2, 509); 497 represents a reference site on the shelf floor; VESP = *in situ* benthic chamber was deployed and yielded video-images for the first time from inside three craters. This map is not a bathymetric map but only shows the position and out-line of the craters.

preferred orientations with bearings of 60° and 120°. These orientations were repeated to a lesser extent by the distribution of pinnacles within individual craters. It is therefore suggested that there may be some structural control on the distribution of the craters.

Strong hyperbola on the boomer records from the floors of several of the craters together with no acoustic penetration by the Parasound suggested a hard irregular surface. This was subsequently proved by sampling as comprising broken fragments of rock. The seafloor surrounding the craters was basically a flat surface with a gentle dip to the south. This surface had a very strong acoustic response attributed to planar erosion such as by glaciers. Locally small mounds occur above this reflector suggesting post glacial deposition adjacent to the craters. The subsurface reflectors dip to the SE.

The friable nature and near monolithic composition of the rock recovered in the box cores suggests that the craters are postglacial in age. The clasts are frequently angular, sometimes with concoidal fractures and compose dark to light grey mudstones and siltstones often with abundant plant fragments. There were only a few subrounded, ice rafted pebbles, including a large clast with glacial straie.

Acoustic reflectors were noted to be downwarped beneath several of the craters (Fig. 50) indicative of significant acoustic velocity differences between the sediment of the crater walls and the water within the craters. Basic calculations on the extent of downwarping revealed that the crater walls have acoustic velocities of 2200 - 2400 m/s which suggested that they comprise solid rock and not unconsolidated glacial products. Such values would be consistent with the lithology of recovered clasts in the box cores.

Enhanced reflectors ("bright spots") were observed below several craters, between 30 and 120 ms (ca. 35-150 m) below the floor of the craters (Fig. 51). Such features have been attributed elsewhere to gas accumulations. No deep reflectors were noted beneath areas devoid of craters. Gas blanking was not observed anywhere suggesting that any concentrations would be low. This would fit with a solid subsurface where porosity is likely to be lower than in unconsolidated Quaternary sediments. With bottom water temperatures of (-0.2°C) and approximately 360 m of hydrostatic pressure on the floor of the craters, any methane and water mixture present is likely to occur within th solid phase as gradient of 40°C/km (ZIELINSKI et al., 1986), free gas could exist at relatively shallow depths beneath the craters (approx 180 m, Fig. 52), below the levels of the enhanced reflectors noted on the boomer water temperatures. However it may be that variations in bottom water temperatures, salinity of pore waters, gas composition and geothermal gradient would create changes in the depth for free gas and explain the range of levels for the enhanced reflectors.

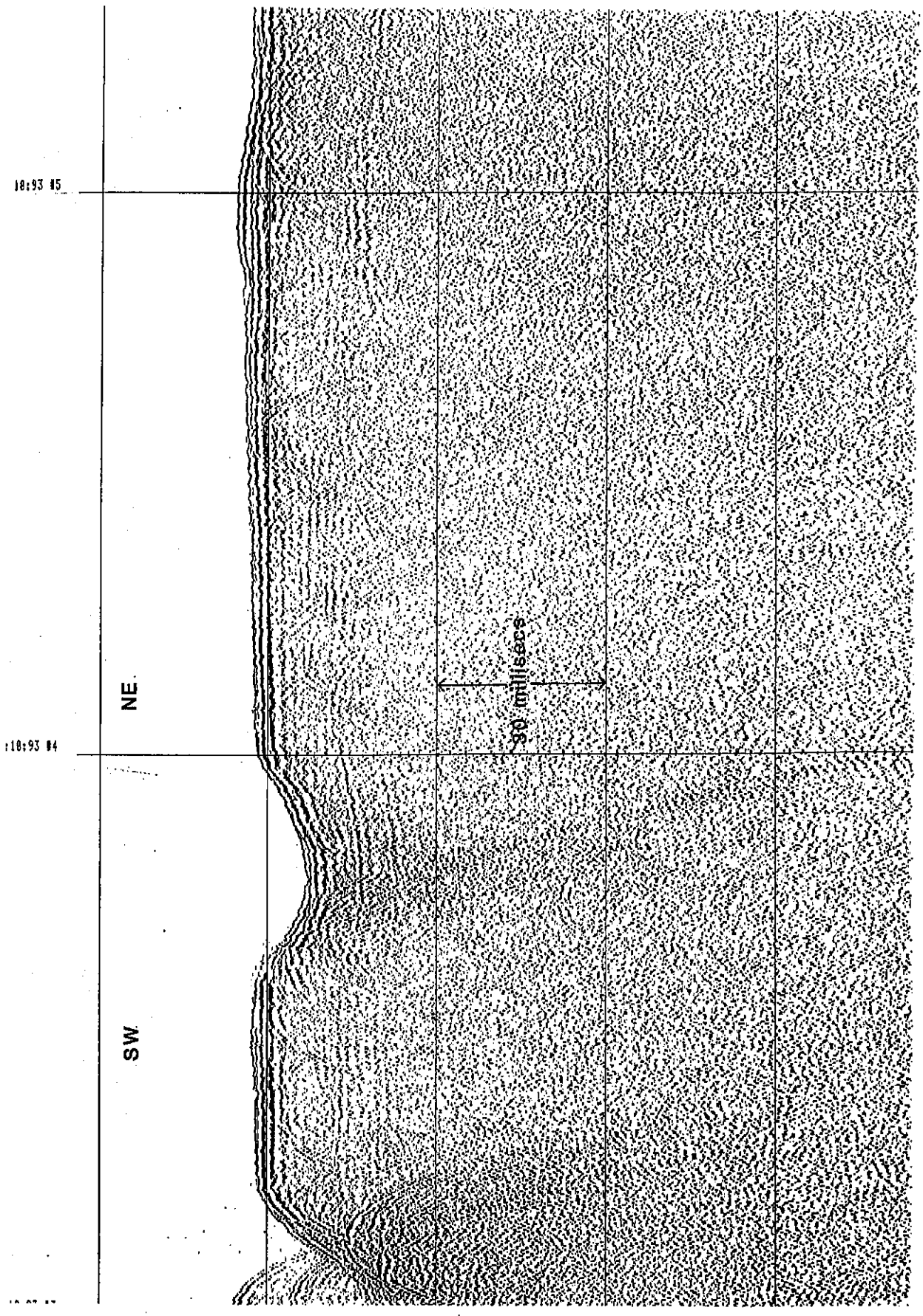

Fig. 50: Displacement of acoustic reflectors beneath small crater located N-E of crater 493.

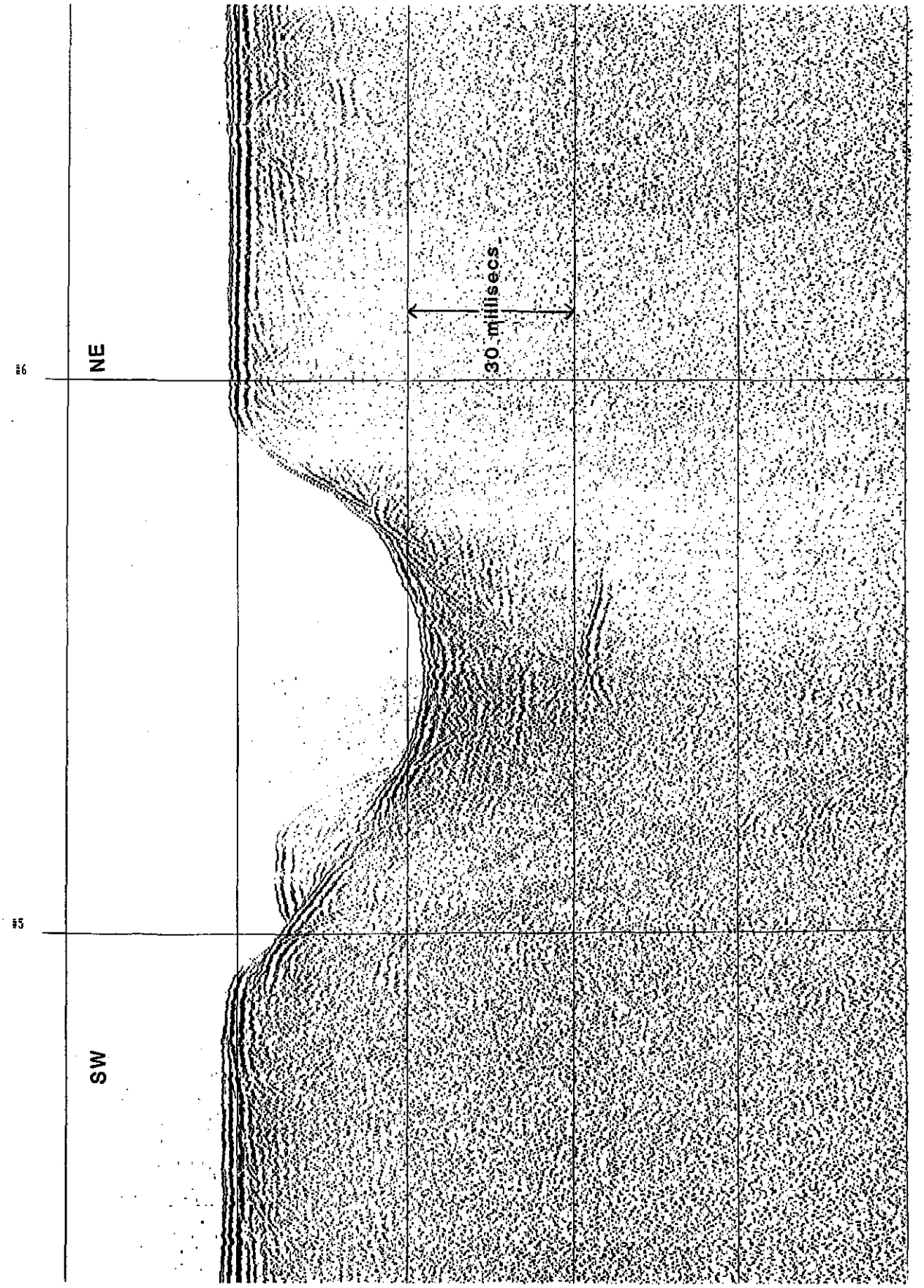

Fig. 51: Enhanced reflector beneath southwesternmost crater

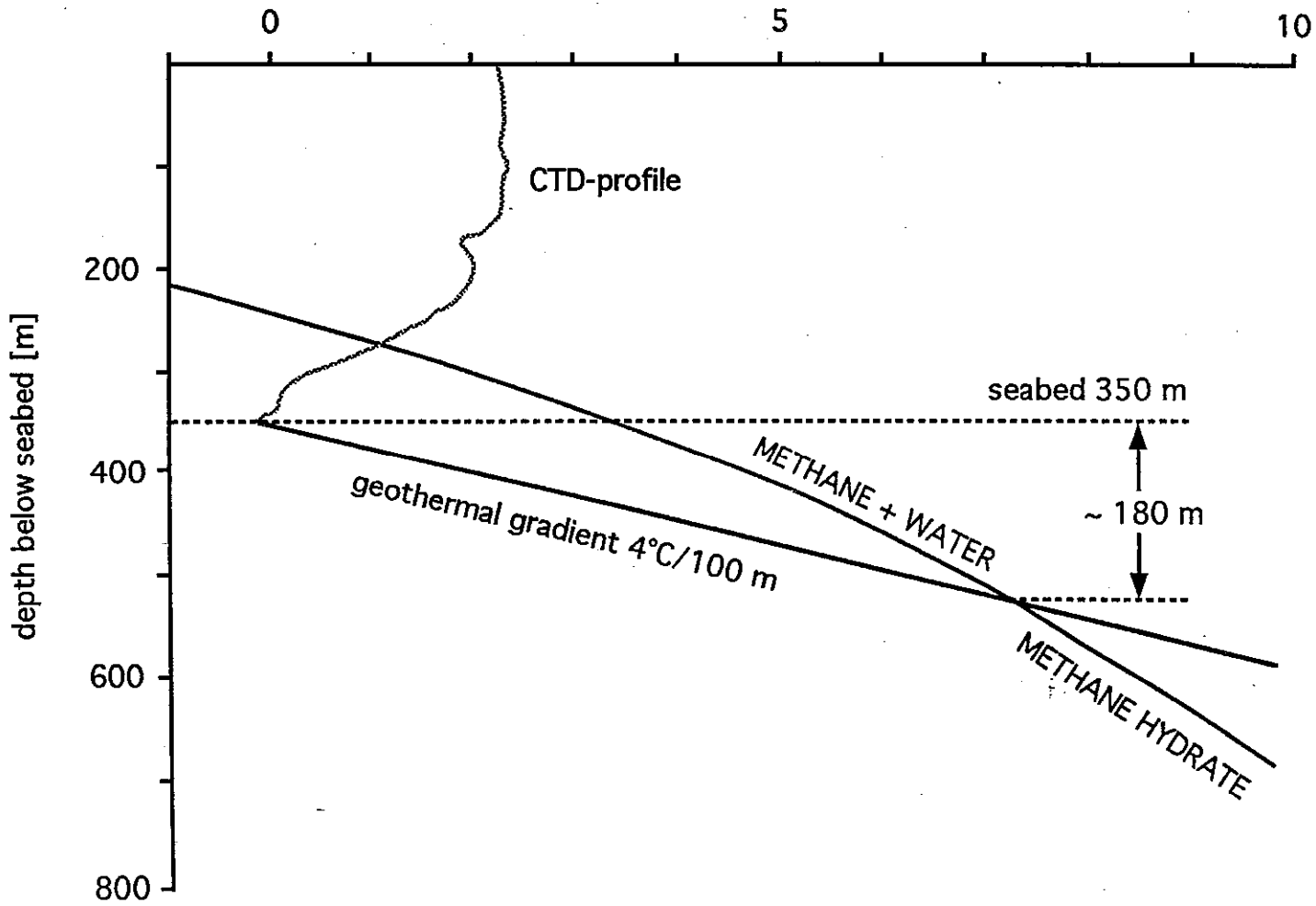

Fig. 52: Hydrate stability diagram illustrating the phase boundary between pure methane and water

5.4.8.2 MEDUSA (G. Wernecke, S. Marx)

MEDUSA (MEthane Detection for UnderSea Application) is an underwater system for the *in situ* measurement of dissolved methane. The range of concentrations is from 50 nl/l up to 100 ml/l. The maximum deployment depth is 300 m. Data are provided by a shipboard computer continuously in real time. Measurement are made by infrared HeNe-laser absorption in the gas phase after the methane has been desorbed from the water phase by membrane modules. The system is incorporated in a tow fish. During this cruise it was planned that MEDUSA would locate seeps by continuously measuring methane concentrations. This can be achieved by conducting a survey grid or by following concentration gradients. If the depletion of methane by bio-degradation and the water current is known, it may also be possible to calculate methane fluxes.

At the beginning of the cruise the optics of the system had to be adjusted because the transport from Geesthacht to Edinburgh damaged the alignment of the laser beam. At the first station in the Skagerrak, the combination of a decreasing ship's voltage, when load was applied, coupled with the voltage attenuation along the 10000 m long cable lead to an unpredictable behaviour of the filtering pump. The resulting sudden pressure impact destroyed the desorption membrane module. The repair took several days and was successful. The voltage problem could not be solved satisfactorily, but the resulting voltage was sufficient for further measurements to be made. These adjustments were aided by the ship's electronic engineers.

In the Barents Sea crater field MEDUSA could have been very useful by carrying out a methane survey to find the source of the high methane concentrations measured with the CTD system. However, due to the severe weather and ship's deck conditions, (snow and ice), the system unfortunately could not be deployed. Instead, surface water was pumped in by ship's cooling system and was measured on deck. Only background concentrations of methane were found in accordance with the CTD measurements since the sea surface degasses quickly. In addition to the crater field area, the surface concentrations were measured while steaming from the crater field south to the Lofoten Island in the same manner, with the same results. The quality of the measurements is poor, because they are affected by the water pumps and by instabilities of the laser beam. The latter problem may be solved later by statistical procedures. If successful, background data of the methane concentration of the areas surveyed could be achieved.

5.4.8.3 Methane in the Water Column (S. Lammers)

Methane analyses of hydrocast samples were originally intended as a vertical high resolution detection in addition to the long-distance surveys of MEDUSA. After the severe storm damage of October 15th, analyses on hydrocasts remained the only opportunity to

geochemically explore active seepage. Of 14 hydrocasts a total of 100 samples were degassed immediately after recovery by application of vacuum and ultrasonic energy (SCHMITT et al., 1991; LAMMERS and SUESS, submitted). Aliquots of the extracted gas were analysed on board for methane with a Shimadzu GC 14A FID system.

Skagerrak

In order to track active seeps in the Skagerrak area, CH_4 analyses were run mostly on bottom-near water samples from 5 hydrocasts (see Fig. 44 for Stations). Bottom water CH_4 anomalies were between 1480 nl/l (Station 463-2) and 370 nl/l (Station 465-1) in all profiles and document the abundance of active seeps over the whole area (Fig. 53). According to the observed gradients, the best result was achieved at Site 463-2, where the CH_4-concentration increased to more than 1300 nl/l within 20 m above the bottom. This indicates a point source nearby, probably an active seep along the line established between the CHALLENGER 82 Site and the METEOR 464 Site.

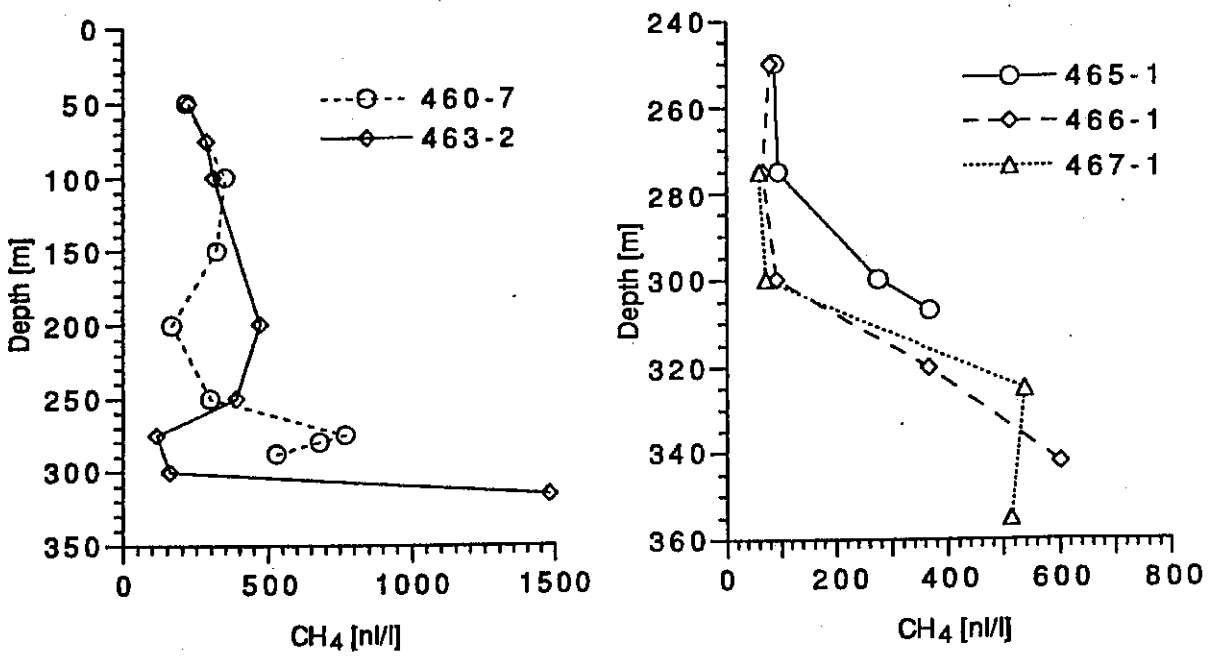

Fig. 53a,b: Methane distribution in the water column at the Skagerrak Sites; station locations 460-7 to 467-1 are shown in Fig. 44. Station 463-2 located closest to the "seep-line", connecting the CHALLENGER 82 Site and the METEOR Station 464-1, has the highest CH_4-content in the bottom water, the other Stations also show strong enrichments of CH_4 in bottom waters, although not as pronounced as Sta. 463-2, indicating methane injection.

A gravity core recovered later at this location supports the evidence for seep activity. Subsamples of the core were preserved in liquid nitrogen for later analyses of total methane. At the Stations 460-7 and 463-2 a second CH_4 maximum above 250 m of water depth indicates additional lateral influences from more remote seeps of gas-rich fluids in the vicinity. At both locations surface-near values were about 200 nl/l, which is about 300% supersaturated with respect to atmospheric concentrations (WIESENBURG and GUINASSO, 1979). Similar patterns may also be expected at Stations 465-1, 466-1, and 467-1 (Fig. 53b). Here only the near-bottom water column was sampled.

In general, the methane measurements confirmed that active seeps greatly affect all near-bottom waters and, to some extent, even the higher water column at the Skagerrak Sites.

North Atlantic and Barents Sea slope

Methane analyses were run on two CTD-casts at the Faeroe-Shetland Channel (Stations 470-2, 472-1) to clarify the existence of gas seepages which had been indicated by previous seismic recordings and which was suspected from the crater-like depression in the channel floor (Fig. 54) Both profiles reveal a typical background distribution, slightly influenced by methane bearing water masses between 400 and 600 m but with no evidence for any methane release from adjacent sedimentary sources (Fig. 55a).

A third typical background methane profile was recorded at the SYNPAL Station 480-1 at the Barents Sea slope, northern Norwegian Sea, where the methane concentration in the surface water was as low as 35 nl/l (Fig. 55b). At equilibrium, this would correspond to only 1.0 ppmv of methane in the atmosphere and therefore indicates a net sink for atmospheric methane at any level higher than 1.0 ppmv.

A comparison with observations of August 1990 (M 13/2) and August 1991 (M17/2) apparently indicates considerably higher methane levels and different distributions in the 1990 profiles (GERLACH and GRAF; 1991, SUESS and ALTENBACH, 1992). The difference is either assumed to reflect higher methane release rates from bottom sources on the shelf (Fig. 55) or could be related to analytical problems, although the degassing method has been in use unchanged for over 3 years. Inspection of the raw data should clarify whether or not analytical problems might be responsible.

The decrease of methane concentrations by 50% in the upper water column between 1991 and 1993 is less significant since the 1991 profile was recorded at greater distance to the slope (Fig. 56). Although these observations were made at about the same time of year and thus do not allow to conlude on the whole range and frequency of these variations, they are assumed to outline the magnitude of annual or longer-term variability of methane discharge on the Barents Sea shelf.

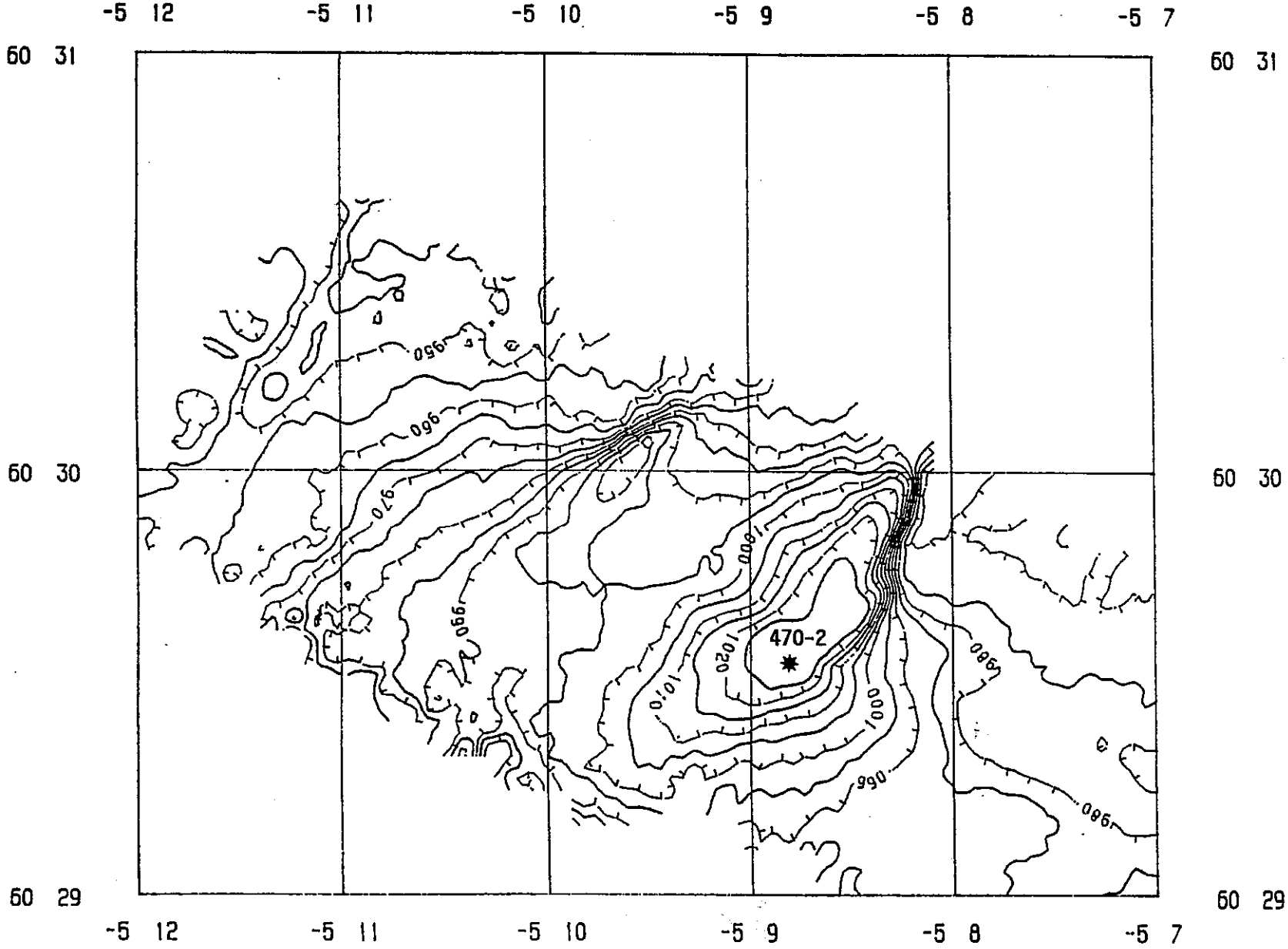

Fig. 54: Depression in the Fearoe-Shetland Channel floor as seen in the Hydrosweep survey. Initially this structure was thought to be a gas hydrate blow-out crater. This hypothesis was however dicounted when no CH_4 anomaly was found in the bottom water (Station 470-2).

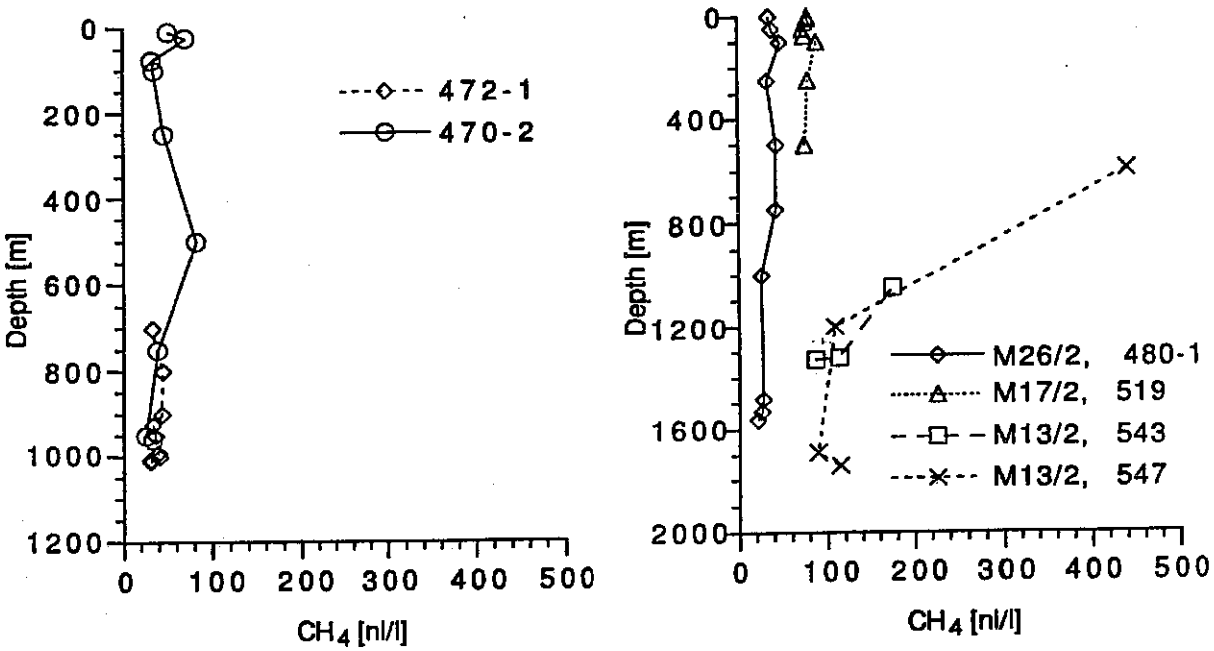

Fig. 55a: CH_4-distribution in the water column at the Fearoe-Shetland Channel above a morphological depression and the deepest part of the channel floor (Station 472-1); with the exception of a small CH_4 anomaly in the mid-water of the channel (500 m), no evidence for currently active CH_4-seeps was found in the Faeroe-Shetland Channel.

Fig. 55b: Typical background of low oceanic CH_4 in the water column of the northern Norwegian Sea (Station 480-1). Comparison with CH_4-contents at this location between 1990 and 1993 might indicate that previously more methane was transported from the Barents Sea shelf by cascading cold water masses.

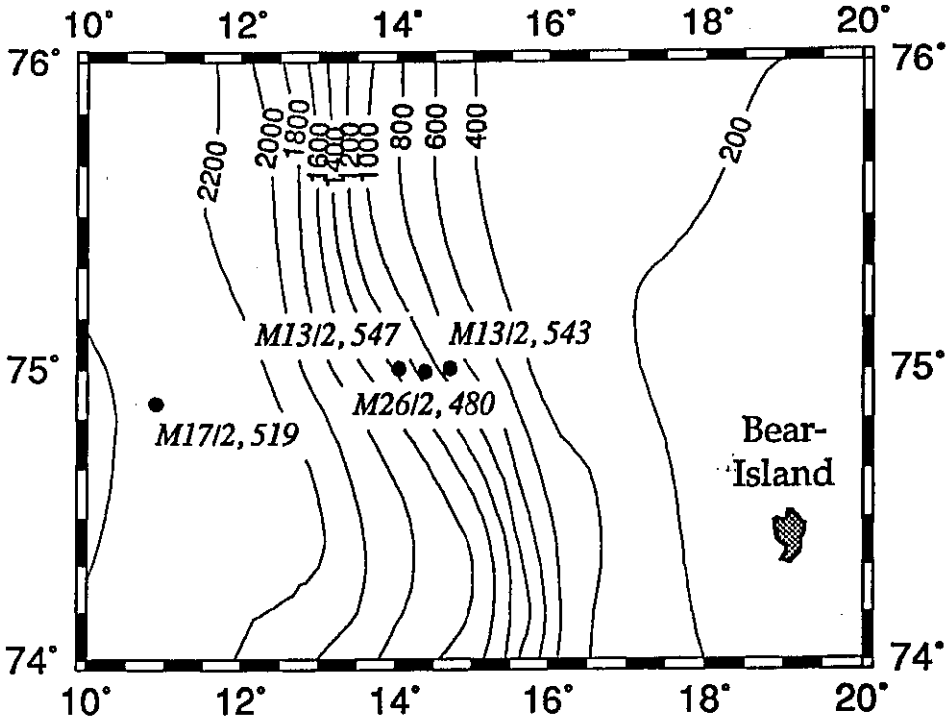

Fig. 56: Barents Sea slope hydrocast Stations taken during METEOR cruises M 13 (August 1990), M 17 (August 1991) and M 26 (Oktober 1993).

Barents Sea crater field

For investigations of known gas seepages and further mapping of a large methane plume that was observed on METEOR cruise 17/2 in August 1991 (LAMMERS et al., submitted; SUESS and ALTENBACH, 1992), methane analyses were run on 35 of near-bottom samples from 5 hydrocasts within a crater area 260 km ENE of Bear Island and at one location about 50 nm north (Fig. 49).

According to previous investigations (SOLHEIM and ELVERHÖI, 1985) and the Parasound sediment profiling on M 26/2 and M 17/2, the craters are thought to have been formed by explosive gas eruptions, although none of them was found to contribute to the presently observed methane anomaly on either survey. A slight decrease of salinity, oxygen, nitrate, and phosphate in the bottom water of a crater at Site 493-1 is not accompanied by any methane gradient and thus is a doubtful indication for seepage.

Methane distributions were similar to those observed in 1991, all showing strong maxima below 280 m water depth. A destinctly increasing concentration level towards the north (Fig. 57), which follows the N-S flow of arctic bottom water in this region. The thickness of the CH_4-plume is about 50 m and corresponds to the hydrographic parameters thought to be characteristic of the Arctic cold water bottom current. Elevated silica and low temperature

(Fig. 58) are the most distiguished features of this water mass and can be traced to follow the CH_4-maxima throughout the region. The gradient towards the north suggests that the source area of the methane is located north of the crater field. However, no major change of the methane distribution was found even 50 nm north at the last Station sampled during the cruise, Site 499-1. Here the transect had to be abandoned on account of ice. The average maximum value of 400-500 nl/l CH_4 in 1993 is about 50 % less than that found in the 17/2 survey in 1991 (LAMMERS et al., submitted).

This discrepancy was also observed in the CH_4-concentration changes at the Barents Sea slope and probably reflects the variability of the supply of marine methane. An increased degassing of methane into the atmosphere caused by weather induced mixing or a variation of the seep activities on the Barents Sea shelf are considered responsible for the lower concentrations in dissolved methane.

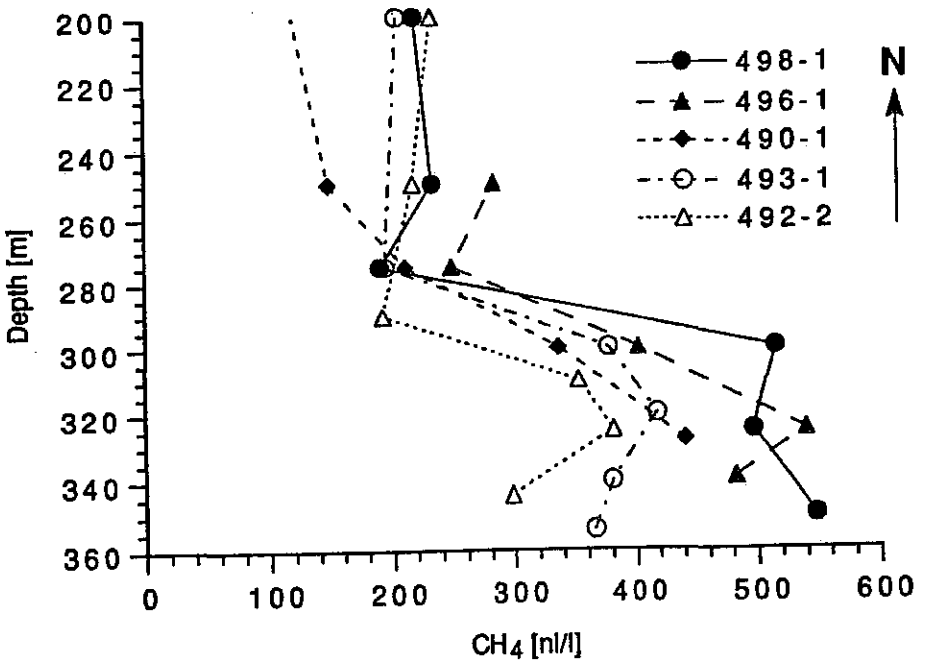

Fig. 57: CH_4 in the bottom water of the Barents Sea shelf in the vicinity of the crater field; not systematic increase of CH_4 towards the north; for Station locations see Fig. 49.

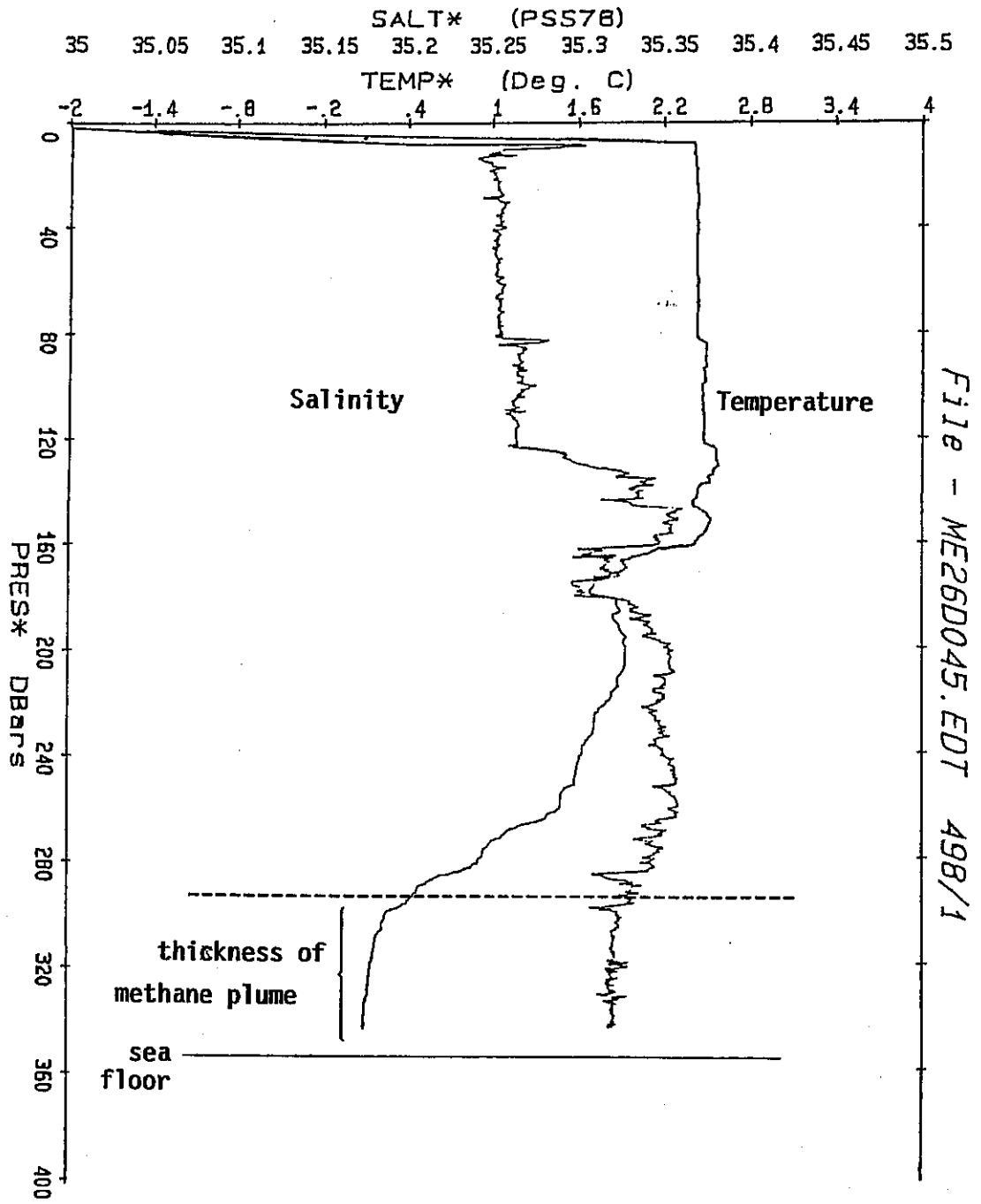

Fig. 58: Salinity and temperature of Barents Sea shelf waters; Station 498-1 shows low temperature bottom water below ~290 m depth; the low temperature water mass corresponds to the thickness of the CH_4 plume found in this area.

5.4.8.4 Sampling for Helium Isotopes (G. Winckler)

According to the initial strategy it was planned to collect seep water samples from the VESP system (s. 5.4.8.5) and analyze them for their helium isotopic ratio. The objective was the detection of an anomaly in the helium isotopic ratio due to gas or fluid input from cold seeps. These fluids are expected to transport a radiogenic, e.g. enriched ^4He isotopes from radioactive delay of uranium compared to the background water depends on the source of the fluids and their residence time in the sediment. Further it was planned to compare the helium isotopes with the data obtained from other typical vent-tracers in order to quantify the seep fluxes and estimate e.g. the flow rates by studying the continuous increase of the tracers in the VESP chamber.

In comparison with methane, the helium isotopic ratio is a less dynamic vent-tracer. It is known from investigations during previous cruises (e.g. RV SONNE cruise no. 78) that the effect on the helium isotopic ratio in conventionally collected samples, with a rosette sampler/CTD is very small and that studies of these water column samples are therefore limited by the resolution of the measurement system. For that reason it was planned to use only the water samples obtained with the VESP-system for the helium isotopic analyses. The VESP-system offers the opportunity to sample the seep fluids or gases directly. Consequently these samples show a much larger effect on their helium isotopic ratio than the CTD-samples do because of less dilution.

Unfortunately, the progress of the cruise prevented this strategy to be followed through. The VESP system could not be used for collecting vent samples during the entire cruise. For that reason the sampling strategy had to be modificated and the conventional rosette sampler be used for collecting water samples. Hence, at a total of six CTD-stations, 44 samples for helium isotope measurements were taken at 7 to 9 depth intervals. The focus was placed on the deeper part of the water column. The samples were taken at the following stations: 5 CTD-stations in the crater field in the Barents Sea: 490/1, 492/2, 493/1, 496/1, 498/1 and 1 CTD-station, ca. 50 nm north of the crater field: 499/1.

The analysis, including the extraction, of these samples will be performed at the helium mass spectrometric system of the working group on "tracer oceanography" at the Institut für Umweltphysik (Universität Heidelberg).

5.4.8.5 Video Images and Survey with VESP (P. Linke, P.R. Dando)

In order to quantify the fluid and geochemical mass fluxes from seeps, an existing device, the Benthic Barrel, was modified and integrated within a lander system (VEnt SPider = VESP) for TV-guided deployment from a surface vessel (LINKE et al., 1994). The Benthic Barrel, an open-bottom barrel with an exhaust port at the top, contains 5 sequentially activated water

bottles and a CTD Probe. A thermistor flowmeter is emplaced within the exhaust and the flowrates are recorded by the CTD probe. Two flowmeters (one as a spare) were calibrated in the temperature range expected for the sample sites on cruise M 26/2. In order to quantify and sample gas bubbles, emanating from the seeps, a gas detector was integrated in the barrel. This detector contains 10 sensors, which measure the gas level within the barrel by the change in conductivity, when the gas/water interface rises. A valve seals the exhaust port below the flowmeter to trap the gas within the barrel.

For TV-guided remote deployment from a conventional surface vessel the barrel is lowered to the sea floor using the main frame of a modified multicorer. The barrel is attached to the central piston of the multicorer, which operates on a water hydraulic basis and assures gentle deployment of the barrel on the sediment surface once the frame has reached the sea floor. The frame is constructed from steel pipes connected by scaffolding clamps; additional diagonal pipes provide more stability, and a platform for mounting of accessory equipment. The frame carries a deep-sea photocamera, a flash, 2 floodlights, a videocamera and telemetry unit for bidirectional data and video transfer to the ship. All functions of the instrument (including the activation of the fluid and gas sampling) and its energy supply are controlled from the surface telemetry unit onboard the ship. CTD-, flowmeter and gas detector data are stored within the storage probe and are recovered after every deployment.

The whole system was sucessfully tested prior to the cruise on a 2-day trip of the RV ALKOR in the Baltic Sea. Several dry runs and 3 survey deployments (Fig. 49) to perform a video and photo survey of the crater field in the Barents Sea were performed during M 26/2, but no active seep site was detected.

Video images and survey description

493-2

VESP was deployed in a 30 m deep pockmark with a vertical pillar of equivalent height to the crater depth (Fig. 59a). The base of this pockmark was of mud with occasional angular slabs of mudstone lying on the bottom or slightly protruding through the sediment cover. Sponges, corals and anemones were common on top of the rocks. Fish, mainly cod, were present in large numbers in the deepest part of the depression (Fig. 59b). Rock slabs were increasingly common towards the pockmark base and at the base of the pillar. The pillar itself had almost vertical slides with small, knobbly but rather angular protuberances (Fig. 59c). It did not have the smoothed surface appearance of the carbonate pillars in the Kattegat and had a sediment covering. Small rocks fell off when the feet of the VESP knocked it. The top was flat and lightly sediment covered with anemones growing on it. The sides of the pockmark were steep with mudstone slabs. Conspicuous mudstone was also observed around the rim of the crater, suggesting explosive release from the crater base.

494-1

The deployment was in the northern pockmark in the previously surveyed area. It had steep sides and no internal protuberances. Sides and base were sediment covered with few physical features except for very occasional small rocks protruding through this cover (Fig. 59e). Small anemones were common and numerous polychaete tubes were visible (Fig. 59d, f). Shrimps and starfish were seen and fish, especially cod, were very numerous in the base. Sediment falling from the feet of the VESP was consolidated and frequently fell as lumps. Crustacean burrows were more common than in the other deployments, suggesting thicker sediment cover.

495-1

The VESP camera was used to survey the base of the pockmark centred at 74°55.5'N and 27°32.5'E. On reaching the bottom, 360 m water depth on the echo sounder, a series of mudstone slabs was observed. These had straight edges and sides, some having almost a 'tombstone' appearance (Fig. 59g). The largest blocks rose 1 - 1.5 m above the pockmark base, were several metres across and frequently had fractured pieces of mudstone lying on their otherwise smooth tops. The tops of the slabs often appeared to be more sediment covered than the rock litter at their bases. Large sponges and corals grew on the edges of the rock and on rock slabs angling out of an apparently thin sediment cover between the large blocks. Crustacean burrows were not common, suggesting shallow sediment. Shrimps were occasionally visible as were dense swarms of Euphaursids. Anemones were particularly common where there was thin sediment cover. Where the rocks were less frequent, perhaps 1 m deeper in the pockmark base, numerous fish, particularly cod, were observed. Occasional *Hippoglossoides* were also seen. No evidence of seepage was observed, e.g. dark sediment, water movement, bacterial mats, seep associated fauna.

The overall impression of the pockmark base was of an old slate quarry (Fig. 59i). Some slabs were seen, lying against others, with their long axis almost vertical (Fig. 59h). What appeared originally to have been a mudstone layer over 1 m thick at the base of the depression had been fractured with lighter pieces of rock flung on top of the larger blocks.

Towards the end of the deployment the ship moved east to allow a view of the 10 m high mound in the northern part of the pockmark. This proved to be a mound of broken mudstone with light sediment covering and the usual epifauna. Beyond this in the western depression was an apparently more heavily sediment covered area, although only a few metres of this were covered before retrieval.

493-2 VESP

Fig. 59a:

Within the pockmark a vertical pillar of equivalent height to the crater depth became visible.

Fig. 59b:

In the deepest part of the depressions fish, mainly cod, were present in large numbers.

Fig. 59c:

The pillar itself had almost vertical slides with small, knobbly but rather angular protuberances colnized by large sponges.

494-1 VESP

Fig. 59d:

Side and base of the pockmark where covered with sediment; polychaete tubes were visible.

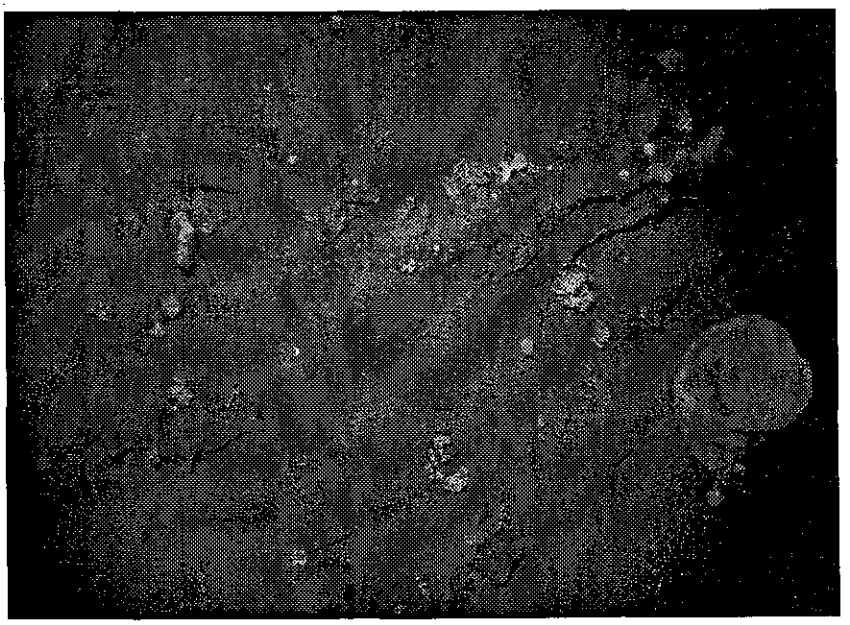

Fig. 59e:

Occasional rocks protruding the sediment were colonized by sponges and anemones.

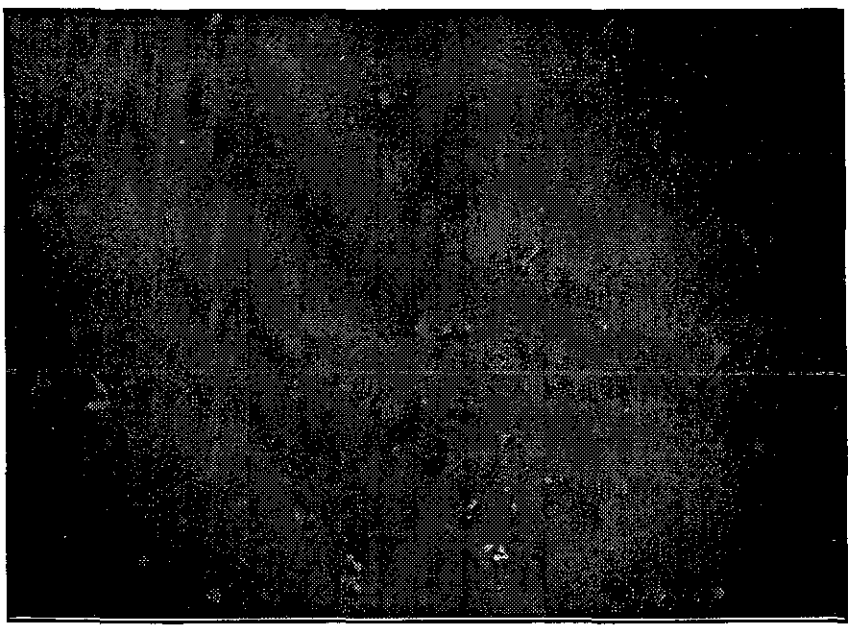

Fig. 59f:

Numerous anemones colonizing small rocks.

495-1 VESP

Fig. 59g:

Within the pockmark a series of mudstones was observed with straight edges and sides.

Fig. 59h:

Some slabs were standing upright, their edges densely colonized.

Fig. 59i:

Large sponges and anemones were seen. The overall impression of the pockmark base was of an old slate quarry.

5.4.8.6 Seep Sulphur System (P. Dando, S.J. Niven, A. Brierly)

Skagerrak

The gravity core 464-1 (Fig. 60) penetrated a seep area at the top of a 1.5 m high ridge. The presence of the seep was indicated by the strong hydrogen sulphide smell on opening the core, high methane concentrations near the surface of the core (>2 m moles dm^{-3} at 50 cm), high ammonia concentrations (up to 6.7 mM), the presence of adult and larval pogonophores, *Siboglinum poseidoni* , and the presence of shells of the bivalve *Thyasira sarsi* at 30 and 35 cm depth. Pore water samples, obtained by filtration through alumina filters of 0.2 μm porosity, were additionally fixed for sulphate, dissolved sulphide, thiosulphate and sulphite analysis. Sediment was fixed for analysis of organic C & N, elemental sulphur, acid-labile and chromous reducible sulphur. Sulphate reduction rate incubations were carried out at 7°C on samples along the length of the core down to 5.05 m. Additional sulphate reduction-rate measurements were performed on bulked sediment from 38-42 cm depth and on sediment from 73-77 cm depth. This material was incubated in the presence and absence of added methane at 1 bar and 35 bar to investigate the effects of methane on the sulphate reduction rate.

The core was sliced in sections longitudinally immediately before sediment samples were taken for methane analysis. A methane maximum occurred at approximately 75 cm depth, a level just below the sediment surface reflector on the 5 kHz Parasound record. Methane concentrations decreased in an approximately linear manner from this maximum towards the sediment surface and also down core to a depth of 3.25 m. Below 4 m methane concentrations increased regularly with increasing depth. The results were interpreted to indicate a lateral flow of methane subsurface at approximately 0.75 m and diffusion of gas upwards and downwards from this point. Towards the base of the core methane increased again at a rate consistent with diffusion upwards from depth. The maximum methane concentration measured was 2.7 m moles dm^{-3} sediment. This would be an underestimate due to degassing during core recovery.

The ammonia concentrations were higher than had previously been recorded in this part of the Skagerrak and showed a double diffusion gradient with a change at 2 m depth, corresponding to the top of a hard reflector on the Parasound. This suggested a dilution of the upward diffusing ammonia at this depth.

No water column hydrogen anomalies were observed in CTD casts 463-2 and 467-1. The presence of very high methane concentrations, 1.8 μl l^{-1} water, in CTD cast 463-2 at 315 m was confirmed. This core extends the line of seep cores collected, during RV CHALLENGER cruise 82, 1.1 km to the SW and suggests that the seeps in the Skagerrak are linear features, probably running along the top of the low sediment ridges.

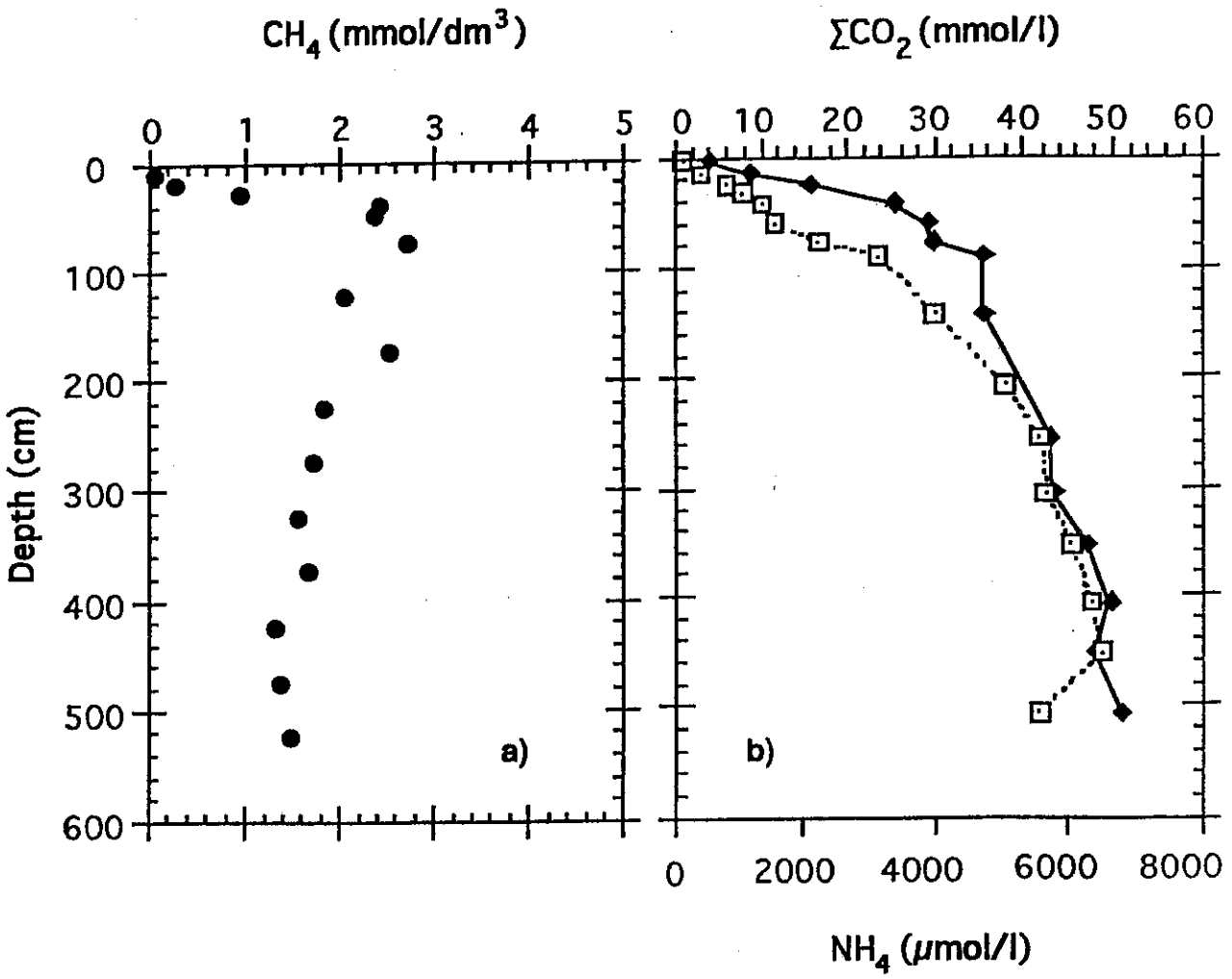

Fig. 60: Pore water profiles from gravity core 464-1 at the Skagerrak seep location

a) CH_4

b) ΣCO_2 and NH_4

Faeroe - Shetland Channel

A multicore sample, 474-1, was studied from this area. Samples were collected, down to a depth of 18 cm, for the determination of soluble and insoluble sulphur species as in the Skagerrak. Sulphate reduction rate measurements were also made. Ammonia concentrations were only detectable (> 2.5 μg at N l^{-1}) in the upper 4 cm of sediment and methane was also slightly elevated in this surface sediment indicating breakdown of organic matter. Samples were taken for organic C & N measurement. Water samples from the CTD cast 470-2 in this area showed no methane anomalies but an increased hydrogen concentration immediately above the level of the south-flowing polar water. The origin of this was unclear.

Barents Sea slope

Two sub-cores from large box core samples, 480-5 and 480-6, were examined. Samples were taken for soluble and insoluble sulphur species, methane, sulphate reduction rates, ammonia, Mn(II), Fe(II), pH, Eh. Ammonia concentrations increased to 113-116 μg at N l^{-1} at 38 cm depth, Mn increased to 96-132 μg at l^{-1} and the Eh had only fallen to +80 mV by 35 cm depth. The side of the box core 480-6 was removed and the positions of pogonophores in the sediment traced by washing and teasing away the surrounding sediment. This was difficult in conditions of poor deck lighting and rapidly freezing seawater. The majority of specimens appeared to grow more or less vertically downwards to just below the region of maximum manganese deposition at 9-10 cm and then to move horizontally into the sediment. Specimens of the dominant species of pogonophores in the sample were dissected from their tubes and assayed for the activity of ribulose-bis-phosphate carboxylase, indicative of chemoautotrophic bacteria. Specimens of a thyasirid bivalve from core 480-5 were similarly treated. No other species which appeared to have a symbiotic association with autotrophic bacteria were observed.

Barents Sea crater field

Multicore and sub-samples from box cores were processed as previously. The first multiple corer taken, from 492-4, was approximately 15 cm deep but proved to have 2 large pieces of shale within it which had been pushed into the sediment, mixing the layers. Multiple core sample 496-8 and a 10 cm diameter sub-core from box core 496-3 were taken from a pockmark. The box core sample had a large piece of mudstone in the sediment and the subcore had numerous small pieces. The maximum ammonia concentrations observed at 35 cm depth were 40 g at N l^{-1}. Evidence for methane seepage was only obtained for core 492-4, from the SE crater in the area surveyed (Fig. 61a). In this core methane concentrations reached 1 mmole dm^{-3} sediment at 10 cm depth. CTD station 492-2 over this crater was the only water sample set, analysed by the head-space method, to show increased methane in the bottom water (Fig. 61b). Multiple core samples 497-1 and 497-2 were taken from a sediment ridge on the seafloor outside the craters and samples were taken for comparison with the crater samples. The sediments inside and outside the pockmarks had similar Eh values down to 20 cm depth.

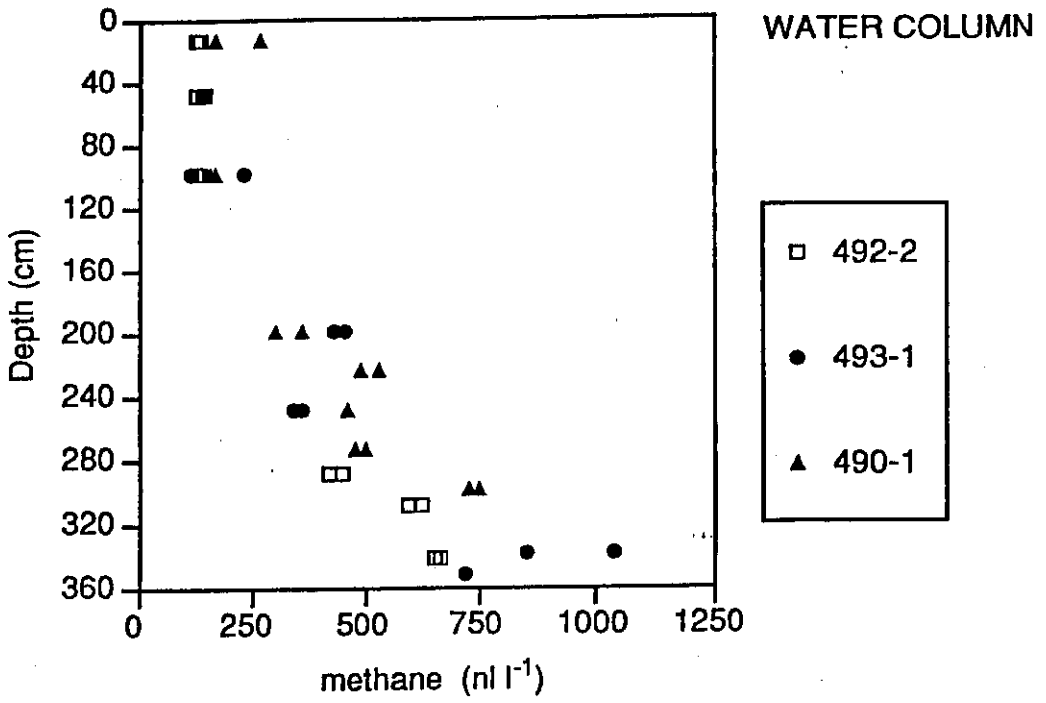

Fig. 61a: Methane profiles of water samples from the Barents Sea crater field showing elevated CH_4-contents in the bottom waters above the craters; these values were obtained by the head-space technique and give considerably higher results than the degassing technique; an intercalibration of both methods should resolve this dicrepancy.

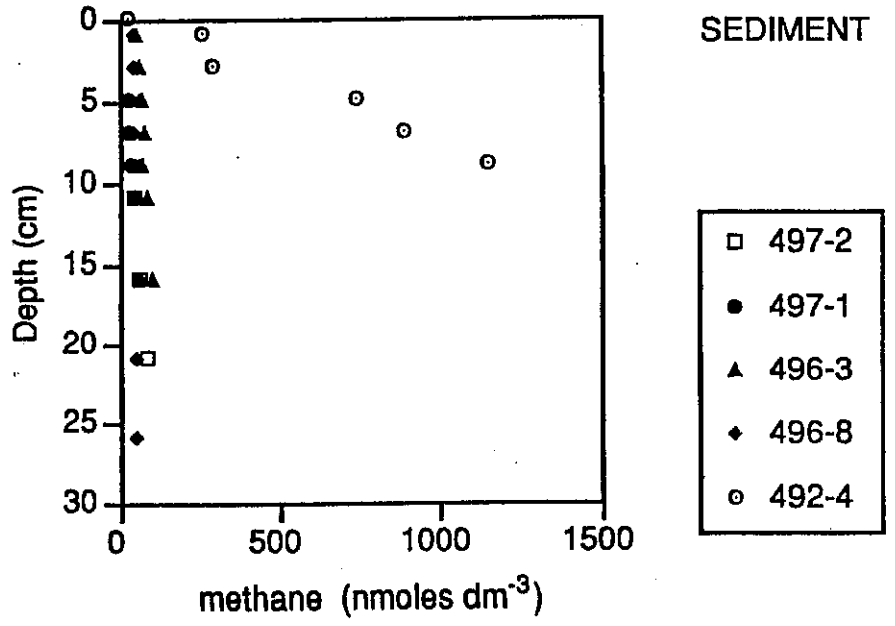

Fig. 61b: Methane contents of sediments samples from the Barents Sea crater field; only core 492-4 shows evidence for methane seepage.

5.4.8.7 Adaptation of Seep Fauna (R. Windoffer, I. Gamenick)

In order to look for structural adaptions of seep fauna at each putative vent station meiofauna samples were taken by boxcorer (GKG) or multicorer (MUC). To also obtain informations on meiofauna abundance and vertical distribution, the samples were fractioned into 0-1 cm, 1-3 cm, 3-5 cm and 5-10 cm layers and separately sieved through a 63 µm sieve. The remaining material including the fauna was then fixed with TRUMPS (glutaraldehyde and formaline in cacodylate buffer) for later quantitative analysis. The special tissue preservation feature of this fixative enables to use the animals also for ultrastructural investigations by electron microscope. The fixation allows also ultrastructural elemental analysis (EELS, ESI) of the material in order to look for possible accumulation of e.g. sulfur. At each station where quantitative meiofauna samples were taken, one subcore was taken for grain size analysis and sectioned into the same horizonts as described earlier. The salinity of the seawater above the sediment was determined using a refractometer.

Skagerrak

In the Skagerrak area a meiofauna sample from 0 - 2 cm was taken from the multicorer (460-1). This sample did not hit a seep and was therefore of minor interest concerning the adaption topic. Still, we investigated the alive material in order to get an impression of the "non-seep meiofauna" community of this area. From the gravity core that was taken very close to a seep (464-1) we got small meiofauna samples from 0 - 5 cm and from 8 - 10 cm sediment depth. In the upper sediment layer we found pogonophorans, few nematodes, two oligochaetes and turbellarians, while in the deeper sediment layer no animals occurred.

Faeroe-Shetland Channel

In this area meiofauna samples were fixed from one MUC (474-1) and two GKG (474-4, 475-1). Since the sediment was not influenced by seepage and also contained large glacial rocks, only samples from the sediment surface (0-5 cm) were taken.

Barents Shelf slope

In the high accumulation area of the Barents slope five subcores (5 cm in diameter) were taken from GKG (480-6). Another subcore was taken for grain size analysis. This sampling site was of interest to us, because typical "vent fauna" like *Thyasira sp.* and pogonophorans were found. Besides the five quantitative samples, we fixed certain animals like nematodes, pogonophores and their larvae and the gills of the bivalve *Thyasira sp* for electron microscopy.

Barents Sea crater field

Within the crater field two stations at the bottom of two craters and one "reference-station" outside a crater were sampled by MUC (492-4, 496-8, 497-1). For quantitative meiofauna analysis three cores (10 cm in diameter) were taken at each station, fractioned and treated as mentioned above. Further on subcores have been taken for grain size analysis at each station

down to 15 cm sediment depth. Since we have samples from two different craters and outside the craters, our data together with the quantitative macrofauna analysis of Dr. A. Tselepides and chemical data from Dr. P. Dando might give a first description of the community living in the Barents Sea crater field.

Of special interest are the samples from station 492-4, since high methane concentrations occur (data by Dr. P. Dando) in the sediment. This core from a seep allows us to analyse the meiofauna seep community as well as investigations on structural adaptations of the fauna to high methane and sulphide concentrations.

5.4.8.8 **Seep Macrofauna** (A. Tselepides)

Cold seeps are recognised as areas with high sulphide, ammonia and trace nutrient concentrations. They are also considered as areas of high benthic productivity due to a food web based on sulphur- and methane-oxidising bacteria. In studies conducted in deeper waters, chemosynthetic carbon fixation has been found to support dense and productive communities of benthic organisms that live near and around seeps. The main objective of our study was to detect and study the chemosynthetic benthic communities that occur around relatively shallow seepage areas in the NE Atlantic European continental margin. In order to do so an extensive sampling program was initiated in the known gas seep site in the Skagerrak, the slope on either side of the Faeroe-Shetland Channel, the Barents Sea slope and the crater field area on the Barents Sea shelf. Despite the very difficult weather conditions that prevailed during most of the cruise, a relatively large number (total of 18) of successful box core samples were retrieved from all three target sites (Table 21). Unfortunately, due to technical difficulties and time constraints typical "seep samples" were not retrieved.

Field Work

Macrofaunal samples were taken with the use of a 0.25 m^2 USNEL box core. Upon retrieval the material was sectioned into four depth layers (0-5, 5-10, 10-20 and 20-40 cm), sieved gently through a 500 µm mesh, stained with Rose Bengal, preserved in 4% buffered formalin and stored in plastic jars for further laboratory analysis. Prior to this, each box core was subsampled for chloroplastic pigments (chlorophyll a and phaeopigments) and organic carbon. Redox potential measurements were undertaken by Dr. P. Dando when reducing conditions were evident. Sediment temperature was recorded at each station. Samples for meiofaunal and particle size analysis were taken by the group from the Univ. of Hamburg on the Barents Sea samples only.

	Sampling Area	GKG Stations	Depth (m)	Latitude	Longitude	Macrofauna Spec. comp. Abun.-Biom.	Chla	Pheo	CPE	OC	Temp. (°C)	Sed. Anal.	Meio-fauna
1	Skagerrak	460-4	320	58° 02.807 N	09° 39.092 E	Y	Y	Y	Y	Y	7,8	N	N
2	Skagerrak	468-2	337	58° 03.148 N	09° 39.506 E	N	Y	Y	Y	Y	7,3	N	N
3	Skagerrak	468-3	334	58° 03.146 N	09° 39.433 E	N	Y	Y	Y	Y			
4	Skagerrak	469-1	329	58° 02.583 N	09° 37.672 E	Y	Y	Y	Y	Y	0,2	N	N
5	Fa-Sh. Chan.	474-2	993	60° 26.024 N	04° 54.478 W	Y	Y	Y	Y	Y	0,9	N	N
6	Fa-Sh. Chan.	474-3	1012	60° 26.119 N	04° 54.598 W	Y	Y	Y	Y	Y			
7	Fa-Sh. Chan.	475-1	983	60° 23.859 N	04° 45.424 W	Y	Y	Y	Y	Y	0,7	N	N
8	Fa-Sh. Chan.	475-2	984	60° 23.695 N	04° 44.259 W	Y	Y	Y	Y	Y			
9	BS Slope	480-5	1601	74° 59.055 N	14° 22.032 E	Y	Y	Y	Y	Y	0,1		
10	BS Slope	480-6	1607	74° 59.025 N	14° 21.600 E	Y	Y	Y	Y	Y		Y	Y-GKG
11	BS Crat. Field	492-5	356	74° 54.228 N	27° 39.214 E	Y	Y	Y	Y	Y	< 0	Y	Y-MUC
12	BS Crat. Field	492-7	356	74° 54.269 N	27° 39.131 E	Y	Y	Y	Y	Y	< 0		
13	BS Crat. Field	492-8	358	74° 54.215 N	27° 39.200 E	Y	Y	Y	Y	Y	< 0		
14	BS Crat. Field	496-3	356	74° 55.434 N	27° 32.421 E	Y	Y	Y	Y	Y	< 0	Y	Y-MUC
15	BS Crat. Field	496-4	351	74° 55.506 N	27° 32.316 E	Y	Y	Y	Y	Y	< 0		
16	BS Crat. Field	496-5	349	74° 55.505 N	27° 32.201 E	Y	Y	Y	Y	Y	< 0		
17	BS Shelf	497-3	341	74° 55.785 N	27° 31.575 E	Y	Y	Y	Y	Y	< 0	Y	Y-MUC
18	BS Shelf	497-5	340	74° 55.852 N	27° 31.764 E	Y	Y	Y	Y	Y	< 0		

Fa-Sh = Faeroe-Shetland-Channel
BS = Barents Sea
Y=Yes
N=No
Chla = Chlorophyll a
Pheo = Phaeopigments
CPE = Chloroplastic equivalent
OC = Organic carbon

Table 21: List of box corer stations taken for macrofaunal analysis.

Further laboratory analysis

The specific objectives of the analyses that will be undertaken in the laboratory are:

- To determine the macrofaunal species composition, abundance, biomass and diversity in the various sampling sites.
- To compare the above indices between the sampling sites.
- To identify differences in species composition both along chemical and vertical gradients.
- To analyse the macrofaunal data statistically and correlate it to the various environmental parameters.

Table 21 gives an overview of the stations that have been sampled as well the biological and chemical analyses that will be performed in the laboratory.

Skagerrak (Stations 460-468-469): Fine, soft, silt-clay sediment of gray colour. Below 20 cm depth the sediment texture became more compact. Sulphidic odour in the deeper layers indicated the existence of reducing conditions. Abundance of organisms observed at all depth layers. Many large Nereid and other sedentary polychaetes were evident in the surface layers. Bivalves, Cumaceans, Amphipods, Sipunculids, Foraminifera, Asteroids and Echinoids were also observed. Actinians were very abundant in the video recordings. These samples were taken as near as possible to the seepage area and will therefore provide us with valuable background information concerning the macrobenthic community structure around these areas in the Skagerrak. It will also be interesting to see how they compare to the original seep samples retrieved during the MAST 1 project. Unfortunately two of the four box-core samples were destroyed due to the storm that we experienced on the the 14-15th of October 1993 in the Barents Sea.

Faeroe-Shetland Channel (Stations 474-475): Coarse, residual sediment with abundant pebbles and rock fragments (lag deposit). Box core penetrated only to a depth of 20 cm. No indication of seepage was evident. Many sponge species were found attached to hard substrate surfaces and were collected by the representative of the Free University of Berlin (Dr. Peter Röpstorf). Ophiuroids, polychaetes and amphipods were abundant as well.

Barents Sea slope (Station 480): Fine, soft, silt-clay sediment of dark brown colour in the surface and gray below a depth of 10 cm. Many thin Pogonophores were found between 2-20 cm depth. Bivalves of the genus *Thyasira* were also found below 10 cm. Both of these species are considered to be characteristic of seep or high organic matter accumulation areas. Polychaetes and ophiuroids were also abundant. Despite the fact that this station showed promising indications of reducing or even seepage conditions, the extremely bad weather conditions in combination with the water depth (1600 m) made it impossible to continue our sampling effort successfully. From the two box cores that were retrieved one was used for the macrofaunal analysis and sulphur chemistry, while the other was subsampled for meiofauna, organic and sulphur chemistry.

Barents Sea crater field and shelf (Stations 492-496-497): Fine, dark brown silt-clay sediment with shales on the surface, that gradually turned gray below 10 cm depth. Below 20 cm the sediment became very compact and sticky. No indication of active seepage was evident. Dense polychaete tubes were found throughout the various depth layers of the box-core. A high percentage of them (approx. 60%) were found to be empty. Large and abundant Bivalves *(Arca glacialis)*, Ophiuroids, Anemones and Pectinarid Polychaetes were evident as well. Few but large Cumaceans, Brachiopods, Asteroids and Holothurians were also collected in this area. Animal biomass seemed to be entirely dominated by the dense clusters of polychaetes that occurred within tubes. Station 497 was outside the crater Field area, on the Barents shelf, and will therefore serve as a reference point. From our initial observations no qualitative difference was evident between this station and those in the craters (492 and 496). On the other hand, the latter probably support a higher animal biomass due to the organic matter that is trapped and accummulated within the crater.

Acquiring these samples was an extremely difficult and dangerous task if one takes into consideration the weather conditions that prevailed throughout this cruise. We should therefore be satisfied with the amount of work that did get done. From the areas that were visited, the Skagerrak remains the most promising and accessible seepage site, while the Faeroe-Shetland Channel should not be taken into consideration in the future. Work still remains to be done in the Barents Sea in order to locate the source that gives rise to the methane plume. The most complete series of biological samples were taken in this remote area and therefore our results are inherently valuable. If an active crater field is discovered in the future further north, then the work done during this expedition will serve as an ideal reference point.

5.4.8.9 Pore Water Nutrients (E. Suess)

Nutrients in pore waters were measured on 57 samples from five cores during M 26/2. Four of these cores were MUCs to obtain high-resolution near-surface gradients and one was a 570 cm long gravity core. Pore waters were extracted by a standard pressure filtration technique at or near *in situ* temperatures. Analyses of labile constituents were performed onboard. The pore water chemistry of gravity core 464-1 and its near-surface companion multicorer 460-1 from the Skagerrak clearly documents ongoing gas-seepage from the sediments at this site. The most interesting preliminary conclusion is based on the combined downcore ΣCO_2 and NH_4-data (Fig. 60a) in conjunction with the CH_4-content (Fig. 60b) and reveals that methane is preferentially oxidized in a subsurface layer between 30-130 cm deep. This layer shows a very significant ΣCO_2 anomaly and also has the highest CH_4 content. It is assumed that methane is supplied either through vertical ascent or lateral flow.

The argument that the excess ΣCO_2 is derived from methane oxidation and is not due to some random NH_4-fluctuations is illustrated in Figure 62. It shows that for the very surface

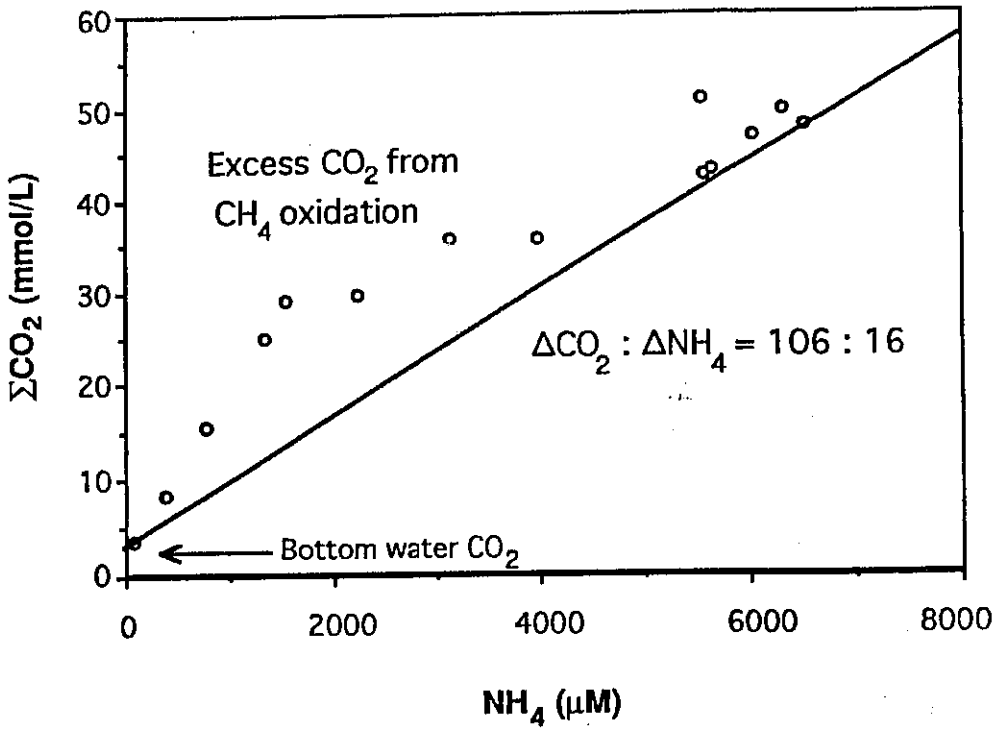

Fig. 62: ΣCO_2 and NH_4 in pore waters from gravity core 464-1; the relationship between both metabolites deviates considerably from the Redfield stoichiometry indicating that there is an excess of ΣCO_2 associated with the maximum CH_4-content in the core (see Fig. 60a); the excess CO_2 is thought to be generated by CH_4-oxidation as previously showed by SUESS and WHITICAR (1989).

and the deepest core sections the generation of ΣCO_2 and NH_4 proceed according to the Redfield ratio of marine organic matter decomposition; i.e. $\Delta CO_2 : \Delta NH_4 = 106 : 16$. However in the subsurface interval between 30-130 cm more ΣCO_2 is generated than would be expected from POC-decomposition. Hence another C-organic substrate must be oxidized but which does not release NH_4. CH_4 very likely is that substrate.

Other evidence to support this idea will come from stable isotope data of the dissolved ΣCO_2 and CH_4 from all core intervals as well as the dissolved sulfate contents (SUESS and WHITICAR, 1989). All precautions on sampling and preserving the labile gas phases for isotope analyses have been taken and the results should be available soon. The shipboard data also indicate that there is enough methane in the samples that they might yield sufficiently large amounts of carbon for ^{12}C-determination. Such data would be valuable in determining the source of the methane and combined with the stable isotope data of carbon and D/H of the

methane might yield information about the efficiency of the near-surface oxidation process. It is interesting that the methane discharge excludes direct expulsion to the bottom water. Instead it appears that a lateral flow or an extremely efficient oxidation process keeps the methane from reaching the sediment surface. Physical properties data, water contents combined with isotope data might elucidate this peculiar situation.

The core at Sta. 480-6 from the Barents Sea slope, a site of high sediment accumulation and subsurface acoustic turbitity, showed strong nitrate reduction within the upper 4 cm of the top and subsequent ammonia generation. This is typical for hemipelagic sediments with some substantial amount of organic matter (> 1.5 wt-%). Silica was high in a subsurface layer at around 5 cm of depth followed by a slight minimum and subsequent gradual increase. This distribution is also typical for hemipelagic sediments. Generally, the same pattern was observed in prior years with the exception that the depth of nitrate penetration varied slightly, i.e. between 4-8 cm. This rather stable nutrient pattern does not suggest substantial influence from venting of methane.

Two MUC-cores from the Barents Sea shelf were used for extraction of pore waters and nutrient analyses. One came from inside a crater (Sta. 496-8) and the other from a sediment mound between craters (Sta. 4972). Both cores showed a characteristic dissolved silica distribution with strong interfacial maxima, i.e. the difference between bottom water silica (10 µM) and subsurface maximum (130 µM) is extremely large. In both cases the maximum is followed by a gradual decrease of silica with depth. Such a pattern is typical for sediments which receive high diatom silica input as is expected for the Barents Sea shelf. Another remarkable feature of the two cores is their dissolved ammonia contents. They show several subsurface maxima, at 4 cm, 8 cm, and 10 cm, which appear to be related to the penetration depths of a very dense polychaete population. At the same time the ammonia remains low in the sediment from inside the crater whereas outside it is about 5-times higher. This is unexpected and difficult to explain. It could be related to the activity of microbial ammonia and methane oxidation which was previously observed in near-surface sediments from inside the crater field. It remains to be seen whether this is an effect of seepage by methane-bearing fluids.

In general, the gradual nutrient concentration gradients which are being maintained across the sediment-water interface at all sites sampled, indicate that any upward advection of fluids must be slow. Estimates indicate that the rate probably is below about 3 cm $year^{-1}$, otherwise the gradients would be "washed out"; i.e. would be vertical up to the interface.

5.4.9 **Boreal Shallow-water Carbonates** (A. Freiwald, P. Röpstorf, H. Meggers)

Cold-water carbonates which were envisaged during M 26/2 include *Lophelia* banks from the Lousy Bank, active balanid production sites on Spitsbergen Bank, bryozoan thickets on

Malangsgrunnen, and one of the largest known *Lophelia* reefs off Trondheim. Due to the severe storms which RV METEOR encountered only the Spitsbergen Bank program could be partly realized. The results however, offer surprisingly new information on the nature of a productive carbonate factory within the photic zone.

The western part of the Spitsbergen Bank is one of the largest occurrence of cold-water carbonate deposits beyond the Arctic Circle. For this reason, it offers an excellent opportunity to study processes of biogenic carbonate production under glaciomarine environmental conditions. The postglacial geological history of the Spitsbergen Bank is reflected by distinct carbonate producing communities which exist on the shelf bank since the last 8.000 years. Most evident is the complete ecological replacement of a former infaunal community, dominated by *Mya truncata* and *Hiatella arctica*, by hardsubstrate encrusting communities. The latter communities consists of *Balanus balanus, Chlamys islandica, Modiolus modiolus* and different species of bryozoans. This faunistic turnover is linked with winnowing processes of the former soft substrate due to isostatic uplift, the shifting of the oceanographic frontal systems over the shelf bank, and finally, the seasonal decline of sea ice coverage. All in all, this large-scaled ecological turnover on this shelf bank is an outstanding example for a taphonomic feedback.

The carbonate deposits on Spitsbergen Bank were studied during previous cruises (M13/1 and M 21/4). On these cruises the sites of carbonate production and deposition in the 120 to 40 m depth interval have been sampled intensively. Therefore, the sampling program on cruise M 26/2 concentrates on a shallow plateau at 75°13.8 N and 18°38.1 E, approximately 80 nm north of Bear Island. Additionally, another site (75°02 N and 22°57.8 E) at 104 m water depth was sampled on the way to the Barents Sea crater field.

The central part of the Spitsbergen Bank area is covered by calcareous sands and gravel formed by the fragmented plates of the balanid *Balanus crenatus*. Due to high energy hydrodynamic conditions, these calcareous sands show a set of current ripples and bars. Epifaunal live on these unstable areas is sparse. The infauna is dominated by amphipods. The lower limit of the *Balanus crenatus* sands is around 40 m water depth. However the production sites are unknown. Therefore, most of the stations are concentrated around a rather shallow plateau at 16 to 25 m water depth forming an isolated shoal on the shelf bank. The main axis of this plateau is oriented from NW to SE and has an extension of 9 nm. The plateau was surveyed with a pan-tilt CCD-Camera system mounted on a frame. After the video surveys, the same area was sampled with a 30 kg Petersen-grab. Sea bed topography is dominated by large outcrops of Jurassic black shale. Slight depressions on the rocky areas are filled by thin veneer of *Balanus crenatus* sands. Most impressingly is the evidence of a far off-shore kelp forest with its lower limit at 25 m water depth. The kelp forest is formed by a single species: *Laminaria saccharina* (Fig. 63.1). The major difference to kelp forests in the boreal realm is the lack of so called understorey algae. These understorey algae are generally dominated by rapidly growing single-year species. However, on the Spitsbergen Bank the

time for growth and reproduction is too short for these ephemeral algae. The extreme seasonality caused by the arctic irradiation regime favors perennial (multi-year) algae to thrive well under these environmental conditions. This is made possible because of their large storage capability in their algal thalli. This is also true for calcifying coralline algae, whose crusts are concentrated close to the rhizoid holdfasts of the *Laminaria saccharina*. Kelp and coralline algae in high latitudes are able to store carbohydrates (amylopectine) during the summer for utilization during the dark winter times. On the other hand, orthophosphorous compounds and nitrogen is stored during dark winter periods and utilized during the summer period, when there is a nutrient depletion in the water column.

The most dominant faunal element within the kelp forest are dense colonies of *Balanus crenatus*. This species forms a single-layered colony on hard substrates. Unlike the deeper water *Balanus balanus,* no reef-like overgrowth occurs in *Balanus crenatus*. Post mortally, the skeletal plates of *Balanus crenatus* are easily dislocated and thus contribute to the sediment supply. Keeping the results of previous sedimentary investigations on the Spitsbergen Bank in mind, it becomes clear that this shoal represents the major resource for sediment supply formed by *Balanus crenatus*. Compared to the spatial distribution of the *Balanus crenatus* sands on the bank, the production sites are very small. The presence of kelp forests and dense accumulations of *Balanus crenatus* on the shallow plateau studied suggests that iceberg-scouring does not occur on this part of the Spitsbergen Bank. Icebergs may strand further east, or, pass through the Storfjord- and the Bear Island-Troughs.

The transit from the shallow plateau to the crater field was used for taking samples with the Petersen-grab from 104 m water depth (75°02. N / 22°57.8 E) which is close to the storm wave base on Spitsbergen Bank. Due to the severe thunderous storm, this transect could not be completed. The sedimentary environment is structured by soft glaciomarine diamictons with a pebbly surface. These pebbles act as hard substrate "islands" for fouling organisms, such as sponges, encrusting and fan-shaped bryozoans, epilithic benthic foramaminifers, zoantharians, serpulids, and limpets (Fig. 63.2). Living *Chlamys islandica* are heavily fouled on their upper (left) valves by reef-like overgrowth of *Balanus balanus* (Figs. 63.3 and 63.4). Additionally, a thin shelly lag-deposit with Holocene bivalves is developed (Fig. 63.5).

Apart from mechanical abrasion due to wave drag in the shallow sites of the Spitsbergen Bank, carbonate removal in the deeper sites is mainly forced by bioerosion at the sediment-seawater interface. The valves are intensely bored by endolithic organisms that are fixed with glutardialdehyde for detailed species determination. Borings are made by sponges, fungi and algae, with burrows measuring 1 to 100 µm in diameter (Fig. 63.6). A postmortem cementation of the borings is very sparsely developed. Therefore, the cold-water carbonates from the storm wave base provide a large potential for storage of hydrocarbons due to their high porosity.

Figure captions

Fig. 63.1: Phylloids of *Laminaria saccharina* in 25 m water depth from the plateau studied.

Fig. 63.2: Encrusting bryozoans (arrow) are very abundant on exposed boulders on the Spitsbergen Bank. The intense overgrowth pattern in the different bryozoan species indicate competition for space.

Fig. 63.3: View on the lower (right) valve of *Chlamys islandica* from Spitsbergen Bank with some bryozoan encrustions. The upper (left) valve is intensely fouled by *Balanus balanus*.

Fig. 63.4: A lateral view of the same specimen showing the enormous settlement of *Balanus balanus*.

Fig. 63.5: Winnowed shelly seatbottom with Holocene (6.000 - 8.000 yB) *Mya truncata* predominately. This type of sediment is widely distributed on the Spitsbergen Bank between 70 to 120 m water depth.

Fig. 63.6: Resin cast of endoliths (sponges?) which live in *Mya truncata* valve. This large intraskeletal porosity is characteristic for cold-water carbonate deposits.

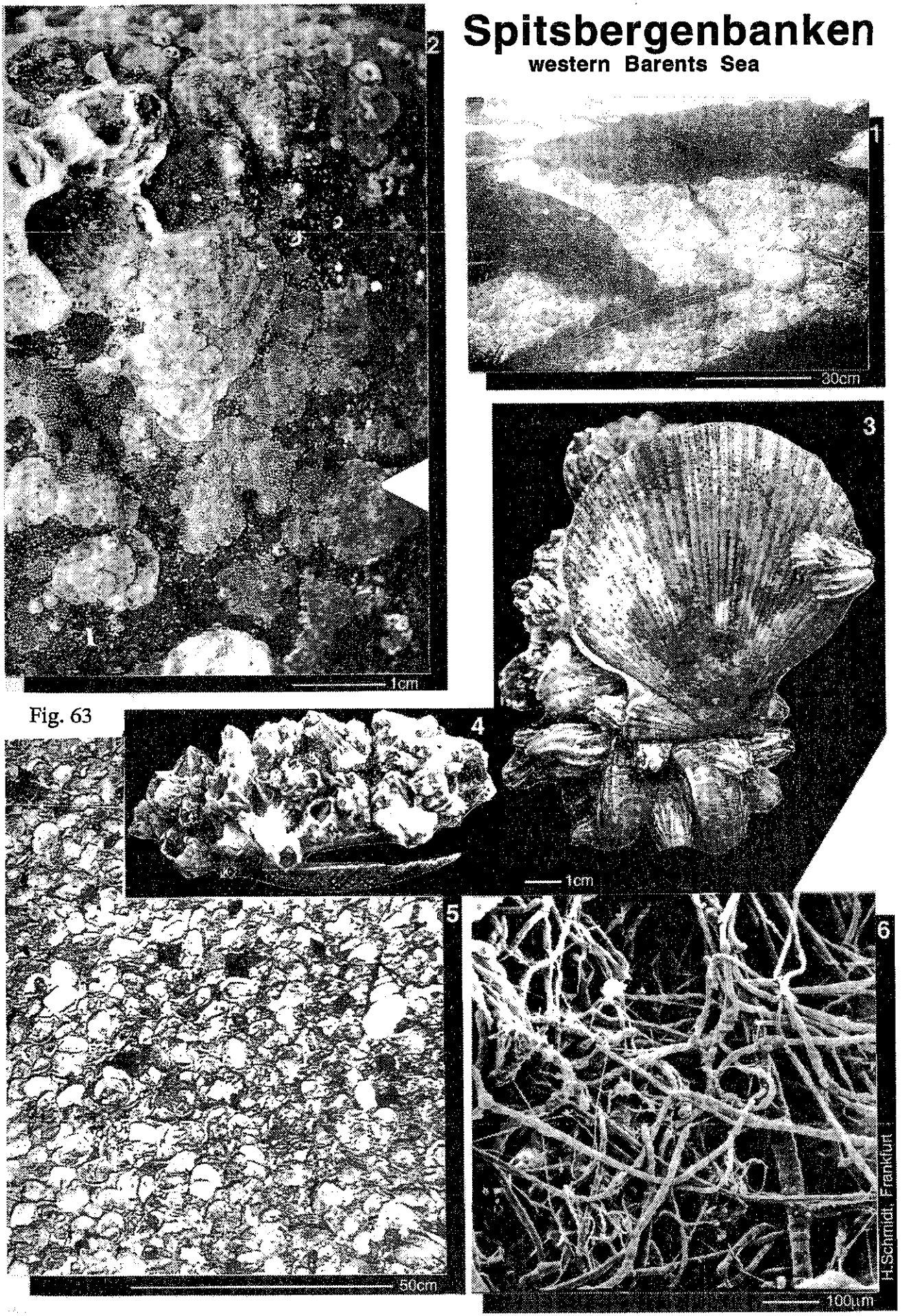
Spitsbergenbanken
western Barents Sea
1
30cm
2
1cm
3
1cm
4
5
50cm
6
100µm
H.Schmidt, Frankfurt

Fig. 63

5.4.10 Porifera Communities and Spiculits (P. Röpstorf)

The main goal of this study was to collect recent sponges and spicules of ancient sponges from different ecological and bathymetric zones for actuopaleontological, histological, and taxonomic research. During leg M 26/2 box core (GKG) and multiple core (MUC) samples were taken from different stations in the Skagerrak, the Faeroe-Shetland Channel, the Aegir Ridge, the Barents Sea slope, and the Barents Sea crater field. On the Spitsbergen Bank a Petersen-grab was used, because of the hard bottom substrate (see 5.4.9). Communities of Porifera were studied during a previous cruise (M21/4) to the Norwegian and Greenland Seas. During leg M 26/2 this work was continued.

In order to record the sponge spicules in different depths, sediment slices were taken at intervals from the box corers or the multiple corers. The spicules separated will be compared to those of the recent sponge fauna. In this way we hope to gather information about the decay of sponges and the composition of the sponge communities in the past. It was of special interest to find spiculits, hard deposits of spicules of ancient sponges. For taxonomic studies on the recent sponges and for ultrastructural research on the morphology of the choanocytes, the sponges were fixed for electron microscopy (TEM & SEM): All sponge samples were fixed in cacodylate buffered 4% glutaraldehyde solution in seawater. The material for histological studies was dehydrated in a series of ethanol up to 70%. Parts of the sponges, which were intended for transmission electron microscopy were postfixed with 2% osmium tetroxide in seawater and after dehydration embedded in LR-White on board ship.

The sponges were examined with a stereomicroscope and spicule samples were prepared in order to determine the species; this task is in progress. Unfortunately no spiculits were found neither with help of the box corers nor with the gravity corer (463-3, 464-1).

Skagerrak

Samples taken in the Skagerrak region contained no sponges. Drop stones, which might act as hard substrates, were absent on the soft silt sediment. Only sediment samples were taken for the spicule report.

Faeroe-Shetland Channel

In five box cores taken from two stations (474, 475; water depth: 1000 m) the coarse residual sediment contained numerous pebbles (1-30 cm), which were populated by Porifera. We collected 38 different sponges, poikilosclerid demosponges and little calcareous sponges were dominant. Hexactinellids were not detected.

Aegir Ridge

In two box corers with silty-muddy sediment, taken from depths of 2250 m and 3300 m only one sponge (*Tentorium semisuberites*) adjacent to a small pebble was found. The low abundance of rocks explains the very poor sponge fauna. The reason for absence of the

typical soft bottom adapted sponges found on a previous cruise could be that the area sampled by the box corer is small compared to that sampled by an Agassiz-trawl, which was not available on cruise M 26/2.

Spitsbergen Bank
Samples were taken with a Petersen grab from the shallowest area (16-35 m) of the Spitsbergen Bank as well as from deeper sites (100 m). On the shallow plateau only one sponge was found, showing a crust-like structure. From the deeper sites five sponges, presumable of different species, were gathered from pebbles. Skeletal plates of *Balanus* and shells of bivalves were colonized by boring-sponges (*Cliona*).

Barents Sea slope and crater field
The samples taken from two slope stations (478-5, 480-6) contained no sponges but spicules were quite abundant. From six box core samples of three stations (489-1, 492-5, 492-6, 496-2, 493-3, 496-4, 496-8) 22 specimens of different sponge-species were collected. Together with encrusting and fan-like bryozoans, the sponges were attached to shale fragments. At station 493-2 the VESP system showed that certain areas of the craters are settled by huge sponges. Unfortunately, we could not obtain specimen of these sponges with the equipment available.

5.4.11 European North Atlantic Margin - Sediment Pathways, Processes and Fluxes (ENAM)

5.4.11.1 Geophysics (D. Evans, C. Brett, D.G. Wallis)

The Storegga Slide, located on the outer shelf and continental slope off Norway, has principally been described in papers by Bugge and his co-workers during the 1980s (BUGGE, 1983; BUGGE et al., 1988; JANSEN et al., 1987). It is one of the world's largest slides, having moved a total of 5600 km^3 of sediment with a thickness of up to 450 m from an area comparable with that of mainland Scotland. Three separate slide movements were identified. It is easily the most significant area of mass movement on the European margin, and is therefore an important component of the ENAM program.

The British Geological Survey (BGS) provided the deep-tow-boomer System (DTBS) for high-resolution seismic profiling around the Storegga Slide. The DTBS is towed at depths down to 800 m, and is able to generate profiles with a resolution of more than one metre in water depths of up to 2000 m. The system had been mobilised on the vessel in Leith and used previously on Leg M 26/2. During the course of that leg the boomer fish had sustained some storm damage but had been repaired successfully.

In general, the intention was to conduct coring operations by day and run profiles using the DTB, Parasound and Hydrosweep overnight. It was also planned to use the DTBS as a sound

source for an Ocean Bottom Hydrophone (OBH) experiment. In addition to the analogue records, all data were recorded on EXabyte tape cartridge using the BGS DAMP16 PC-based digital recording system. These data will be processed at BGS/Edinburgh.

In total, almost 400 km of boomer profile was acquired (Figs. 64 and 65; Table 22), and in general it is of good quality, with penetration of up to 300 ms. The data over the first three nights suffered from 50 Hz noise (see for example Figs. 66a, 67c and 68b) which became a nuisance in deep water. The noise was traced to an earth-loop problem in the power supply; this was solved by simply reversing the ship's main connections to the power supply. Subsequent data were all of a very high quality.

Tab. 22: Deep-tow-boomer lines recorded on Leg M 26-3

Line	Start		End		Line	METEOR
Number	Date	Time	Date	Time	Length (km)	Profil No.
1	11/1	21:15	11/2	03:25	52	511-1
2	11/2	03:30	11/2	10:30	56	511-2
3	11/2	20:45	11/3	04:20	58	516-1
4	11/3	04:25	11/3	09:10	42	516-2
5	11/3	20:05	11/4	02:05	50	521-1
6	11/4	02:10	11/4	04:45	22	521-2
7	11/4	14:37	11/4	15:30	8	Kiel OBH
8	11/7	05:40	11/7	10:25	40	541-2
9	11/7	20:45	11/7	23:45	24	544-1
10	11/7	23:50	11/8	01:15	9	544-2
11	11/8	01:20	11/8	05:00	36	544-3

Log of normal operations

Operations commenced in the Storegga Slide area on 11/1/93 when the boomer was deployed at 20:50 and run overnight, completing BGS Lines 93/04/1 and 2 (METEOR Profile 511-1 and 511-2). The fish was recovered at 12:00 on 11/2/93 and deployed later the same day at 19:50. BGS Lines 93/04/3 and 4 (METEOR Profile 516-1 and 516-2) were run overnight with the fish being recovered at 09:55 11/3/93. The boomer was deployed again at 19:30 when BGS Lines 93/04/5 and 6 (METEOR Profile 521-1 and 521-2) were completed overnight; the fish was recovered at 06:45 on 11/4/93.

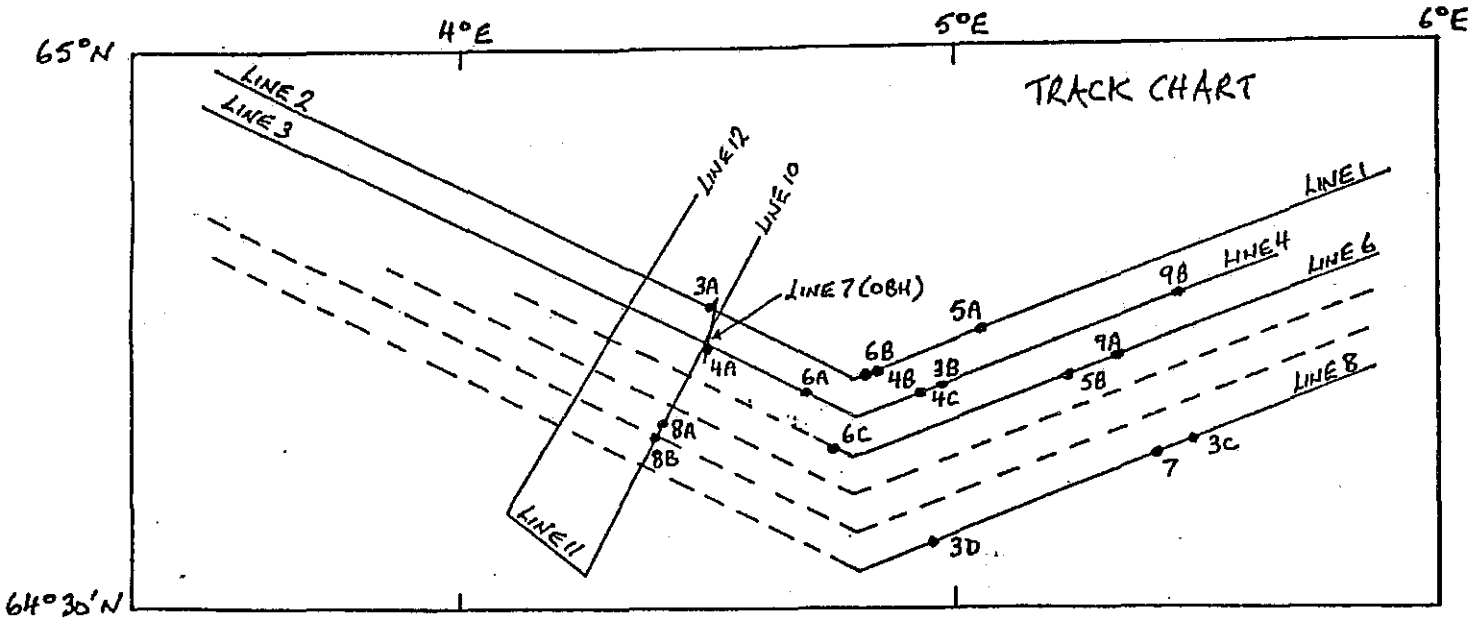

Fig. 64: Generalized track chart showing the locations of selected profiles. Solidlines = deep-tow-boomer, Parasound and Hydrosweep; dashed lines = Parasound and Hydrosweep; dots = approximate locations of Figures 66-72.

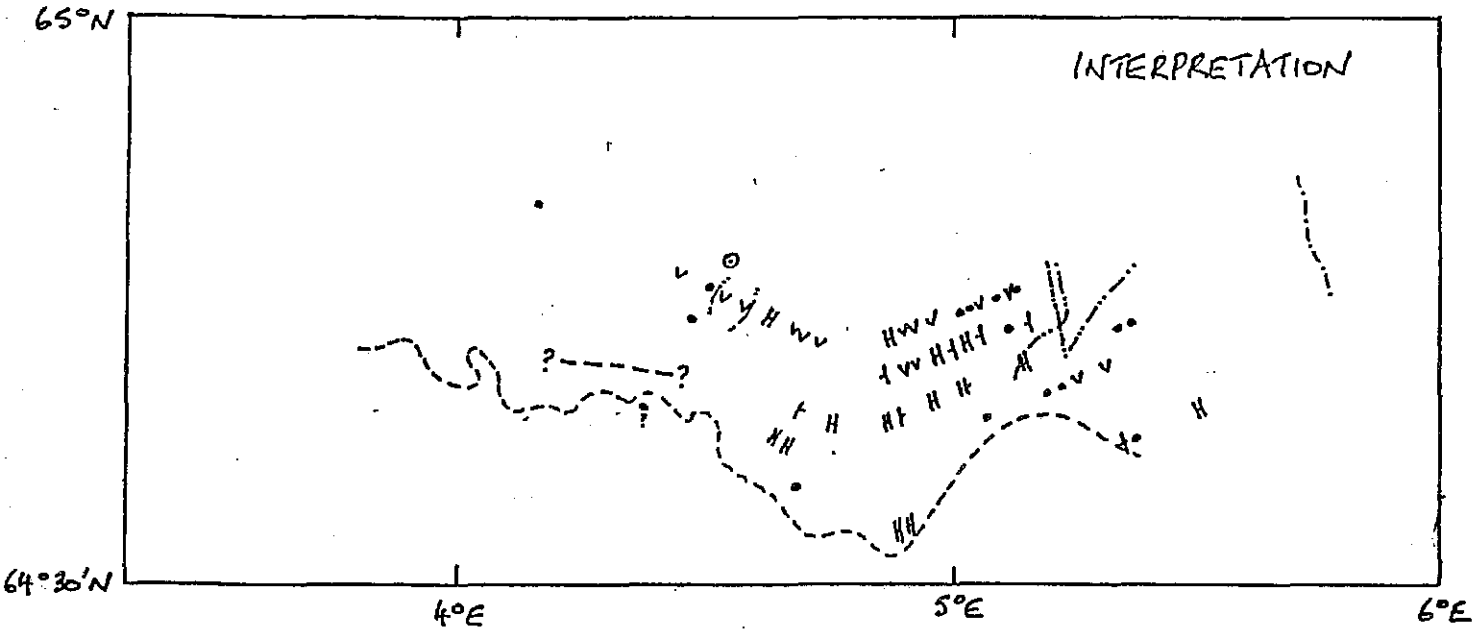

Fig. 65: Distribution of selected features on the northern edge of the Storegga Slide. Open circle with dot = mud volcano (Parasound); solid dot = pockmark (some fossil); V = vent; - - line = landward limit of well-bedded upper unit; - - - line = sea-bed breakup; = seaward limit of debris flows; light - - slide scarp; heavy - - line with question marks = buried slide scarp; brick sign = graben; ∧ - fault.

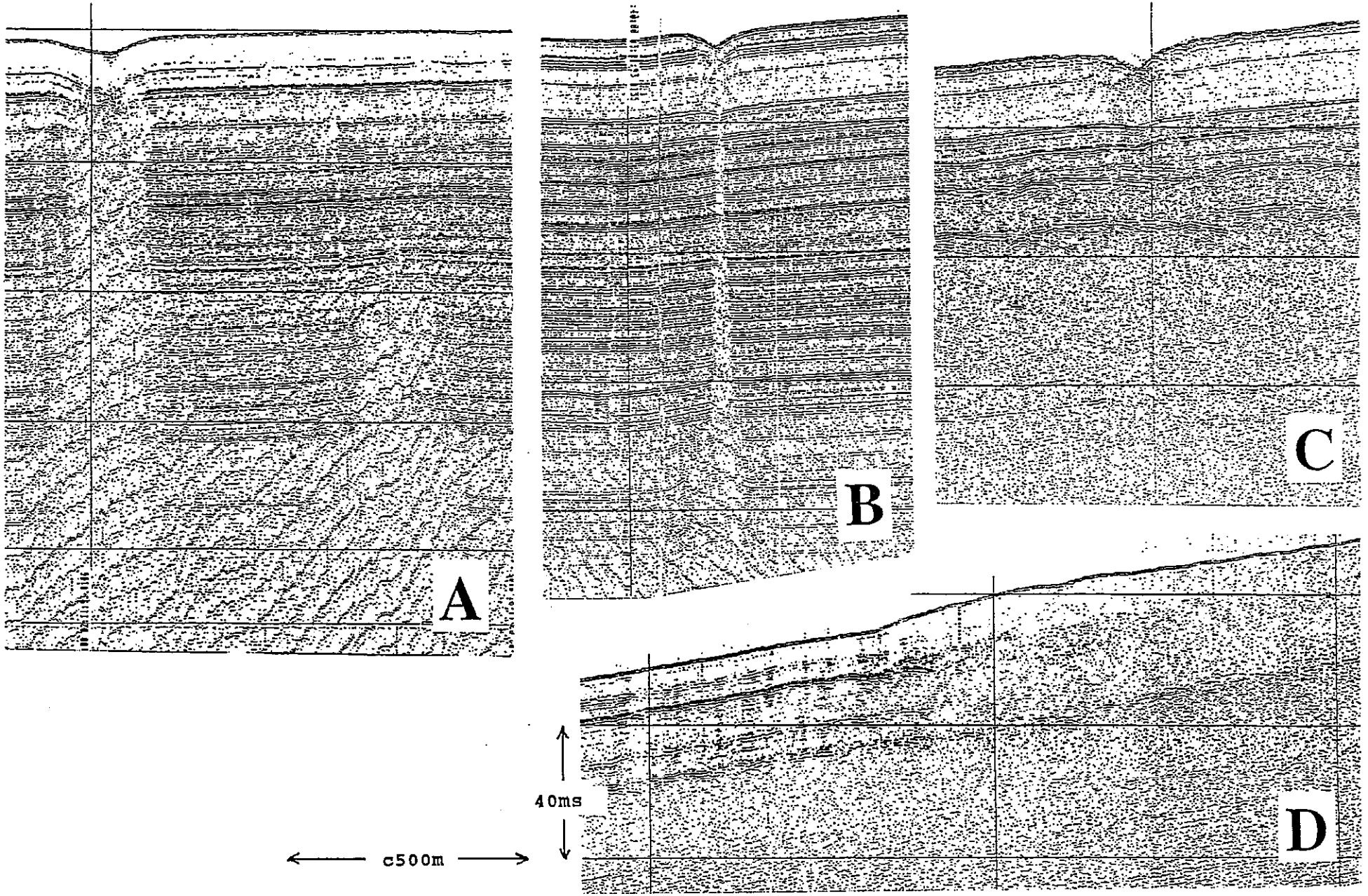

Fig. 66: BGS deep-tow-boomer profiles from the Storegga Slide area. For locations see Fig. 64. a) pockmark with subsurface vent. b) pockmark with chimney. c) single pockmark. d) sediment aggradation at the edge of a slide scarp.

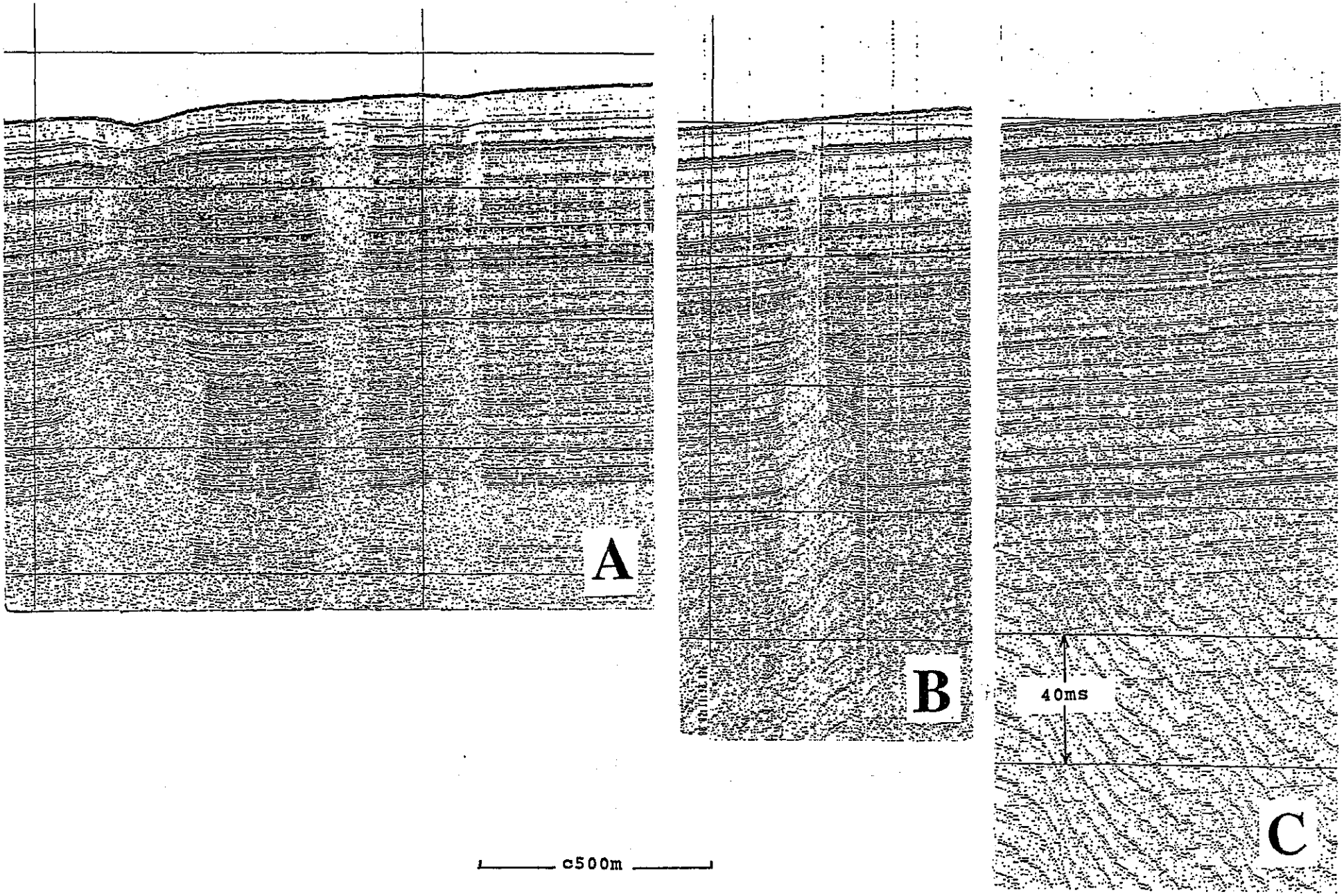

Fig. 67: BGS deep-tow-boomer profiles from the Storegga Slide area. For locations see Fig. 64. a) gas vents, note the upward thinning of the left vent and chimney. b) gas vent. c) chimneys associated with faulting.

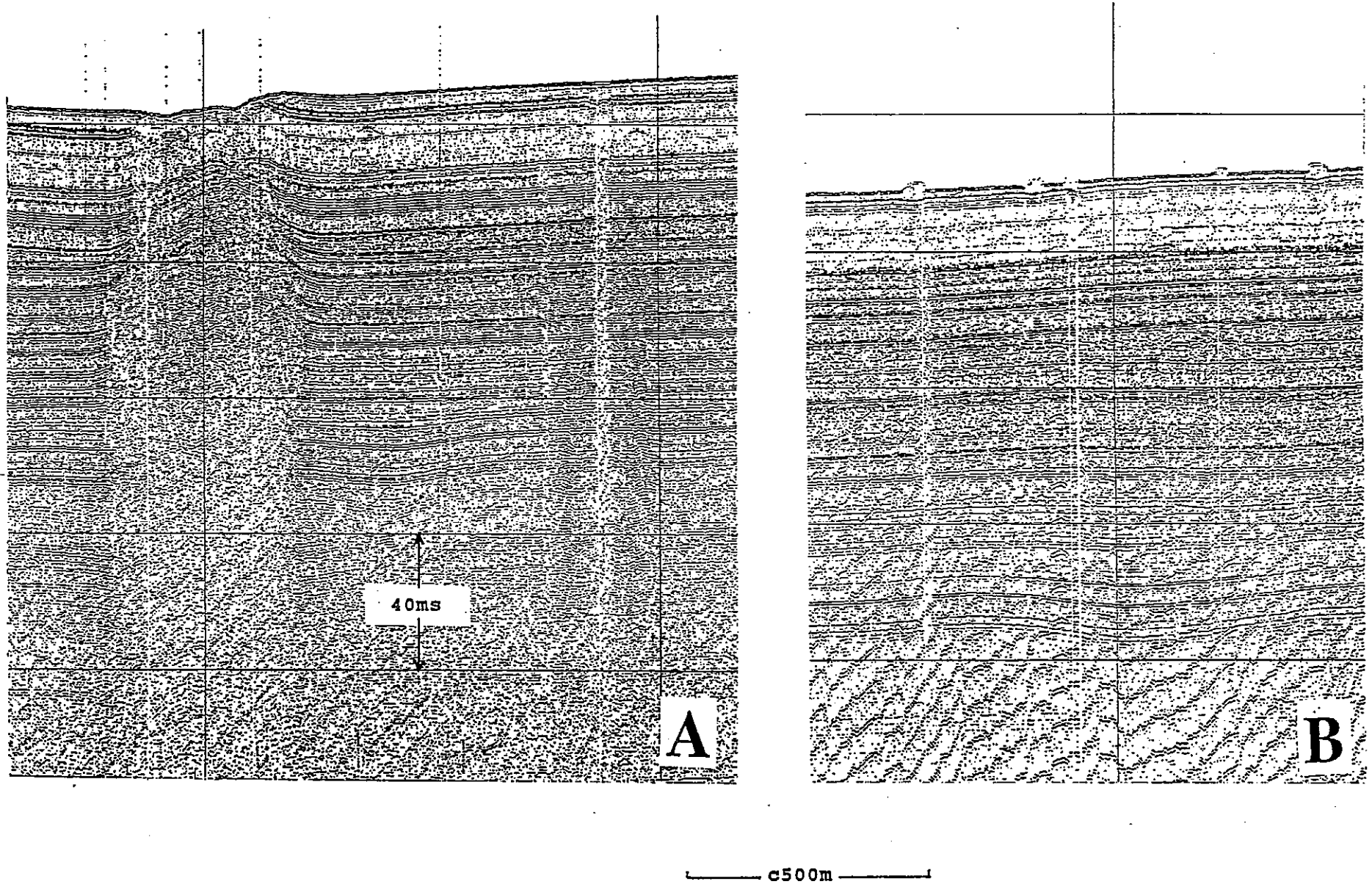

Fig. 68: BGS deep-tow-boomer profiles from the Storegga Slide area. For locations see Fig. 64. a) upward turning of reflectors at the sides of a gas vent, note the rimmed pockmark on the surface. b) bright reflectors and sea-bed breakup.

The boomer was next deployed on 11/6/93 at 21:40 but failed while winching down before the start of the line. This failure was caused by water damage in the trigger connector to the Energy Storage Unit in the fish. This affected the high voltage power supply on board the vessel. The fish was recovered at 00:15 on 11/7/93 and the connector cleaned and resealed and the power supply repaired. The fish was redeployed at 0445 UTC and BGS Line 93/04/8 (METEOR Profile 541-2) was run throughout the remainder of the night, the boomer being recovered at 11:30.
The system was deployed again at 19:10 on 11/6/93 to run BGS Lines 93/04/9,10 and 11 (METEOR Profile 544-1 and 544-2) overnight, with Line 11 ending at 05:00 on 11/8/93. This was the last of the planned lines in this area and during recovery of the boomer fish the electro-hydraulic power pack supplying the winch failed with 400 m of cable still out. It was suspected that the motor had failed and was shorting out the ship's supply. On opening the cover, the motor was found to be full of sea water. This was drained, flushed out with fresh water and dried, but it remained inoperable. It can only be assumed that the sea water entry had occurred during the storm on the previous leg, but that somehow the motor had continued to operate. The fish was recovered using a tugger winch and then the capstan.

OBH experiment
The Ocean Bottom Hydrophone (OBH) is designed to measure the propagation velocity of compressional waves in shallow sediments. The OBH experiment proved most successful. A very good vertical profile recorded from the DTBS should make an excellent comparison with the wide-angle data recorded on the OBH. The OBH data will be processed and analysed in Kiel, as part of B1 project in the SFB 313 and ENAM.

Results
Initial interpretation of the data has been carried out onboard; these analyses have been combined with the ship's Parasound profiles, and with Hydrosweep data as it has become available after initial processing. The profiles were collected from an area on the northern margin of the slide (Fig. 64). It was intended that a grid of lines also be run to the south of the slide, but this was not possible due to bad weather. The profiles were run as shallow chevron-shaped track lines over largely undisturbed sediments north of the slide, but the southernmost lines cross its edge. Two crosslines were run, and a further transverse profile was run in conjunction with an Ocean Bottom Hydrophone (OBH) experiment.

The sedimentary sequence to the north of the slide edge comprises largely undisturbed, parallel, gently seaward-dipping, seismically well-bedded reflectors. The sequence is apparently of almost constant thickness when short lengths of record are examined, but there is an overall downslope reduction in thickness. This reflects a constant pattern of deposition, particularly in the upper 80 ms of section, and a stratigraphy that will be investigated further. Below 80 ms, there are many local changes to this regular pattern, such as reflector warping and lensoid development. These anomalous features are in some cases reflected in topographic changes at the sea bed, despite the overlying drape. The stratigraphical

relationships of these features will be clarified when copies of the profiles are available for detailed interpretation, and when cores will have been analysed. For the present, the main interest lies in the features that vary from this regular pattern. These have been identified and are discussed below. Their distribution has been mapped (Fig. 65), and it is evident that the features are concentrated in the eastern portion of the grid, and are absent in the deeper water to the west.

Pockmarks

Pockmarks are shallow depressions in the sea bed which are thought to be formed by the escape of gas or fluid (e.g. HOVLAND and JUDD, 1988). As the gas vents, it throws out sediment from which the finest component is carried away by currents, leaving only the coarser grades to fall back. This process may be gradual or explosive, and leads to the formation of a depression at the sea bed. This process can only take place in argillaceous sediment. Several such depressions have been identified in the study area (Figs. 66a-c), the largest of which is ca. 300 m in diameter and 5 m in depth. The true distribution of features of this dimension is difficult to assess without side scan sonar; in at least one instance (at a PUPPI site), a pockmark was identified on Parasound data immediately beneath the ship, but was not recorded by the DTBS which at that point was probably flying along a line to the side of the ship's track. The pockmarks in the area are commonly, but by no means ubiquitously, underlain by "vents" or "chimneys" which appear to confirm the presence of gas. Some pockmarks do not appear to have been active for some time, as they are buried - these are termed fossil pockmarks.

Vents

The features defined here as vents are recognised as vertical pillars of "wipe-outs" of acoustic features, up to ca. 200 m wide, from which a much reduced signal is returned (Figs. 67a-b). In some cases there are hyperbolic reflection patterns off their sides, upward turning of the reflectors at the sides of the vent (Fig. 68a), or doming of reflectors over a width of ca. 300 m. They may or may not reach the surface, and in one case there is upward lateral truncation of the wipe-out, resulting in thinning of the column (Fig. 67a). It is thought most likely that these are gas escape pathways; in some cases they are associated with pockmarks.

Chimneys

Chimneys, as recognised in the study area, are vertical or sub-vertical columns of wipe-out zones. They are narrower than vents, from which they differ more significantly by never appearing to disrupt the reflector pattern (e.g. Figs. 67a and 67c). However, they grade in width to become small vents, and vary from clearly defined to barely distinguishable. It is therefore commonly difficult to identify them and map their distribution (Fig. 64). In some instances they are associated with faults (Fig. 69a).

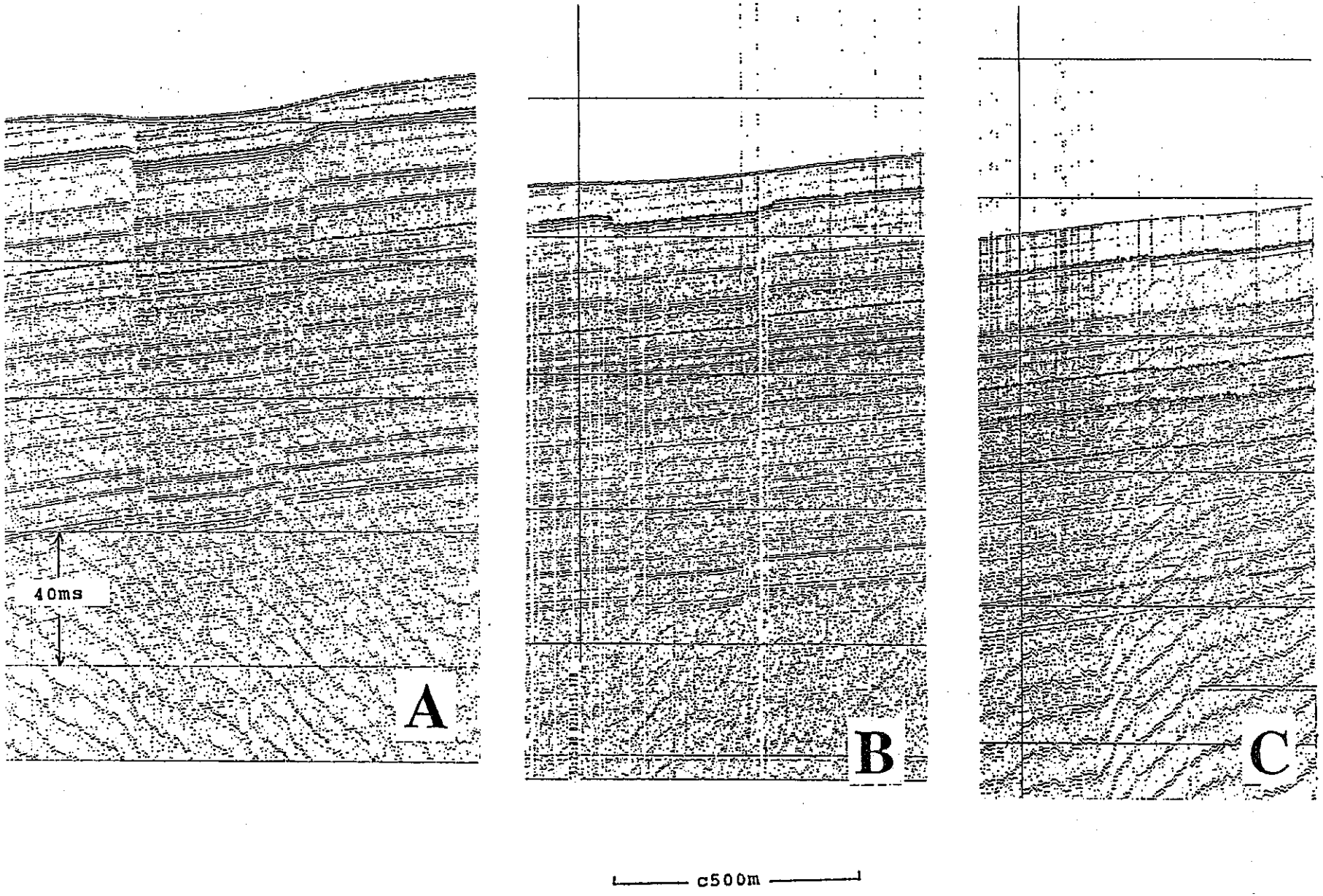

Fig. 69: BGS deep-tow-boomer profiles from the Storegga Slide area. For locations see Fig. 64. a) graben with associated chimneys. b) graben, c) single vertical fault.

Bright/hyperbolic reflectors

Throughout the upper part of the record there are scattered instances of short, stronger reflectors, commonly with associated hyperbolic reflection patterns (Fig. 68). They would appear to have a random depth distribution, and are probably due to the local presence of coarser-grained sediment layers deposited from icebergs, or less likely to the presence of gas.

Mud volcanoes

Only one possible instance of this phenomenon has been recorded by the DTBS, and the term "mud volcano" is used here rather speculatively. The feature is similar to a pockmark except that it has a weakly-defined topographic rim on the profile and upturned marginal reflectors suggesting forceful movement through the sediment (Fig. 68a). A better-defined feature is recorded on a line run only with the Parasound, and another Parasound profile shows a topographic blister which may represent a "pre-eruption" condition of a mud volcano.

Faults and grabens

Several faults have been recorded on the profiles (Fig. 69). They are predominantly vertical, but some are inclined; the maximum recorded throw is ca. 4 m. All faults either reach the sea bed or come within a very few metres of it, despite the softness of the sediment; shear strengths of about 6 kPa were measured by the Module Geotechnique within 2 m of the sea bed. It is suspected that, in similarity with investigated deep-sea sediments, these apparently single-plane faults may in reality be the sum of many smaller movements within a narrow zone.

Single faults generally have a downthrow towards the topographically lower sea bed, but there are examples of the opposite sense of movement (Fig. 69c). Many of the faults occur in conjugate pairs to form graben, which are typically some 150 m in width (Figs. 67c and 69a-b). They generally generate sea-bed depressions of similar dimensions to their throws. From the line spacing of the survey, it is not possible to map the orientation of the faults; the topographic depressions are too subtle to be recorded by the Hydrosweep.

Slide scarps

The edge of the Storegga Slide in this area is generally defined by a sharp downslope scarp. This is well defined on DTBS records, and can be accurately mapped with the aid of the Hydrosweep data (Fig. 65). Excellent definition of the internal structure of both the slumped and *in situ* sediment has been obtained; Figure 70 shows displacement of a large block of the sedimentary sequence at the scarp, with more-disturbed sediments giving a markedly irregular surface farther from the scarp. In one instance, at about 5° E (Fig. 65), there is a record of aggradation of sediment at the edge (Fig. 66d) - this is similar to that recorded at the southern edge of the Storegga Slide. Sediment moving from the headwall to the north and east has here evidently overridden the southward-projecting spur of undisturbed sediment.

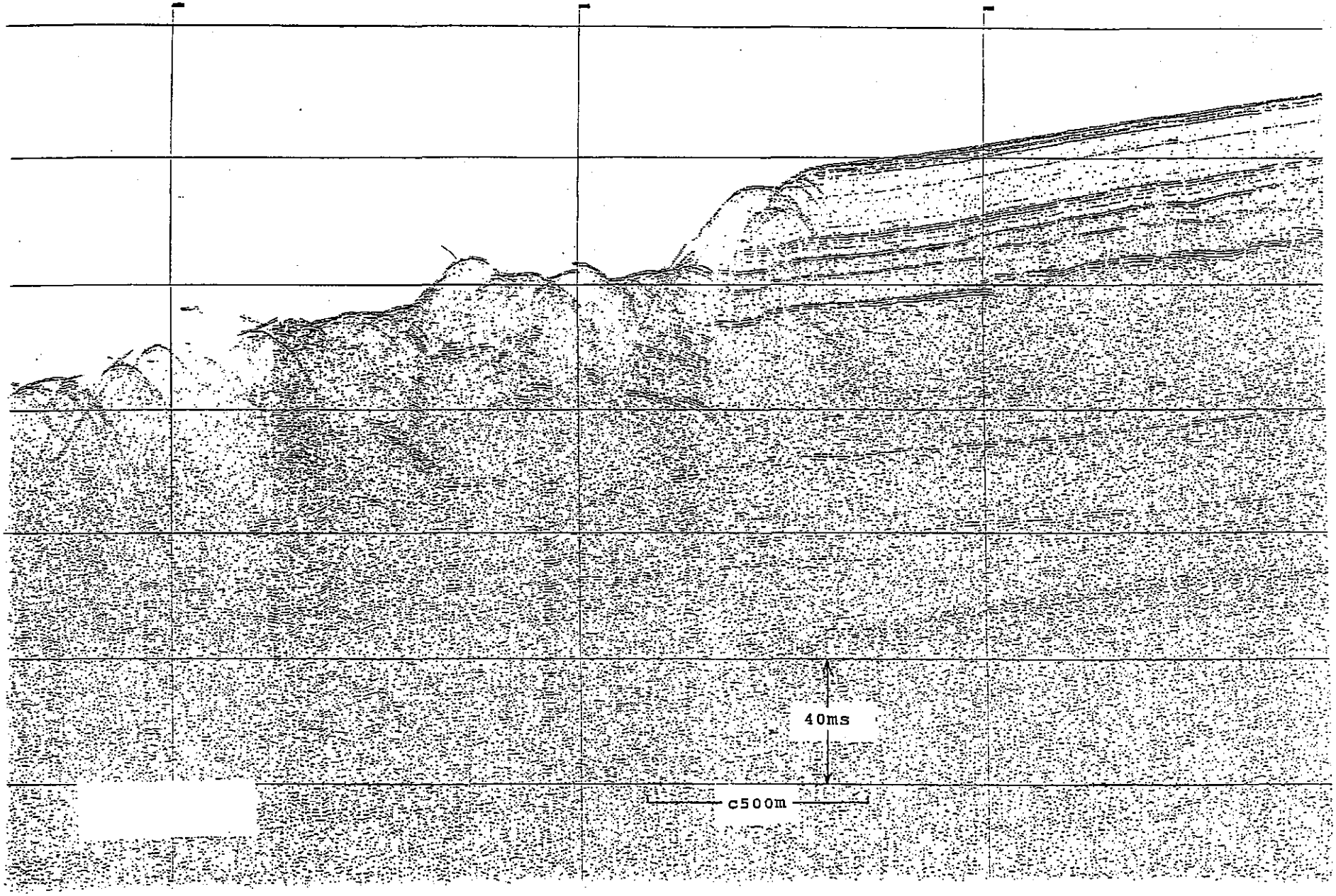

Fig. 70: BGS deep-tow-boomer profiles from the Storegga Slide area. For locations see Fig. 64. Displacement of a large block of a sedimentary sequence. The edge of the slide scarp is seen in the middle of the profile separating continuous layers (right) from massive deposits with varied sea-bed relief (left).

Buried scarps

A particularly interesting discovery has been that there is at least one slide that pre-dates the "First slide" of BUGGE et al., 1988. The profile in Figure 71a is interpreted as showing a slump deposit with its head defined by the truncation of a strong reflector. The massive deposit is overlain by up to 80 m of the undisturbed sequence, which is cut by the "First Slide". If the age of the sequence can be determined, the timing of this ancient slide could be established. The location of the ancient slide remains discernible from sea bed topography. Other slides pre-dating the "First Slide" may be identifiable by examination of the sea-bed topography; one possible location is noted in Figure 65. Following this discovery, re-examination of IKU sparker records suggests that a yet older slide is also present, overlain by up to 200 ms of the sedimentary sequence. These observations are particularly pertinent in the light of the discovery by the Bergen group of an older slide to the south of the Storegga Slide.

Debris flows

As the well-bedded sedimentary sequence is followed upslope, much of its upper part grades into, or is replaced laterally by massive sediments interpreted to be a succession of mass-flow deposits, possibly debris flows (Fig. 72). The uppermost debris-flow unit is overlain at its farthest downslope extent by almost 40 ms (ca. 30-35 m) of the well-bedded sequence. This well-bedded section above the debris flows dies out as the water shallows so that the debris-flow crops out at the sea bed in shallow water. It is to be hoped that dating of the overlying sediments will allow the age of the youngest debris flow to be determined.

Sea bed break-up

Two zones have been recognised in which the sea bed gives a broken return with occasional hyperbolic reflectors derived from points about 3 m above the sea bed (Figs. 68b and 72). The main occurrence is coincident with the pinching out of the debris flows in the shallower water. Gas escape may be a factor in producing these features, but an alternative explanation is that they could be due to patches of cold-water coral (*Lophelia poiglera*), which is common in this area.

Slide deposits

The allochthonous deposits, those that have been moved, below the slide scarp can be divided into two types. The first is a massive deposit with a particularly varied sea bed relief (Fig. 70); the second is composed of large portions of the undisturbed sedimentary sequence which have been variably folded, stretched or compressed (Fig. 71b). Examination of the IKU sparker records also shows both types, but with the latter underlain by disturbed, massive deposits at a depth beyond the penetration of the DTBS.

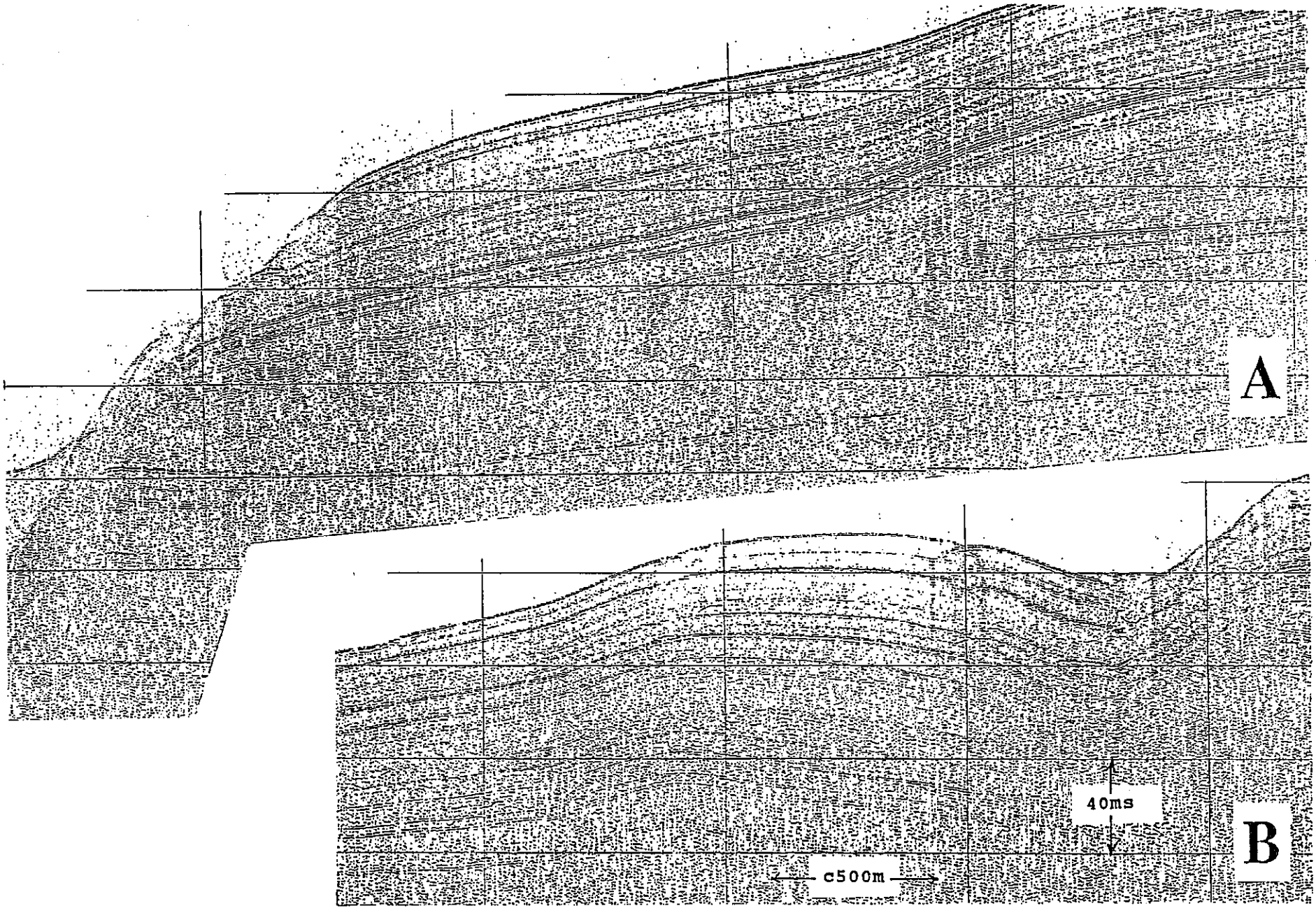

Fig. 71: BGS deep-tow-boomer profiles from the Storegga Slide area. For locations see Fig. 64: a) slump deposit with its head defined by truncation of a strong reflector. b) allochthonous folded, partly strechted and partly compressed sedimentary sequence.

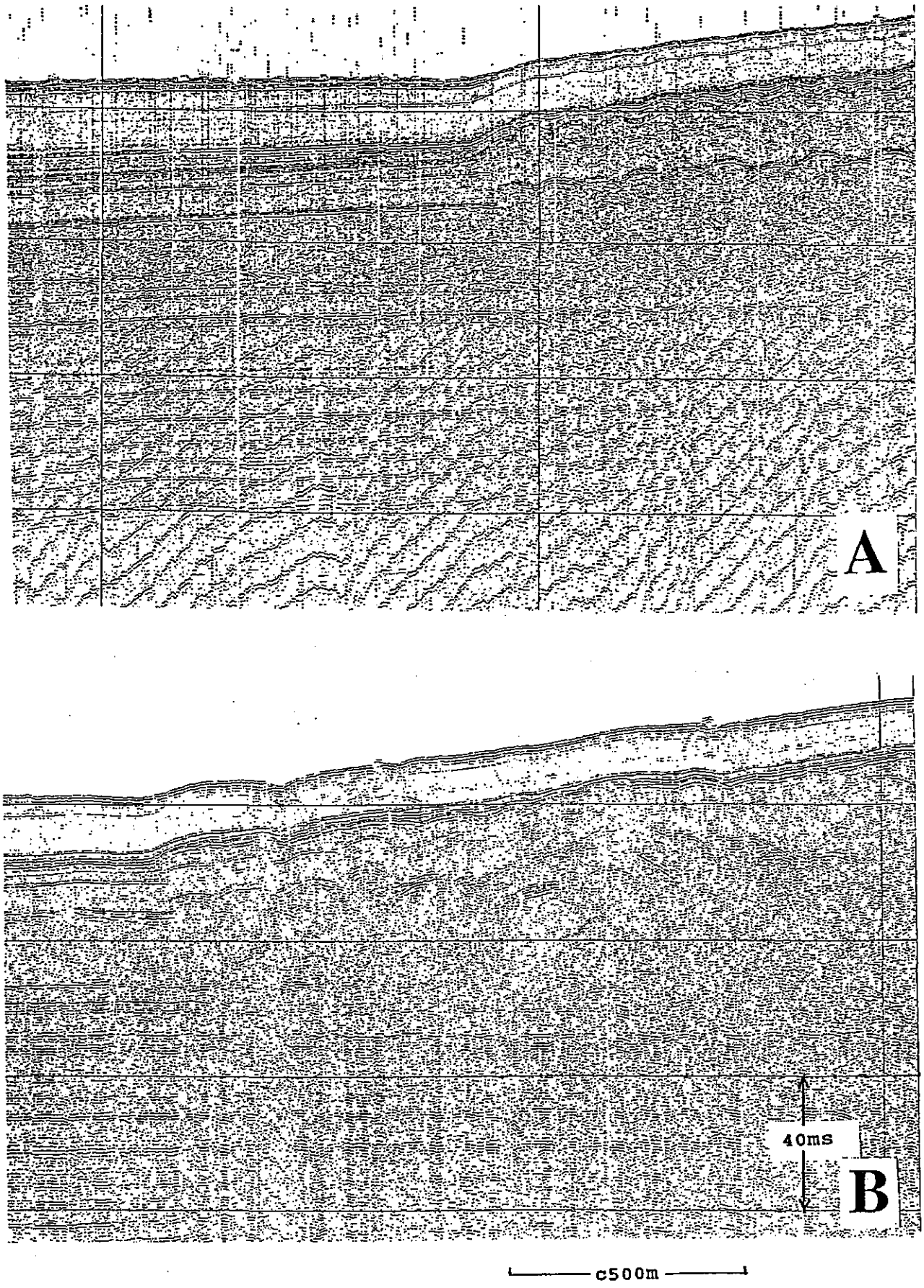

Fig. 72: BGS deep-tow-boomer profiles from the Storegga Slide area. For locations see Fig. 64. a) debris flow deposit (to the right). b) debris flow deposit and sea bed breakup.

CONCLUSIONS

1 The DTBS has proved to be a particularly appropriate system for investigation of the northern margin of the Storegga Slide. Good-quality profiles were obtained, from which much information has been abstracted, including detailed tracing of the slide scarp in conjunction with Hydrosweep data. Future work will allow further deductions to be made.

2 There is much evidence for the presence of gas in the undisturbed sediments to the north of the slide edge.

3 One DTBS profile is interpreted as showing evidence for a major slide that pre-dates the "First slide" of BUGGE et al., 1988.

4 Given that the Storegga Slide is such a major geological feature so close to the coast of Europe, survey coverage of it is surprisingly limited. During this leg, more detail has been discovered over a very small part of the slide, and already it is clear that the history of the area is more complex than hitherto proposed from limited data. Much further work is necessary, in particular the following should be considered:

A Further deep-tow-boomer profiling around the margins of the slide, together with a sparker system for deeper penetration. A sparker profile along the DTBS line which shows an ancient slide would be most informative.

B Side scan sonar would allow the distribution of sea bed features to be mapped.

C A shallow bore hole drilled into the undisturbed sediment sequence to a depth of about 200 m (compare STOKER et al., 1994) would reveal much about its stratigraphy, age, climatic influence on sedimentation and mass movement, and many other aspects of the geology.

5.4.11.2 *In situ* Pore Pressure and Geotechnical Properties of Sediments

(P. Schultheiss, E. Darlington, M. Langseth, G. Auffret, G. Floch, J.Y. Landure, C. Toularastel)

Pore Pressures and Shear Strength

Subseafloor pore pressures that deviate from hydrostatic equilibrium drive pore water through permeable sea floor sediments and through the sea floor. Non-hydrostatic pressures can result from a number of mechanisms. For example, rapid loading or unloading of sediments due to slumping or tectonic deformation can lead to pore waters being overpressured (rapid loading) or underpressured (rapid unloading) relative to hydrostatic. The pore pressure anomalies

caused by such events are transient. However, because of the very low permeability of most marine sediments they can survive for a very long time after the perturbating event. Temperature anomalies in the oceanic crust or gas-charged pore fluids lead to lateral density variations that can drive fluid flow. This flow is induced by buoyancy forces as well as pressure gradients and will last as long as the sources of anomalous temperature or gas exist.

Extensive evidence has been discovered for subseafloor overpressures within sedimentary wedges formed at subduction zones (WESTBROOK and SMITH, 1983). These overpressures result from the rapid burial and loading of water-saturated low-permeability sediments as the wedge grows, and cause a significant flux of pore fluids from the wedge. Overpressures also play an important role in the deformation of wedges because they reduce the internal shear strength of sediments in the wedge by reducing the effective stress (effective stress = total stress - pore pressure).

Underpressured conditions have been observed in the crust and sediments of midoceanic ridges where thermally driven water circulation results in non-hydrostatic pressure gradients. The fluid flow through the igneous crust at the axis and on the flanks of mid-ocean ridges dominates the transport of heat and chemicals through the sea floor, and is the principal cause of the chemical alteration mechanism in ocean crustal rocks. These conditions lead to a downward flux of pore waters through the overlying sediments (LANGSETH et al., 1992).

Slope failures occur at certain depths in the sedimentary column when the tangential stress exceeds the internal friction stress. Until now the assessment of slope stability has relied on geophysical data and on physical properties measured in the laboratory on collected cores; the state of which has been altered due to changes in the ambient pore pressure and temperature.

Anomalous pore pressures (non-hydrostatic) and shear strengths might be expected in the Storegga Slide area for a number of reasons. Slope failure itself, and the ensuing downslope movement of massive volumes of sea floor material, may be caused by overpressured pore waters in the sediment, locally decreasing the shear strength of the sediment to near zero, in a manner similar to that observed in sediment accretionary complexes at subduction zones.

When a transient primary trigger (such as the shear stresses induced by earthquakes) is responsible for a submarine sediment failure, the area of initial failure is likely to be where the sediments are weakest. Consequently, sediment areas with higher pore pressures are more likely to fail in the event of a trigger mechanism occurring than in areas with lower or negative pore pressures (relative to hydrostatic).

Whatever the initiating mechanism, the slide event itself will result in large anomalous subseafloor pore pressure by rapidly unloading large areas upslope and rapidly loading downslope sediments buried by the debris flow. These will lead to transient fluxes of water through the sea floor for the period whilst the anomalous pore pressures are still decaying.

The length of time that it takes for anomalous subseafloor pore pressures produced by a huge event such as the Storegga Slide to dissipate depends primarily on the permeability of the sediment and the depth of the anomalous zone.

There is also evidence of localised upward movement of gas-charged pore waters through the sediments in this area (Fig. 73). Numerous small depressions (pockmarks) in the sea floor are present in this region. High-resolution seismic reflection profiles show that below these depressions the normal acoustic stratigraphy is highly disturbed. The pockmarks are believed to be sites where lower density gas-charged pore fluids are escaping. *In situ* pore pressure gradient measurements in and around these pockmarks should detect any expulsion of pore waters and may provide a rough estimate of the rate. However, significant caution must be exercised when interpreting pore pressure results where free gas may be present adjacent to the measuring probe, as our understanding of the complex local pressure field and exactly what is being measured is unclear. The PUPPI and Module Geotechnique (MG) instruments were used to make measurements in an area where pockmarks and gas seeps are abundant.

Pore Pressure Measurements

Direct *in situ* measurements of pore pressure gradients in sea floor sediments is one of the primary ways to detect and quantify fluid flow through the sea floor and to estimate the subseafloor pressures at greater depths. The rates of pore fluid flow are related to the pore pressure gradient through Darcy's law, i.e. the flux of pore fluid is equal to the pore pressure gradient times the permeability. Pore pressure at greater depths can be estimated by extrapolation of the shallow pore pressure gradient to depth assuming a uniform upward flux and estimates of the permeability of the sediment deeper in the section (LANGSETH et al., 1992).

The Pop Up Pore Pressure Instrument (PUPPI), originally developed at the Institute of Oceanographic Sciences (SCHULTHEISS and McPHAIL, 1986; SCHULTHEISS and NOEL, 1987), is designed and constructed to make accurate *in situ* measurements of the vertical pore pressure gradient in the sea floor. The PUPPI measures differential pore pressures at two ports on a lance, with a resolution of about 15 Pa. The length of lance that can be used depends on the sediment stiffness. It is a free-fall instrument that can be ballasted with lead or steel weights to penetrate a range of sediment types in water depths of up to 6,000 m. Typically a 4 m lance can be used successfully in soft hemipelagic sediments although 6 m long lances have been successfully used in deep-sea pelagic muds.

Pore pressures are measured relative to hydrostatic at the porous ports on the 50 mm diameters lance using specially adapted differential pressure transducers connected to the pressure ports and the open sea water. A programmable solid state data logger is used to record the data at a maximum rate of 1 sample per 2 s.

Just prior to recovery an acoustic command is sent to the instrument to activate the pre-release pipe cutter. This opens both sides of each differential pressure transducer to the open sea water hence providing an *in situ* zero pressure calibration just before recovery. This is an important part of the measurement process for obtaining high resolution differential pressures for estimating fluid fluxes. Recovery is accomplished using an acoustic command which activates a release mechanism severing the disposable from recoverable parts; the lance and ballast weight assembly is left on the sea floor while the buoyant instrument package ascends to the surface for recovery. In addition to the acoustic command for release, the instrument also houses a back-up release timer that can be set to release the instrument at any required time.

Currently the PUPPI is the only instrument with sufficient resolution and accuracy to measure the small pressure gradients (a few hundred Pa/m maximum) that are associated with the low level fluxes of pore fluids (several mm per year) typical for sea floor sediments (SCHULTHEISS, 1990a-b). In addition to the ambient pore pressure the pore pressure transients produced by the penetration of the PUPPI probe and by tidally induced pressure variations on the sea floor also provide information of geotechnical interest. The maximum insertion pressure is indicative of the shear strength whilst modelling of the decay curve and tidally induced signals can provide estimates of the permeability of the sediments. The analysis of the tidal cycles can also provide estimates of the frame modulus of the sediment structure (HURLY and SCHULTHEISS, 1990; FANG et al., 1993).

Module Geotechnique

The Module Geotechnique has been developed to investigate *in situ* physical properties of the sea floor and to collect two-metre long cores. It allows correlation of *in situ* physical properties with core lithology and comparison with geotechnical measurements made in the laboratory (OLLIER et al., 1992; COCHONAT, 1991). Following successful operations in the Baltic under the "Geophysical *In situ* Probes" (GISP) (MAST I) program, a new phase of MG development began in late 1992 to allow the operation of a gamma-density probe and to obtain acoustically triggered bottom photographs. This included mechanical and software modifications. Due to time constraints it had not been possible to test these new developments at sea prior to this cruise. During this cruise the operation of the following tools was expected: (1) Penetrometer: The resistance to penetration (Q_c) recorded by means of a piezocone, with three possible ranges (0 to 1000 kPa, 0 to 1500 kPa, 0 to 5000 kPa) and the induced excess pore pressure, U_t (0 to 1000 kPa) measured by the deformation of a membrane. Both sets of data are recorded every 2 cm. (2) Core sampler: The module can also recover one 2-m long, piston-assisted, push core (penetration speed - 2 cm/s). Such cores are of a higher quality than conventional gravity cores as they do not usually compress the sediments, hence providing a more representative sample for measurements of geotechnical properties. (3) Gamma-density-probe: This sensor was developed within the GISP program (MAST II) and has been finalised under the ENAM program. It allows for the first time the *in situ* measurement of sediment density. All safety clearances for handling the gamma ray source were obtained prior to the

cruise. (4) Acoustically triggered bottom photographs: This system allows us to take photographs at a distance of about 5 m above the bottom, before landing the module. This information is useful because it reveals the intensity of bioturbation and/or erosional features, which are relevant to the interpretation of physical properties.

PUPPI operational log

31 October

A wire test was performed using two acoustic units and 2 PUPPI data loggers to test all the main functions of the systems. This included the main acoustic command functions as well as the main release back up timers. Four differential pressure transducers were also tested with the main loggers together with the "pipe-cut" zero calibration facility. The water depth was approximately 1000 m and in the area of the subsequent deployment locations. All systems operated successfully and after examination on board both units were deemed fit for deployment.

1 November

The first PUPPI deployment (Station 510), using a 3 m probe with 3 lead weights, was made at 17:40 at 64°44.00'N, 04°26.97'E in a water depth of 961 m. It was deployed from the main deck beneath the CTD winch where the side rail can be removed and where the freeboard is about 3 m. The launch frame was modified to fit the deck fittings. This first deployment from METEOR went smoothly.

2 November

The second PUPPI deployment (Station 514), using a 4 m probe with 4 lead weights, was made at 19:21 at 64°56.98'N, 03°32.19'E in a water depth of 1454 m.

3 November

A second wire test was performed using a new acoustic unit. Some difficulties were experienced with the performance of this unit but the major release functions worked.

5 November

We returned to the first PUPPI site (Station 510) and remotely turned on the acoustic command unit at 06:32. At 06:37 we transmitted briefly on the release channel to fire the pre-release pipe cutter (this provides the *in situ* zero reference pressure). Five minutes later we continued to transmit on the release frequency. However, the instrument failed to release from the sea floor despite strong signals from the acoustic command unit and apparently faultless behaviour. We continued to transmit at and around the release frequency for approx. 1.5 h before moving on to the next station. At approx. 11:30 we returned to the site and again made good acoustic contact. Again we transmitted at the release frequency but to no avail. At 11:55 we stopped transmitting and waited whilst the back-up release timer fired at 12:00. A duplicate back-up timer was set and run in parallel in the laboratory. This fired at 12:00 as planned, as we assume the sea floor timer did. However, the PUPPI remained "glued" to the

sea bed. Further transmissions of the release frequency failed to have any effect although all surface indications showed the acoustic system to be behaving faultlessly. At this stage the instrument had to be provisionally declared "LOST".

The second PUPPI (Station 514) had a back-up timer set to fire at 19:00. We arrived a little late at this station for the recovery (Station 530) at 19:15, turned on the acoustic command channel and found that the instrument was, as expected, already on its way to the surface, having been released by the back-up timer. It surfaced at 19:30 and was safely on board by 20:00.

6 November
The third PUPPI deployment (Station 536), again using a 4 m probe but with 3 lead weights, was made at 13:37 at a location of 64°46.29'N, 04° 30.06'E (close to the first PUPPI deployment) in a water depth of 893 m and about 200-300 m from a gas seep as revealed from the Parasound record. Following the launch of the third PUPPI we went back to the first PUPPI site. Again the instrument responded well to the acoustic command but failed to release.

8 November
The third PUPPI deployment was ended prematurely after only 2 days on the sea floor by releasing the instrument acoustically at 10:15 (Station 545). This was caused by impending bad weather and the necessity to temporarily leave the area. The recovery was made without incident and the instrument immediately prepared for the next deployment. The fourth PUPPI deployment was made (Station 546) with a 4 m probe and 3 weights at a location of 64°46.083'N, 04°30.085'E in a pock mark made by an obvious gas seep. Despite a steadily worsening sea state the deployment was again made without any significant difficulty.

11 November
PUPPI station 4 was recovered without incident at 08:18 (Station 550). We then proceeded to the PUPPI station 1 site for a final attempt at release before leaving the area. Once again all indications were that the acoustic system was working faultlessly but the instrument failed to ascend. The acoustic system was put to sleep prior to leaving.

Module Geotechnique operational log
While it was anticipated that the module would be launched from the side of the RV METEOR, it was realised on board that the module had to be handled by the stern A-frame, because it could not be operated from the side concurrently with the gravity corer.

2 November
After a series of "on-deck" positive tests the module was launched on at 13:00 (Station 512) on a site at 64°56.70N, 3°31.20'E. and in a water depth of 1400 m near to PUPPI station 2.

Three operational sequences were programmed: (1) sequence 1: penetrometer (2) sequence 2: penetrometer (3) sequence 3: penetrometer, gamma (test without electronics) and corer.

The Benthos camera was not fixed on the frame because of the risk of damage if the module hit the ship during launch and recovery.
The delay time required for launching and lowering the MG to the sea floor was set at 1 h. Sequence 1 was due to begin at 14:00, sequence 2 at 14:30 and sequence 3 at 15:00. The wind and sea conditions were good, it took 16 minutes to fix the glass spheres and pinger on the cable and to launch the frame. A shock to the frame from collision with the stern side-board occurred during this launch operation.

The sites (S1, S2 and S3) were offset by half a mile from each other. During transits between sites the module was raised 150 m above the sea floor and towed at an average speed of 2 knts. The height of the module above the sea floor was monitored by the direct and sea floor-reflected signals of the pinger. Clear pinger records enabled good control of the module height (the echo from the module was also clearly distinguished). When the Module was raised to the surface at 16:00 the corer was found to be projecting beneath the main frame. Recovery of the corer was made possible only by setting the module on its side along the stern ramp which caused the upper part of the barrel to bend. The corer was then secured and finally disconnected.

We also discovered that an electric cable from the gamma probe had been broken, probably by the module connection and/or cable intrusion within the frame. The command panel of the module was immediately examined in the laboratory and found to be out of order. An unusual amount of condensation was found in the electronics pressure housing. No data were obtained from this deployment. In agreement with the chief scientist it was decided to prepare the module ready for another trial with only the penetrometer operational.

3 November
We repaired all the electronic boards by careful drying and cleaning process and then submitted the MG to a series of tests which it passed successfully.

4 November
During the course of further tests, the progress of the penetrometer was interrupted. The command card was again tested, and a defective component discovered. After changing this component late in the afternoon the unit was successfully tested (using 3 program sequences).

5 November
Despite marginal sea state and wind conditions (with water coming occasionally on the deck, we decided, in agreement with the chief scientist, to launch the MG as the weather forecast indicated no improvement for the next few days.

The module was launched at 12:00 (Station 529). At 12:45 the pinger was fixed 43 m above the MG on the main wire and the it was lowered to the sea floor near to PUPPI station 1. Three sequences were performed. The MG was set on the bottom 2 minutes before the beginning of each sequence. Between sequences it was raised 150 m above the bottom and towed a distance of 0.5 miles at an average speed of 2 knots.

	Sequence 1	**Sequence 2**	**Sequence 3**
Time	13:30	14:05	14:40
Depth	950 m	950 m	961 m
Latitude	64°44.11'N	64°43.90'N	64°43.70'N
Longitude	4°27.17'E	4°27.2'E	4°27.09'E

At about 15:15 the MG was retrieved in good condition despite heavy seas. The command panel was connected, the data transferred, printed and the profiles drawn with the exception of the excess pressure probe, which was not recorded.

6-9 November
While calibrating the excess pore pressure probe, a failure interrupted communications with the module. All subsequent investigations failed to identify the cause of the electronic failure. Whilst sheltering from bad weather behind Fröya Island on 9 November, we dismantled and secured the MG before sailing to the Greenland Margin.

PUPPI Summary
The relative positions of PUPPI stations 1, 3 and 4 to the prominent pockmark and associated gas seep are shown in Figure 73 and Table 23.

PUPPI 1 - Station No. 510.
This station in 961 m water depth was approximately 10 nm from the northern edge of the Storegga Slide, an area that shows many gas seeps and pockmarks. The location itself was offset from a prominent gas seep and pockmark by approximately 2.5 nm. The failure to recover this instrument is a complete mystery. All systems were tested on a wire prior to deployment and functioned normally. The acoustic commands sent to the instrument, once on the sea floor, gave the appropriate acoustic responses yet it failed to release. Furthermore, the back-up timer should have fired successfully, we have no reason to suppose it didn't, yet still it did not release. Assuming that at least one of the release functions operated correctly then the most likely causes for the failure seem to be:

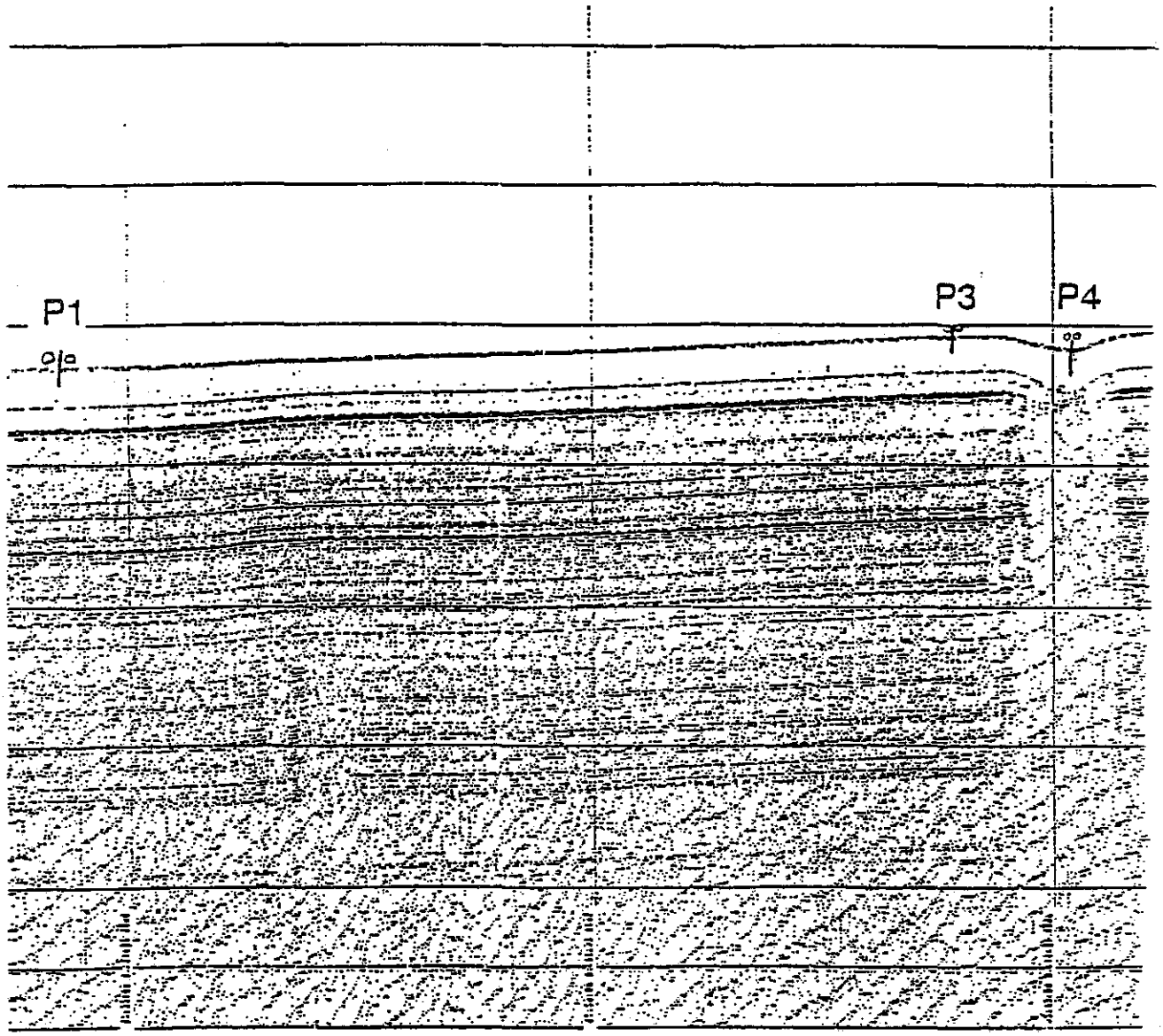

Fig. 73: Illustrative seismic reflection profile (BGS deep-tow-boomer) showing relative positions of PUPPI stations 1, 3 and 4 in relation to the location of a prominent pock mark and gas seep.

Table 23: Summary of station information for the 4 PUPPI deployments

PUPPI SUMMARY LOG	PUPPI 1	PUPPI 2	PUPPI 3	PUPPI 4
Station No	510	514/530	536/545	546/550
Latitude	64.44.00N	64.56.984N	64.46.29N	64. 46.083N
Longitude	04.26.97E	03.32.20E	04.30.06E	04. 30.085E
Water Depth (m)	961	1454.5	893	872
CONFIGURATION				
Probe/pres ports	3 m & 1.5 m	4 m & 2 m	4 m & 2 m	4 m & 2 m
No. of lead Weights	3	4	3	3
BACK-UP CLOCK	11/5/1993 12:00	11/5/1993 19:00	11/10/1993 15:00	Not Set
DEPLOYMENT				
Date	11/1/93	11/2/93	11/6/93	11/8/93
Time Set Logger	17:06	18:49	13:10	12:42
Time of Launch	17:40	19:21	13:37	13:06
RECOVERY				
Date	11/5/93	11/5/93	11/8/93	11/11/93
Time Pipe Cut (release ch.)	6:37	1900 on BU clock	10:03	7:19
Time Released from sea bed	Failed to release	19:02	10:13	7:30
Time on board	19:40			8:18
Time Logger off	LOST	20:12	10:03	9:00
Total Time on (Hrs)		73.5	45	68.5

- Loss of buoyancy - a leak in 1 glass sphere. Catastrophic failure seems unlikely as the spheres are rated for a working depth of 6000 m and it is probable that this type of failure would severely damage the acoustic electronics.

- Overpenetration - if the release mechanism was covered by cohesive sediment it is conceivable that the resulting suction would overcome the buoyancy forces. However, one might expect the unit to slowly creep out of the mud. This it had not done within a period of 6 days, the final time the system was monitored. The subsequent successful recovery of the other PUPPI deployments makes this a highly unlikely scenario.

In conclusion, the balance of evidence would suggest that the unit had somehow lost buoyancy. It is, therefore, unlikely to pop-up in the future even after some corrosion, and must be considered lost.

PUPPI 2 - Station No. 514/530

This station in 1454 m water depth was approximately 10 nm from the northern edge of the Storegga Slide on an area of the slope deemed to be a reference site as it had parallel uninterrupted bedding and was at least 10 nm from the nearest known prominent pock mark or gas seep. The data from both upper and lower pore pressure ports is excellent (Figs. 74 and 75). The pipe cut occurred at a time of 72.18 h with release from the sea bed at 72.21 hours This short time between cut and release occurs when the instrument releases using the back-up clock. As the sampling rate did not reset to 2 s sampling there are only 2 data points during the calibration period. However, close examination of the records enables the zero calibration level to be accurately determined.

The upper port (Channel A - 2 m) and lower port (Channel B - 4 m) show maximum insertion pressures of 26 kPa and 48 kPa, respectively with smoothly decaying pressures reaching a minimum after about 20 h insertion. There is no discernible pressure difference at the time of the pipe cut on either pressure port. A small tidal cycle signature is discernible on Channel A with a more pronounced signature on Channel B. Both channels show a small upward drift in pressure (of about 140 Pa) between 20 and 72 h. This has been observed previously and has been attributed to a small mechanical creep in the transducers with time. It is curious, however, that both drift by approximately the same amount and consequently the possibility of this drift being real should not be eliminated. If true it would indicate a time-varying pore pressure that, prior to the instrument release, was negative.

PUPPI 3 - Station No. 536/545

This station in 893 m water depth was again approximately 10 nm from the northern edge of the Storegga Slide again in an area which shows many gas seeps and pockmarks . The location itself was offset from a prominent gas seep and pock mark by about 200-300 m. The data from PUPPI 3 is believed to be accurate as no instrumental problems were encountered.

However, this relatively short record does show some unusual and interesting features (Figs. 76 and 77). The pipe cut occurred at a time of 44.12 h with release from the sea bed occurring 10 minutes later at 44.29 h. Although the sampling rate did not reset to 2 s sampling there is a clear period for the zero pressure calibration to be accurately determined.

The upper port (Channel A - 2 m) and lower port (Channel B - 4 m) show maximum insertion pressures of 32 kPa and 30 kPa respectively with pressures generally decaying all the time until the pipe cut. The slightly lower insertion pressure at the lower port indicates that the lower port came to rest in a weaker sediment type than the upper port. The decay of insertion pressure on the lower port is also unusual compared with the smooth decay of the upper port.

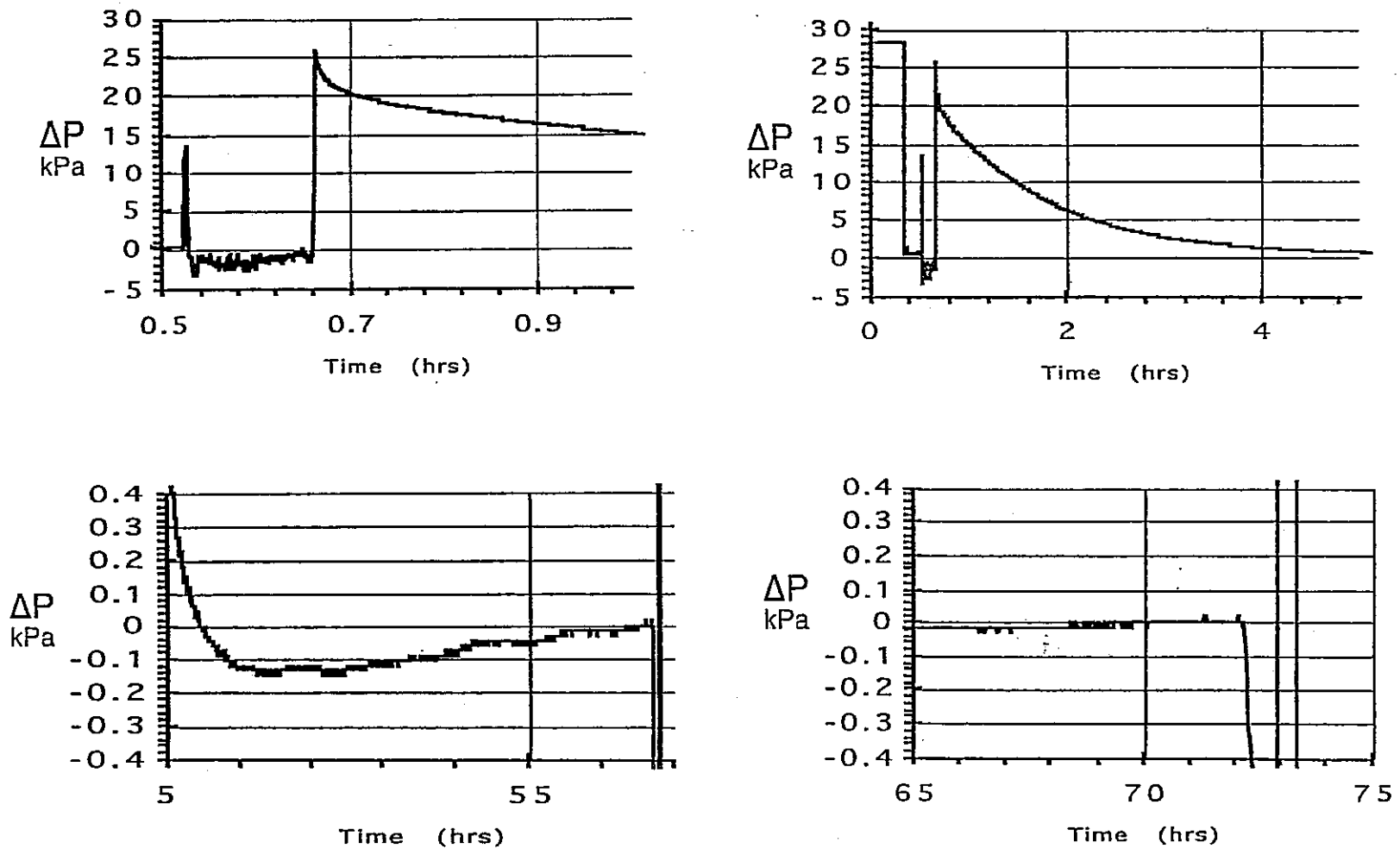

Fig. 74: PUPPI 2 data (Channel A-upper port) show features of the record at different pressure and time scales. Top left - the data during descent through the water column and the penetration event. Top right - the first 4 h of the decay curve. Bottom left - the end of the decay curve and the slight upward drift in pressure. Bottom right - the time around the pipe cut showing zero excess pore pressure.

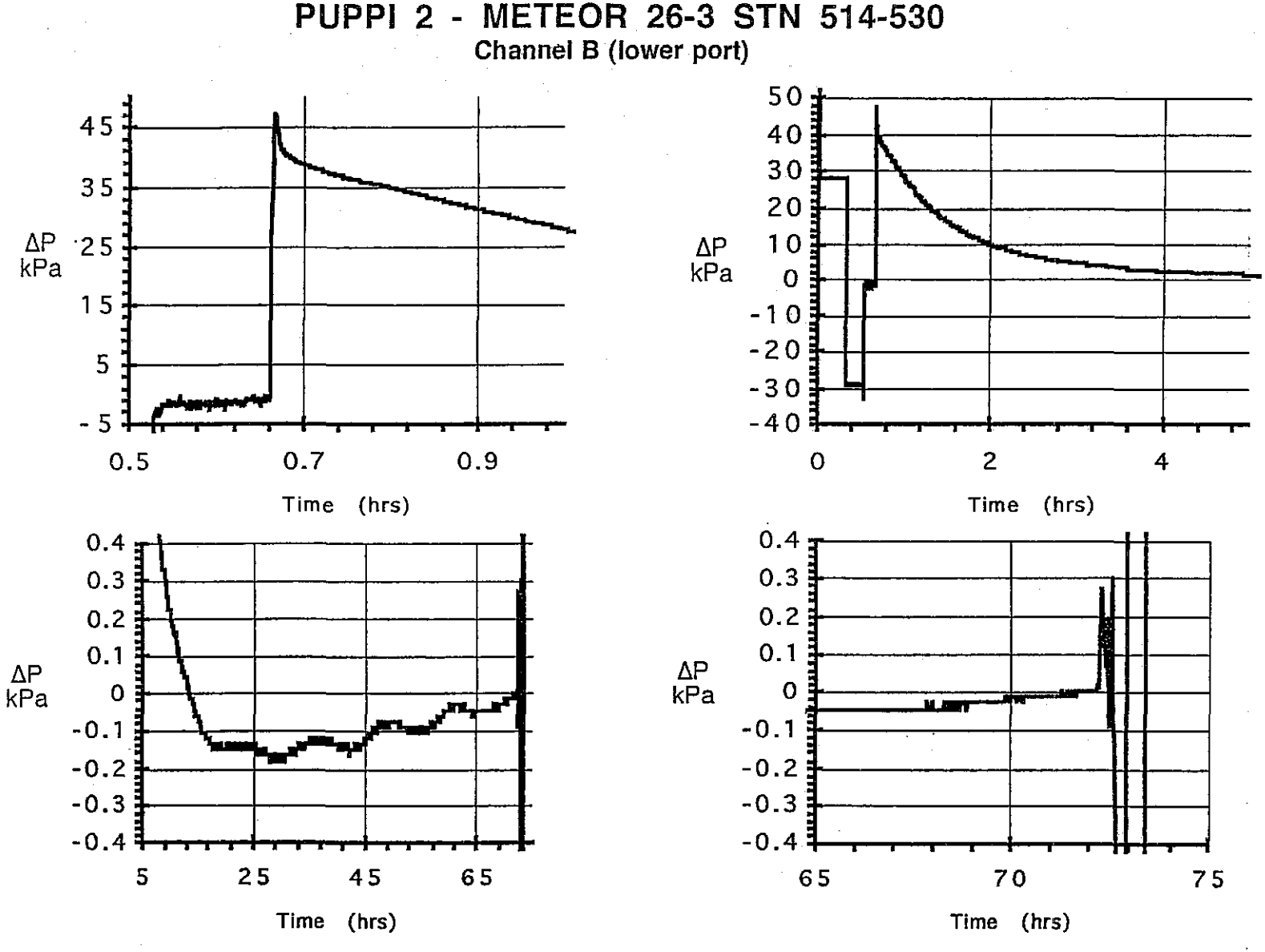

Fig. 75: PUPPI 2 data (Channel B-lower port) show features of the record at different pressure and time scales. Top left - the data during descent through the water column and the penetration event. Top right - the first 4 h of the decay curve. Bottom left - the end of the decay curve and the slight upward drift with the superimposed tidal cycles. Bottom right - the time around the pipe cut showing zero excess pore pressure.

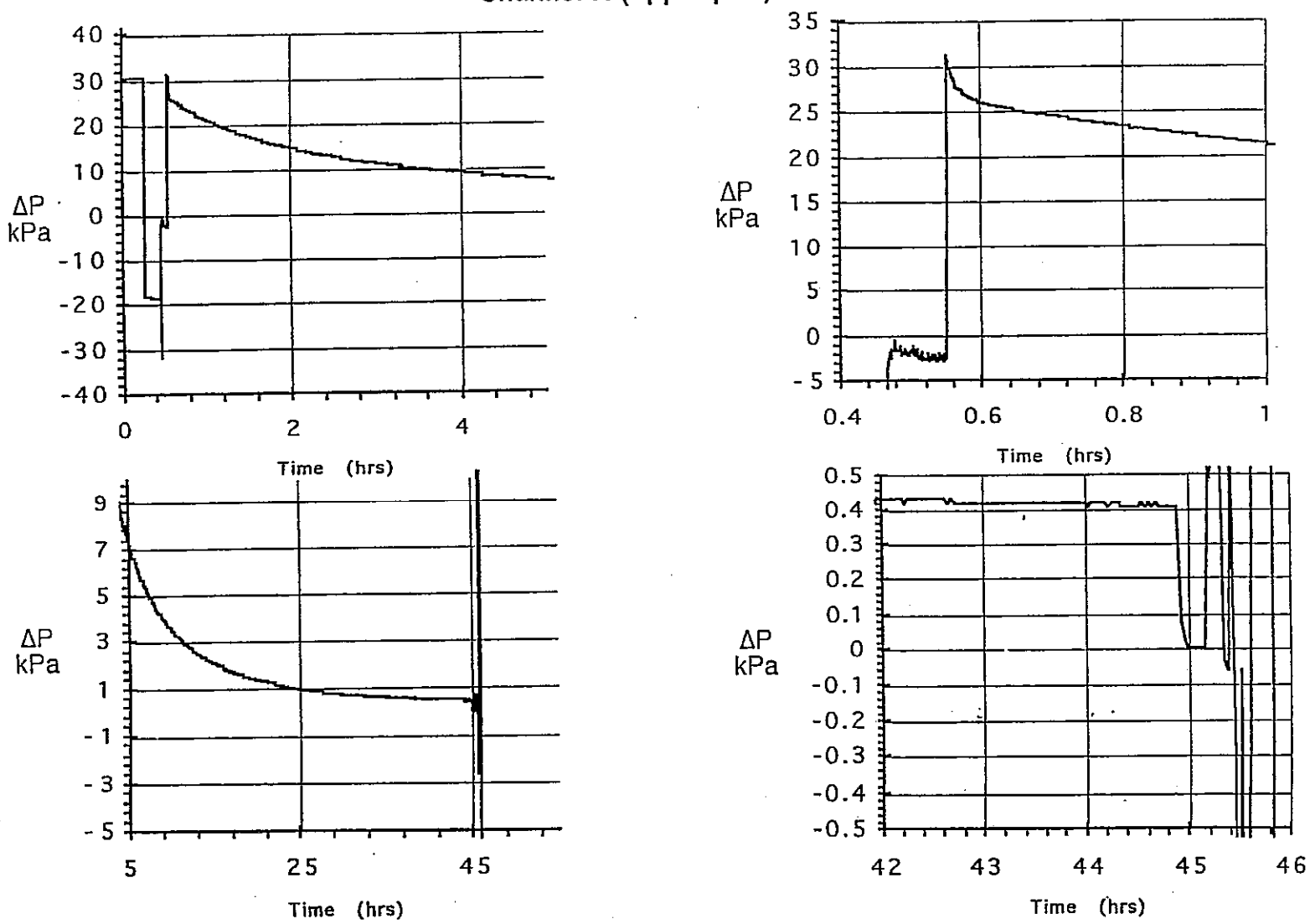

Fig. 76: PUPPI 3 data (Channel A-upper port) show features of the record at different pressure and time scales. Top left - the first 4 h of the decay curve. Top right - the data during descent through the water column and the penetration event. Bottom left - the last 40 h of the decay curve. Bottom right - the time around the pipe cut showing a large positive excess pore pressure at the time of the cut.

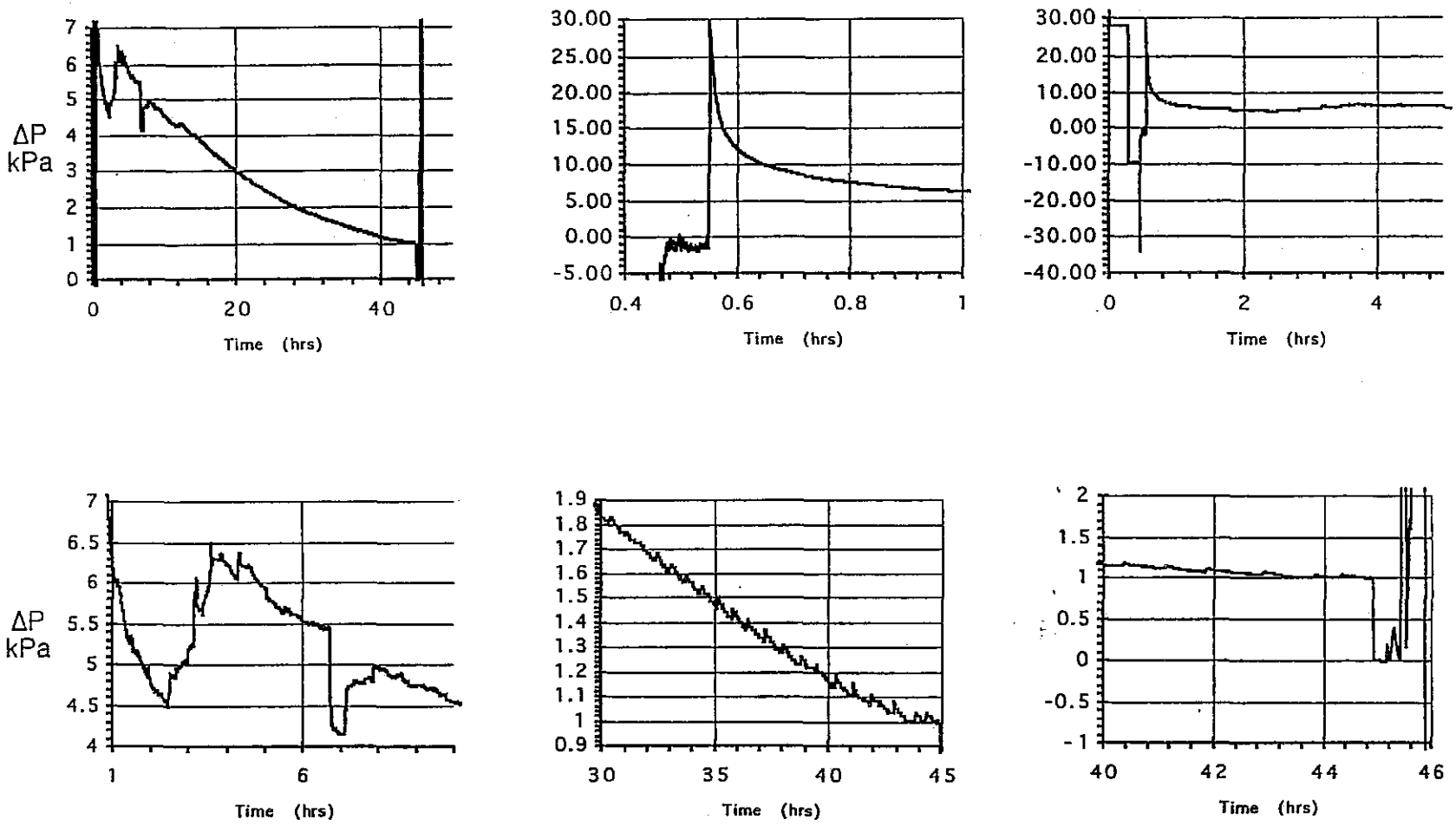

Fig. 77: PUPPI 3 data (Channel B-lower port) show features of the record at different pressure and time scales. Top right - the first 4 h of the decay curve. Top centre - the data during descent through the water column and the penetration event. Top left - the complete decay curve showing the erratic behaviour in the first few hours which is expanded in the botom left graph. Bottom centre - the saw-tooth nature of the final part of the decay curve. Bottom right - the time around the pipe cut showing a large positive excess pore pressure at the time of the cut.

The fast initial decay is followed by considerable fluctuations in pressure of up to nearly 2 kPa between 1 h and 14 h. A detailed look at the data shows no apparent instrumental problems with the conclusion being that they are real. In addition, even during the later smoother period of the curve there is a very small saw-tooth pattern that has not been observed previously. This pattern consists of small increases in pore pressure (approximate amplitude 40 Pa) with slower decays and continues until the pipe is cut. The low insertion pressure, the irregular behaviour at the beginning of the decay and the small saw-tooth pattern indicates some form of dynamic behaviour around the lower port. This is tentatively attributed to the possibility of a quantity of free gas.

Examination of the records around the pipe cut shows that there are positive differential pressures being exerted on both channels (0.41 kPa on the upper port and 1.0 kPa on the lower port). However, the pressure at both ports is still decaying at this time hence any equilibrium differential pore pressure will be lower than these values.

PUPPI 4 - Station No. 546/550

This station in 872 m water depth was again approximately 10 nm from the northern edge of the Storegga Slide (very close to PUPPI station 3) and in the centre of a pock mark above a prominent gas seep, as revealed on the high resolution seismic profiles (see Fig. 73).

Unfortunately on recovery a small amount of water (approx. 2 ml) was found in the data logger tube (more than could be explained by condensation). A detailed inspection of the electronics, the data and laboratory testing, lead us to the conclusion that a small low pressure leak had occurred soon after deployment. Water got onto the electronics board controlling the signal conditioning which had a number of detrimental effects on the data soon after penetration. The first sign of a problem with the data (Figs. 78 and 79) does not occur until a time of about 0.6 h. Consequently, the maximum insertion pressure is believed to be accurate, showing 36 kPa on the upper port and 43 kPa on the lower port. The upper port shows a dramatic problem after 0.6 h (Fig. 78) with the data completely unreliable through to the end.

The lower port behaviour (Fig. 79), however, is very different and does not show the usual signs of electronic problems caused by water because there are no rapid changes in signal level. Consequently, the possibility that this data is good should be examined. The pressure decays relatively smoothly for the first 4 h and then a more erratic behaviour begins with the pressure reaching a minimum after 12 h and then increasing until the pipe cut at 66.63 h. Following the pipe cut but prior to the release the pressure decays at a time when it should remain constant (zero pressure). This may have been caused by a poor cut of the tubing connecting the ports with the transducer (observed on retrieval). Following release the behaviour looks normal apart from the fact that the pressure is offset by about +1.5 kPa. Only during recovery does the behaviour show the erratic pattern that one might expect if small amounts of water have been touching parts of the electronics. It is interesting to observe that at this stage the upper port comes back to life showing the same behaviour as the lower port.

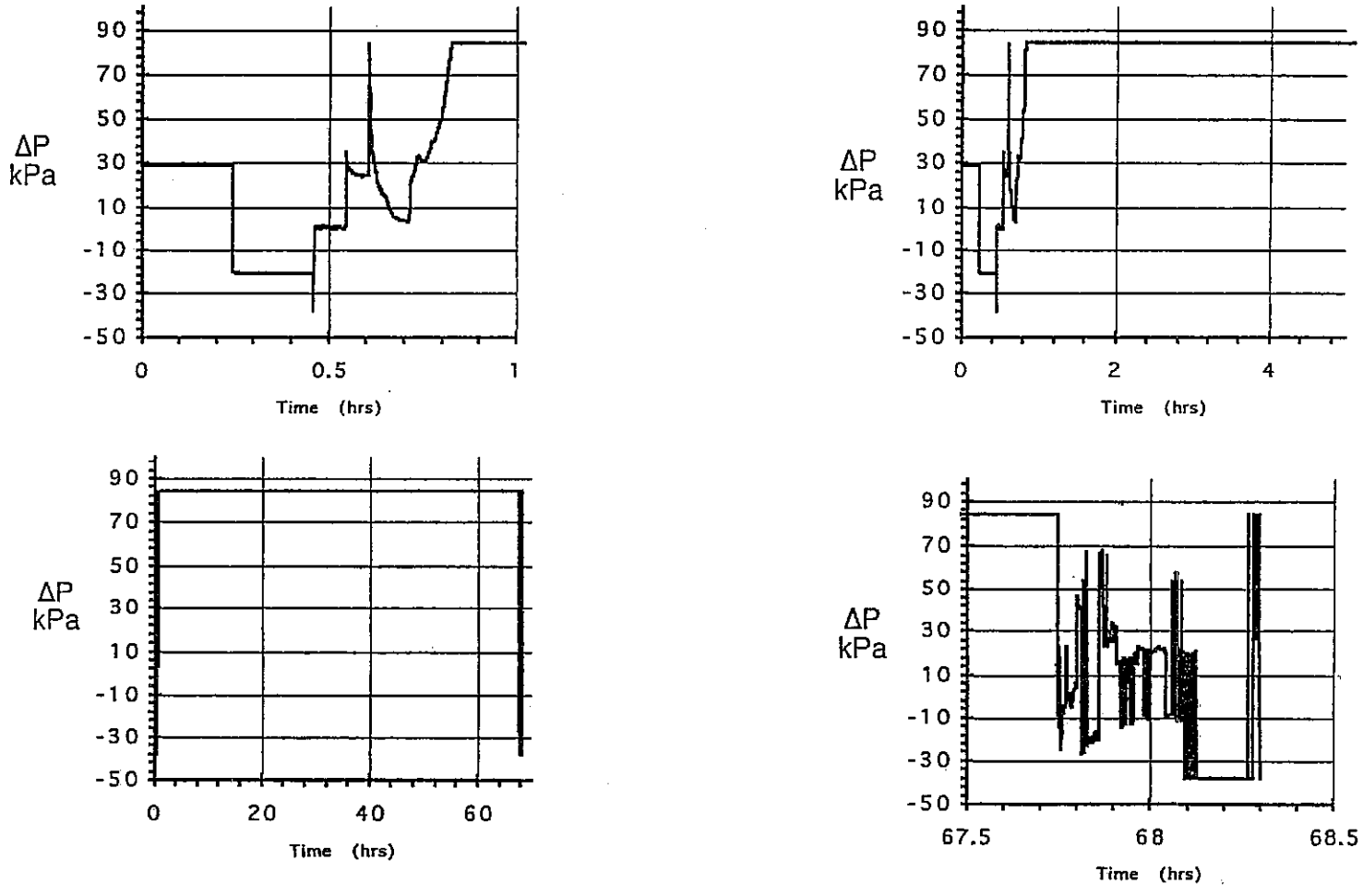

Fig. 78: PUPPI 4 data (Channel A-upper port) show features of the record at different pressure and time scales. Top left and right - the first 5 h of the record showing good descent and penetration data up to about 0.6 h. Bottom left - complete time record showing data problems (over-range values) for most of the record. Bottom right - the final hour where the system started to work during ascent.

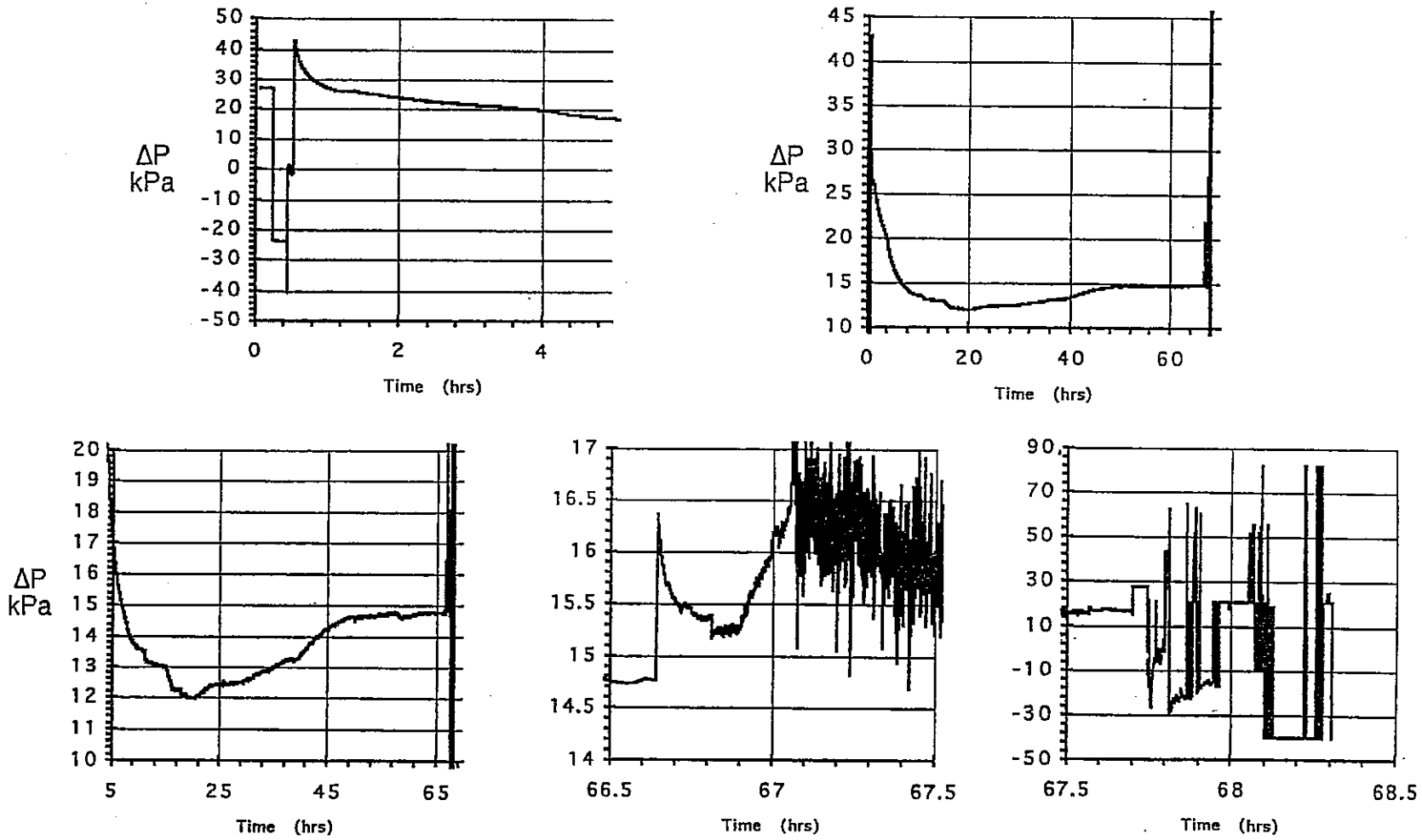

Fig. 79: PUPPI 4 data (Channel B-lower port) show features of the record at different pressure and time scales. Top left - the first 5 h of the record showing good penetration and decay data. Top right - the complete record showing the large erratic behavior and upward drift which is shown on an expanded scale in the bottom left. Bottom centre - the time around the pipe cut, ascent and surface. Bottom right - the final hour where the system shows an erratic behaviour similar to Channel A.

The lower port data cannot be completely correct because of the offset that has occurred between the launch of the instrument and its recovery. However, there are indications that at least some of the dynamic behaviour may be real and consequently, as with the PUPPI 3 deployment, it may be tentatively attributed to the existence of free gas within the sediments.

Module Geotechnique

Data from the three penetrometer tests only gave an indication of the cohesion of the sediment because of the lack of pore pressure data. The measured penetration resistance (Q_c) should be corrected according to the value of the induced excess pore pressure, (U_t) by: $Q_t=Q_c-(1-a)U_t$ where "a" is an instrumental factor ($0.5< a< 0.9$).

Since excess pore pressure can be of the same order of magnitude as the resistance to penetration the corrected value can be as low as 50% of the measured value. The cohesion (Su) is related to the corrected Q_c value (Qt) by : $S_u= Q_t/N_k$

Nk is a function of the physical properties of the sediment, a commonly adopted value is 15. Using an estimated value for the induced pore pressure and including the above approximations, an average cohesion value at 2 m, for a resistance to penetration of 100 kPa (see Fig. 80), is about 6 kPa. A 130 cm long core was collected at the first station. It is probable that the first 70 cm were not recovered due to their low cohesion, which was not sufficient to open the core catcher. Despite the fact that no *in situ* data were obtained during this deployment, the core will be investigated at IFREMER to assess its physical properties.

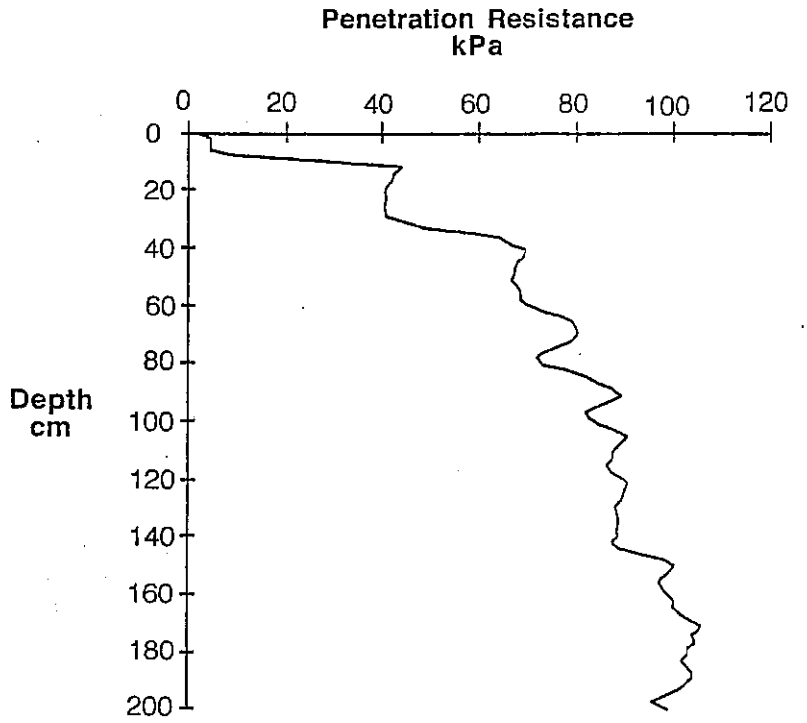

Penetration resistance profile from the Geotechnical Module
Stn. 529

Fig. 80: Profile of penetration resistance vs. depth for the Geotechnical Module at Station 529.

Conclusions

PUPPI

Four PUPPI deployments were made on the continental slope on the northern side of the Storegga Slide. We failed to recover the first instrument for unknown reasons but loss of buoyancy seems the most likely explanation. Deployment 2 provided excellent data at the reference site showing zero differential pore pressures and a well defined tidal signature. Deployment 3, near to a pock mark and gas seep showed large positive differential pressures at the time of recovery and a dynamic behaviour at a depth of 4 m which is tentatively ascribed to the presence of free gas in the surrounding sediments. Deployment 4 suffered a small leak in the electronics housing which throws an uncertainty on the reliability of much of the data obtained from the centre of a pock mark above a gas seep. However, there is some evidence to suggest that once again there is a dynamic behaviour which may be caused by the presence of free gas. The quantitative interpretation of pore pressure records where free gas is present is notoriously difficult .

Module Geotechnique

In sediments in a water depth of 950 m the best estimate for an average cohesion value at a burial depth of 2 m is 6 kPa. A 130 cm long core was collected during the first MG station (water depth 1473 m) which will be investigated at IFREMER to assess its physical properties.

Shear strengths from the PUPPI and the MG

Maximum insertion pressures (I_{max}) at depths (x) of 2 m and 4 m using the PUPPI range between 26 to 35 kPa and 30 to 49 kPa respectively. Using the approximation $C_u=I_{max}/6$ then the shear strength (C_u) varies from a low of 4.3 kPa at 2 m to a high of 8.1 kPa at 4 m. The comparative data from the MG indicates a cohesion value, at 2 m to be approximately 6 kPa. This combined data set is shown graphically in Figure 81. It is interesting to note that at the reference site PUPPI 2 in deeper water the shear strength increases with depth at a rate normal for hemipelagic sediments, whereas at both PUPPI stations in and around the pock mark/gas seep the lower port indicates weaker sediments. This is further evidence suggesting that some free gas may exist at 3-4 m below the sediment surface.

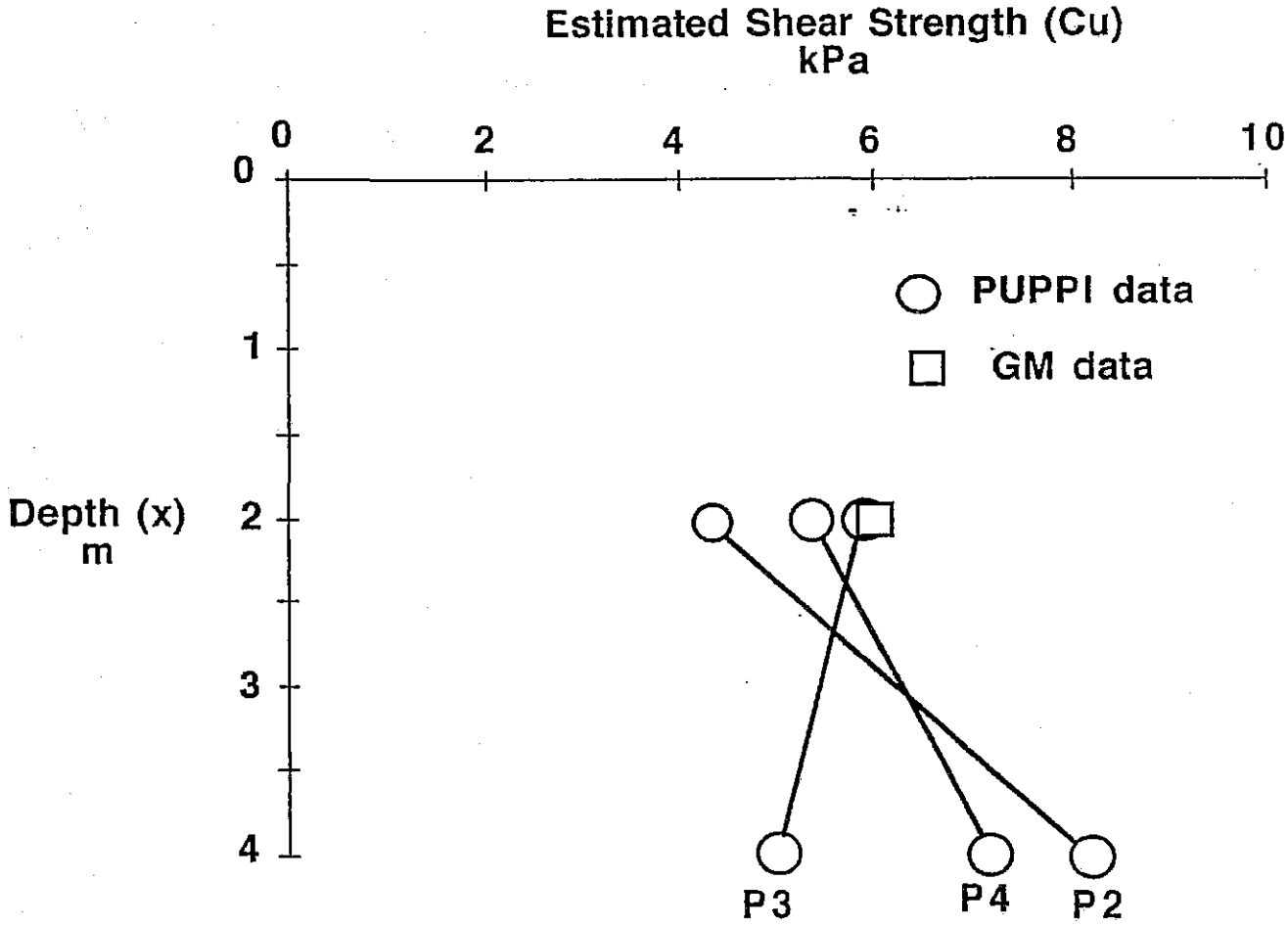

Estimated sediment shear strengths.
Data based on all maximum insertion pressures generated by PUPPI deployments 2,3 & 4 & by the Geotechnical Module (GM)

Fig. 81: Estimated shear strength values obtained from a) the maximum insertion pressures of PUPPI Stations 2, 3 and 4 and b) the penetration resistance of the Geotechnical Module at Station 529.

5.4.11.3 Geoacoustic Hydrophone-Pinger Experiments (M.Bobsien, J. Mienert)

The HF-OBH provides high resolution measurements of p-wave velocities in the upper 200 m of the sediments. It is an *in situ* sea floor platform that was developed by the Special Research Project 313 of the University of Kiel during the last two years. The system is well adapted for finding gassy sediments because there p-wave velocities are drastically reduced. The complete HF-OBH-System forms a unit which stands upright on the sea floor (Fig. 82). The buoyancy element is made of synthetic foam that can be deployed down to a depth of 6000 m. For locating the OBH there is a strobe light, a radio transmitter and a signal flag at the upper part of the OBH frame. In order to make sure that the system will go up to surface there are two independent release mechanisms which can disconnect the OBH from its anchor weight. The first is an acoustic release, and the second is an electro-chemical release which is activated by the internal clock of the electronic registration unit. The electronic unit is placed in a cylindrical pressure housing made of aluminium. The acoustic signals are to be received by three hydrophones. They are connected with the electronic unit by cables that pass through one of the end caps of the cylinder. The recording unit consists of a programmable logic, a 12 bit A/D-converter, a digital audio tape recorder, an internal clock, and a power pack.

Deployment

For the *in situ* measurements, the OBH together with an acoustic source (3.5 kHz Transducer) are lowered to a height of 50 m above the sea floor. Subsequently the OBH, hanging directly under the source, is disconnected by an acoustic release from the towing fish. Profiling then starts with a towing speed of 2.5 knts and a towing height of about 50 m above the ocean bottom. The length of the seismic profile is 1 nm, with a shot rate of 1 shot per second. Lowering of source and OBH together is necessary because the source must pass the OBH position within a horizontal range of 20 m.

Owing to a common and synchronised time basis for shot instance and OBH clock, it is possible to measure the travel time of the signal on its way from the source to the receiver. At the end of data processing and after having made all corrections, all shots are plotted together according to their distance from the receiver. The results are travel time curves which are reflection hyperbolas for each reflector. Since the degree of the curvature of the hyperbolas is a function of p-wave velocity in the sediments above the reflector, interval velocities can be computed.

HF-OBH measurement in the Storegga Slide area

The main goal of the geophysical investigations at the Storegga Slide was the determination of changes of p-wave velocities in gassy sediments. The position chosen for the OBH employment was at the northern border of the Storegga Slide at a depth of 890 m; this is an area charaterized by many gas vents. Exact positioning was done with deep-tow-boomer (Fig. 83) and Parasound profiles. Deep penetration of the signals into the sediment, undisturbed and horizontal layering of the layers, together with the occurrence of gas, are

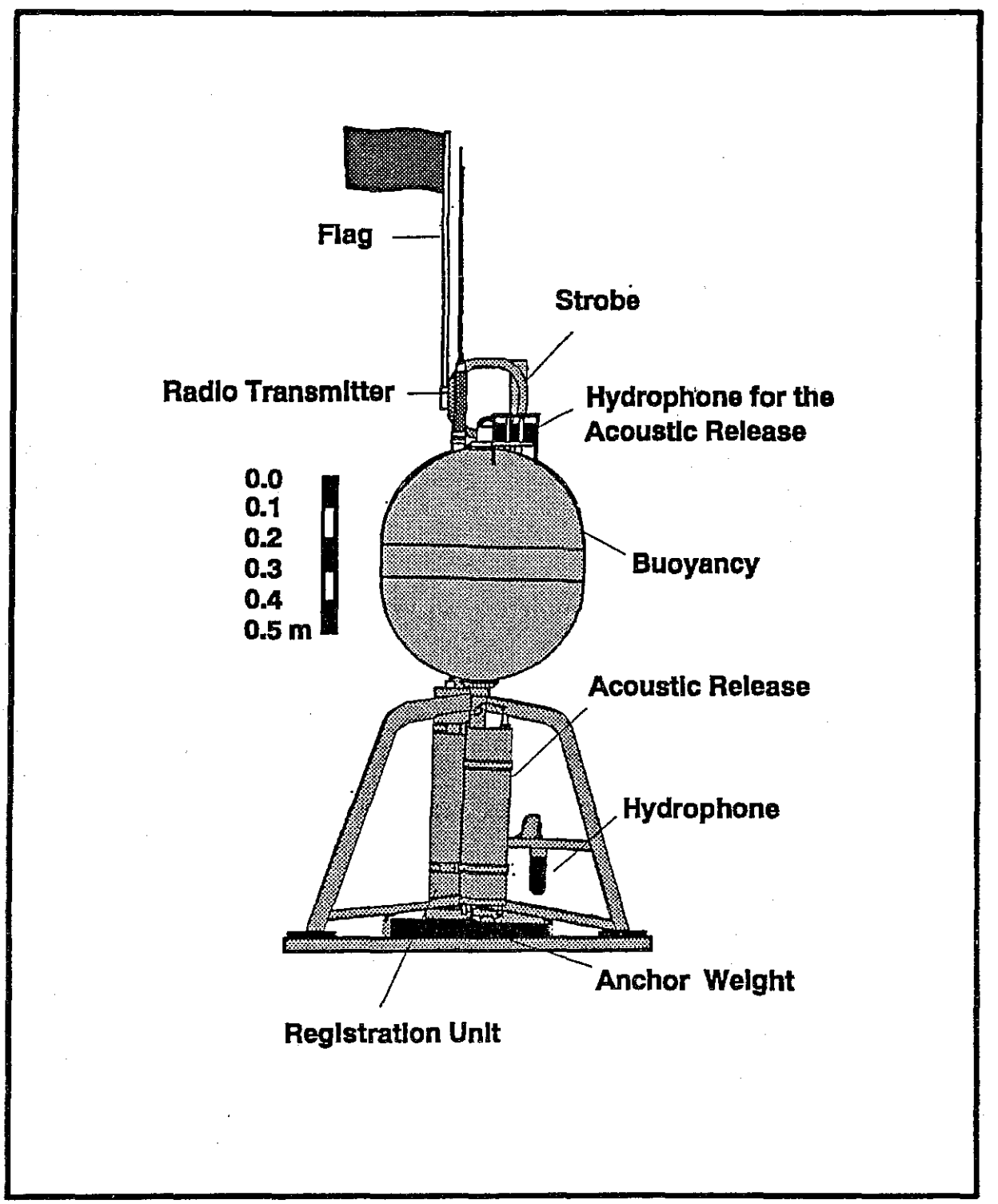

Fig. 82: HF-OBH configuration of the various components of the acoustic system.

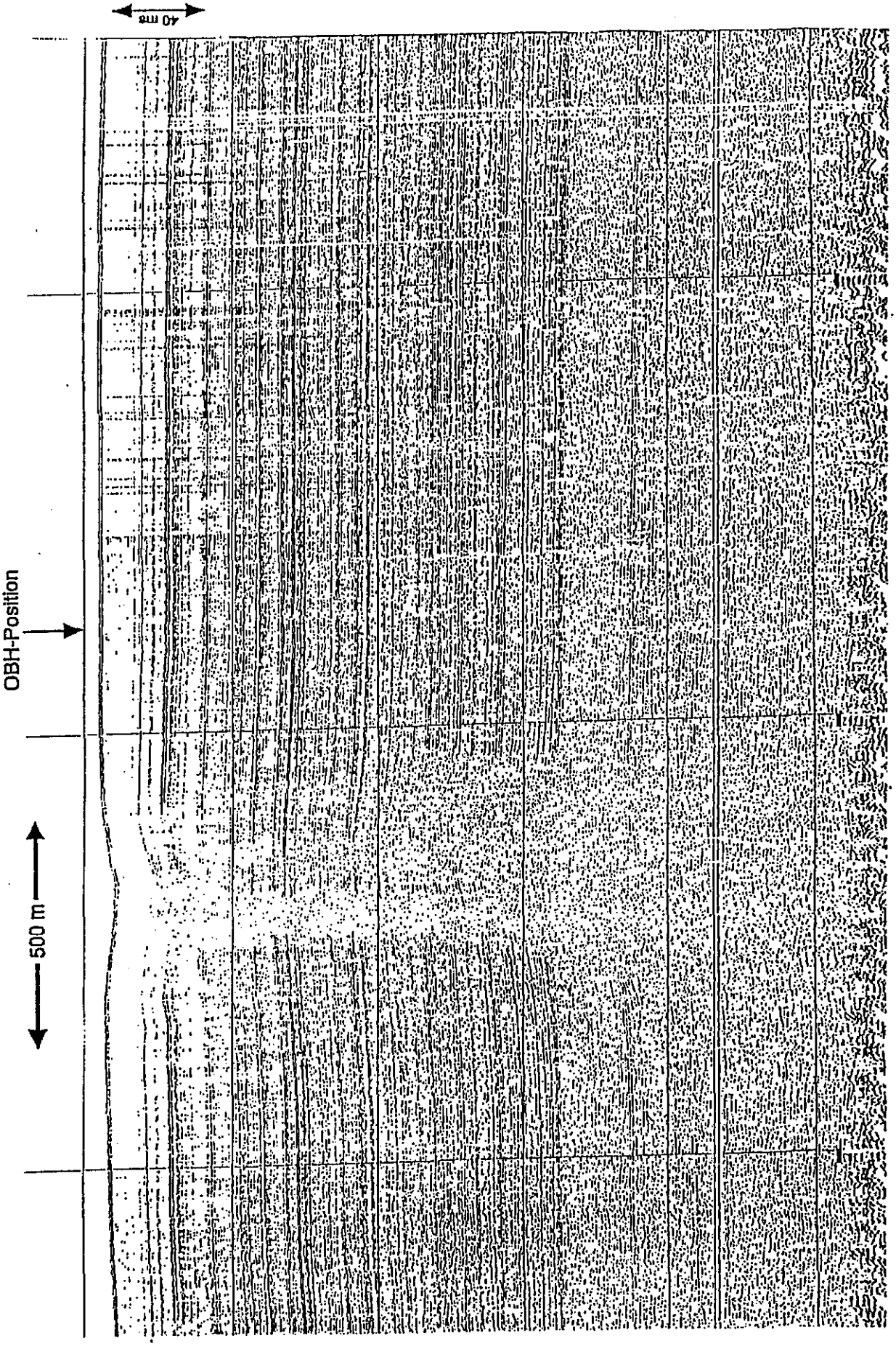

Fig. 83: Boomer profile with OBH-position and gas vent (middle left side).

ideal conditions for OBH measurements (Fig. 84). The position is close to a gas vent (Fig. 83). Figure 85a,b shows single shots of a boomer profile (Fig. 85a) and a Pinger profile (Fig. 85b).

The OBH deployment took place on 4 November. During this cruise there was the opportunity to use another source besides that specifically developed for the OBH system; the BGS deep-tow-boomer system (0.5 - 3 kHz). With the help and support of BGS, a combined investigation was undertaken. The program was divided into two parts, with two time windows for registrations since the total registration time is limited to two hours. During the first period of the program the OBH was lowered to the sea floor together with the pinger. After release of OBH the first profile was run. Subsequently, the pinger was brought on deck and the BGS boomer was deployed. With the beginning of the second time window, the boomer profile was started.

The hydrophone-pinger experiment started at 10:58. Low wind velocities and a calm sea provided almost perfect conditions for the deployment. With a winch velocity of 0.5 m/s the platform was lowered to a depth of 840 m. At 12:02 the acoustic command for the release of the OBH was given since the first time window was programd from 12:00 to 12:40. At 64°46.20'N, 4°30.30'E the OBH sank to the ocean bottom and the first profile (OBH 523-1) started at a speed of 1-2 knts. During the profile the sea floor reflections were also registered by the pinger and sent up to the ship by the wire. The signals were displayed on a graphic recorder (EPC 4800) so that the towing height could be controlled. The profile ended at 12:35 at 64°45.62'N, 4°29.79'E (water depth 897 m). The pinger was back on deck at 13:00. At 13:45, deployment of the BGS boomer and the approach to the second profile began. The second time window was programd from 15:30 to 16:50 and profile OBH 523-2 started at 64°47.46'N, 4°30.95'E, coincident with the opening of the window. During the profiling, the actual towing height has to be recorded minute by minute in the log book since the height is only displayed and not stored. The length of the towing cable was 1311 m. The time between two shot instances varied about 1.2 s due to a depth compensation feature of the boomer. Knowledge of the absolute shot instance is of great importance for the processing of the OBH data. For that reason the time code of the clock that started the OBH clock was recorded together with the TTL impulse of the shot instance delivered by the boomer system. The profile ended at 16:30 at 64°43.98'N, 4°29.27'E. After the recovery of the boomer, and after having released the OBH at 17:55, the OBH was sighted at 18:06. About 30 minutes later it was brought on deck.

A first look at the data by a D/A conversion and output to a loudspeaker showed that both profiles were recorded well. As expected, the noise level was low compared to previous investigations in the shallow waters of the Baltic Sea.

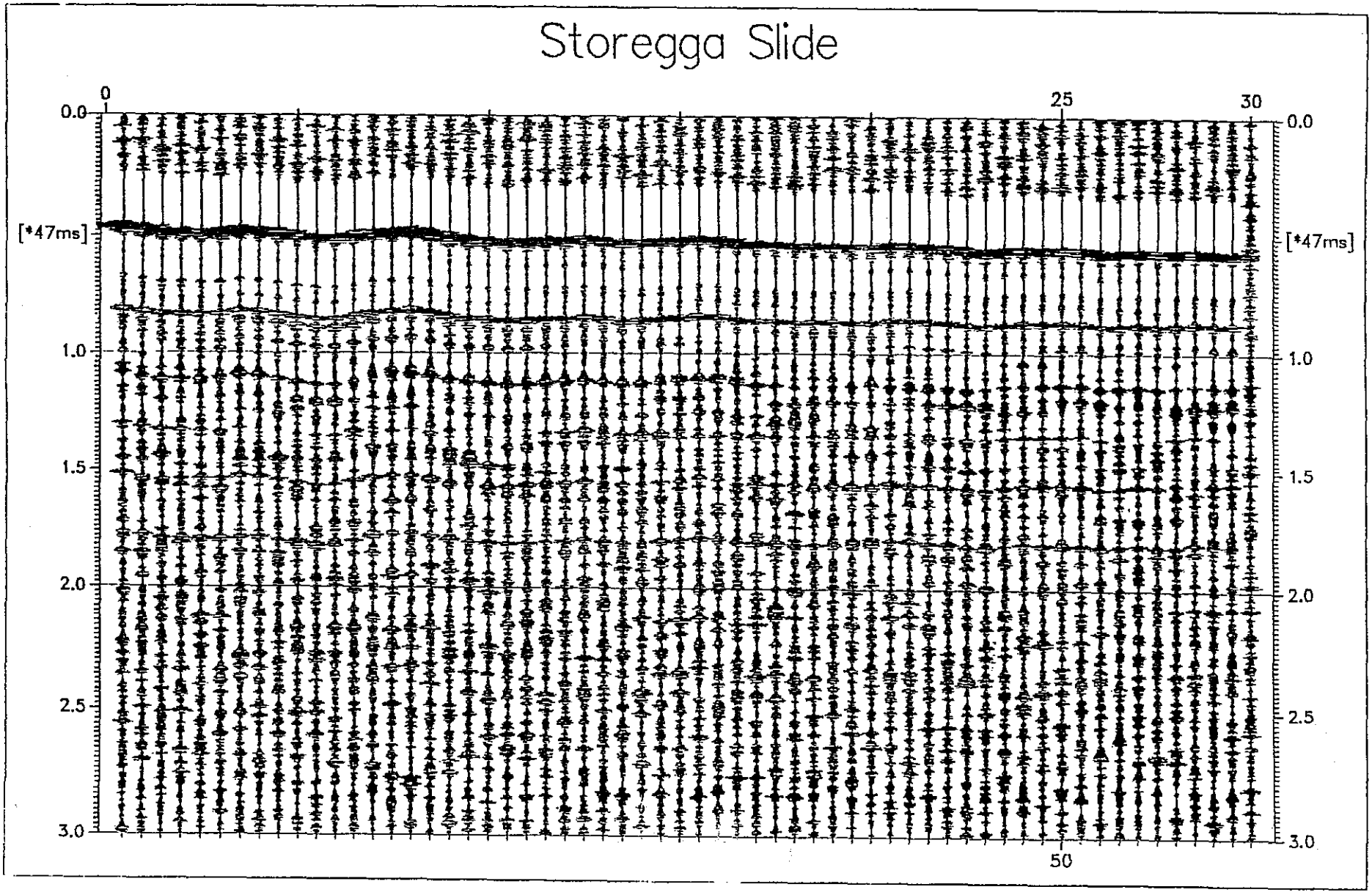

Fig. 84: Sample of uncorrected raw data of OBH measurement.

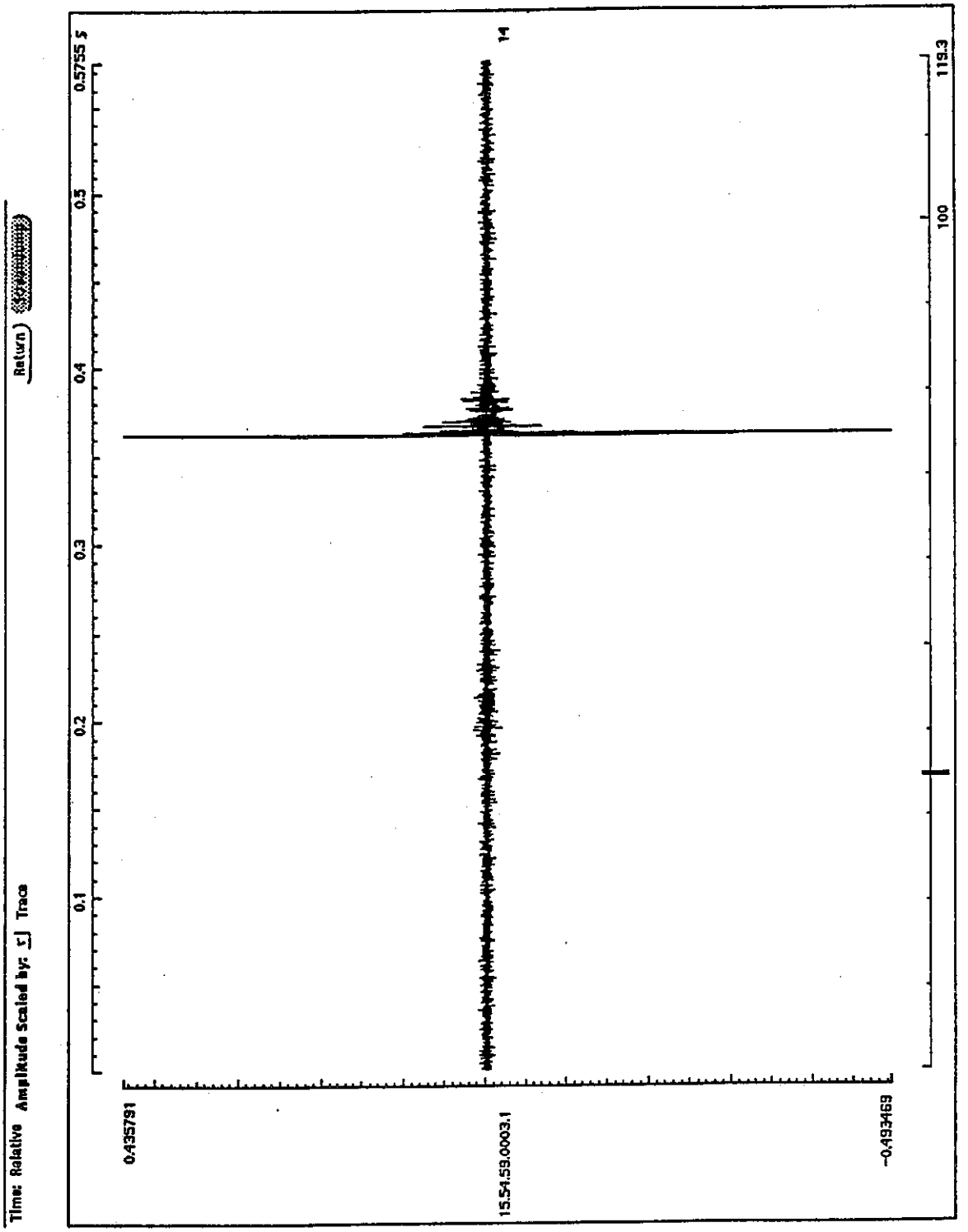

Fig. 85a: Single shot of OBH-registration. (a) Boomer profile.

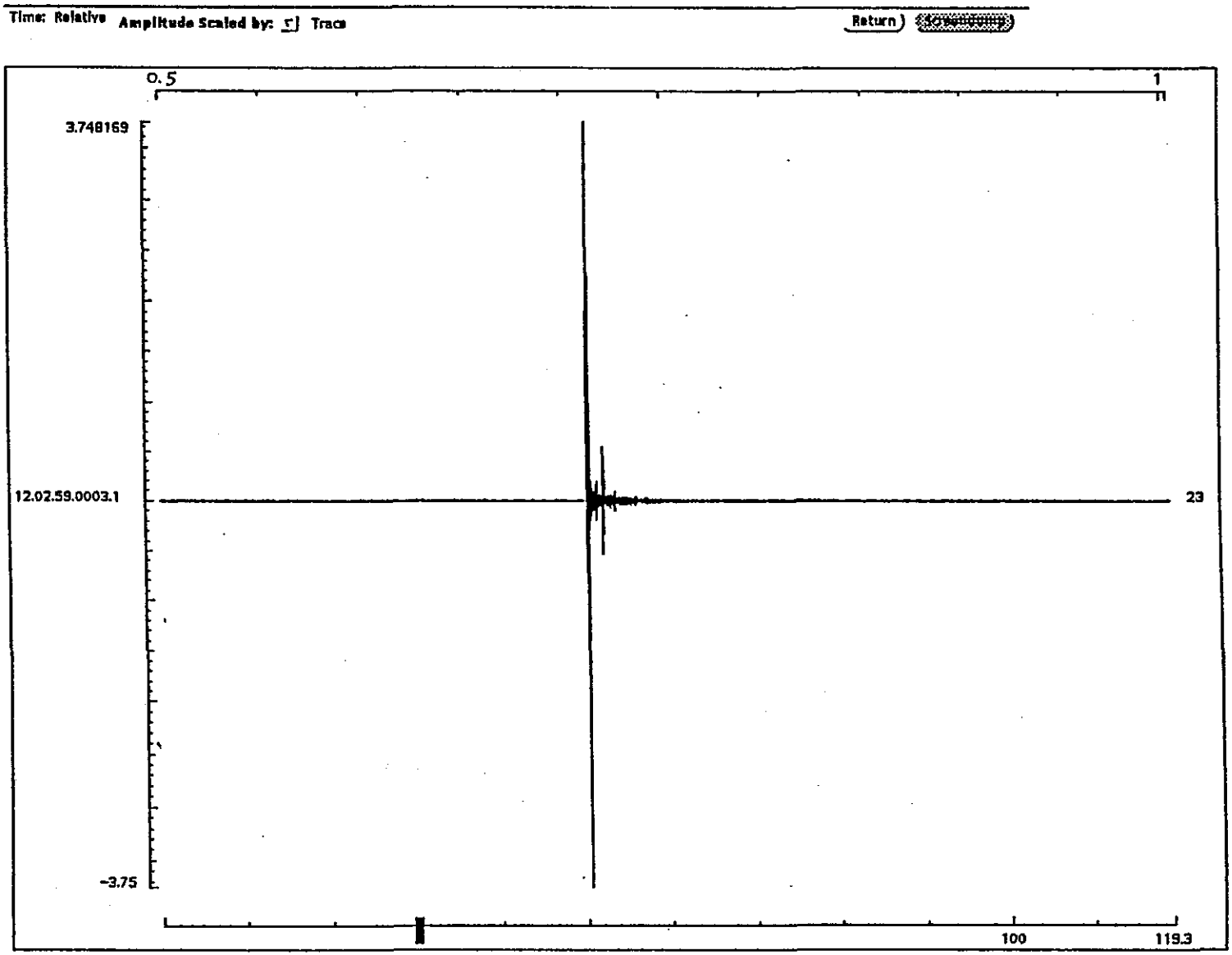

Fig. 85b: Single shot of OBH-registration. (b) Pinger profile.

5.4.11.4 Parasound and Hydrosweep Profiling

(J. Baas, F.-J. Hollender, M. Bobsien, C. Baumgärtner, N. Kenyon)

The Storegga Slide off the continental slope of Norway was surveyed as part of the ENAM-project. The study concentrated on the northern rim of the slide in water depths between 400 and 1500 m. Several techniques were used to assess the distribution and effects of free gas and gas hydrates in the slope sediments. In this chapter the preliminary results of Parasound and Hydrosweep profiling are presented. The Parasound echo-sounder is a sediment subbottom profiler. It works with two simultaneous primary frequencies (a fixed frequency of 18 kHz and a variable frequency of 18 to 23.5 kHz). Through the Parametric Effect in water, a secondary frequency is produced in the range 2.5 to 5.5 kHz. In ocean sediments, a penetration of up to 100 m is possible. Analogue plots are available for preliminary interpretation on board. In addition, digital data are preserved on magnetic tape so that details can be studied with post-processing techniques. The Hydrosweep system, a multibeam echo sounder system, was also used. It operates at a frequency of 50 kHz. The combined use of the Parasound and Hydrosweep systems provides three-dimensional imaging of superficial seismic units in the study area.

Results

The Parasound and Hydrosweep records of the Storegga Slide area are of good quality, owing to good weather conditions and locally deep penetration. Preliminary results, presented in this chapter, are based on the analogue data. Details will become available after the post-processing of the digital data. Six chevron-shaped profiles (511, 516, 521, 525, 531 and 541) were run parallel to the northern rim of the Storegga Slide, in SW-NE and NW-SE directions. They range in water depths between 400 m and 1500 m. The northernmost four profiles (511, 516, 521 and 525) were taken on the undisturbed slope. The southernmost profile (541) extended over the Storegga Slide. The remaining profile (531) was taken at the rim of the slide, so that undisturbed as well as disturbed areas were studied. Additionally, two profiles were obtained perpendicular to the rim (544 and 549).

Slope sediments

Profiles 511, 516, 521 and 525 on the undisturbed slope show similar downslope sequences of seismic features. At depths less than about 500 m the sea bottom has a wavy configuration with a chaotic seismic unit present at and beneath the sea bed. The penetration depth here is usually less than 10 m. Downslope, the chaotic unit is buried under a progressively thickening, regularly stratified sequence. The chaotic unit extends down to 600-700 m depth. The maximum thickness of the stratified seismic unit is confined by the maximum depth of penetration. The data typically shows a sequence of 55 m thickness and up to 15 bright reflectors (Fig. 86). The reflectors tend to occur in bundles, separated by weak or no reflectors. Offlap is seen in the uppermost sequences which progressively thicken downslope.

Between water depths of 600 m and 1000 m, several features demonstrate the presence of gas, denoted here as vents, chimneys and bubbles (Figs. 86-88). Graben-like structures are also present with vertical displacements of several metres. Normally the sea-bottom reflector drapes the underlying displaced reflectors (Fig. 89). The grabens may be associated with gas escape.

Evidence of gas in sediments

In water depths between 600 m and 1000 m various morphological and seismic features are believed to demonstrate the presence of gas. The preliminary classification presented here is based on what may be various development stages of pressure build-up:

- **Gas bubbles** show up as individual elliptical bright spots on the analogue Parasound profiles (Fig. 86). Their apparent long axis is perpendicular to the sea bottom and they are several tens of metres wide.
- **Gas chimneys** are vertical, seismically transparent features which hardly interrupt the stratified sequence. Their small width distinguishes them from gas vents (Fig. 88).
- **Pressure domes** are seismically transparent columns which are overlain by continuous reflectors. They measure up to several hundreds of metres in width. It is thought that an impermeable layer prevents upward escape of gas. In at least one example, a hummock is present on the sea bottom (Fig. 88). This feature may indicate very slow escape of gas or pressure build-up against a sediment layer close to the sea bottom.
- **Gas vents** are wide transparent features which extend to the sea bottom. Hence, gas has escaped out of the sedimentary sequence into the water column. In some instances, the location of a former pressure dome can be recognised. The escape route above these pressure domes is commonly narrower than the width of the pressure dome itself.
- **Pockmarks** on the sea bottom may accompany gas vents. They have various shapes. Most frequently, they are V-shaped, either with or without levees (Fig. 87) and they measure several metres in a vertical section and several hundreds of metres in cross-section.

Storegga Slide sediments

The rim of the Storegga Slide is a prominent feature on the Parasound (Fig. 90) and Hydrosweep profiles. The stratified sequence is abruptly cut off by a steep erosional truncation. Slide deposits are represented by chaotic seismic units with low penetration (up to 20 m) at the base of the truncation. The profiles perpendicular to the rim of the Storegga Slide show secondary creep and slumping. The debris has a hummocky upper surface. Locally, large blocks of the stratified sequence, several hundreds of metres in cross section, are incorporated. Stratified sequences also underlie slide masses. Erosional truncations are not confined to the rim but also occur within the Storegga Slide. This may point to various periods of mass movement. Our observations broadly support the interpretations of published

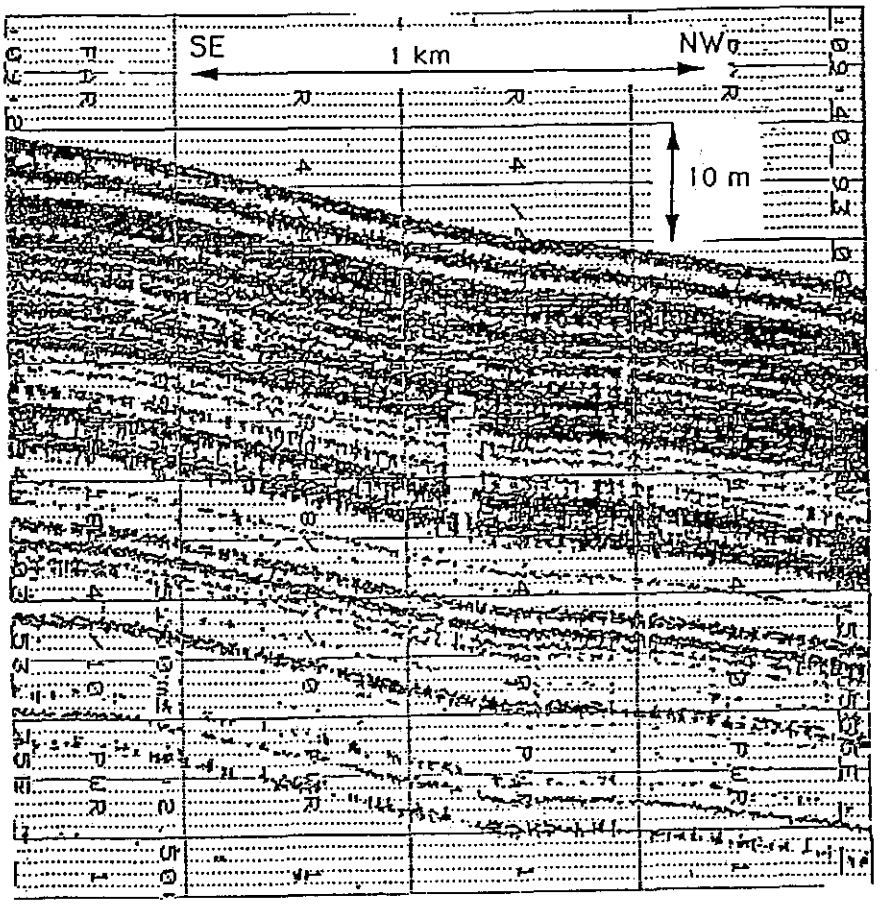

Fig. 86: "Acoustic transparency zones". Profile 511. Water depth: 1160 m. Location: 64°54.270'N, 3°52.360'E.

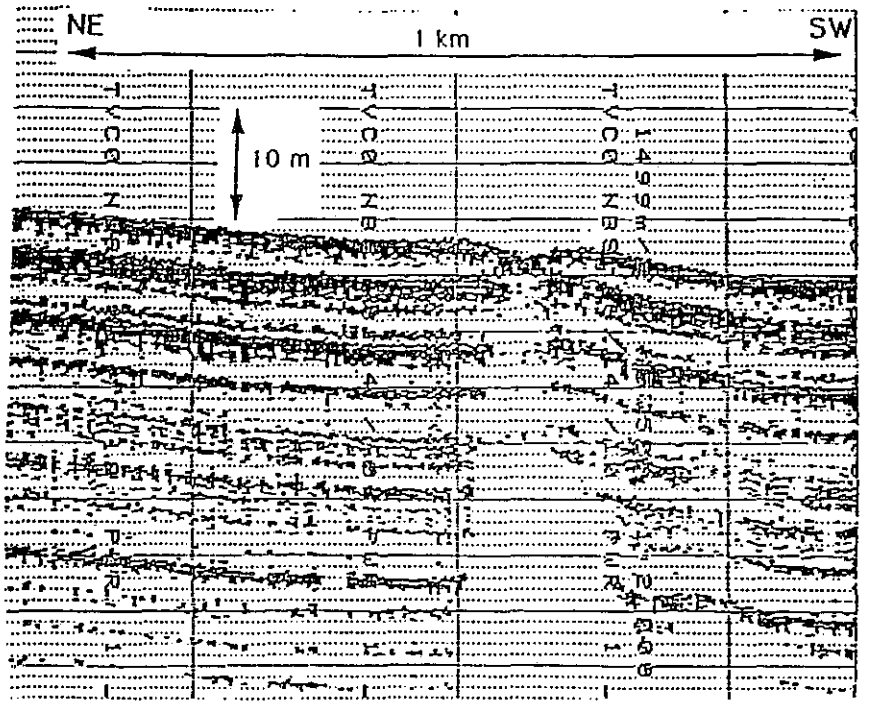

Fig. 87: Gas vent with leveed pock mark. Note decrease in width in upper 18 m. Profile 511. Water depth: 720 m. Location: 64°45.268'N 5°06.500'E.

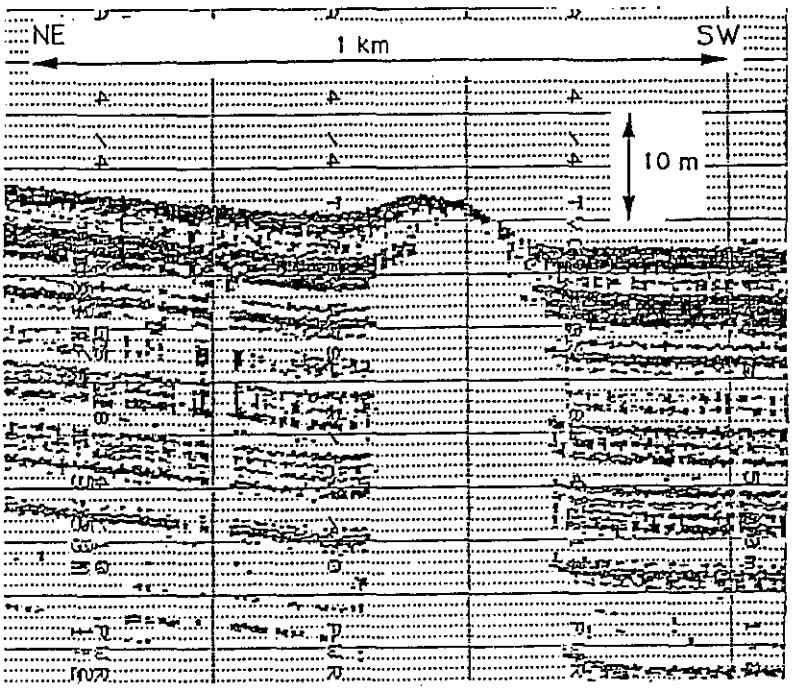

Fig. 88: Gas vent with hummock on sea bottom. Profile 511. Water depth: 735 m. Location: 64°44.611'N, 5°02.815'E.

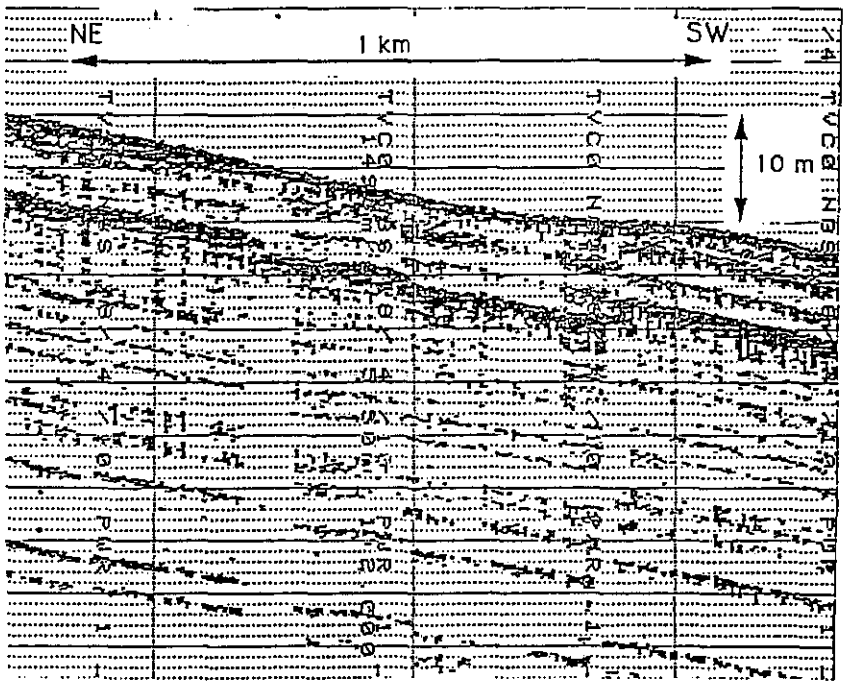

Fig. 89: Indication of Graben structure. Profile 511. Water depth: 800 m. Location: 64°43.282'N, 4°54.038'E.

data but provide much more detail in the slide area (BUGGE et al., 1987, 1988; JANSEN et al., 1987). Details will become available by further analysis of the digital Parasound data and the deep-tow-boomer data.

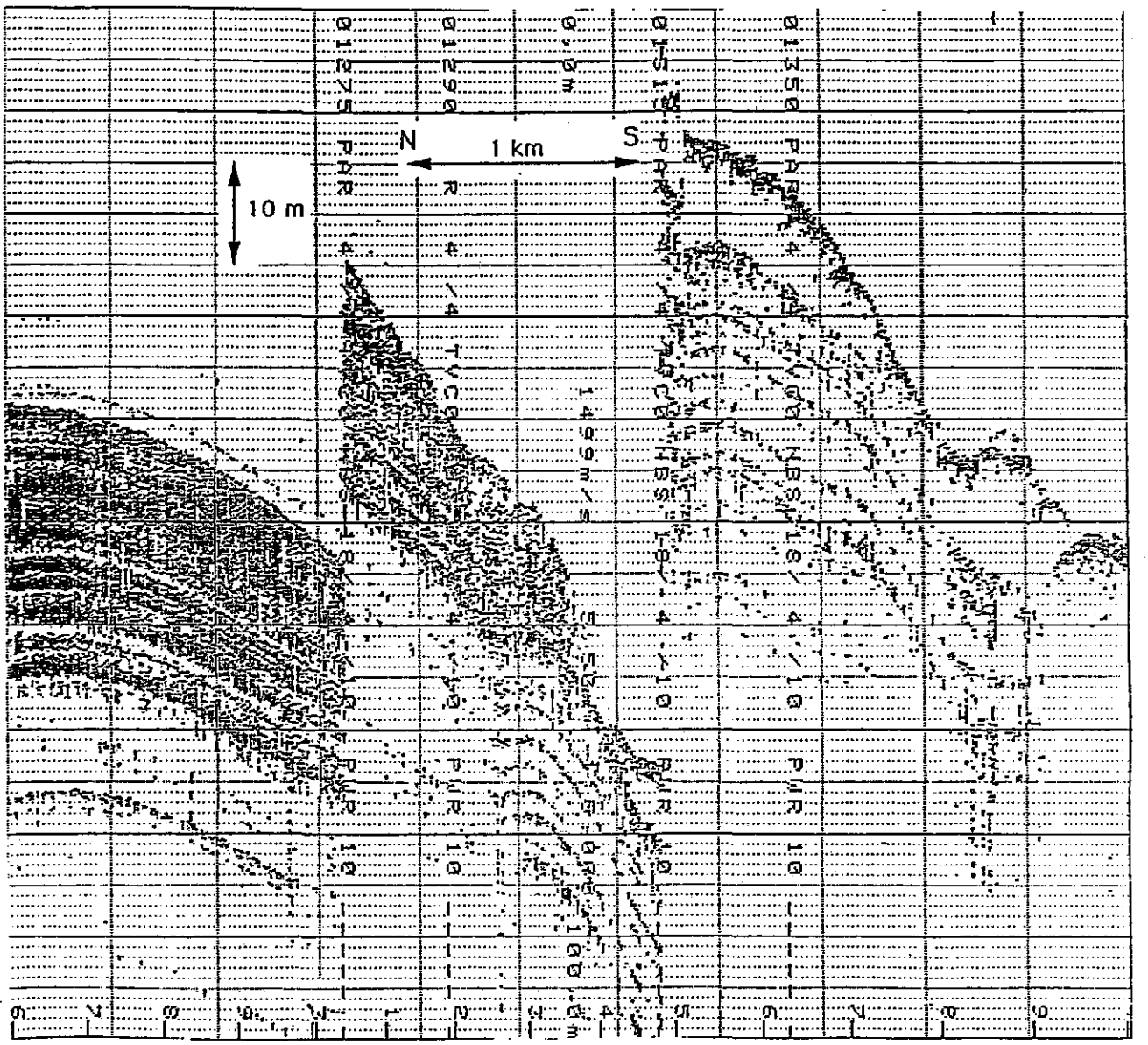

Fig. 90: Northern rim of Storegga Slide. Profile 540. Water depth: 1265-1366 m. Location: 64°37.699'N, 4°26.556'E - 64°35.356'N, 4°26.906'E.

5.4.11.5 Sedimentary Processes - Storegga Slide (N. Kenyon, J. Mienert)

There is a variety of relief features on the continental slope of NW-Europe that are formed by mass wasting processes. Submarine canyons and leveed channels are the conduits through which much sediment is transferred to the deep-sea floor, where the volume of transferred sediment is greater than the size of the conduit. Another major category of feature are the scars left by submarine slides, where the amount of material displaced has the same volume as the scar. They have a great variety of sizes but by far the largest is the Storegga Slide off mid Norway.

The available data suggests that the Storegga Slide consists of three major events with further minor or secondary associated slides (BUGGE et al., 1988). The "First" Storegga Slide was the largest and created a slide scar with a 290 km wide headwall. The slide extends down the continental slope and into the Abyssal Plain for a distance of more than 800 km. The sediments that were removed are presumed to have been the relatively soft, mainly Plio-Quaternary clays now found downslope as acoustically transparent deposits with small-scale surface roughness. The "Second" and "Third" slides cut down up to 200 m deeper into more consolidated sediments and cut a new headwall some 5-8 km further back into the shelf edge. The deposits have a characteristically blocky appearance on seismic profiles and include some huge, largely unbroken sediment slabs. The "First" slide is dated at 30.000-50.000 years BP and displaced about 3900 km^3 of material, while the "Second" and "Third" slide occurred in near succession, about 6000-8000 years ago, and involved about 1700 km^3 of sediment. A thick (more than 6 m) fine-grained turbidite in the Abyssal Plain is related to the "Second" slide. In places its thickness is more than 20 m. There is also evidence for a tsunami which accompanied the Second Slide, leaving dated deposits on the coasts of Scotland and Norway (DAWSON et al., 1988).

It is believed that earthquake loading and gas hydrate decomposition caused liquefaction which triggered these catastrophic events. There appears to be significant earthquake activity in the Storegga area. Immediately outside the northern margin of the slide scar gas has been observed on two sparker profiles in water depths of 1000-1300 m. It is believed that there is free gas and also a gas hydrate layer parallel to the sea floor and cutting across bedding planes (seen as a bottom simulating reflector) at a sub-bottom depth of 300 m. The observed gas is presently at about the same sub-bottom depth as the glide plain of the "First" slide.

5.4.12 History of the Norwegian Shelf Uplift During the Neogene
(M. Weinelt, K. Rokoengen, A. Aichinger, J. Saettem, A. Hamich)

Based on extensive work by NTH (Kåre Rokoengen) and IKU (Joar Saettem, Leif Rise) the deployment of a vibrocorer on the Norwegian Continental Shelf became an exciting scientific task. Since the 1970s seismic data have been documenting the existence of large sedimentary

basins off Mid-Norway. In the course of increased exploration activities a number of bore holes have been made, which gave access to Upper Triassic to Tertiary sediments. But due to the drilling routines within the offshore industry, the Quaternary and the younger parts of Pliocene sediments (consisting of immature sands) have not been sampled. However, many ideas of sedimentological and lithological properties of these strata were interpreted from seismic data. This led to an outline of the characteristics of the Pliocene sediments off Mid-Norway. They can be subdivided into 11 regional sequences prograding roughly from east to west. Sequence bounding and internal reflectors show dips up to 15°. The sediments could have been deposited as clayey sand in delta bodies.

Seismic data document a very thin or absent Quaternary cover on the Pliocene wedges between Friyabanken and Haltenbanken. This information made it worthwhile to try to recover Late Tertiary sediments by deploying a relatively short sample device: the 5 m long vibrocorer. Successful operation would give access to sediments which suggest a dramatic environmental change on the Norwegian shelf.

During M 26/3 such a sampling program was carried out. The SFB 313 of the University of Kiel provided 48 hours of ship-time and the vibrocorer. BGR completed the equipment with a power supply cable of 400 m length. Based on the IKU seismic data, 10 sample locations were selected (Table 24; Fig. 91).

Tab. 24: List of the vibrocorer locations. Codes and seismic profiles are indicated in Fig. 91.

code	line	shot point	latitude	longitude	station (m)	waterdepth
A	B73-157-2	1444	64° 20.733'N	8° 23.664'E	501	289.2m
B	B73-157-2	1502	64° 21.634'N	8° 21.378'E	502	276.7m
C	B73-155	2108	64° 17.333'N	8° 12.418'E	505	334.4m
E	B73-155	2056	64° 18.023'N	8° 09.575'E	503	284.0m
F	B73-155	2051	64° 18.356'N	8° 09.244'E	504	283.8m

Operational log

After reaching the working area (Fig. 91) at about 21:00 on 28 October 1993, the sample locations were surveyed by multibeam-echo sounder (Hydrosweep) and subbottom-profiler (Parasound) during the night (Station 500). The systems were tuned on these first profiles. Problems of lack of penetration, bad resolution, overmodulation and "ghosts" initially occurred. Nevertheless, the characteristic configuration of the reflectors within the Pliocene

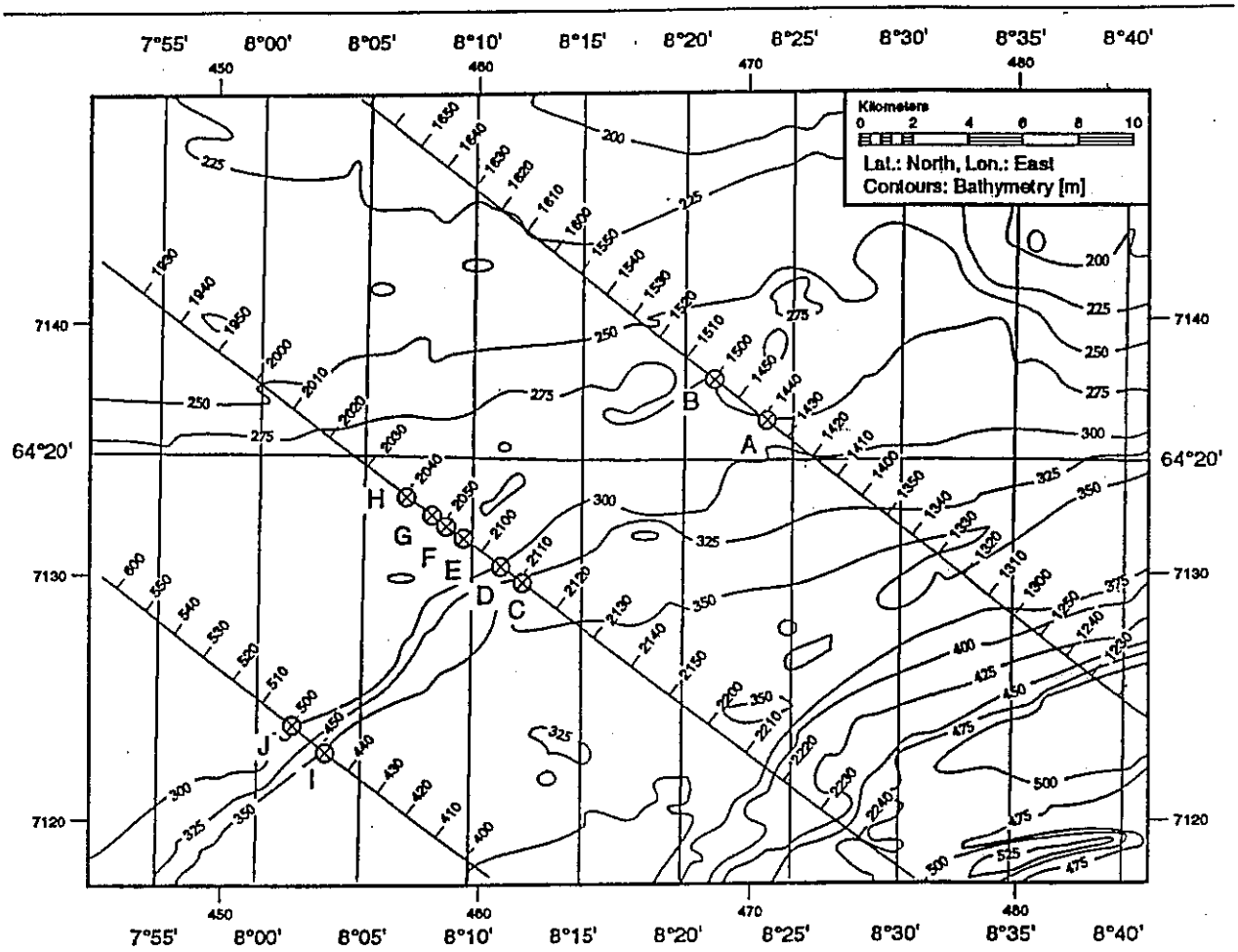

Fig. 91: List of the most prospective core locations based on IKU seismic data (shot point annotated lines). Positions A, B, C, E, and F have been sampled on this cruise (see also Table 24).

wedges could be detected with the Parasound system. The subbottom data gave no reason for altering the sample locations determined from the IKU profiles.

On 29 October Station 501 (first vibrocorer station, water depth: 289.2 m) was reached at about 6:00. The equipment was prepared for the first deployment (about 8:30). This attempt was a failure. The spring cover, supposed to close the corebox after deployment, had obviously been triggered before the device reached the sea floor and prevented the core-box from penetrating the sediment. A second attempt (10:30) at this station was successful. Penetration was 408 cm (see appendix core number 23490-2). But this time the spring cover

did not function at all and the deeper parts of the core were lost during recovery. 312 cm of grey-brownish silty clay, containing erratic clasts below 12 cm, were recovered. The lithology suggests a Quaternary age of the core.

After sailing to Station 502 (water depth: 277.0 m) coring started at about 10:45. The attempt was successful with a penetration of 490 cm and a recovery of 477 cm (see appendix core number 23491-1). The core only contains Quaternary material. At the next station located on the central profile (503-3, Fig. 91), the problem with a premature triggering of the spring cover occurred again. During the second attempt on this station the ship obviously drifted off station, putting tension on the wire. The corer was tilted during deployment and the box was bent. It could not be pulled back into the rig and the box had to be cut losing the material. The third attempt was successful. The device penetrated 270 cm into the sea floor (see appendix core number 23492-3). The box bent again and the spring cover did not close the box. About 40 cm of the core were lost. Nevertheless, this deployment was a success. The recovered sediments consist of clayey and pure sand of dark to blackish-greenish colour (glauconite?). The boundaries between the individual sand layers at 50 cm and 85 cm are oblique. The upper 50 cm of the core contain foraminifera and molluscs. At about 100 cm trace fossils were observed. At 180 cm and 190 cm layers of firm clayey sand occur within the non-stratified sands. From 210 cm to the base at 234 cm the inner part of the core was washed out.

At Station 504 (water depth: 283.8 m) the first deployment was successful. After penetrating 430 cm a core of 380 cm length was recovered at about 19:00. The upper 285 cm of the core consist of clayey and silty layers, partly with erratic clasts and shells (see appendix core number 23495-1). Below, dark green (glauconite?) sand with little clay was found. At 318 cm and 358 cm layers of erratic clasts (dropstones?) are present.

The last core was recovered at Station 505 (water depth: 334 m) with a penetration of 490 cm and a recovery of 482 cm (see appendix core number 23496-1). The sediment is a silty clay with dropstones, apart from the uppermost 4 cm which are sandy. Sandy intercalations with oblique boundaries occur at 150 cm and 160 cm. Between 165 cm and 200 cm the lithology changes to a dark greenish sand. Below 200 cm down to the base of the core the material is dark grey clay with dropstones. The core tore off its upper part at 333 cm and slided down in the core box about 17 cm. Between 350 cm and 420 cm the outer part of the core box was covered with dark greenish sand. On the morning of 30 October the vibrocorer program could not be resumed. Heavy winds (> 8 Bft) and a strong swell made further deployment impossible.

Summary

The cores which consist of clayey and silty material and contain erratic clasts (interpreted as dropstones) have been assigned a Quaternary age. With the core recovered at Station 503 the main objective of this program was achieved. Sediment of the Pliocene wedges was recovered. From seismic data we concluded that the strata were deposited with relatively

steep dips. This was confirmed by dipping sandy layers in the cores. The layering and the lithology may support the delta-model. First questions are raised by the sedimentological characteristics of the successions:

- Is the greenish colour of the sediments caused by glauconite, and if so, is this authigenic glauconite?
- What is the sand/clay ratio? Within a delta facies one would expect a considerable amount of clay in the sands.

The core recovered at Station 505 shows sandy layers within Quaternary sediments. Age and physical properties of these sands may give indications about the glacial history of the study area.

5.5. **Coring Operations** (E. Steen, M. Schumann, Chr. Franke)

Sediment layers near the surface have been collected with a box corer (GKG) and multicorer (MUC), longer sediment columns with a gravity corer (SL). In sandy sediment layers on the shelf, the vibrocorer-VK 500 (VC) has been deployed.

1	Box corer (GKG): box size:	50 x 50 x 60 cm
	dead weight of normal model:	approx. 900 kg
	of deep sea model:	approx. 1100 kg
	manufacturer:	Fa. Wuttke, Henstedt-Ulzburg
2	Multicorer:	8 sampling tubes, Ø 10 cm
	weight:	400 kg

For target sampling, an UW-camera was installed in the frame of the MUC, leaving 7 sample tubes.

3	Vibrocorer VK 500 (VC): box size:	10 x 10 x 500 cm
	striking power:	approx.700 kp
	core length:	up to 500 cm
	manufacturer:	Hydrowerkstätten, Kiel-Hassee

4 Combined gravity- (SL) and piston corer (KOL) type 446:

total weight:	2000 kg
diameter of corer:	14 cm
diameter of liner:	12 cm
length:	multiple of 575 cm
manufacturer:	Hydrowerkstätten, Kiel-Hassee

Table 25 gives a summary listing of the deployments of the various coring devices and their total sediment recovery. Rough weather conditions as frost, high sea and storm put high demands to crew and coring devices. The crew did great work on deck, enhancing security and success during coring operations.

Tab. 25: Deployment statistics of sampling devices.

	Sample device	Number of deployments	Number of successful deployments	Total recovery (m)
M 26/2	MUC	8	7	19.46
	TV-MUC	1	1	4.06
	GKG	26	22	8.23
	SL-6 m	2	2	11.23
M 26/3	VK	8	5	23.06
	GKG	8	7	3.02
	SL -6 m	1	1	5.74
	SL -12 m	11	11	77.24

6 Ship's Meteorological Station

6.1 Weather and Meteorological Conditions During Leg M 26/1

(H. Ulbricht)

The cruise started in the evening of August 24 at a temperature of 27° C and 80 % relative humidity. The course to station M2, crossing the western Mediterranean was relatively calm. Just when passing two convergence lines and a coldfront, nocturnal thunderstorms occurred and the wind increased up to 6 and 7 Beaufort. Also the following part of the voyage was quite undisturbed. Between a flat depression over Morocco/Sahara and a wedge of the Azores anticyclone, constant northerly to northeasterly tradewinds of 3 or 4 Bft were blowing. With the beginning of the further cruise to station W2 and L2 the synoptic situation and development changed significantly and remained thus until the end of leg M 26/1.

An intense blocking high was situated over Greenland and in a far southerly frontal zone extraordinary intense cyclones developed in comparison to the season.
Thus the formation of a secondary depression to a storm low began from September 4. On September 6 it tracked north of our position and caused a severe gale of Bft 9. When the storm centre drifted away to the Celtic Sea, the wind ceased and the work at station L2 was not impaired anymore.

Some days later on September 10 another secondary low developed from the former tropical storm "Floyd". It deepened rapidly, becoming a low of hurricane force and moved to the Bay of Biscay until September 12. At this time METEOR was already north of 50 degrees North, so that only an indirect influence of a northwesterly wind force 6 to 7 occurred and the work at the station was not handicaped.

Cruises and measurements between the stations F" and E1/E2 developed rather calm at the edge of a high over Greenland/Iceland and easterly winds. On September 15 a new secondary low developed near Newfoundland. It moved along the 55th degree of latitude and intensified to a complex low hurricane of wind force and a central pressure of 965 hPa near 40 degrees West.

The influence on the rest of M 26/1 was direct. The work at station D2 could still be finished on September 16 when a southeasterly wind increased. But during the next night a violent storm (11 Bft) set in. Due to the expected developement of the weather the planned track to the last station A2 was cancelled and the course was set for Edingburgh. The violent storm lasted until morning of September 18 but ceased rapidly, when the occlusion passed. Then easterly winds of only Bft 6 to 7 were encountered.
Until the Pentland Firth this weakening storm centre dominated the weather of the cruise of METEOR. At the end of the leg there were only remnants of this system left, so that the Northsea welcomed us with a calm-glassy sea and sunshine.

6.2 Weather and Meteorological Conditions During Leg M 26/2

(H. Ulbricht, D. Bassek)

The transit of RV METEOR from Edinburgh to the Skagerrak was influenced by a high pressure cell located over Scandinavia and light winds (4-6) from the southeast (Fig. 92). During station work from early in the day on 30 Sept. to about noon on 2 Oct., a strong southeasterly flow of air prevailed between a storm centered over Great Britain/Ireland (975 hPa) and a strong high pressure cell (> 1030 hPa) over Finland and the Baltic states. Winds were between 6-7 and increased to force 8-9 after METEOR left the working area and steamed a northwesterly course.

The second area of work, the Faeroe-Shetland Channel, was reached crossing under light winds (3-4) the northern flank of a weak low pressure cell over the North Sea. During that time and preceeding the transit, a strong North Atlantic low (57°N/26°W) had moved east while a strong high developed over Greenland. In addition, the high pressure over Scandinavia decreased and was replaced from the west, primarily from the vicinity of the Lofoten Islands, by a low pressure cell. As a consequence, a continuous and increasing flow of cold air developed which originated from the Barents Sea, passed the vicinity of the Faeroe

DAT.	00	06	12	18	DAT	00	06	12	18
28. 09.			56.0 03.2W 9 131 97 12 5 2 12,5 5	56.3 01.6W 10 112 98 13 6 7 11,6 5 3	12. 10.	74.4 11.4E -3 089 98 12 -11 5,5 2	74.9 13.0E -2 087 98 05 -9 5 5,0 5 2	75.0 14.3E -5 112 96 12 -9 8 6,2 4 1	75.0 14.4E -5 118 98 03 -10 8 6,3 5
09.	56.6 00.4E 12 111 96 01 11 12,1 3	56.9 02.3E 13 122 96 09 11 8 12,8 5 3	57.2 04.2E 12 166 96 18 12 2 11,9 5 2	57.4 05.7E 11 192 97 18 10 5 11,4 5 2	13. 10.	75.0 14.7E -6 112 96 09 -10 6,3 1	74.8 16.9E -8 096 98 05 -13 5 3,0 5 2	75.2 18.4E -9 090 97 05 -13 5 3,0 5 2	75.2 19.3E -6 059 98 18 -10 1,2 1
30. 09.	57.7 07.6E 11 218 97 07 8 11,1 2	58.0 09.5E 10 224 98 06 7 4 11,2 5 3	58.0 09.7E 10 218 97 07 7 3 11,3 5	58.1 09.7E 10 198 98 07 6 7 11,4 5 1	14. 10.	75.1 20.2E -6 044 97 12 -7 0,8 1	75.1 21.5E -7 022 98 18 -7 8 0,2 5 1	75.0 23.0E 5 986 97 22 -6 8 -0,3 5 1	74.9 25.1E -1 934 97 10 -5 0,8 1
01. 10.	58.1 09.7E 9 183 98 08 4 11,1	58.1 09.7E 8 145 97 23 4 6 10,3 5 1	58.0 09.7E 8 125 98 19 3 7 10,1 5	58.1 09.7E 10 095 98 09 3 6 10,1 5	15. 10.	74.9 25.6E -3 955 97 09 -5 1,0 1	75.2 26.0E -4 950 96 08 -6 8 1,5 4 1	75.1 26.7E -5 989 93 23 -8 6 2,1 4 1	75.2 27.3E -5 000 97 07 -9 8 2,2 5 1
02. 10.	58.1 09.7E 8 092 97 07 5 10,0.	58.1 09.7E 8 075 97 06 5 7 9,5 5	58.0 08.8E 9 072 97 06 6 5 11,0 5 2	58.1 06.2E 10 045 97 05 6 8 10,9 5 3	16. 10.	75.2 27.6E -5 988 98 05 -9 3,2 1	75.1 28.0E -7 030 97 12 -13 8 3,2 5 1	74.5 26.6E -8 052 95 22 -12 8 3,9 5 2	73.9 25.9E -7 073 96 07 -12 5,0 2
03. 10.	58.6 04.1E 11 051 96 01 8 11.6 3	59.0 01.9E 11 042 97 05 8 8 11,4 5 3	59.4 00.1W 11 031 97 07 9 8 11,0 5 3	59.8 02.1W 11 997 95 06 9 5 10,8 5 3	17. 10.	74.0 25.9E -7 074 97 03 -11 4,9 2	74.6 26.9E -8 060 97 08 -14 5 4,0 5 2	74.9 27.3E -7 060 97 00 -12 8 2,2 5 2	74.9 27.6E -8 053 97 03 -14 8 2,2 5 1
04. 10.	60.2 04.1W 10 970 97 13 9 11,1 2	60.4 04.7W 10 955 96 05 9 8 9,9 4 1	60.5 05.3W 9 956 97 03 8 7,9 9,6 5 1	60.5 04.9W 8 963 97 06 7 8 9,6 5 1	18. 10.	74.9 27.5E -8 050 97 02 -12 2,5 1	74.9 27.5E -9 051 96 03 -13 8 2,2 4	74.9 27.6E -8 048 97 04 -14 8 2,3 5	74.9 27.6E -9 038 95 02 -14 8 2,2 3
05. 10.	60.4 04.6W 9 972 95 13 9 9,8 1	60.4 04.9W 8 997 97 12 7 8 9,5 5	60.4 04.7W 7 029 98 012 6 8 9,7 5 1	60.5 04.8W 6 055 98 12 2 8 9,3 5 1	19. 10.	74.9 27.6E -9 048 97 02 -13 2,1	74.9 27.5E -8 059 98 06 -13 7 2,2 5	74.9 27.5E -8 080 94 11 -11 8 2,2 3	75.0 27.6E -9 081 94 00 -12 8 3,1 4 1
06. 10.	60.9 05.4W 6 076 98 12 0 9,0 2	61.4 06.1W 6 122 98 30 1 7 9,3 5 2	62.0 06.7W 7 170 98 18 -2 6 9,0 5 2	62.0 06.8W 6 179 98 05 -1 8,9	20. 10.	75.8 27.8E -13 097 97 12 -15 -0,2 2	75.5 27.0E -7 099 97 04 -11 8 1,2 4 2	74.2 26.4E -8 099 93 03 -11 8 4,3 3 2	73.4 23.3E -6 129 94 03 -9 8 5,2 4 2
07. 10.	62.0 06.8W 5 184 98 04 1 8,9.	62.0 06.8W 6 189 98 04 1 3 8,9 5	62.0 06.7W 7 183 98 07 -1 6 8,9 5 1	62.6 05.9W 7 200 98 09 3 6 9,1 5 2	21. 10.	72.4 21.0E -3 167 97 21 -3 5,6 2	71.4 19.0E -1 204 98 17 -8 6 6,4 5 2	70.4 17.0E 2 238 98 08 -5 6 6,6 5 2	69.5 15.1E 95 08 0 8 6,6 4 3
08. 10.	63.4 05.3W 5 184 98 01 -1 7,7 2	63.8 05.0W 6 207 98 07 1 7 7,7 5 1	64.7 04.1W 7 206 98 01 1 3 7,2 5 1	65.7 03.2W 6 203 98 01 1 7,1 1	22. 10.	68.7 13.5E 4 261 98 03 0 7,2 2	67.8 12.1E 5 267 98 06 1 7 7,8 5 2	66.9 11.0E 5 278 98 00 1 5 7,8 5 2	66.0 10.6E 7 267 98 07 1 8 8,4 5 2
09. 10.	65.8 03.3W 6 200 98 07 1 7,6.	66.2 02.9W 7 191 98 02 5 8 7,6 5 2	67.3 02.1W 7 212 98 09 3 4 8,3 5 3	68.6 01.1W 5 215 98 01 -0 7 8,0 5 3	23. 10.	65.0 10.1E 7 257 98 06 5 8,5 2	64.2 09.6E 5 241 97 05 1 8 8,1 5 2	64.1 09.5E 8 223 97 10 4 8 8,7 5 1	63.9 09.4E 9 194 97 17 4 6 8,4 4 1
10. 10.	69.5 00.4W 4 212 98 02 -2 7,7.	70.0 00.0 3 204 98 08 -1 6 7,5 5	70.0 00.1W 3 218 98 09 -3 3 7,9 5 1	70.6 01.3E 1 221 98 02 -4 8 7,8 5 2	24. 10.	64.0 09.5E 7 191 97 05 -2 8,2 1	64.1 09.5E 5 171 97 15 1 7 9,1 5 1	63.9 09.4E 4 217 98 19 2 6 8,4 5 1	64.1 09.5E 6 211 97 07 0 8 8,0 5 1
11. 10.	71.4 03.3E -0 214 98 05 -6 7,0 2	72.3 05.1E -0 168 98 26 -7 8 6,9 5 3	73.1 07.7E -1 134 96 18 -2 8 6,7 3 2	73.9 09.8E -1 113 96 11 -5 8 6,3 5 2					

Fig. 92: Weather and meteorological conditions during leg M 26/2.

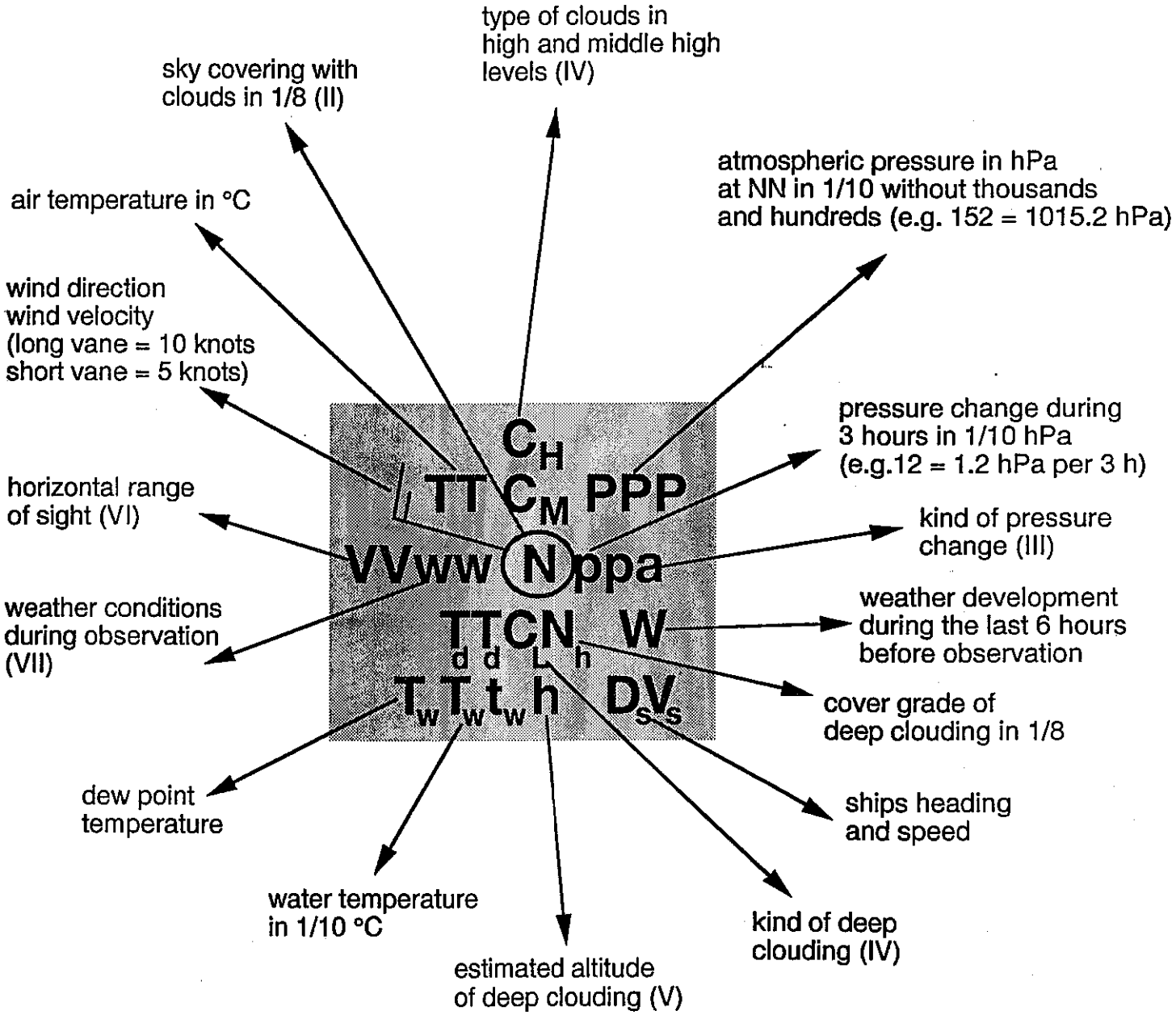

Fig. 92: Legend I

II

N

- cloudless
- 1/8
- 2/8
- 3/8
- 4/8
- 5/8
- 6/8
- 7/8
- 8/8
- covering for meterological reasons not recognizable
- covering not observed

III

a

- inclined, then declined
- inclined, then constant
- constant incline
- declined, then inclined
- constant
- declined, then inclined
- declined, then constant
- constant declined
- inclined, then declined

IV

- Cirrus
- loose Altocumulus
- lenticular Altocumulus
- Stratocumulus
- Stratus
- broken Stratus
- Cumulus
- Cumulonimbus
- Nimbostratus

V

0	0 - 50 m
1	50 - 100 m
2	100 - 200 m
3	200 - 300 m
4	300 - 600 m
5	600 - 1000 m
6	1000 - 1500 m
7	1500 - 2000 m
8	2000 - 2500 m
9	> 2500 m

VI

90	below	0.03 sm	heavy fog
91	from	0.03 sm	
92	from	0.1 sm	
93	from	0.3 sm	weak fog
94	from	0.5 sm	misty
95	from	1.1 sm	
96	from	2.2 sm	steamy
97	from	5.4 sm	good sight
98	from	11.0 sm	very good sight
99	from	27.0 sm	

VII (simplified)

- sand-storm
- snow-storm
- fog
- drizzle
- rain
- snow
- shower
- with or without rainfall
- snow-shower
- snow-rain
- shower in the last hour, but not in time

Fig. 92: Legend II-VII

Islands and Iceland, and reached far into the central North Atlantic Ocean, thereby affecting the area of operation by METEOR. A NE-storm with force between 9-10 developed and persisted for some time during station work. As this situation appeared to be stable, scientific work aboard the vessel was halted and a decision reached to not commence work in the Lousy Banka area, located directly in the path of the strom. Instead Torshavn/Faeroe Islands was reached under strong NE-winds on Oct. 6.

The meteorological situation had changed little by 7 October when METEOR began a long transit to eventually head for 75°N/13°E. However, during the transit the pressure gradients diminished and hence the air flow decreased initially to 7-8 and finally to force 4-5. These conditions did not affect station work on the Iceland-Faeroe Ridge, the Aegir Ridge and the central Norwegian Sea. The more than 1000 km long air stream of Arctic air in soutwesterly direction lowered the air temperature to below freezing and caused repeated strong snow flurries.

During the subsequent work in the area south of Spitsbergen (75°N/13°E to 75°N/28°E) the inflow of Arctic air was maintained between a remarkably stable high over east-central Greenland and several lows moving in easterly or northerly directions from the Spitsbergen/Nowaja Semlja and Scandinavia, respectively. This caused the temperatures to further drop to 9° below freezing and combined with high wind velocities of force 6 accelerated the formation of heavy ice on the structures of the vessel.

This situation escaled dramatically during 14/15 October, when a low pressure cell, originating in the eastern North Sea, developed into a storm over central Sweden and continued to increase further into a very strong storm over northern Norway (958 hPa). Winds of force 12, the maximum speed measured was 70 knots, hit METEOR in transit just 20 nm away from to the final working area on the evening of 14 October and continued well into the following day. The temperatures dropped from -1°C to -4°C and the waves crested at 15 m. The low pressure cell moved slowly in the direction of Nowaja Semlja during the day and winds decreased gradually to force 9 and eventually dropped to force 6 on 16 October; the temperatures continued to decrease to -7°C.

Station work during 17-19 October continued to be affected by Arctic air flow with velocities between Bft 5-7. Temperatures also dropped and reached the lowest value recorded during the cruise of -12.7°C early on 20 October. An attempt to occupy a station around 76°N/27°E had to be abandoned when new ice was encountered; large ice fields with scattered growlers were deemed to dangerous for further work.

Because of renewed severe storm forecast during transit to the final station at 72°N/13°E, the return voyage to Trondheim was begun late during 20 October, 2 days erlier than planned. Initially a slight high pressure cell generated calm seas and increasing temperatures, but storm

warnings had to be posted for the 21/22 October. During the final third of the return leg winds increased steadily and a SW-storm (Bft 9) accompanied the vessel to port in Trondheim.

6.3 Weather and Meteorological Conditions during Leg M 26/3

(H. Ulbricht, D. Bassek)

During the transit from the port of Trondheim to the Norwegian shelf the wind rapidly decreased because we were on the backside of a southeastward moving low pressure cell that came from the Barents Sea. These ideal sea conditions allowed preparation of the equipment on deck and in the laboratories. The continuation of the voyage, however was somewhat delayed by another low pressure cell that passed through our working area. The low arrived on the 29/10 - 30/10 from the Denmark Strait and moved towards the Barents Sea. On the open sea it generated wind intensities of Bft 10-11. Fortunately, METEOR was able to reach shelter at Fröya Island, where winds reached only Bft 9 and in gales Bft 10. Subsequently, a strong high-pressure cell moved in from the southwest and the storm field quickly collapsed. The high pressure cell became stationary above Scandinavia and created nearly ideal weather conditions from 2 to 8 November. Only during the passing of two low pressure fronts the wind intensity increased to Bft 6 and 7 from south to southwest directions.

From 8 to 9 November a gale developed to hurricane force in the Irminger Sea. With still increasing intensities its centre moved towards Iceland. During the morning of 9 November, METEOR reached shelter in the lee of Fröya Island for a second time. On the open sea southwest winds reached Bft 10-11 but behind Fröya only Bft 9. A marginal low-pressure cell above the southern North Sea caused a sudden end to the storm in the morning of 10 November.

Under conditions of Bft 5 - 6, METEOR returned to the Storegga Slide area and therefore sailed to the mooring station NB 7. The south to southwest flowing currents reached ideal water temperatures of 8-6°C. Even north of 75° N, water temperatures were above 0°C. These conditions, however, changed quickly on 13 November at mooring station OG6. Another intensifying low developed over Iceland from a low pressure cell (hurricane force) in the Irminger Sea. This low passed westward from our station towards the north and later to the northeast. As this cold front passed the wind increased to Bft 8-9 blowing from southeast to south. On the back of this cold front cold air invaded from the Arctic with temperatures decreasing to between -1 and -5 ° C, with accompanying heavy snow falls.

When we approached the East Greenland Margin, temperatures decreased to -10 °C, or lower during northwest winds. Unfortunately, the weather changed quickly to give extreme conditions. Because the low-pressure cell pathways from the Atlantic to Europe were blocked by an enormous high-pressure cell over eastern Europe and Scandinavia, the low pressure cells took a northern route over Iceland and our working area. Under the influence of the low

pressure cells we experienced hurricane force winds (16/11: Bft 11) and hurricane force gales (during the night from 18/11.-19/11: Bft > 12, wind speed 93 knts, average wind speed 76 knts). In addition, strong temperature gradients between -12° C and + 2° C, accompanied by snow fall made working conditions even worse. Only quick response during the weather windows, and careful planning, allowed the station work to be completed with success.

7. Lists

7.1 Station list leg M26/1

7.1.1 List of mooring and sampling stations (JGOFS/WOCE)

Date	Station No.	Position latitude	Position longitude	water depth (m)	equipment
30.08. - 31.08	450 (M2)	32°34,3´N	10°03,0´W	2065	CTD, recovery experiment of WOCE mooring M2
01.09.	451	32°15,8´N	16°01,0´W		surface sampling for trace elements with rubber boat
02.09. - 03.09	452 (L1)	33°09,8´N 33°08,5´N	22°00,2´W 21°58,5´W	5317	2 x CTD, 3 x MSN, 2 x PN, MC, GFO, deployment of JGOFS mooring L193
05.09.	453 (W2)	40°29,9´N	20°00,9´W	4950	recovery of German-French acoustic mooring
05.09	454	41°16,9´N	19°59,4´W	4800	GFO
08.09. - 09.09	455 (L2)	47°46,9´N 47°48,0´N	19°46,8´W 19°47,6´W	4568	2 x CTD, 3 x MSN, 2 x PN, MC, deployment of JGOFS mooring L293
10.09. -	456 (F2)	52°22,1´N	16°21,8´W	3484	2 x CTD, 3 x MSN, 2 x PN, GFO, recovery of WOCE mooring F2,
11.09		52°24,1´N	16°22,2´W	3484	deployment of WOCE mooring F2
12.09. - 13.09	457 (L3)	54°39,8´N 54°39,8´N	21°13,0´W 21°13,6´W	3057	2 x CTD, 3 x MSN, 2 x PN, MC, deployment of JGOFS-mooring L393
14.09. -	458 (E2)	54°17,3´N	25°52,5´W	3070	2 x CTD, 3 x MSN, MC, recovery of WOCE mooring E2,
15.09.		54°24,8´N	25°51,7´W	3125	deployment of WOCE mooring E2
16.09.	459 (D2)	57°24,5´N	28°14,7´W	2568	CTD, MSN, MC, recovery experiment of WOCE mooring D2
		57°33,3´N	28°10,4´W	2294	deployment of WOCE mooring D2

List of gears:

CTD = battery water sampler (12 l)
MSN = multi-closing-net
PN = plankton net
GFO = Goflo-water sampler
MC = multicorer

7.1.2. List of surface water sampling stations

(JGOFS; by continous pumping from ca. 7m water depth)

Station	Datum	Latitude	Longitude	T	S	NUT	TM	PC	Chl.a	OPT	SPM	OS	AS
1	24.08.93	35°58,1´ N	13°59,4´ E	x	x	x	x	x	x	x			x
2	25.08.93	36°09,5´ N	13°35,3´ E	x	x	x	x	x	x	x			
3	25.08.93	36°25,6 ´N	13°01,3´ E	x	x	x	x	x	x	x			x
4	25.08.93	36°41,2´ N	12°28,6´ E	x	x	x	x	x	x	x			
5	25.08.93	36°56,2´ N	11°57,0´ E	x	x	x	x	x	x	x			x
6	25.08.93	37°07,5´ N	11°23,4´ E	x	x	x	x	x	x	x			
7	25.08.93	37°21,2´ N	10°48,6´ E	x	x	x	x	x	x	x			x
8	25.08.93	37°32,4´ N	10°14,4´ E	x	x	x	x	x	x	x			
9	25.08.93	37°38,0´ N	09°37,0´ E	x	x	x	x	x	x	x			x
10	25.08.93	37°42,3´ N	09°00,4´ E	x	x	x	x	x	x	x			
11	26.08.93	37°43,2´ N	08°22,7´ E	x	x	x	x	x	x	x	x		x
12	26.08.93	37°38,6´ N	07°44,6´ E	x	x	x	x	x	x	x	x		
13	26.08.93	37°34,1´ N	07°07,3´ E	x	x	x	x	x	x	x	x	x	x
14	26.08.93	37°29,7´ N	06°30,5´ E	x	x	x	x	x	x	x	x	x	
15	26.08.93	37°25,0´ N	05°50,2´ E	x	x	x	x	x	x	x	x	x	x
16	26.08.93	37°20,5´ N	05°13,9´ E	x	x	x	x	x	x	x	x	x	
17	26.08.93	37°16,0´ N	04°38,2´ E	x	x	x	x	x	x	x	x	x	x
18	26.08.93	37°11,5´ N	04°00,1´ E	x	x	x	x	x	x	x	x	x	
19	27.08.93	37°06,9´ N	03°21,7´ E	x	x	x	x	x	x	x	x	x	x
20	27.08.93	37°02,8´ N	02°47,1´ E	x	x	x	x	x	x	x	x	x	
21	27.08.93	36°58,4´ N	02°10,0´ E	x	x	x	x	x	x	x	x	x	x
22	27.08.93	36°53,7´ N	01°31,1´ E	x	x	x	x	x	x	x	x	x	
23	27.08.93	36°48,9´ N	00°54,3´ E	x	x	x	x	x	x	x	x	x	x
24	27.08.93	36°44,1´ N	00°16,1´ E	x	x	x	x	x	x	x	x	x	
25	27.08.93	36°39,6´ N	00°19,9´ W	x	x	x	x	x	x	x	x		x
26	28.08.93	36°35,1´ N	00°55,7´ W	x	x	x	x	x	x	x	x		
27	28.08.93	36°29,9´ N	01°37,7´ W	x	x	x	x	x	x	x	x		
28	28.08.93	36°25,9´ N	02°12,4´ W	x	x	x	x	x	x	x	x	x	x
30	28.08.93	36°16,6´ N	03°23,8´ W	x	x	x	x	x	x	x	x	x	x
31	28.08.93	36°12,0´ N	04°00,5´ W	x	x	x	x	x	x	x	x	x	x
32	28.08.93	36°06,9´ N	04°26,5´ W	x	x	x	x	x	x	x	x	x	
33	28.08.93	36°02,7´ N	05°14,1´ W	x	x	x	x	x	x	x	x	x	x
34	29.08.93	35°57,6´ N	05°50,0´ W	x	x	x	x	x	x	x	x		x
35	29.08.93	35°49,7´ N	06°25,3´ W	x	x	x	x	x	x	x	x		
36	29.08.93	35°27,8´ N	06°48,1´ W	x	x	x	x	x	x	x			x
39	29.08.93	34°14,9´ N	08°06,4´ W	x	x	x	x	x	x	x	x	x	x
40	29.08.93	33°35,7´ N	08°06,8´ W	x	x	x	x	x	x	x	x	x	
41	29.08.93	33°35,9´ N	08°47,8´ W	x	x	x	x	x	x	x	x	x	
42	29.08.93	33°12,5´ N	09°12,6´ W	x	x	x	x	x	x	x	x	x	
43	30.08.93	32°50,7´ N	09°35,4´ W	x	x	x	x	x	x	x		x	
44	30.08.93	32°18,2´ N	09°59,0´ W	x	x	x	x	x	x	x			x
45	31.08.93	32°23,8´ N	10°22,8´ W	x	x	x	x	x	x	x	x		
46	31.08.93	32°23,0´ N	10°57,8´ W	x	x	x	x	x	x	x	x	x	x
47	31.08.93	32°22,0´ N	11°33,4´ W	x	x	x	x	x	x	x	x	x	
48	31.08.93	32°21,1´ N	12°12,2´ W	x	x	x	x	x	x	x	x	x	x

49	31.08.93	32°20,1´ N	12°48,5´ W	x	x	x	x	x	x	x	x	x		
50	01.09.93	32°19,6´ N	13°18,4´ W	x	x	x	x	x	x	x	x	x	x	x
51	01.09.93	32°18,7´ N	13°54,6´ W	x	x	x	x	x	x	x		x		
52	01.09.93	32°17,9´ N	14°30,8´ W	x	x	x	x	x	x	x		x	x	
53	01.09.93	32°17,0´ N	15°06,7´ W	x	x	x	x	x	x	x		x		
54	01.09.93	32°16,2´ N	15°41,6´ W	x	x	x	x	x	x	x	x	x	x	
55	01.09.93	32°14,7´ N	16°16,9´ W	x	x	x	x	x	x	x	x	x		
56	01.09.93	32°18,4´ N	16°54,9´ W	x	x	x	x	x	x	x	x	x	x	
57	01.09.93	32°22,6´ N	17°26,5´ W	x	x	x	x	x	x	x	x	x		
58	01.09.93	32°27,8´ N	18°03,3´ W	x	x	x	x	x	x	x	x	x	x	
59	02.09.93	32°38,5´ N	18°39,4´ W	x	x	x	x	x	x	x	x	x		
60	02.09.93	32°37,8´ N	19°12,2´ W	x	x	x	x	x	x	x	x	x	x	
61	02.09.93	32°44,8´ N	19°48,3´ W	x	x	x	x	x	x	x	x	x		
62	02.09.93	32°52,0´ N	20°26,6´ W	x	x	x	x	x	x	x	x	x	x	
63	02.09.93	32°57,3´ N	20°55.0´ W	x	x	x	x	x	x	x		x		
64	02.09.93	33°04,0´ N	21°30,1´ W	x	x	x	x	x	x	x		x	x	
65	03.09.93	33°35,9´ N	21°53,9´ W	x	x	x	x	x	x	x		x		
66	04.09.93	34°04,5´ N	21°46,2´ W	x	x	x	x	x	x	x		x	x	
67	04.09.93	34°34,0´ N	21°38,2´ W	x	x	x	x	x	x	x		x		
68	04.09.93	35°05,9´ N	21°30,1´ W	x	x	x	x	x	x	x	x	x	x	
69	04.09.93	35°32,5´ N	21°22,7´ W	x	x	x	x	x	x	x	x	x		
70	04.09.93	36°02,9´ N	21°14,7´ W	x	x	x	x	x	x	x	x		x	
71	04.09.93	36°31,2´ N	21°06,9´ W	x	x	x	x	x	x	x	x			
72	04.09.93	37°01,1´ N	20°58,9´ W	x	x	x	x	x	x	x	x		x	
73	04.09.93	37°30,8´ N	20°50,7´ W	x	x	x	x	x	x	x	x			
74	04.09.93	37°58,9´ N	20°43,4´ W	x	x	x	x	x	x	x	x		x	
75	05.09.93	38°28,4´ N	20°34,9´ W	x	x	x	x	x	x	x	x			
76	05.09.93	38°57,7´ N	20°16,9´ W	x	x	x	x	x	x	x			x	
77	05.09.93	39°27,0´ N	20°18,6´ W	x	x	x	x	x	x	x			x	
78	05.09.93	39°57,7´ N	20°09,7´ W	x	x	x	x	x	x	x			x	
79	05.09.93	40°25,6´ N	20°02,0´ W	x	x	x	x	x	x	x	x	x		
80	05.09.93	41°02,9´ N	19°59,0´ W	x	x	x	x	x	x	x	x	x	x	
81	05.09.93	41°29,9´ N	19°59,3´ W	x	x	x	x	x	x	x	x	x		
82	06.09.93	41°57,7´ N	19°58,3´ W	x	x	x	x	x	x	x	x	x	x	
83	06.09.93	42°27,9´ N	19°57,3´ W	x	x	x	x	x	x	x		x		
84	06.09.93	42°57,3´ N	19°56,4´ W	x	x	x	x	x	x	x		x	x	
85	06.09.93	43°29,2´ N	19°55,3´ W	x	x	x	x	x	x	x		x		
86	06.09.93	43°29,2´ N	20°28,4´ W	x	x	x	x	x	x	x		x	x	
87	06.09.93	44°24,6´ N	20°28,4´ W	x	x	x	x	x	x	x				
88	07.09.93	44°54,1´ N	20°40,3´ W	x	x	x	x	x	x	x			x	
89	07.09.93	45°23,8´ N	20°50,3´ W	x	x	x	x	x	x	x		x		
90	07.09.93	45°53,8´ N	20°49,1´ W	x	x	x	x	x	x	x		x	x	
91	07.09.93	46°23,9´ N	20°37,0´ W	x	x	x	x	x	x	x		x		
92	07.09.93	46°51,2´ N	20°19,5´ W	x	x	x	x	x	x	x		x	x	
93	08.09.93	47°18,7´ N	19°58,4´ W	x	x	x	x	x	x	x	x	x		
94	09.09.93	48°00,7´ N	19°38,7´ W	x	x	x	x	x	x	x	x		x	
95	09.09.93	48°28,4´ N	19°18,6´ W	x	x	x	x	x	x	x	x	x		
96	09.09.93	48°56,8´ N	18°58,1´ W	x	x	x	x	x	x	x	x	x	x	
97	09.09.93	49°23,9´ N	18°38,4´ W	x	x	x	x	x	x	x	x	x		
98	10.09.93	49°50,7´ N	18°18,2´ W	x	x	x	x	x	x	x	x	x	x	
99	10.09.93	50°15,3´ N	17°59,4´ W	x	x	x	x	x	x	x	x	x		

100	10.09.93	50°44,2´ N	17°38,1´ W	x	x	x	x	x	x	x	x	x	x
101	10.09.93	51°11,8´ N	17°17,0´ W	x	x	x	x	x	x	x	x		
102	10.09.93	51°37,9´ N	16°56,8° W	x	x	x	x	x	x	x	x		x
103	10.09.93	52°04,2´ N	16°36,2´ W	x	x	x	x	x	x	x	x		
104	11.09.93	52°40,0´ N	16°58,7´ W	x	x	x	x	x	x	x	x		x
105	11.09.93	52°58,8´ N	17°38,8´ W	x	x	x	x	x	x	x	x	x	
106	12.09.93	53°17,5´ N	18°19,7´ W	x	x	x	x	x	x	x	x	x	x
107	12.09.93	53°35,1´ N	18°55,8´ W	x	x	x	x	x	x	x		x	
108	12.09.93	53°53,4´ N	19°38,3´ W	x	x	x	x	x	x	x	x	x	x
109	12.09.93	54°11,9´ N	20°18,8´ W	x	x	x	x	x	x	x	x	x	x
110	12.09.93	54°31,1´ N	20°58,4´ W	x	x	x	x	x	x	x	x	x	
111	13.09.93	54°37,6´ N	21°38,9´ W	x	x	x	x	x	x	x	x		x
112	13.09.93	54°33,2´ N	22°32,2´ W	x	x	x	x	x	x	x	x	x	
113	13.09.93	54°29,8´ N	23°24,3´ W	x	x	x	x	x	x	x	x	x	x
114	13.09.93	54°25,0´ N	24°14,1´ W	x	x	x	x	x	x	x	x	x	
115	13.09.93	54°20,0´ N	25°04,9´ W	x	x	x	x	x	x	x	x	x	x
116	15.09.93	54°54,1´ N	26°15,1´ W	x	x	x	x	x	x	x	x	x	
117	15.09.93	55°25,9´ N	26°39,4´ W	x	x	x	x	x	x	x	x	x	x
119	15.09.93	56°17,2´ N	27°19,5´ W	x	x	x	x	x	x	x	x	x	
120	15.09.93	56°44,1´ N	27°40,8´ W	x	x	x	x	x	x	x		x	x
121	16.09.93	57°11,6´ N	28°02,9´ W	x	x	x	x	x	x	x	x	x	
122	16.09.93	57°40,5´ N	29°05,3´ W	x	x	x	x	x	x	x	x	x	x
123	17.09.93	57°53,7´ N	29°50,4´ W	x	x	x	x	x	x	x	x	x	
124	17.09.93	58°09,2´ N	30°42,8´ W	x	x	x	x	x	x	x	x	x	x
125	17.09.93	58°22,2´ N	31°26,2´ W	x	x	x	x	x	x	x	x	x	x
126	18.09.93	58°21,0´ N	28°03,8´ W	x	x	x	x	x	x			x	
127	18.09.93	58°21,8´ N	27°07,7´ W	x	x	x	x	x	x				x
128	18.09.93	58°22,7´ N	26°07,0´ W	x	x	x	x	x	x				
129	18.09.93	58°23,3´ N	25°10,3´ W	x	x	x	x	x	x				x
130	18.09.93	58°24,5´ N	24°13,6´ W	x	x	x	x	x	x				
131	19.09.93	58°25,1´ N	23°17,3´ W	x	x	x	x	x	x				x
132	19.09.93	58°26,0´ N	22°13,5´ W	x	x	x	x	x					
133	19.09.93	58°26,7´ N	21°21,1´ W	x	x	x	x	x	x				x
134	19.09.93	58°27,6´ N	20°24,6´ W	x	x	x	x	x	x				
135	19.09.93	58°28,5´ N	19°27,9´ W	x	x	x	x	x	x				x
136	19.09.93	58°29,4´ N	18°27,8´ W	x	x	x	x	x	x				
137	19.09.93	58°30,3´ N	17°30,3´ W	x	x	x	x	x	x				
138	19.09.93	58°31,2´ N	16°36,7´ W	x	x	x	x	x	x				
139	20.09.93	58°31,9´ N	15°39,0´ W	x	x	x	x	x	x				
140	20.09.93	58°32,7´ N	14°40,9´ W	x	x	x	x	x	x				
141	20.09.93	58°33,6´ N	13°44,2´ W	x	x	x	x	x	x				
142	20.09.93	58°34,6´ N	12°45,7´ W	x	x	x	x	x	x				
143	20.09.93	58°35,5´ N	11°47,9´ W	x	x	x	x	x	x				
144	20.09.93	58°36,0´ N	10°46,0´ W	x	x	x	x	x	x				
145	20.09.93	58°36,9´ N	09°51,7´ W	x	x	x	x	x	x				
146	20.09.93	58°37,7´ N	08°56,1´ W	x	x	x	x	x	x				
147	21.09.93	58°38,6´ N	07°57,4´ W	x	x	x	x	x	x				
148	21.09.93	58°39,3´ N	06°59,1´ W	x	x	x	x	x	x				
149	21.09.93	58°40,2´ N	06°03,0´ W	x	x	x	x	x	x				

150	21.09.93	58°42,1´N	05°04,6´W	x	x	x	x	x	x				
151	21.09.93	58°42,0´N	04°06,4´W	x	x	x	x	x	x				
152	21.09.93	58°42,9´N	03°08,1´W	x	x	x	x	x	x				
153	21.09.93	58°20,1´N	02°32,5´W	x	x	x	x	x	x				
154	22.09.93	57°55,9` N	01°59,7´W	x	x	x	x	x	x				
155	22.09.93	57°30,2´N	01°24,9´W	x	x	x	x	x	x				
156	22.09.93	57°02,2´N	01°24,0´W	x	x	x	x	x	x				
157	22.09.93	56°44,3´N	01°24,5´W	x	x	x	x	x	x				

T = water temperature
S = salinity
NUT = nutrients
TM = trace elements
PC = POC/PON

Chl.a = chlorophyll a
OPT = fluorescence
SPM = suspended part. material
OS = organic acids
AS = amino acids

7.2 Leg M26/2

7.2.1 List of Stations

Station - No. METEOR	Date 1993	Device Profile	Time (UTC) from Deck	at Depth	on Deck	Geographic Position Latitude °N	Longitude °E	Water depth (m)	Wire-length (m)	Penetration Depth/ Recovery (cm/cm)	Remarks
460-1	30.9.	TV-MUC		09:39		58°02.935	09°38.670	336		55-58	
460-2		MUC		10:51		58°02.800	09°38.000	324		60	
460-3		MUC		11:28		58°02.711	09°38.385	312		47-55	
460-4		GKG		12:34		58°02.807	09°38.092	320		50	
460-5		GKG		13:24		58°02.769	09°38.039	320		0	
460-6		GKG		13:46		58°02.773	09°38.990	319		53	
460-7		CTD		14:39		58°02.605	09°39.791	304			no T-S-recording
461-1		SISS	from	18:47		58°03.510	09°41.160				
			until	19:22		58°02.300	09°38.300				
461-2		SISS	from	19:48		58°02.560	09°38.100				
			until	20:45		58°03.750	09°40.900				
461-3		SISS	from	20:55		58°03.973	09°40.759				
			until	21:32		58°02.700	09°37.800				
461-4		SISS	from	22:23		58°02.202	09°36.026				
			until	23:30		58°04.500	09°41.500				
461-5	1.10.	SISS	from	01:42		58°04.567	09°35.699				
			until	02:45		58°04302	09°39.113				
461-6		SISS	from	03:45		58°04.302	09°39.113				
			until	04:17		58°03.040	09°41.266				
461-7		SISS	from	05:32		58°04.138	09°39.194				
			until	05:52		58°03.373	09°40.492				
462-1		MEDUSA	from	12:30		58°02.100	09°46.000				
			until	13:40		58°02.400	09°36.400				
463-1		CTD		14:01		58°02.973	09°39.116	336			Bottles were not closed
463-2		CTD		15:41		58°02.813	09°39.195	321	300		
	Sampling intervals:		25m, 50m, 75m, 100m, 200m, 250m, 275m, 300m, 315m								
463-3		SL		17:39		58°03.105	09°39.462	332		573	no surface
464-1		SL		18:45		58°02.702	09°37.697	336		550	
465-1		CTD		20:13		58°03.326	09°40.822	327	300		
	Sampling intervals:		25m, 50m, 75m, 100m, 150m, 200m, 250m, 275m, 300m, 307m								
466-1		CTD		21:29		58°03.699	09°40.167	352	342		
	Sampling intervals:		25m, 50m, 75m, 100m, 150m 200m, 250m, 275m, 300m, 320m, 342m								
467-1		CTD		22:54		58°03.576	09°39.027	362	355		
	Sampling intervals:		25m, 50m, 75m, 100m, 150m 200m, 250m, 300m, 325m, 355m								
467-2		ISP		23:35		58°03.661	09°39.104	368	100		
468-1	2.10.	MUC		04:30		58°03.154	09°39.505	335		60	
468-2		GKG		05:21		58°03.148	09°39.507	334		55	
468-3		GKG		05:59		58°03.146	09°39.431	334		48	
469-1		GKG		07:01		58°02.635	09°37.914	332		45	
469-2		GKG		07:38		58°02.582	09°37.688	328		55	
470-1	4.10.	SISS	from	02:30		60°19.866	04°27.413W	643			
			until	10:27		60°32.221	05°11.541W	808			
470-2		CTD		13:10		60°29.488	05°08.541W	1021	1011		
	Sampling intervals:		500m, 550m, 600m, 650m, 700m, 750m, 800m, 850m, 900m, 925m, 950m, 980m, 990m, 1000m, 1005m, 1011m								
471-1		DTBS	from	16:26		60°25.000	04°55.500W				HS, PS
			until	17:12		60°27.500	04°52.900W				
471-2		DTBS	from	18:45		60°26.200	04°54.400W				HS, PS
			until	21:09		60°22.100	04°36.800W				
472-1	5.10.	CTD		01:26		60°25.908	04°54.250W	993	960		
	Sampling intervals:		15m, 25m, 50m, 75m, 100m, 125m, 250m, 500m, 600m, 700m, 750m, 800m, 900m, 950m, 960m								
473-1		ISP		02:24		60°25.901	04°54.301W	994	200		
474-1		MUC		06:29		60°26.013	04°54.481W	991		28	
474-2		GKG		07:34		60°26.024	04°54.478W	993		30	
474-3		GKG		08:28		60°26.119	04°54.589W	1012		35	
474-4		GKG		09:45		60°26.324	04°54.163W	1018		20	
475-1		GKG		11:06		60°23.859	04°45.424W	983		25	
475-2		GKG		12:01		60°23.695	04°44.259W	984		35	
476-1	8.10.	CTD		03:55		63°45.068	05°00.040W	2901	2850		
	Sampling intervals:		8m, 43m, 68m, 93m, 150m, 300m, 600m, 1000m, 1500m, 2000m, 2500m, 2850m,								
477-1		CTD		19:53		65°49.404	03°16.415W	2291	2285		
	Sampling intervals:		8m, 18m, 33m, 42m, 75m, 100m, 150m, 200m, 300m, 600m, 1000m, 1500m, 2000m, 2265m								
477-2		RSN		22:29		65°49.769	03°18.834W	2326	1000		
477-3		RSN		23:57		65°50.033	03°19.220W	2301	500		failure
477-4	9.10.	RSN		00:30		65°50.183	03°19.425W	2378	500		
477-5		RSN		01:20		65°50.462	03°19.662W	2612	100		

Station - No. METEOR	Date 1993	Device Profile	Time (UTC) from Deck	at Depth	on Deck	Geographic Latitude °N	Position Longitude °E	Water depth (m)	Wire-length (m)	Penetration Depth/ Recovery (cm/cm)	Remarks
477-6		GKG		02:54		65°49.393	03°16.125W	2275		35	
478-1	10.10.	CTD		03:31		70°00.000	00°00.006W	3297			
	Sampling intervals:			15m, 25m, 50m, 100m, 150m, 200m, 500m, 1000m, 1500m, 1700m, 2000m, 2300m, 2500m, 2800m, 3000m, 3238m							
478-2		RSN		06:00		70°00.005	00°00.116W	3297	1000		
478-3		RSN		06:59		70°00.084	00°00.069W	3298	500		
478-4		RSN		07:34		70°00.054	00°00.151W	3301	100		
478-5		ISP		08:16		70°00.037	00°01.281W	3300	100		
478-6		GKG		11:43		70°00.335	00°03.793W	3296		50	
479-1	12.10.	PS	from	07:09		74°58.967	13°20.332				
			until	10:25		74°59.000	14°55.000				
480-1		CTD		12:40		74°59.114	14°22.532	1589	1564		
	Sampling intervals:			15m, 50m, 100m, 250m, 750m, 1000m, 1480m, 1530m, 1564m							
480-2		ISP		14:32		74°59.218	14°22.192	1582	1500		
480-3		RN		16:58		74°59.345	14°22.358				Mistake at deployment
480-4		MN		17:48		74°59.974	14°22.449	1542	1000		
480-5		GKG		20:10		74°59.055	14°22.032	1600		43	
480-6		GKG		22:00		74°59.025	14°22.600	1607		43	
481-1	13.10.	CTD		05:49		74°50.940	16°56.943	308	300		
	Sampling intervals:			20m, 25m, 50m, 80m, 100m, 120m, 150m, 170m, 200m, 230m, 250m, 280m, 291m							
481-2		GWS		06:50		74°51.014	16°57.245	308	120		
482-1		TV		12:51		75°13.816	18°38.085	25			
482-2		BG		13:08		75°13.828	18°38.103	25			10 times
483-1		TV		13:59		75°13.926	18°43.840	25			
483-2		BG		14:18		75°13.897	18°43.660	25			10 times
484-1		TV		15:06		75°13.916	18°49.624	25			connector failure
484-2		BG		15:16		75°13.916	18°49.621	25			10 times
485-1		TV		16:17		75°10.980	19°00.173	25			
485-2		BG		16:25		75°10.952	18°59.617	28			10 times
486-1		TV		20:44		75°07.651	19°49.356	42			
486-2		BG		21:13		75°08.289	19°49.450	42			10 times
487-1	14.10.	BG		11:29		75°02.031	22°57.806	104			9 times
488-1	17.10.	DTBS	from	11:57		74°53.100	27°24.600				
			until	13:10		74°55.300	27°40.000				
488-2		DTBS	from	13:46		74°54.100	27°40.00				
			until	14:41		74°56.200	27°30.000				
488-3		DTBS	from	15:15		74°54.700	27°32.000				
			until	15:48		74°55.500	27°40.000				
489-1		GKG		17:58		74°55.351	27°33.770	358		15-23	
489-2		GKG		18:58		74°55.347	27°33.783	351		empty	
490-1		CTD		19:15		74°55.597	27°33.728	340	321		
	Sampling intervals:			15m, 50m, 100m, 200m, 225m, 250m, 275m, 300m, 321m							
491-1		HS-PS	from	20:45		74°56.000	27°34.000				
			until	21:20		75°00.000	27°33.600				
491-2		HS-PS	from	21:35		75°00.000	27°33.300				
			until	22:12		74°55.500	27°34.000				
491-3		HS-PS	from	22:26		74°55.000	27°34.00				
			until	23:07		75°00.000	27°20.900				
491-4		HS-PS	from	23:13		74°59.900	27°20.000				
			until	23:54		74°54.500	27°34.000				
491-5	18.10.	HS-PS	from	00:04		74°54.000	27°34.000				
			until	00:39		74°58.000	27°23.700				
491-6		HS-PS	from	00:47		74°58.000	27°22.400				
			until	01:23		74°53.600	27°34.000				
491-7		HS-PS	from	01:31		74°53.100	27°34.000				
			until	02:24		74°58.000	27°21.100				
491-8		HS-PS	from	02:26		74°58.000	27°20.000				
			until	03:06		74°52.600	27°34.000				
491-9		HS-PS	from	03:17		74°51.100	27°34.000				
			until	04:13		74°57.500	27°20.000				
491-10		HS-PS	from	04:21		74°57.000	27°20.000				
			until	05:01		74°52.000	27°22.900				
491-11		HS-PS	from	05:11		74°52.000	27°31.700				
			until	05:54		74°56.500	27°20.000				
491-12		HS-PS	from	06:02		74°56.100	27°20.000				
			until	06:33		74°52.000	27°30.400				
491-13		HS-PS	from	07:14		74°52.000	27°29.100				
			until	07:45		74°55.600	27°19.600				
492-1		CTD		08:23		74°54.365	27°39.133	347	350		5 bottles did not close
492-2		CTD		09:03		74°54.227	27°39.130	353	344		
	Sampling intervals:			15m, 50m, 100m, 200m, 250m, 270m, 290m, 310m, 325m, 344m							
492-3		MUC		10:06		74°54.203	27°39.000	351		18	1 tube filled
492-4		MUC		10:27		74°54.212	27°39.178	351		18-23	

Station - No. METEOR	Date 1993	Device Profile	Time (UTC) from Deck	Time (UTC) at Depth	Time (UTC) on Deck	Geographic Position Latitude °N	Geographic Position Longitude °E	Water depth (m)	Wire-length (m)	Penetration Depth/ Recovery (cm/cm)	Remarks
492-5		GKG		11:20		74°54.228	27°39.214	356		49	
492-6		GKG		12:01		74°54.279	27°39.179	352		empty	
492-7		GKG		12:42		74°54.269	27°39.131	356		25	
492-8		GKG		13:17		74°54.215	27°39.200	358		38-45	
493-1		CTD		14:19		74°55.057	27°34.948	347	353		
		Sampling intervals:		15m, 50m, 100m, 200m, 250m, 275m, 300m, 320m, 340m, 354m							
493-2		VESP				74°54.996	27°34.749	325			
494-1	19.10.	VESP				74°57.000	27°36.000				
495-1		VESP				74°55.600	27°32.500				
496-1		CTD		06:43		74°55.300	27°31.496	345	339		
		Sampling intervals:		15m, 50m, 100m, 200m, 250m, 275m, 300m, 325m, 339m							
496-2		GKG		07:38		74°55.259	27°31.601	370		15	
496-3		GKG		08:32		74°55.434	27°32.421	356		30	
496-4		GKG		09:10		74°55.506	27°32.316	351			
496-5		GKG		09:52		74°55.505	27°32.201	349		25	
496-6		GKG		10:35		74°55.486	27°32.211	340			washed out
496-7		MUC		11:31		74°55.508	27°32.372	359			frozen
496-8		MUC		12:31		74°55.531	27°32.527	356		25	
497-1		MUC		13:15		74°55.720	27°31.654	341		20	
497-2		MUC		13:48		74°55.787	27°31.489	342		30	
497-3		GKG		14:35		74°55.785	27°31.575	341		35	
497-4		GKG		15:08		74°55.793	27°31.636	340		empty	
497-5		GKG		15:50		74°55.852	27°31.764	340		38	
498-1		CTD		16:50		74°57.000	27°35.900	340	339		
		Sampling intervals:		15m, 50m, 100m, 200m, 250m, 275m, 300m, 315m, 335m							
499-1		CTD		23:32		75°45.000	27°47.700	261			0 - 60m no CTD-Data
		Sampling intervals:		15m, 25m, 50m, 75m, 100m, 150m, 200m, 220m, 230m, 241m							

7.3 Leg M26-3

7.3.1 List of Stations

Station Meteor 1993	Number GPI	Date	Device	Time UTC (+1h)	Geographical Position Latitude Longitude	Water depth uncorrected (m)	Wire length (m)	Comments
500		28.10.	HS+PS	20.50	64°21,3´N 008°22,2´E	280		Profile start 500-1
				21.06	64°22,2´N 008°18,6´E	278		Profile end 500-1
				21.20	64°22,2´N 008°18,6´E	274		Profile start 500-2
				21.56	64°19,8´N 008°26,4´E	311		Profile end 500-2
				22.59	64°15,9´N 008°15,6´E	364		Profile start 500-3
				23.55	64°20,4´N 008°02,4´E	313		Profile end 500-3
		29.10.	HS+PS	00.35	64°15,0´N 007°58,8´E	287		Profile start 500-4
				01.00	64°12,9´N 008°04,8´E	375		Profile end 500-4
				01.35	64°12,0´N 008°15,6´E	308		Profile start 500-5
				03.10	64°19,8´N 007°53,4´E	283		Profile end 500-5
				03.47	64°24,0´N 008°01,5´E	232		Profile start 500-6
				05.19	64°16,2´N 008°24,0´E	367		Profile end 500-6
501			VC	08.47	64°20,7´N 008°23,7´E	287	291	Bottom contact, Failure
	23490-2		VC	10.04	64°20,7´N 008°23,7´E	288	284	Bottom contact
502	23491-1		VC	12.42	64°21,6´N 008°21,4´E	277	273	Bottom contact
503			VC	15.03	64°18,1´N 008°09,5´E	283	280	Bottom contact, Failure
			VC	16.08	64°18,3´N 008°09,4´E	282	280	Bottom contact, Failure
	23492-3		VC	17.40	64°18,1´N 008°09,7´E	283	280	Bottom contact
504	23495-1		VC	19.48	64°18,4´N 008°09,1´E	283	295	Bottom contact
505	23496-1		VC	21.26	64°17,3´N 008°12,3´E	333	335	Bottom contact
506			HS+PS	23.11	64°17,7´N 008°25,8´E	346		Profile start 506-1
		30.10.		02.39	64°28,5´N 007°54,6´E	300		Profile end 506-1
				03.10	64°26,4´N 007°50,4´E	234		Profile start 506-2
				05.15	64°15,4´N 008°21,6´E	363		Profile end 506-2
				05.44	64°13,5´N 008°18,0´E	350		Profile start 506-3
				07.19	64°21,0´N 007°55,8´E	280		Profile end 506-3
				08.00	64°18,5´N 007°52,8´E	298		Profile start 506-4

Station Meteor 1993	Number GPI	Date	Device	Time UTC (+1h)	Geographical Position Latitude Longitude	Water depth uncorrected (m)	Wire length (m)	Comments
				09.27	64°11,4´N 008°13,8´E	353		Profile end 506-4
507		01.11.	HS+PS	08.59	64°40,0´N 004°37,0´E	1050		Profile start 507
				09.33	64°44,0´N 004°27,0´E	980		Profile end 507
508			PP	10.22	64°44,3´N 004°26,4´E			Test on the wire
509	23497-1		SL(12)	13.43	64°44,0´N 004°27,1´E	947	974	Core recovery 8.92 m
	23497-2		SL(6)	14.46	64°44,0´N 004°26,9´E	961	980	Core recovery 5.74 m
510			PP1	17.40	64°44,0´N 004°27,0´E			PP in the water
511			DTBS+	22.12	64°52,8´N 005°52,8´E	378		Profile start 511-1
		02.11.	HS+PS	04.45	64°42,3´N 004°48,0´E	862		Profile end 511-1
				04.45	64°42,3´N 004°48,0´E	862		Profile start 511-2
				13.08	64°59,1´N 003°30,0´E	1429		Profile end 511-2
512			MG	14.58	64°57,0´N 003°32,1´E	1455	1431	Bottom contact
				15.28	64°56,8´N 003°31,6´E	1468	1439	Bottom contact
				15.58	64°56,6´N 003°31,2´E	1480	1445	Bottom contact
513	23498-1		SL(12)	18.13	64°57,0´N 003°31,9´E	1442	1434	Core recovery *
514			PP2	19.20	64°57,0´N 003°32,2´E	1454		PP located /on deck
515			CTD	19.39	64°57,0´N 003°32,3´E	1460	550	Test
516			DTBS+	21.14	64°57,0´N 003°30,0´E	1462		Profile start 516-1
		03.11.	HS+PS	05.26	64°40,3´N 004°48,0´E	941		Profile end 516-1
				05.26	64°40,3´N 004°48,0´E	941		Profile start 516-2
				10.50	64°49,0´N 005°24,0´E	492		Profile end 516-2
517	23499-1		SL(12)	12.20	64°46,3´N 005°24,0´E	645	635	Core recovery 5.37 m
518	23500-1		SL(12)	14.54	64°43,4´N 004°55,0´E	804	789	Core recovery 8.26 m
519			OBH	15.42	64°43,7´N 004°55,2´E			Test on the wire
			Hyd	15.36	64°43,7´N 004°55,2´E			Hydrophon release test
			OBH	17.04	64°43,7´N 004°55,2´E			Resurfacing test
520			PP	17.14				Test on the wire 521
			DTBS+	20.35	64°49,0´N 005°52,8´E	346		Profile start 521-1
		04.11.	HS+PS	03.10	64°38,1´N 004°47,6´E	1032		Profile end 521-1
				03.10	64°38,1´N 004°47,6´E	1032		Profile start 521-2
				07.41	64°47,3´N 004°05,7´E	1043		Profile end 521-2
522			CTD	09.20	64°55,9´N 004°30,4´E	890	868	

Station Meteor 1993	Number GPI	Date	Device	Time UTC (+1h)	Geographical Position Latitude Longitude	Water depth uncorrected (m)	Wire length (m)	Comments
523			OBH	10.54	64°46,2´N 004°30,2´E			OBH and fish in the water
				12.03	64°46,2´N 004°30,3´E	890		OBH and fish separated
								Profile start OBH 523-1
				12.36	64°45,6´N 004°29,8´E			Profile end OBH 523-1
			14.00		64°49,2´N 004°32,7´E			Profile start OBH 523-2
				16.30	64°49,9´N 004°29,3´E			Profile end OBH 523-2
			18.29					OBH on deck
524			MSN	18.50	64°46,3´N 004°30,0´E		100	
				19.03	64°46,3´N 004°30,1´E		700	
525			HS+PS	23.07	64°47,0´N 005°52,8´E	349		Profile start 525-1
		05.11.		02.05	64°36,0´N 004°48,0´E	1105		Profile end 525-1
				02.05	64°36,0´N 004°48,0´E	1105		Profile start 525-2
				04.45	64°48,1´N 003°52,2´E	1185		Profile end 525-2
526	23501-1		SL	08.53	64°43,0´N 004°27,3´E	997	977	Core recovery 8.57 m
527			MSN	10.22	64°42,1´N 004°48,2´E		100	
528			Hyd.	11.47	64°44,1´N 004°27,1´E			in the water
				12.44				on deck
529			MG	14.22	64°44,1´N 004°27,2´E	942	947	Bottom contact
				15.01	64°43,8´N 004°27,2´E	949	950	Bottom contact
				15.38	64°43,7´N 004°27,0´E	961	967	Bottom contact
530			PP2	19.28	64°57,3´N 003°32,1´E	1454		PP located/on deck
531			HS+PS	20.34	64°51,0´N 003°30,0´E	1505		Profile start 531-1
		06.11.		00.22	64°34,0´N 004°48,0´E	1179		Profile end 531-1
				00.22	64°34,0´N 004°48,0´E	1179		Profile start 531-2
				03.22	64°45,0´N 005°52,8´E	337		Profile end 531-2
532			CTD	04.43	64°41,6´N 005°33,1´E	589	578	
533			MSN	05.19	64°41,5´N 005°33,1´E		100	
			MSN	05.33	64°41,6´N 005°33,0´E		500	
534			CTD	08.00	64°36,0´N 004°59,6´E	998	893	
535			MSN	09.12	64°36,0´N 005°00,1´E		100	
			MSN	09.26	64°36,0´N 005°00,1´E		700	

Station Meteor 1993	Number GPI	Date	Device	Time UTC (+1h)	Geographical Position Latitude Longitude	Water depth uncorrected (m)	Wire length (m)	Comments
536			PP	13.37	64°46,3´N 004°30,1´E			PP in the water
537	23502-1		SL(12)	15.40	64°37,0´N 004°27,1´E	1311	1260	Core recovery 8.19 m
538			CTD	17.36	64°38,4´N 004°22,8´E	1295	1261	
539			MSN	18.11	64°38,6´N 004°23,1´E		100	
			MSN	18.25	64°38,7´N 004°23,3´E		700	
540			HS+PS	19.40	64°35,2´N 004°26,7´E	1366		Profile start 540
				22.20	64°47,0´N 003°30,0´E	1612		Profile end 540
541			DTBS+	22.42	64°49,0´N 003°30,0´E	1548		Profile start 541-1
		07.11.	HS+PS	06.45	64°32,1´N 004°48,7´E	1287		Profile end 541-1
				06.45	64°32,1´N 004°48,7´E	1287		Profile start 541-2
				12.14	64°41,7´N 005°43,3´E	455		Profile end 541-2
542	23503-1		SL(12)	15.46	64°46,0´N 004°30,1´E	873	873	Core recovery 9.92 m
543	23504-1		SL(12)	17.49	64°46,0´N 004°30,1´E	878	885	Core recovery 11.41 m
544			DTBS+	20.10	64°50,7´N 004°37,4´E	864		Profile start 544-1
		08.11.	HS+PS	00.48	64°32,0´N 004°15,0´E	1539		Profile end 544-1
				00.48	64°32,0´N 004°15,0´E	1539		Profile start 544-2
				02.24	64°35,0´N 004°06,1´E	1527		Profile end 544-2
				02.42	64°35,0´N 004°06,1´E	1468		Profile start 544-3
				06.22	64°32,5´N 004°28,9´E	925		Profile end 544-3,
				06.30				Loss of boomer winch
				09.08				Boomer on deck
545			PP3	10.37	64°46,3´N 004°30,1´E			PP located/on deck
546			PP4	13.08	64°46,0´N 004°30,1´E			PP in the water
547			CTD	13.58	64°45,6´N 004°30,2´E	865	854	
548			MSN	14.31	64°45,5´N 004°30,8´E		100	
			MSN	14.45	64°44,8´N 004°30,8´E		700	
				15.35				Weathering
549		10.11.	HS+PS	22.59	64°51,5´N 004°33,0´E	902		Profile start 549-1
		11.11.		01.17	64°32,5´N 004°10,5´E	1563		Profile end 549-1
				01.17	64°32,5´N 004°10,5´E	1563		Profile start 549-2
				01.42	64°30,5´N 004°19,0´E	1532		Profile end 549-2
				01.42	64°30,5´N 004°19,0´E	1532		Profile start 549-3
				03.42	64°50,0´N 004°42,0´E	840		Profile end 549-3

Station Meteor 1993	Number GPI	Date	Device	Time UTC (+1h)	Geographical Position Latitude	Longitude	Water depth uncorrected (m)	Wire length (m)	Comments
				03.42	64°50,0´N	004°42,0´E	840		Profile start 549-4
				03.54	64°49,0´N	004°46,5´E	809		Profile end 549-4
				03.54	64°49,0´N	004°46,5´E	809		Profile start 549-5
				05.00	64°39,6´N	004°35,8´E	1076		Profile end 549-5
				05.00	64°39,6´N	004°35,8´E	1076		Profile start 549-6
				05.12	64°38,9´N	004°40,0´E	1063		Profile end 549-6
				05.12	64°38,9´N	004°40,0´E	1063		Profile start 549-7
				06.12	64°48,0´N	004°50,8´E	777		Profile end 549-7
550			PP4	08.15	64°46,1´N	004°29,9´E	872		PP on deck
551		12.11.	NB7	11.37	69°41,6´N	000°29,0´E	3291		Hydr. in the water
				11.55					Mooring released
				12.06					Mooring located
				12.23	69°41,4´N	000°28,5´E			Top buoy on deck
				13.41					Mooring salvaged
			CTD	15.39	69°41,3´N	000°28,9´E	3291	3237	
			MSN	17.01	69°41,3´N	000°28,8´E		100	
				17.14	69°41,3´N	000°28,8´E		700	
				19.42	69°41,4´N	000°28,9´E	3291	3000	
	23505-1		GKG	22.32	69°41,4´N	000°28,8´E	3291	3261	Core recovery 0.55m
552		13.11.	GWS	20.00	72°23,6´N	007°36,1´W	1050		
			CTD	22.35	72°23,6´N	007°35,9´W	2668	2616	
		14.11.	MSN	00.03	72°23,6´N	007°35,6´W	100		
			MSN	00.20	72°23,6´N	007°35,6´W	700		
			MSN	01.19	72°23,6´N	007°36,1´W	2500		Failure W3: 03.05-03.37
	23506-1		GKG	07.32	72°23,6´N	007°36,2´W	2670	2622	Core recovery 0.35m
553			OG6	10.12	72°21,8´N	007°35,5´W			Hydr. in the water
				10.17					Mooring released
				10.32-					div. search courses and
				14.00					hydrophon measurements
554			HS+PS	14.00	72°21,6´N	007°35,9´W	2581		Profile start 554
				21.13	73°30,0´N	010°00,0´W	330		Profile end 554
555				21.13	73°30,0´N	010°00,0´W	330		Profile start 555-1
				22.00	73°35,0´N	010°24,0´W	334		Profile end 555-1

Station Meteor 1993	Number GPI	Date	Device	Time UTC (+1h)	Geographical Position Latitude Longitude	Water depth uncorrected (m)	Wire length (m)	Comments
			HS+PS	22.00	73°35,0´N 010°24,0´W	334		Profile start 555-2
				22.14	73°37,9´N 010°18,6´W	2964		Profile end 555-2
				22.14	73°37,9´N 010°18,6´W	2964		Profile start 555-3
				23.11	73°32,1´N 009°54,5´W	2955		Profile end 555-3
				23.11	73°32,1´N 009°54,5´W	2955		Profile start 555-4
				23.26	73°34,2´N 009°49,0´W	2952		Profile end 555-4
				23.26	73°34,2´N 009°49,0´W	2952		Profile start 555-5
		15.11.		00.14	73°39,2´N 010°13,2´W	2995		Profile end 555-5
				00.14	73°39,2´N 010°13,2´W	2995		Profile start 555-6
				00.28	73°41,2´N 010°07,8´W	2996		Profile end 555-6
				00.28	73°41,2´N 010°07,8´W	2996		Profile start 555-7
				01.26	73°36,4´N 009°43,4´W	3027		Profile end 555-7
				01.26	73°36,4´N 009°43,4´W	3027		Profile start 555-8
				01.40	73°38,4´N 009°37,9´W	3042		Profile end 555-8
		15.11		01.40	73°38,4´N 009°37,9´W	3042		Profile start 555-9
				02.38	73°43,4´N 010°02,4´W	3084		Profile end 555-9
				02.38	73°43,4´N 010°02,4´W	3084		Profile start 555-10
				02.52	73°45,5´N 009°05,7´W	3051		Profile end 555-10
				02.52	73°45,5´N 009°05,7´W	3051		Profile start 555-11
				03.48	73°40,5´N 009°32,5´W	3035		Profile end 555-11
				03.48	73°40,5´N 009°32,5´W	3035		Profile start 555-12
				04.00	73°42,6´N 009°26,9´W	3083		Profile end 555-12
				04.00	73°42,6´N 009°26,9´W	3083		Profile start 555-13
				05.00	73°47,5´N 009°50,9´W	3127		Profile end 555-13
				05.00	73°47,5´N 009°50,9´W	3127		Profile start 555-14
				05.16	73°49,6´N 009°46,3´W	3080		Profile end 555-14
				05.16	73°49,6´N 009°46,3´W	3080		Profile start 555-15
				06.07	73°44,9´N 009°21,0´W	3025		Profile end 555-15
				06.07	73°44,9´N 009°21,0´W	3025		Profile start 555-16
				06.21	73°46,9´N 009°17,0´W	3125		Profile end 555-16
				06.21	73°46,9´N 009°17,0´W	3125		Profile start 555-17
				07.35	73°51,9´N 009°40,2´W	3150		Profile end 555-17
				07.35	73°51,9´N 009°40,2´W	3150		Profile start 555-18

Station Meteor 1993	Number GPI	Date	Device	Time UTC (+1h)	Geographical Position Latitude Longitude	Water depth uncorrected (m)	Wire length (m)	Comments
			HS+PS	07.51	73°53,7´N 009°34,9´W	3090		Profile end 555-18
				07.51	73°53,7´N 009°34,9´W	3090		Profile start 555-19
				08.47	73°48,9´N 009°10,5´W	3081		Profile end 555-19
556	23507-1		GKG	11.00	73°49,8´N 009°15,1´W	3150	3095	Core recovery 0.47m
557	23508-1		GKG	13.45	73°51,6´N 009°23,7´W	3202	3142	Core recovery 0.47m
			CTD	16.20	73°51,6´N 009°23,7´W	3202	3147	
558			HS+PS	17.54	73°51,6´N 009°23,7´W	3120		Profile start 558
				23.16	73°50,0´N 012°00,0´W	2845		Profile end 558
		16.11.		00.00				Weathering
			HS+PS	09.50	73°50,0´N 012°00,0´W	2839		Continuation Profil 558
				12.35	73°50,1´N 013°31,3´W	2571		Profile end 558
				12.35				Weathering
559		17.11.	CTD	03.28	73°49,9´N 013°30,0´W	2579	1000	
			MSN	04.03	73°50,0´N 013°30,7´W	100		
			MSN	04.18	73°50,0´N 013°30,8´W	700		
	23509-1		GKG	06.45	73°50,0´N 013°30,1´W	2576	2534	Core recovery 0.37m
560			CTD	12.07	73°40,1´N 012°00,3´W	2865	1000	
			MSN	12.38	73°40,1´N 012°00,3´W	100		
			MSN	12.53	73°40,1´N 012°00,3´W	700		
561			HS+PS	13.52	73°40,0´N 012°00,2´W	2870		Profile start 561
				17.10	73°26,2´N 013°32,8´W	2633		Profile end 561
562	23510-1		SL (12)	19.09	73°27,2´N 013°25,9´W	2643	2593	Core recovery 7.01m
563			HS+PS	20.34	73°27,2´N 013°27,2´W	2640		Profile start 563
		18.11.		00.24	73°13,0´N 015°00,0´W	2244		Profile end 563
564	23511-1		SL (12)	01.14	73°13,0´N 015°00,9´W	2295	2230	Core recovery 2.61m
	23511-2		GKG	03.43	73°12,9´N 015°00,1´W	2295	2242	Core recovery 0.4m
565			HS+PS	04.47	73°13,0´N 015°00,0´W	2240		Profile start 565
				07.03	73°03,0´N 014°05,0´W	2530		Profile end 565
566			CTD	07.38	73°03,2´N 014°05,3´W	2532	1000	
			MSN	08.05	73°03,2´N 014°05,3´W	100		
			MSN	08.19	73°03,1´N 014°05,2´W	700		
567			HS+PS	09.12	73°03,0´N 014°05,0´W	2540		Profile start 567
				10.49	72°56,5´N 013°25,0´W	2550		Profile end 567

Station Meteor 1993	Number GPI	Date	Device	Time UTC (+1h)	Geographical Position Latitude Longitude	Water depth uncorrected (m)	Wire length (m)	Comments
568	23512-1		GKG	12.13	72°56,5´N 013°25,4´W	2610	2562	Core recovery 0.41m
	23512-2		SL(12)	14.16	72°56,5´N 013°25,4´W	2612	2557	Core recovery 6.98m
569			HS+PS	15.49	72°56,5´N 013°25,1´W	2550		Profile start 569
				22.25	72°33,5´N 011°17,4´W	2235		ceasing of Profil 569
570	23513-1	19.11	GKG	13.05	72°32,8´N 011°12,5´W	2174	2145	Failure
571			HS+PS	14.24	72°32,5´N 011°09,8´W	2104		Profile start 571
				15.47	72°25,0´N 010°30,1´W	2098		Profile end 571
572			HS+PS	16.08	72°22,2´N 010°37,7´W	2241		Profile start 572
				20.29	72°49,0´N 013°00,0´W	2582		Profile end 572
573			HS+PS	20.46	72°47,0´N 013°00,0´W	2594		Profile start 573
		20.11.		01.52	72°19,0´N 010°30,0´W	2150		Profile end 573
574				01.52	72°19,0´N 010°40,0´W	2150		Profile start 574
				06.53	72°21,6´N 007°36,1´W	2578		Profile end 574
575			OG6	07.00	72°21,7´N 007°36,1´W			Hydrophon in the water
			07.15	End of scientific station work				

7.3.2 Core Descriptions of Gravity and Box Cores

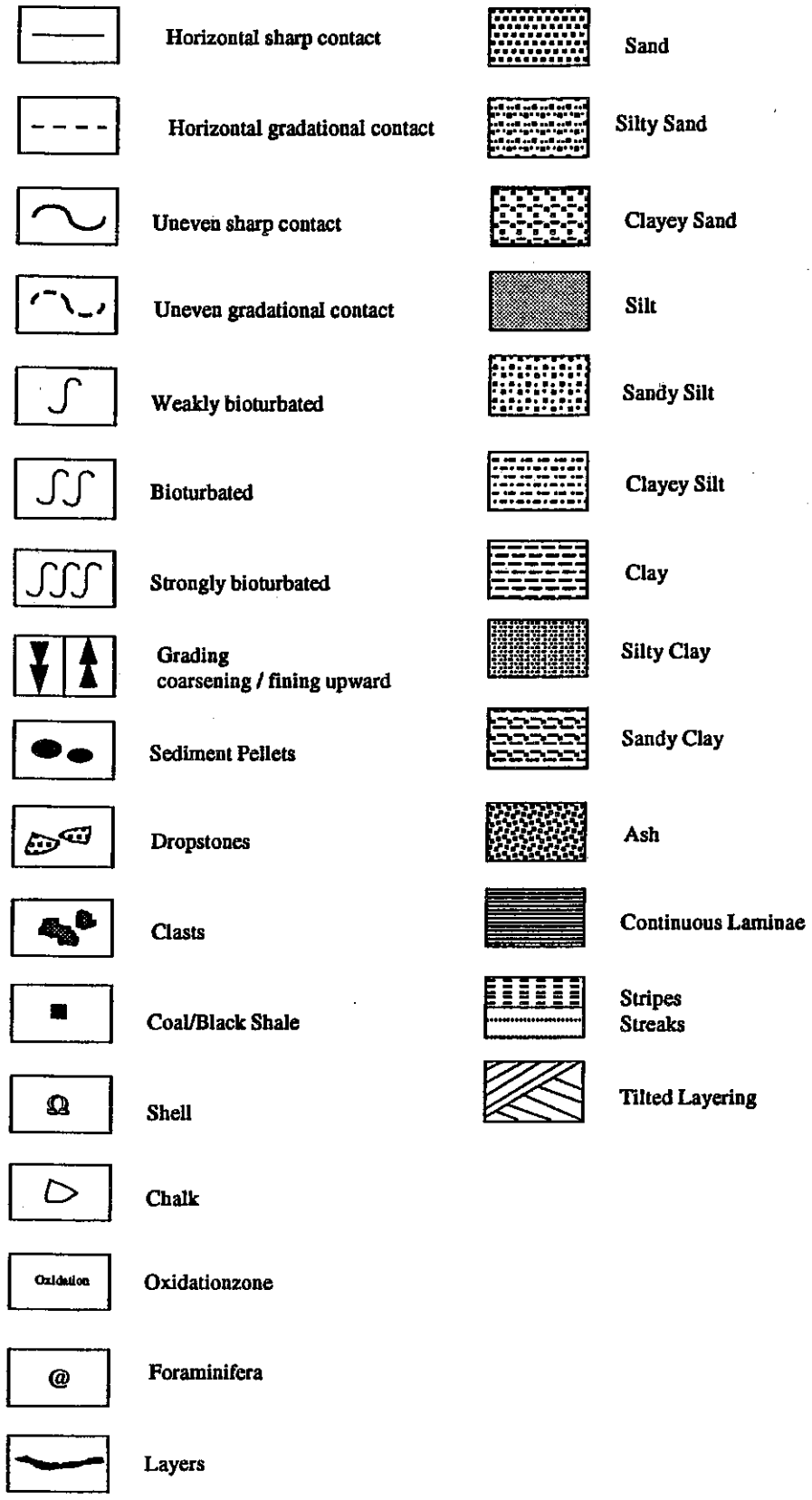

Figure . Legend: lithology symbols and symbols used to describe sediments

METEOR 26/3 — 27.10.1993 - 25.11.1993
Station: M 26/3-501 — Date: 29.10.1993
Position: 64° 20,732´ N ; 8° 23,664´ E — Water Depth: 289,2 m

Core: M 26/3 GIK 23490-2 — Core Recovery: 312 cm
Section: 0 - 150 cm

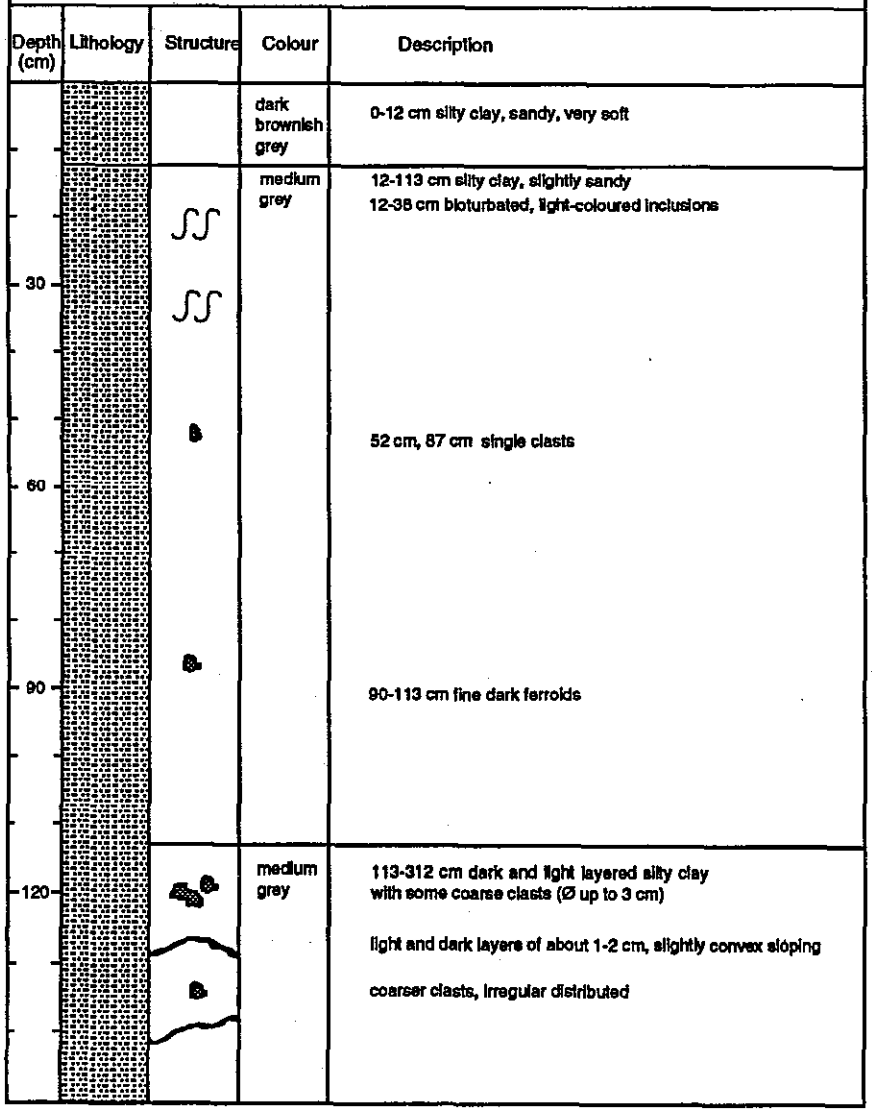

Figure . Description of sediment column of core GIK 23490-2

METEOR 26/3 — 27.10.1993 - 25.11.1993
Station: M 26/3-501 — Date: 29.10.1993
Position: 64° 20,732´ N ; 8° 23,664´ E — Water Depth: 289,2 m

Core: M 26/3 GIK 23490-2 — Core Recovery: 312 cm
Section: 150 - 300 cm

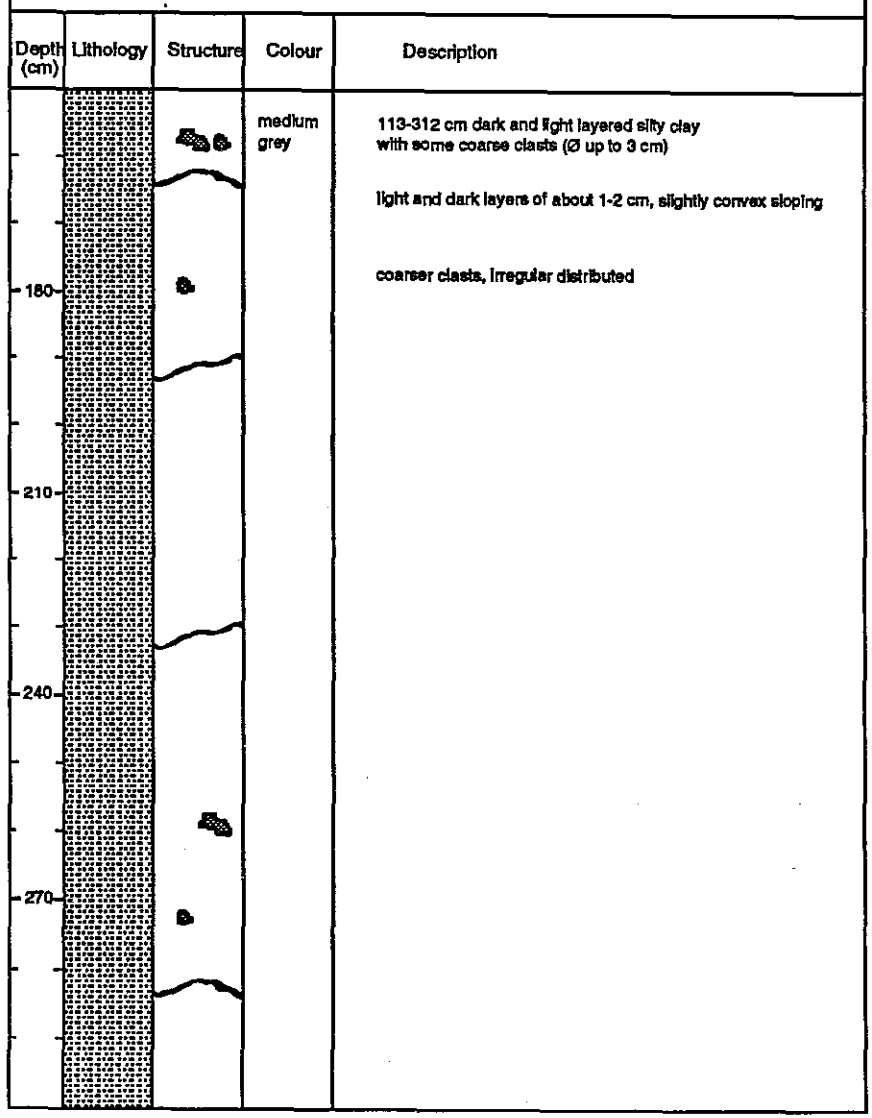

Figure . continued

METEOR 26/3	27.10.1993 - 25.11.1993
Station: M 26/3-501	Date: 29.10.1993
Position: 64° 20,732´ N ; 8° 23,664´ E	Water Depth: 289,2 m

Core: M 26/3 GIK 23490-2 — Core Recovery: 312 cm
Section: 300 - 312 cm

Depth (cm)	Lithology	Structure	Colour	Description
			grey	layered silty clay
				EOC: 312 cm
				loss of the rest of the core
330				
360				
390				
420				

Figure . continued

METEOR 26/3	27.10.1993 - 25.11.1993
Station: M 26/3-502	Date: 29.10.1993
Position: 64° 21,634´ N ; 8° 21,378´ E	Water Depth: 276,7 m

Core: M 26/3 GIK 23491-1 — Core Recovery: 477 cm
Section: 0 - 150 cm

Depth (cm)	Lithology	Structure	Colour	Description
			brownish-grey	0-4 cm silty clay, sandy, with foraminifera, high water content 4-9 cm silty clay, sandy with foraminifera and single gastropods stiffer
			brownish-grey	9-31 cm silty clay, slightly sandy, mottled with dark traces
30			dark grey, slightly brown	31-224 cm silty clay with small blackish spots, single "Dentalien", gastropods
60				
90				
			dark brownish grey	
120				

Figure . Description of sediment column of core GIK 23491-1

METEOR 26/3 — **27.10.1993 - 25.11.1993**
Station: M 26/3-502 — **Date: 29.10.1993**
Position: 64° 21,634´ N; 8° 21,378´ E — **Water Depth: 276,7 m**

Core: M 26/3 GIK 23491-1 — **Core Recovery: 477 cm**
Section: 150 - 300 cm

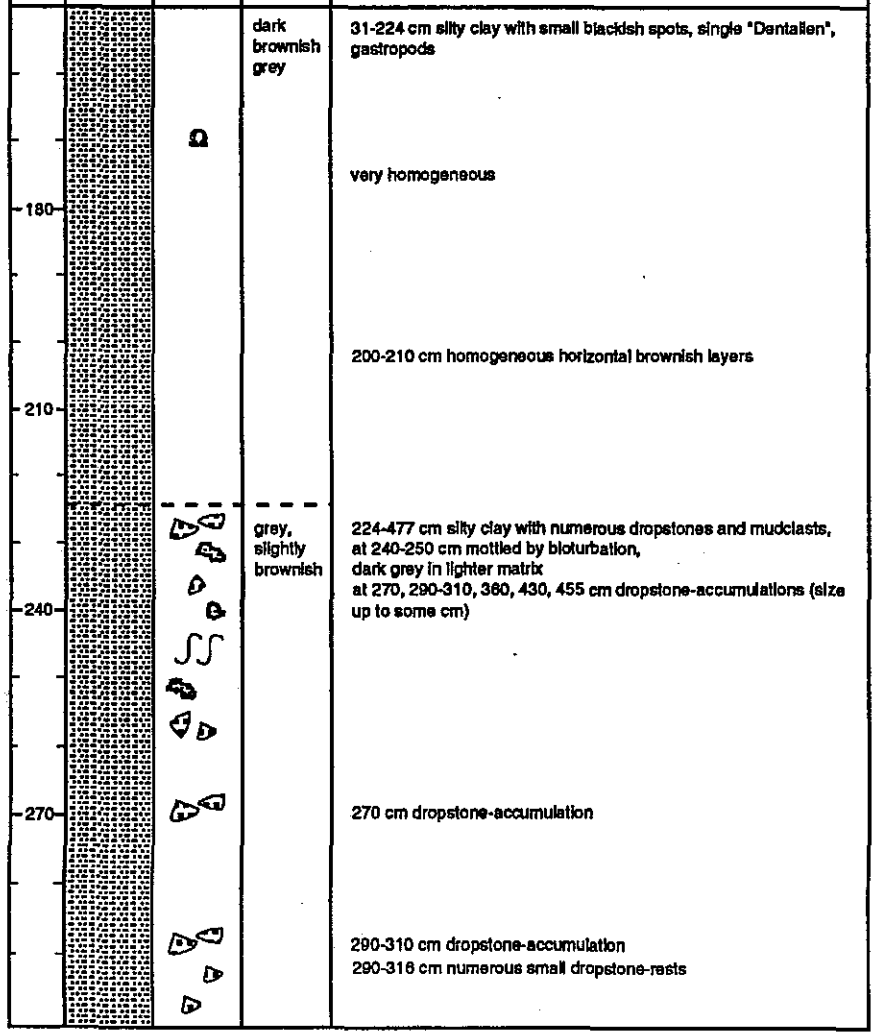

Figure . continued

METEOR 26/3 — **27.10.1993 - 25.11.1993**
Station: M 26/3-502 — **Date: 29.10.1993**
Position: 64° 21,634´ N; 8° 21,378´ E — **Water Depth: 276,7 m**

Core: M 26/3 GIK 23491-1 — **Core Recovery: 477 cm**
Section: 300 - 450 cm

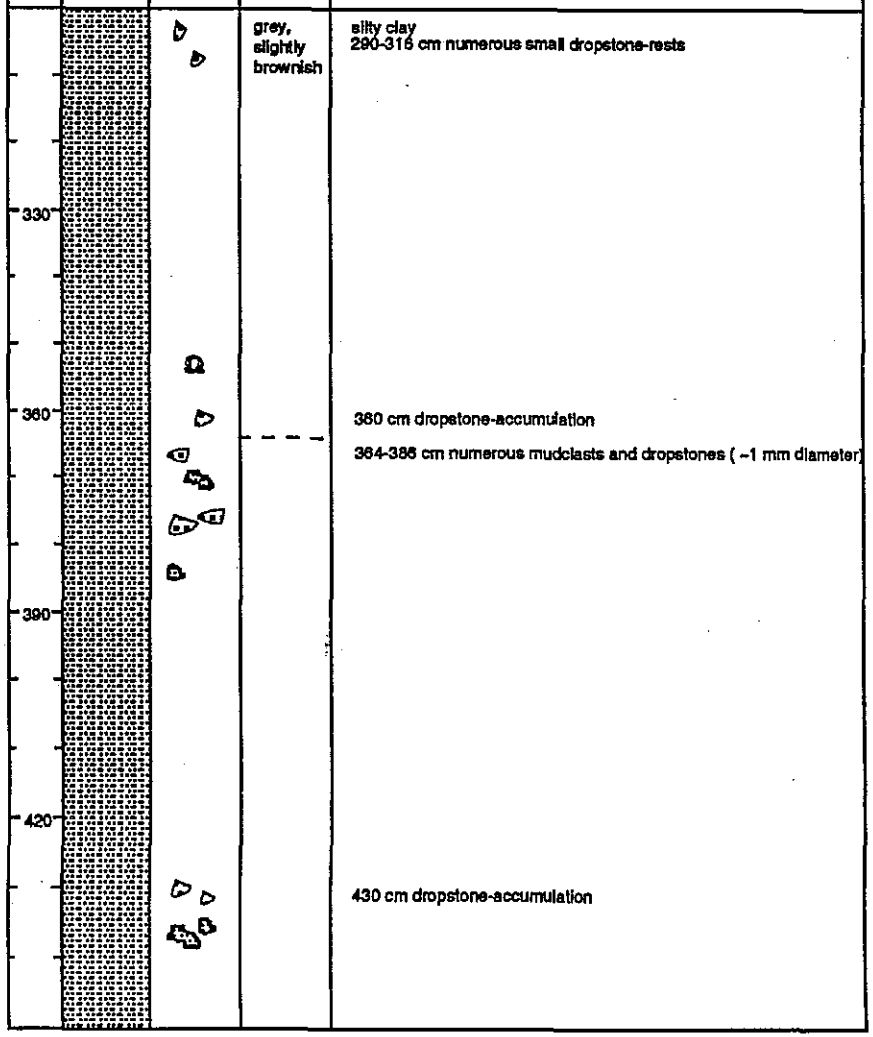

Figure . continued

Meteor 26/3 — 27.10.1993 - 25.11.1993
Station: M 26/3-502 — Date: 29.10.1993
Position: 64° 21,634´ N ; 8° 21,378´ E — Water Depth: 276,7 m

Core: M 26/3 GIK 23491-1 — Core Recovery: 477 cm
Section: 450-477 cm

Depth (cm)	Lithology	Structure	Colour	Description
			grey, slightly brownish	silty clay, with numerous dropstones 455 cm dropstone-accumulation
				EOC: 477cm
480				
510				
540				
570				

Figure . continued

METEOR 26/3 — 27.10.1993 - 25.11.1993
Station: M 26/3-503-3 — Date: 29.10.1993
Position: 64° 18.023´ N ; 8° 09.575´ E — Water Depth: 284 m

Core: M 26/3 GIK 23492-3 — Core Recovery: 234 cm
Section: 0 - 150 cm

Depth (cm)	Lithology	Structure	Colour	Description
			dark green	0-24 cm glauconite sand, nearly without clay, with foraminifera, single molluscs,high water content, disturbance due to water outflow
30			grey, greenish	24-50 cm clayey silt, sandy, with some large molluscs, base is sloping from 46-55 cm
60			black-green	50-84 cm glauconite sand base is sloping as well
90			grey-green	84-99 cm slightly more fine-grained glauconite sand with dark bioturbation at the horizontal base
120			dark green	99-176 cm coarse glauconite sand indistinct horizontal layered, no graded bedding visible, sharp contact at base homogeneous

Figure . Description of sediment column of core GIK 23492-3

METEOR 26/3
Station: M 26/3-503-3
Position: 64° 18.023´ N ; 8° 09.575´ E

27.10.1993 - 25.11.1993
Date: 29.10.1993
Water Depth: 284 m

Core: M 26/3 GIK 23492-3
Section: 150 - 300 cm

Core Recovery: 234 cm

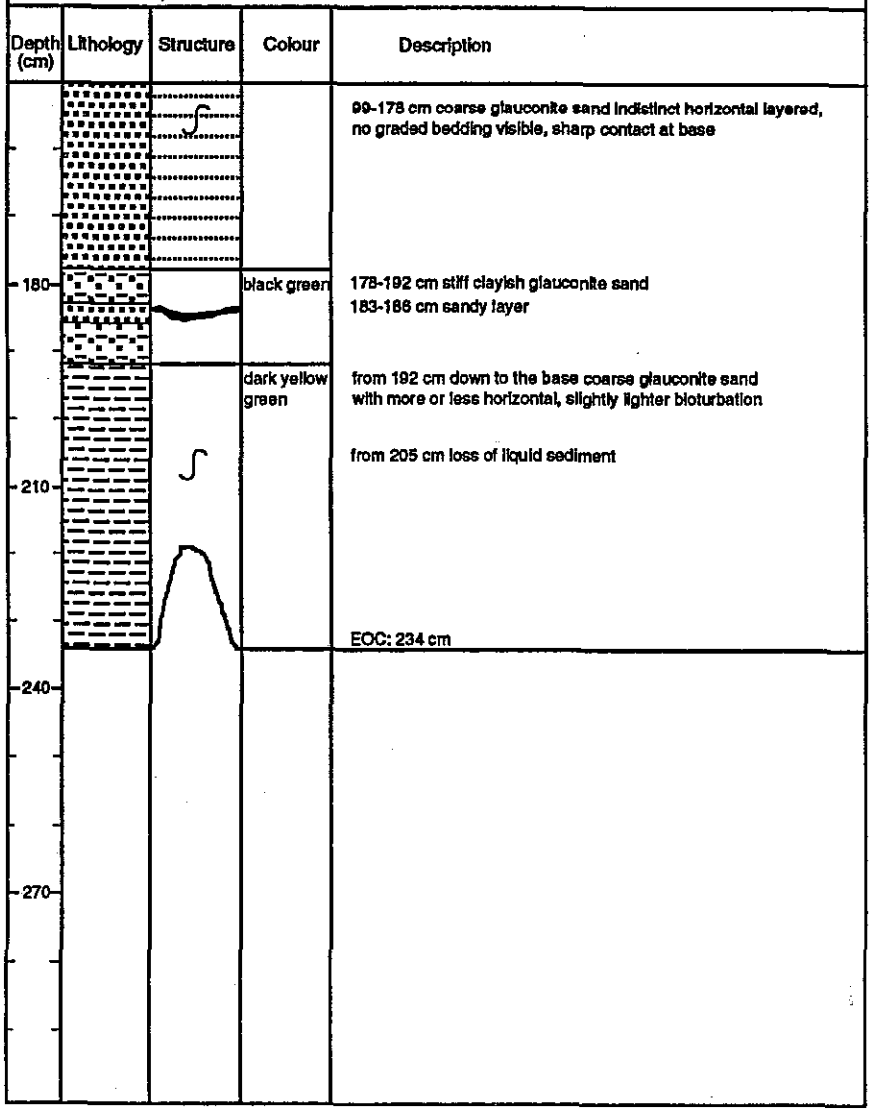

Figure . continued

METEOR 26/3
Station: M 26/3-504
Position: 64° 18.356´ N ; 8° 09.244´ E

27.10.1993 - 25.11.1993
Date: 29.10.1993
Water Depth: 283,8 m

Core: M 26/3 GIK 23495-1
Section: 0 - 150 cm

Core Recovery: 382 cm

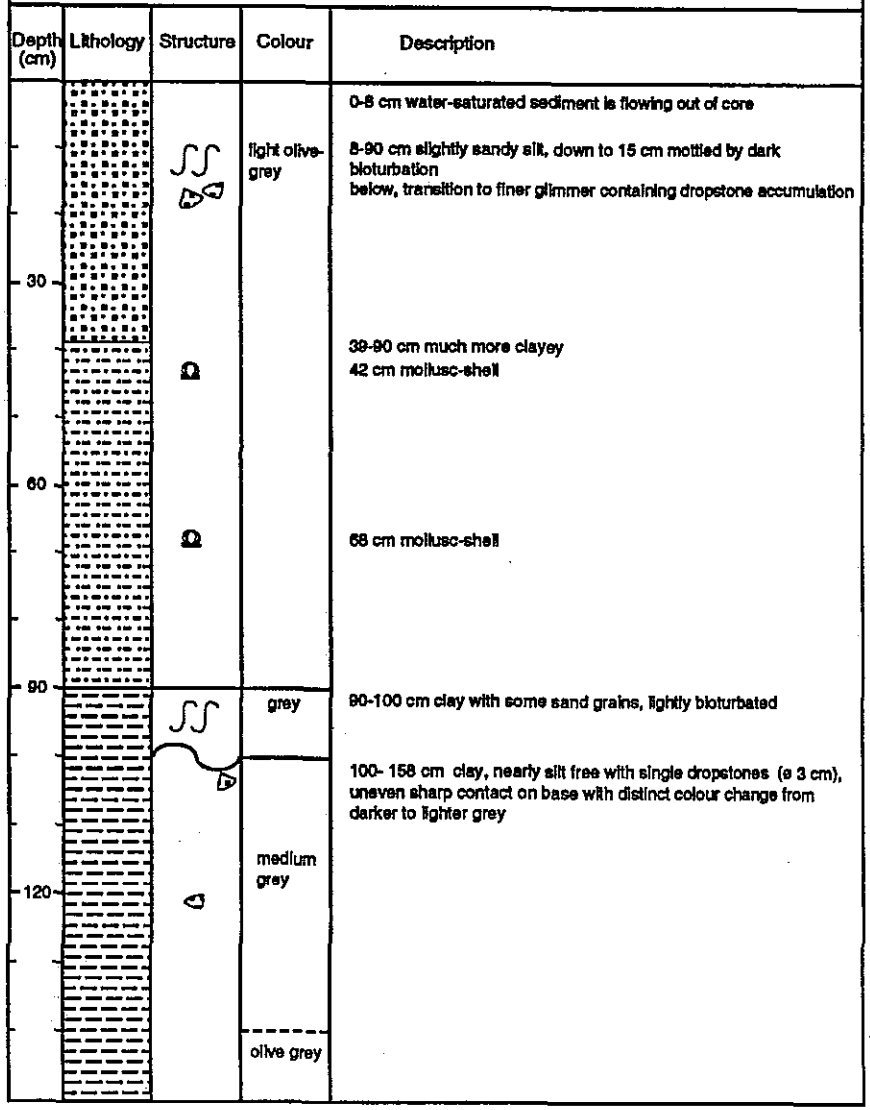

Figure . Description of sediment column of core GIK 23495-1

METEOR 26/3 — 27.10.1993 - 25.11.1993
Station: M 26/3-504 — Date: 29.10.1993
Position: 64° 18.356´ N ; 8° 09.244´ E — Water Depth: 283.8 m

Core: M 26/3 GIK 23495-1 — Core Recovery: 382 cm
Section: 150 - 300 cm

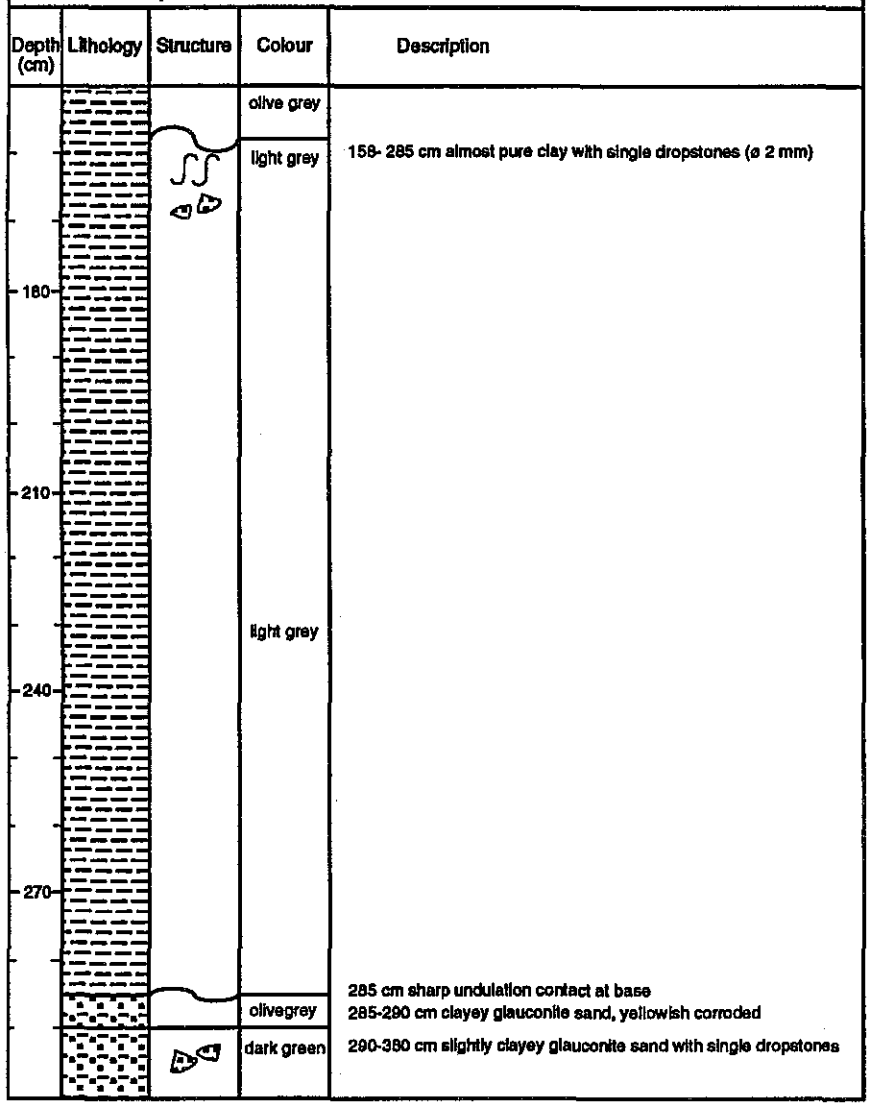

Figure . continued

METEOR 26/3 — 27.10.1993 - 25.11.1993
Station: M 26/3-504 — Date: 29.10.1993
Position: 64° 18.356´ N ; 8° 09.244´ E — Water Depth: 283.8 m

Core: M 26/3 GIK 23495-1 — Core Recovery: 382 cm
Section: 300 - 450 cm

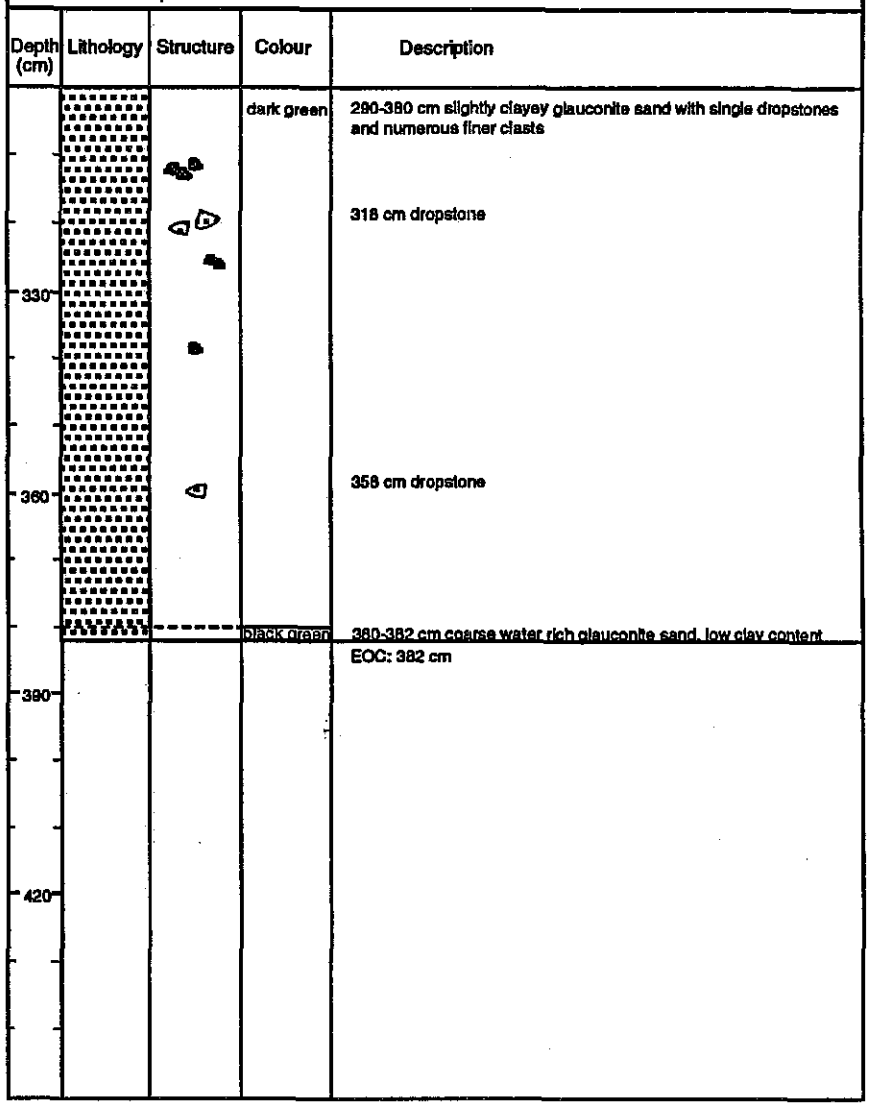

Figure . continued

METEOR 26/3 — **27.10.1993 - 25.11.1993**
Station: M 26/3-505 — **Date: 29.10.1993**
Position: 64° 17.333´ N ; 8° 12.418´ E — **Water Depth: 334.4 m**

Core: M 26/3 GIK 23496-1 — **Core Recovery: 471 cm**
Section: 0 - 150 cm

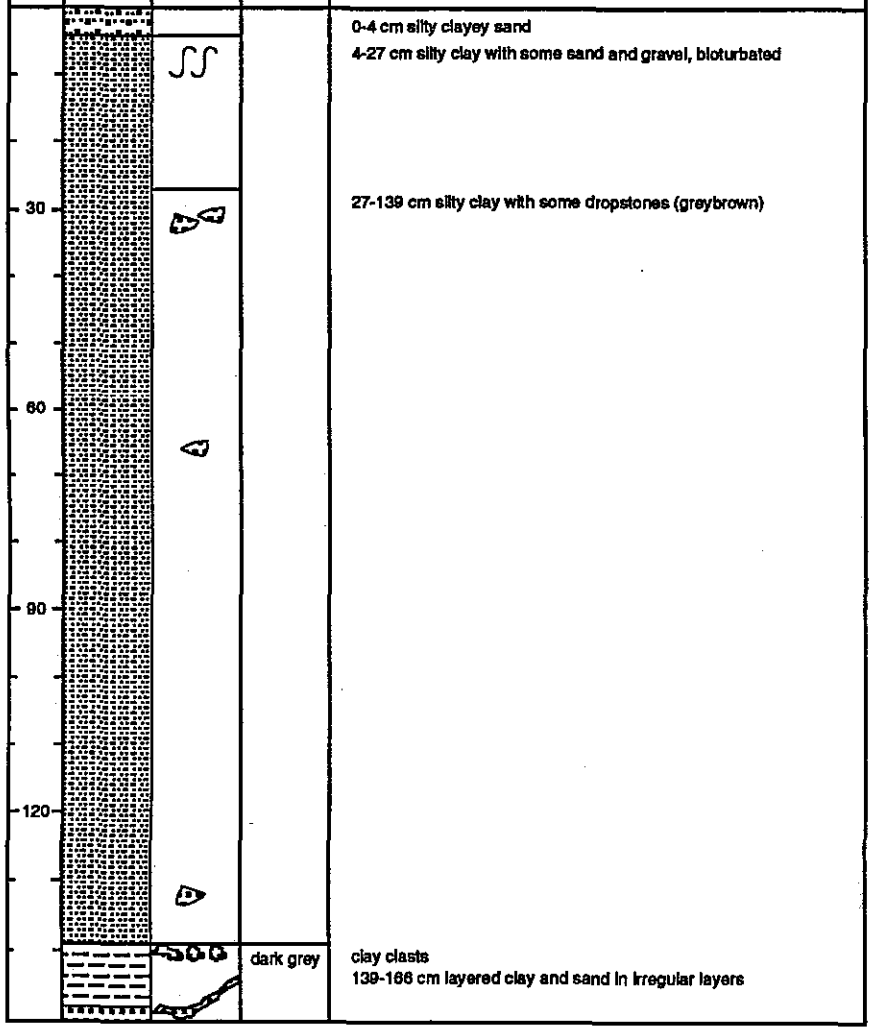

Figure . Description of sediment column of core GIK 23496-1

METEOR 26/3 — **27.10.1993 - 25.11.1993**
Station: M 26/3-505 — **Date: 29.10.1993**
Position: 64° 17.333´ N ; 8° 12.418´ E — **Water Depth: 334.4 m**

Core: M 26/3 GIK 23496-1 — **Core Recovery: 471 cm**
Section: 150 - 300 cm

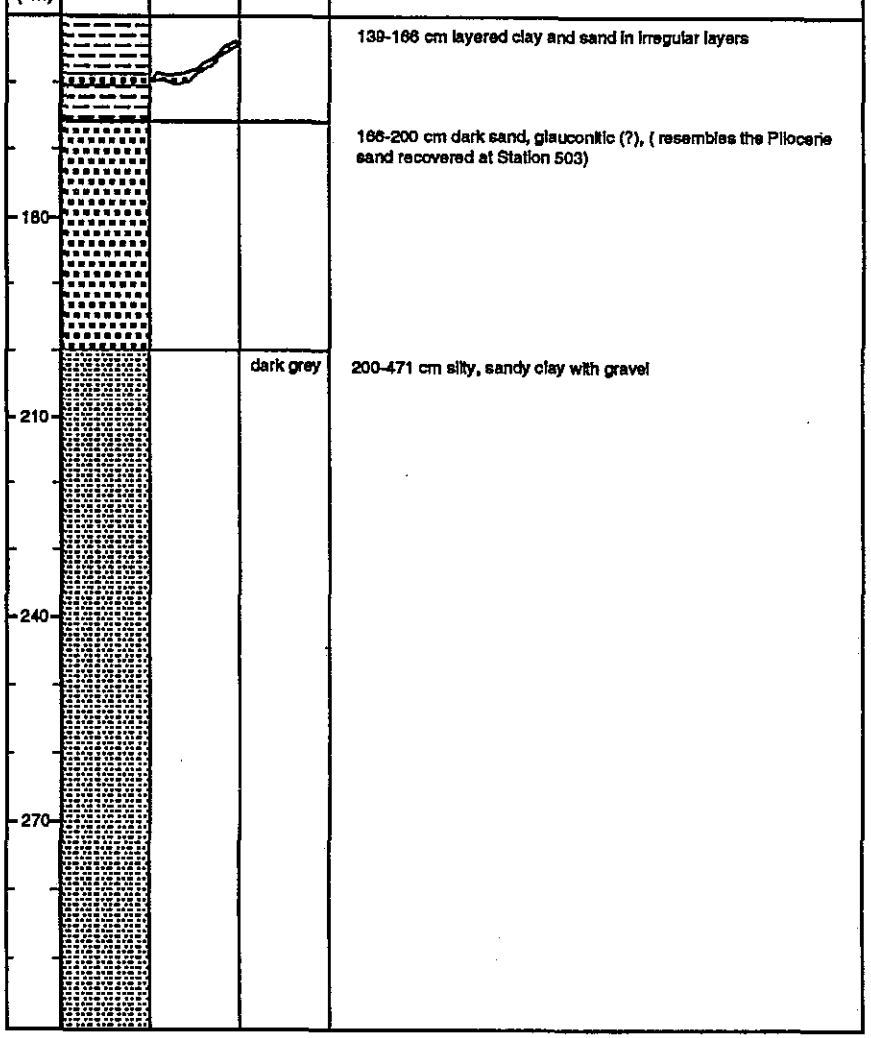

Figure . continued

METEOR 26/3	27.10.1993 - 25.11.1993
Station: M 26/3-505	Date: 29.10.1993
Position: 64° 17.333´ N ; 8° 12.418´ E	Water Depth: 334.4 m

Core: M 26/3 GIK 23496-1 — Core Recovery: 471 cm
Section: 300 - 450 cm

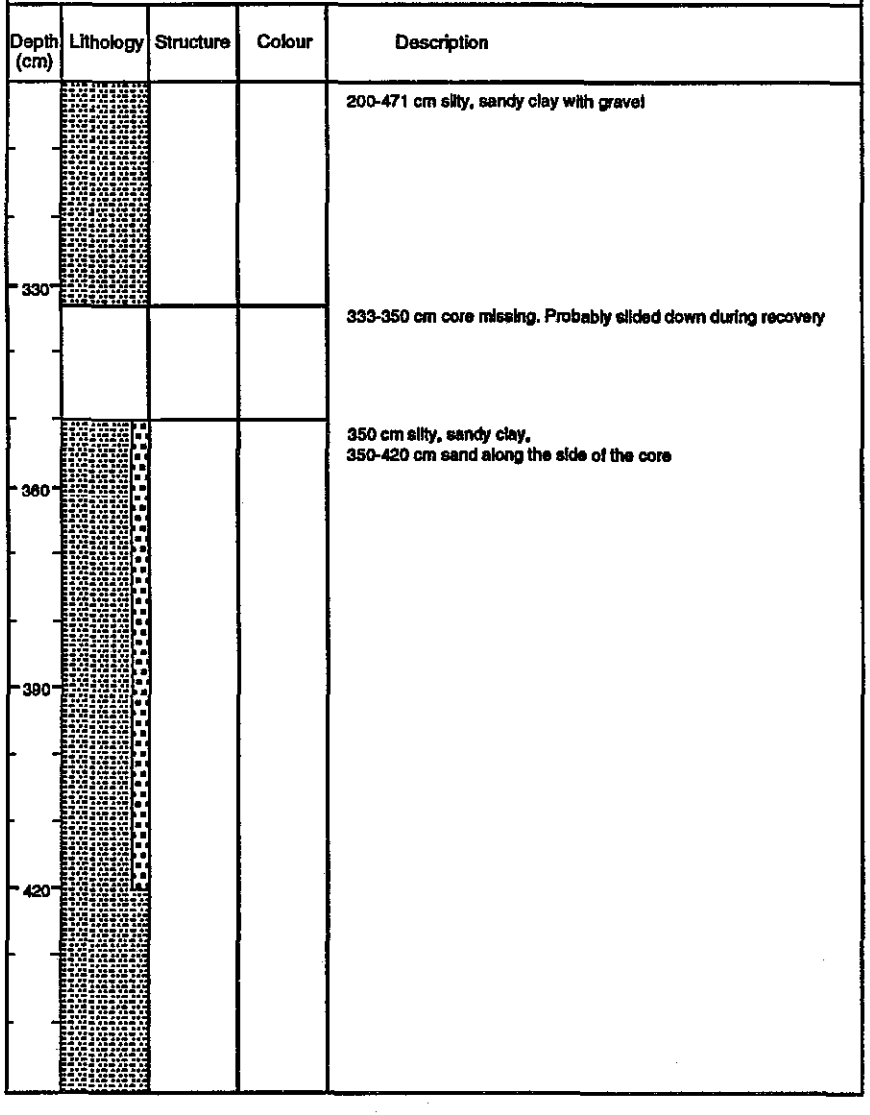

Figure . continued

Meteor 26/3	27.10.1993 - 25.11.1993
Station: M 26/3-505	Date: 29.10.1993
Position: 64° 17.333´ N ; 8° 12.418´ E	Water Depth: 334.4 m

Core: M 26/3 GIK 23496-1 — Core Recovery: 471 cm
Section: 450-471 cm

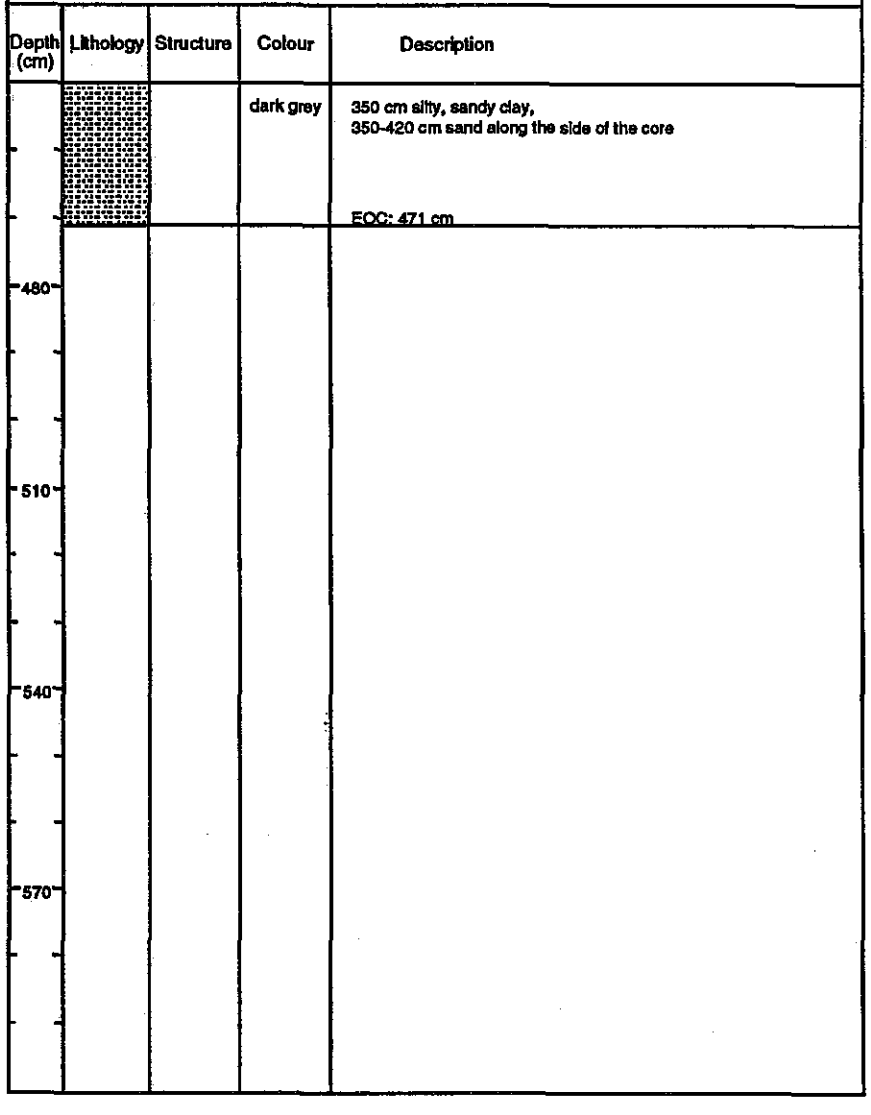

Figure . continued

METEOR 26/3 — **27.10.1993 - 25.11.1993**
Station: M 26/3-526 — **Date: 05.11.1993**
Position: 64° 43,04´ N ; 4° 27,34´ E — **Water Depth: 997 m**

Core: M 26/3 GIK 23501-1 — **Core Recovery: 857 cm**
Section: 0 - 150 cm

Depth (cm)	Lithology	Structure	Colour	Description
			light olive brown	0-4 cm silty clay with heavily bioturbated, sediment surface flown out, gradational contact at base
			olive brown	4-41 cm slightly silty clay, bioturbations very indistinct, towards base transition to dark-grey to blackish bioturbations
30				
				41-72 cm as above with numerous burrows (ø 2 mm)
60				
				72-200 cm as above, coarse Fucoids
90				
120				

Figure . Description of sediment column of core GIK 23501-1

METEOR 26/3 — **27.10.1993 - 25.11.1993**
Station: M 26/3-526 — **Date: 05.11.1993**
Position: 64° 43,04´ N ; 4° 27,34´ E — **Water Depth: 997 m**

Core: M 26/3 GIK 23501-1 — **Core Recovery: 857 cm**
Section: 150 - 300 cm

Depth (cm)	Lithology	Structure	Colour	Description
			olive brown	slightly silty clay
180				
				200-203 cm gap caused by shrinking
210				203 cm as above
240				
270				272-280 cm darkgreen mottled bioturbation

Figure . continued

METEOR 26/3	27.10.1993 - 25.11.1993
Station: M 26/3-526	Date: 05.11.1993
Position: 64° 43,04´ N ; 4° 27,34´ E	Water Depth: 997 m

Core: M 26/3 GIK 23501-1 — Core Recovery: 857 cm
Section: 300 - 450 cm

Depth (cm)	Lithology	Structure	Colour	Description
				72-325 cm slightly silty clay with dark coarse Fucoids
330			olive brown	325-374 cm slightly silty clay, weakly bioturbated
			light grey	345-360 cm vertical burrow, greenish 346 cm dropstone consisting of bryaozoen limestone, sandy
360				
			olive brown	374-388 cm slightly silty clay with numerous black distinct bioturbations,gradational contact at base
390				388-409 cm silty clay with dark bioturbation
				409-420 cm some,fine Fucoids
420				420-453 cm less bioturbation

Figure . continued

Meteor 26/3	27.10.1993 - 25.11.1993
Station: M 26/3-526	Date: 05.11.1993
Position: 64° 43,04´ N ; 4° 27,34´ E	Water Depth: 997 m

Core: M 26/3 GIK 23501-1 — Core Recovery: 857 cm
Section: 450-600 cm

Depth (cm)	Lithology	Structure	Colour	Description
			olive brown	453-475 cm silty clay with grey burrows (ø 2 mm) clear in contrast
480				475-670 cm as above, black burrows mostly vertical in the upper part, below regularly spread in all directions
510				silty clay with black bioturbation, regularly spread
540				
570				

Figure . continued

METEOR 26/3 — **27.10.1993 - 25.11.1993**
Station: M 26/3-526 — **Date: 05.11.1993**
Position: 64° 43,04´ N ; 4° 27,34´ E — **Water Depth: 997 m**

Core: M 26/3 GIK 23501-1 — **Core Recovery: 857 cm**
Section: 600 - 750 cm

Depth (cm)	Lithology	Structure	Colour	Description
				475-670 cm silty clay, black burrows regularly spread in all directions, fill-in material is clayey; base very indistinct but marked by the disappearance of bioturbations
630				
660			olive brown	670-748 cm silty clay with some dropstones and mudclasts, mottled by bioturbation 676 cm dropstone (ø 2 cm)
690				
				714 cm fine light grey Fucoids
720				
				base indistinct, 748-792 cm silty clay with black, clay-filled burrows, very regularly spread

Figure . continued

METEOR 26/3 — **27.10.1993 - 25.11.1993**
Station: M 26/3-526 — **Date: 05.11.1993**
Position: 64° 43,04´ N ; 4° 27,34´ E — **Water Depth: 997 m**

Core: M 26/3 GIK 23501-1 — **Core Recovery: 857 cm**
Section: 750 - 857 cm

Depth (cm)	Lithology	Structure	Colour	Description
			olive brown	748-792 cm silty clay with black, clay-filled burrows, very regularly spread
780				
				792-857 cm silty clay heavily bioturbated, matrix and bioturbations hard to distinguish, single dropstones
810				
840				
				EOC: 857 cm
870				

Figure . continued

METEOR 26/3 — **27.10.1993 - 25.11.1993**
Station: M 26/3-542 — **Date: 07.11.1993**
Position: 64° 46,00´ N ; 4° 30,15´ E — **Water Depth: 872 m**

Core: M 26/3 GIK 23503-1 — **Core Recovery: 991 cm**
Section: 0 - 150 cm

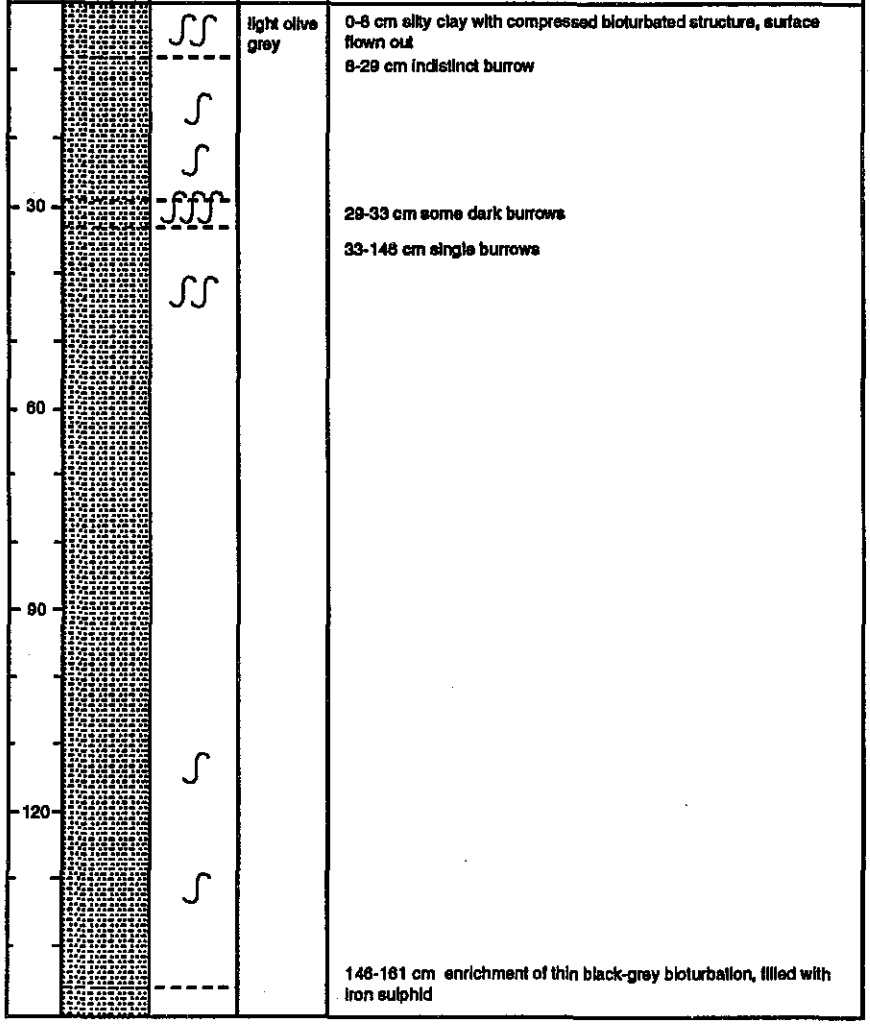

Figure . Description of sediment column of core GIK 23503-1

METEOR 26/3 — **27.10.1993 - 25.11.1993**
Station: M 26/3-542 — **Date: 07.11.1993**
Position: 64° 46,00´ N ; 4° 30,15´ E — **Water Depth: 872 m**

Core: M 26/3 GIK 23503-1 — **Core Recovery: 991 cm**
Section: 150 - 300 cm

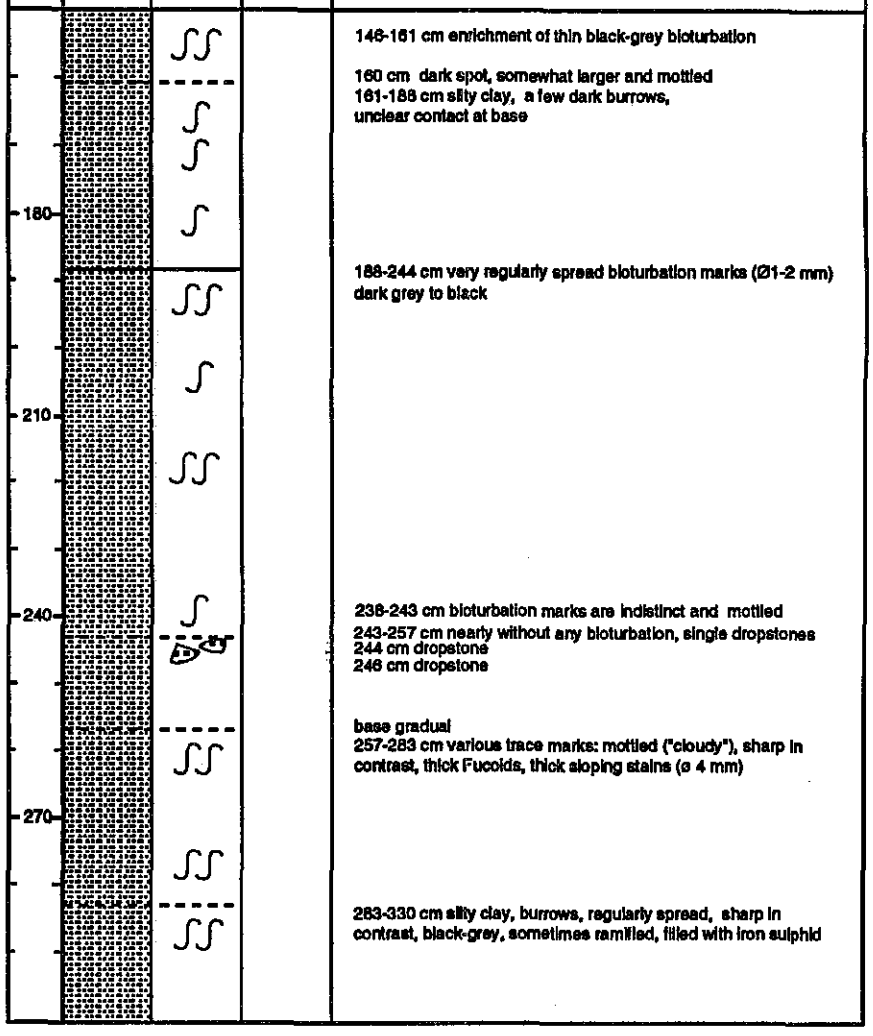

Figure . continued

METEOR 26/3 — **27.10.1993 - 25.11.1993**
Station: M 26/3-542 — **Date: 29.10.1993**
Position: 64° 46,00´ N ; 4° 30,15´ E — **Water Depth: 872 m**

Core: M 26/3 GIK 23503-1 — **Core Recovery: 991 cm**
Section: 300 - 450 cm

Depth (cm)	Lithology	Structure	Colour	Description
330				283-330 cm slightly silty clay, burrows, regularly spread, sharp in contrast, black-grey, sometimes ramified, filled with iron sulphid 302 cm narrow layer with horizontally orientated Lamellibranchiata shells
360				
390				
420				400-429 cm slightly silty clay with distinct, irregularly shaped, black stains of iron sulphid 429-436 cm gap caused by shrinking 429-436 cm slightly silty clay with distinct, irregularly shaped, black stains of iron sulphid

Figure . continued

Meteor 26/3 — **27.10.1993 - 25.11.1993**
Station: M 26/3-542 — **Date: 07.11.1993**
Position: 64° 46,00´ N ; 4° 30,15´ E — **Water Depth: 872 m**

Core: M 26/3 GIK 23503-1 — **Core Recovery: 991 cm**
Section: 450-600 cm

Depth (cm)	Lithology	Structure	Colour	Description
				450-529 cm slightly silty clay
		∫		470-496 cm mottled (and hazy)
480				
		∫		
510				
		∫		529-548 cm "flag" with hazy contours 548-560 cm same below, a bit lighter
540				
		∫		
570				

Figure . continued

METEOR 26/3	27.10.1993 - 25.11.1993
Station: M 26/3-542	Date: 07.11.1993
Position: 64° 46,00´ N ; 4° 30,15´ E	Water Depth: 872 m

Core: M 26/3 GIK 23503-1 — Core Recovery: 991 cm
Section: 600 - 750 cm

Depth (cm)	Lithology	Structure	Colour	Description
			dark grey	615-631 cm slightly silty clay, colour of matrix changes to dark grey, it remains olive grey (as above) around the dark stains
630			olive grey	631-645 cm as above but again olive grey
				645-664 cm as above but only a few blackish spots, grey bioturbation, between 654-662 cm diffuse
680				664-711 cm slightly silty clay, clear in contrast, sometimes sloping stains 671-682 cm diffuse
690				
			grey	711-731 cm silty clay 711-717 cm diffuse indistinct dark grey stains
720				722-724 cm big dropstone (cristalline)
			olive grey	731-763 cm olive grey silty clay with blackish worm-like spatula stains

Figure . continued

METEOR 26/3	27.10.1993 - 25.11.1993
Station: M 26/3-542	Date: 07.11.1993
Position: 64° 46,00´ N ; 4° 30,15´ E	Water Depth: 872 m

Core: M 26/3 GIK 23503-1 — Core Recovery: 991 cm
Section: 750 - 900 cm

Depth (cm)	Lithology	Structure	Colour	Description
				731-763 cm olive grey silty clay with blackish worm-like spatula stains
				763-795 cm nearly without stains but diffuse black-grey mottled
780				780-784 cm thin Floekus layer
			grey	795-855 cm silty clay dark mottled "spätels"
810				
840				844-852 cm single small shell remains
				base gradual 855-899 cm silty clay, hardly any stains, contact at top as well at bottom a bit sloping
870				874-886 cm again black spatula with dark surroundings

Figure . continued

METEOR 26/3 — **27.10.1993 - 25.11.1993**
Station: M 26/3-542 — **Date: 07.11.1993**
Position: 64° 46,00´ N ; 4° 30,15´ E — **Water Depth: 872 m**

Core: M 26/3 GIK 23503-1 — **Core Recovery: 991 cm**
Section: 900 - 991 cm

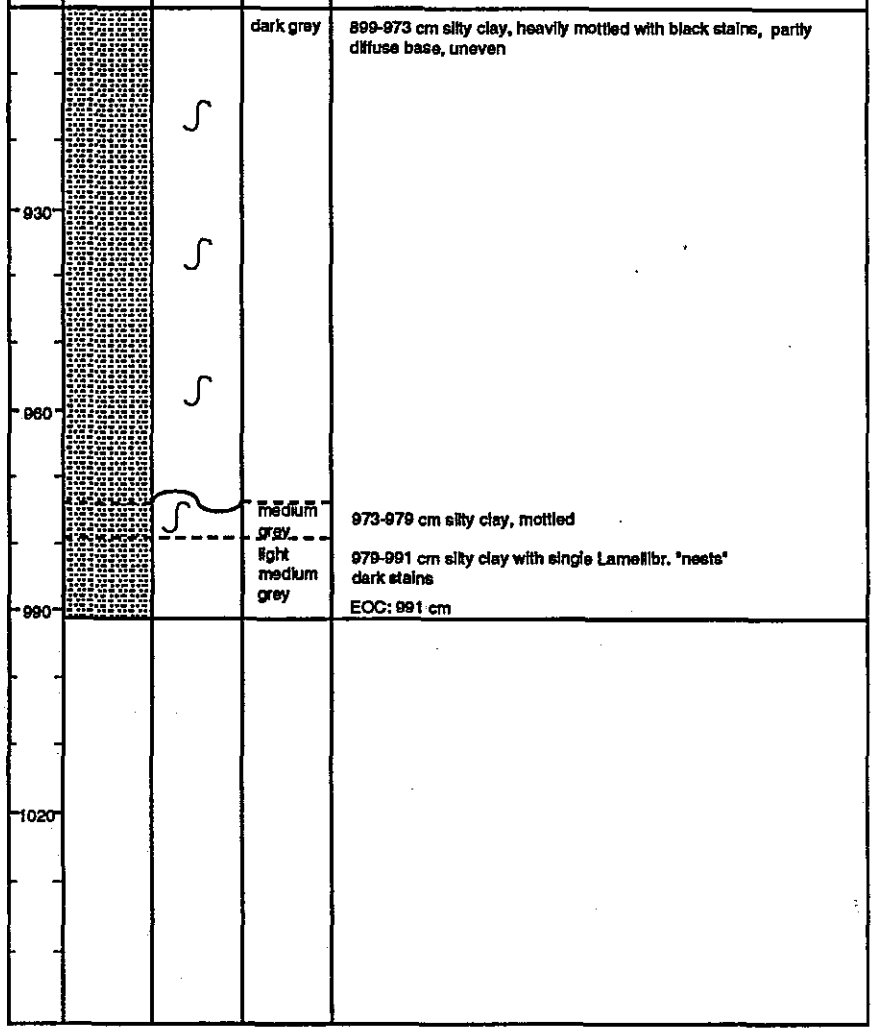

Figure . continued

Meteor 26/3 — **27.10.1993 - 25.11.1993**
Station: M 26/3-551 — **Date: 12.11.1993**
Position: 69° 41,45´ N ; 08° 28,68´ E — **Water Depth: 3291 m**

Core: M 26/3 GIK 23505-1 — **Core Recovery: 55 cm**
Section: 0 - 55 cm

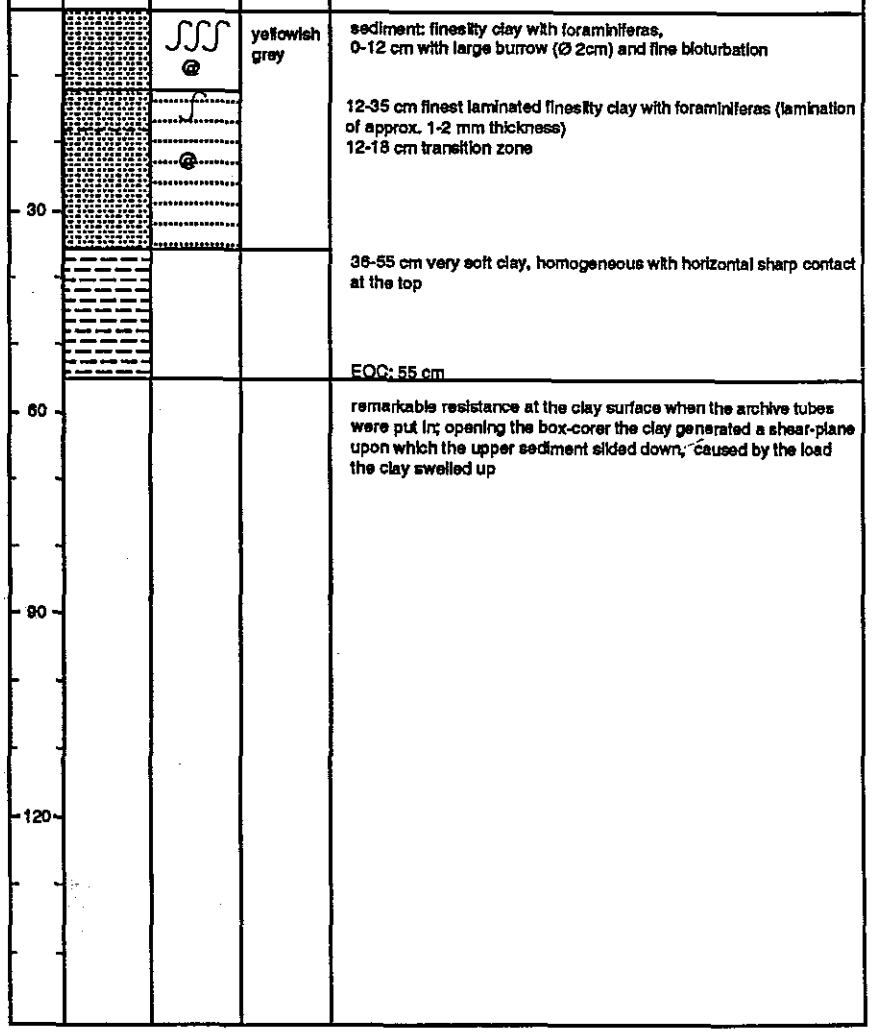

Figure . Description of sediment column of core GIK 23505-1

Meteor 26/3 — 27.10.1993 - 25.11.1993
Station: M 26/3-552-4 — Date: 14.11.1993
Position: 72° 23,60´ N ; 07° 36,26 W — Water Depth: 2666 m

Core: M 26/3 GIK 23506-1 — Core Recovery: 35 cm
Section: 0 - 35 cm

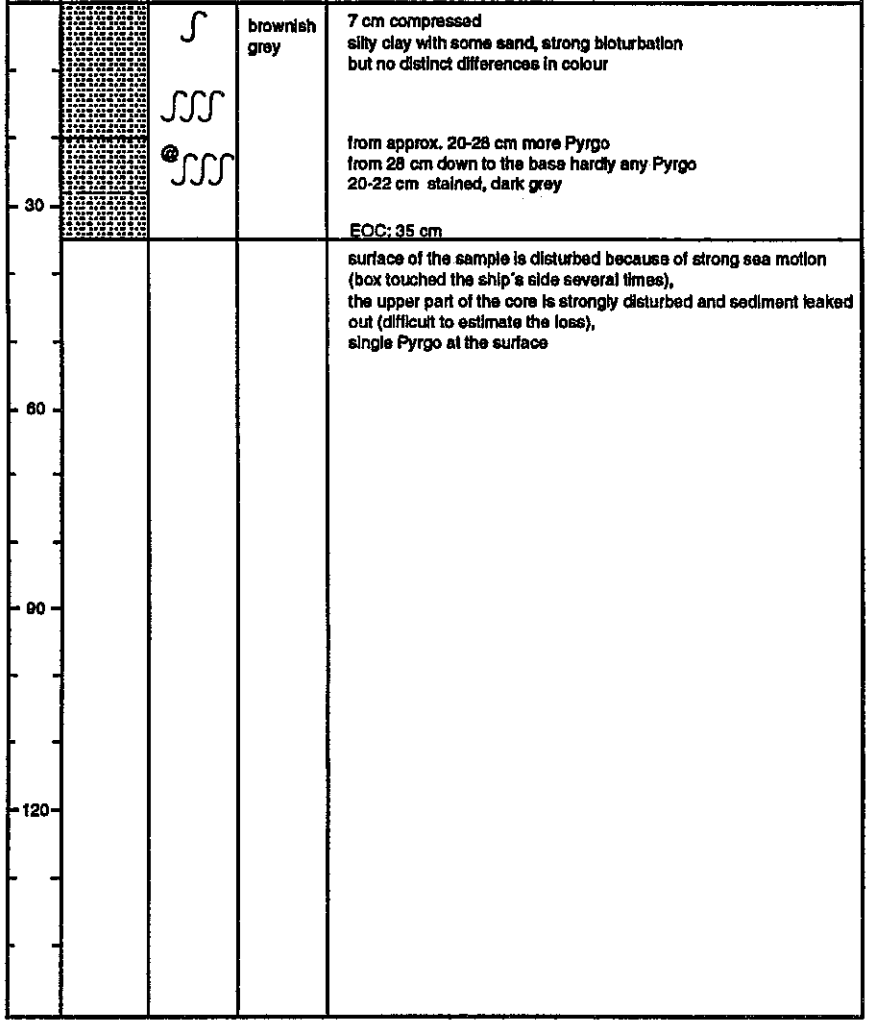

Figure . Description of sediment column of core GIK 23506-1

Meteor 26/3 — 27.10.1993 - 25.11.1993
Station: M 26/3-556 — Date: 15.11.1993
Position: 73° 49,73´ N ; 09° 14,87´ W — Water Depth: 3149 m

Core: M 26/3 GIK 23507-1 — Core Recovery: 47 cm
Section: 0 - 47 cm

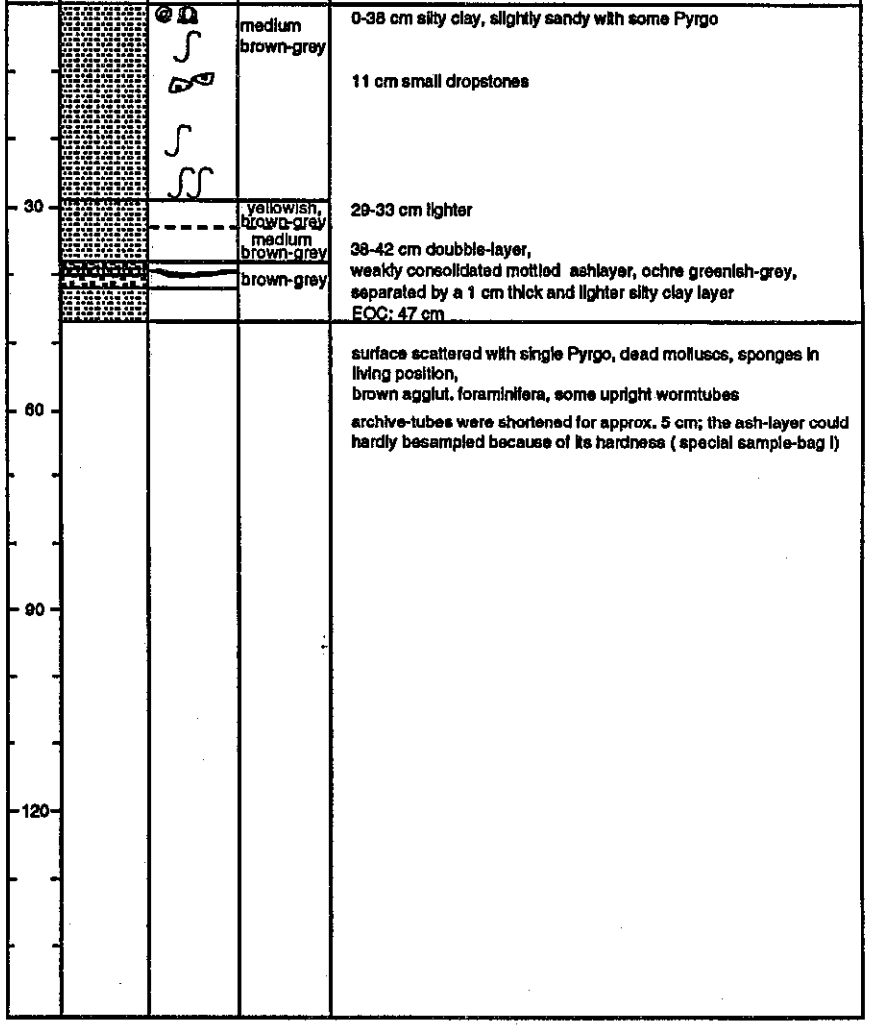

Figure . Description of sediment column of core GIK 23507-1

Meteor 26/3 — 27.10.1993 - 25.11.1993
Station: M 26/3-557 — Date: 15.11.1993
Position: 73° 51,60´ N ; 09° 23,60´ W — Water Depth: 3201 m

Core: M 26/3 GIK 23508-1 — Core Recovery: 47 cm
Section: 0 - 47 cm

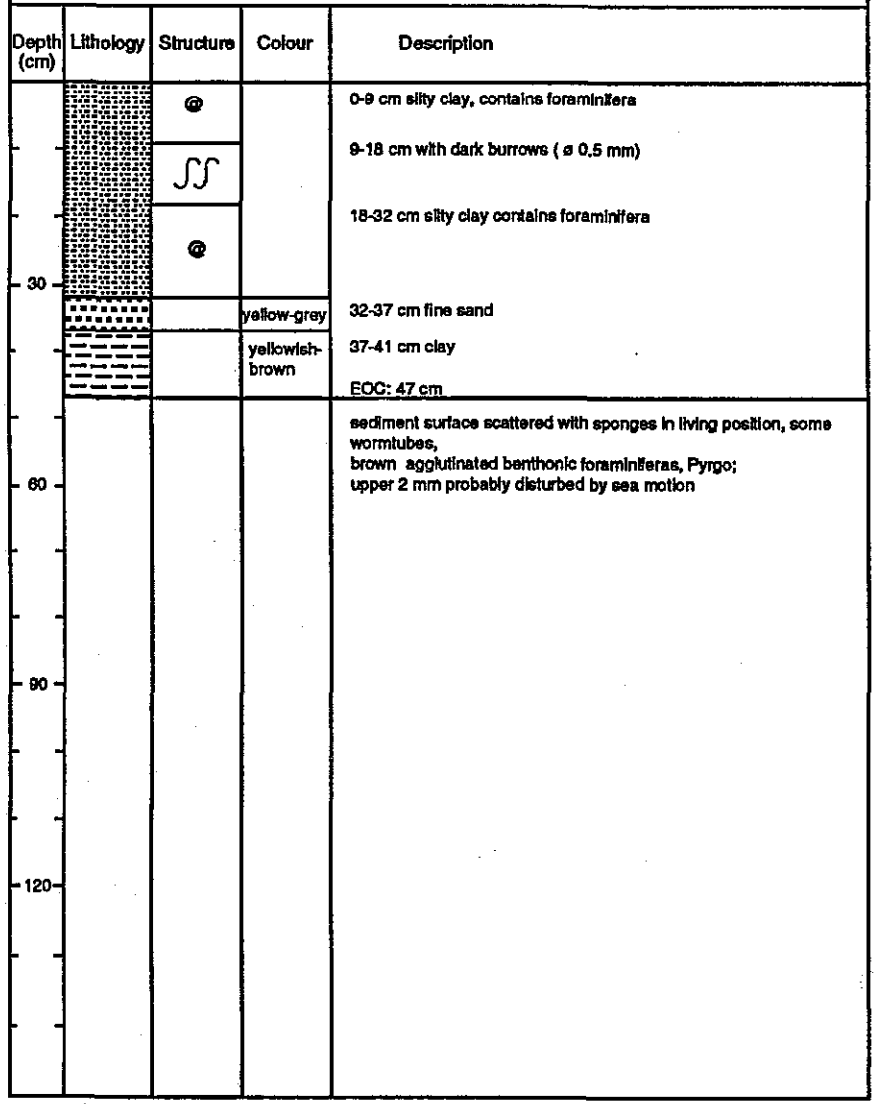

Figure . Description of sediment column of core GIK 23508-1

METEOR 26/3 — 27.10.1993 - 25.11.1993
Station: M 26/3-559 — Date: 17.11.1993
Position: 73° 50,0´ N ; 13° 30,1´ W — Water Depth: 2576 m

Core: M 26/3 GIK 23509-1 — Core Recovery: 37 cm
Section: 0 - 37 cm

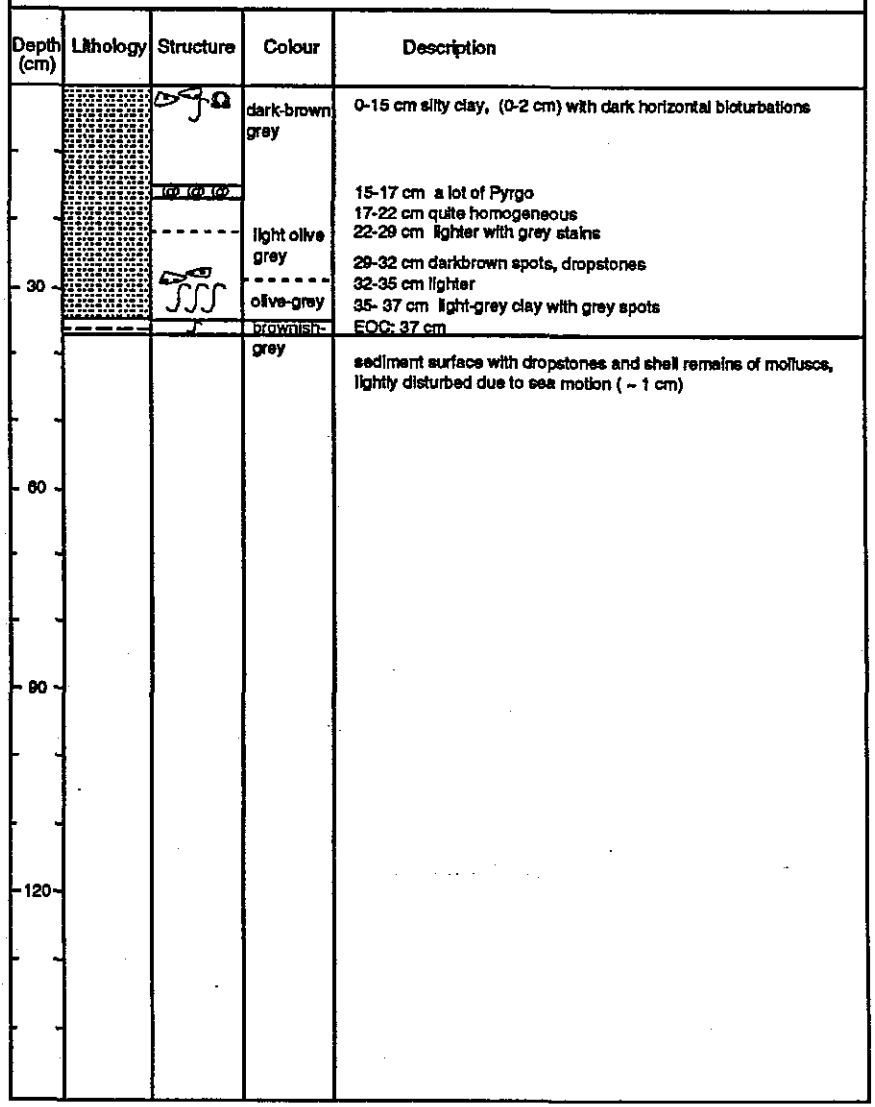

Figure . Description of sediment column of core GIK 23509-1

Meteor 26/3 — 27.10.1993 - 25.11.1993
Station: M 26/3-564 — Date: 17.11.1993
Position: 73° 13,09´ N ; 15° 01,20´ W — Water Depth: 2298 m

Core: M 26/3 GIK 23511-2 — Core Recovery: 42 cm
Section: 0 - 42 cm

Depth (cm)	Lithology	Structure	Colour	Description
			greenish-grey	0-5 cm silty clay, bioturbated
			olive-grey	5-31 cm silty clay, weakly bioturbated
30				31-35 cm brownish and black stains of sulphur with dark burrows
				35-42 cm same but greyer
				EOC: 42 cm
				sediment surface disturbed by sea motion (~2 cm) single sponges
60				
90				
120				

Figure . Description of sediment column of core GIK 23511-2

Meteor 26/3 — 27.10.1993 - 25.11.1993
Station: M 26/3-568 — Date: 18.11.1993
Position: 72° 56,44´ N ; 13° 25,39´ W — Water Depth: 2612 m

Core: M 26/3 GIK 23512-1 — Core Recovery: 41 cm
Section: 0 - 41 cm

Depth (cm)	Lithology	Structure	Colour	Description
			medium-brown	0-25 cm homogeneous silty clay, upper 1-2 cm with dark horizontal big burrows
				17-25 cm some more Pyrgo
				from 18 cm down smaller dropstones
30			slightly lighter brown	25-29 cm lighter
				29-34 cm darker again
			reddish-brown	34-41 cm reddish
				EOC: 41 cm
				sediment surface with empty shells, crinoids on stalks, tube-building structures slightly disturbed
60				
90				
120				

Figure . Description of sediment column of core GIK 23512-1

Meteor 26/3	**28.10.1993 - 26.11.1993**
Station:501	**Date:** 29.10.1993
Position: 64° 20.732' N, 8° 23.664' E	**Water Depth:** 289 m

Core: VB 23490 - 2	**Core Recovery:** 312cm
Section: 0 - 100 cm	**Sheet:** 1/4

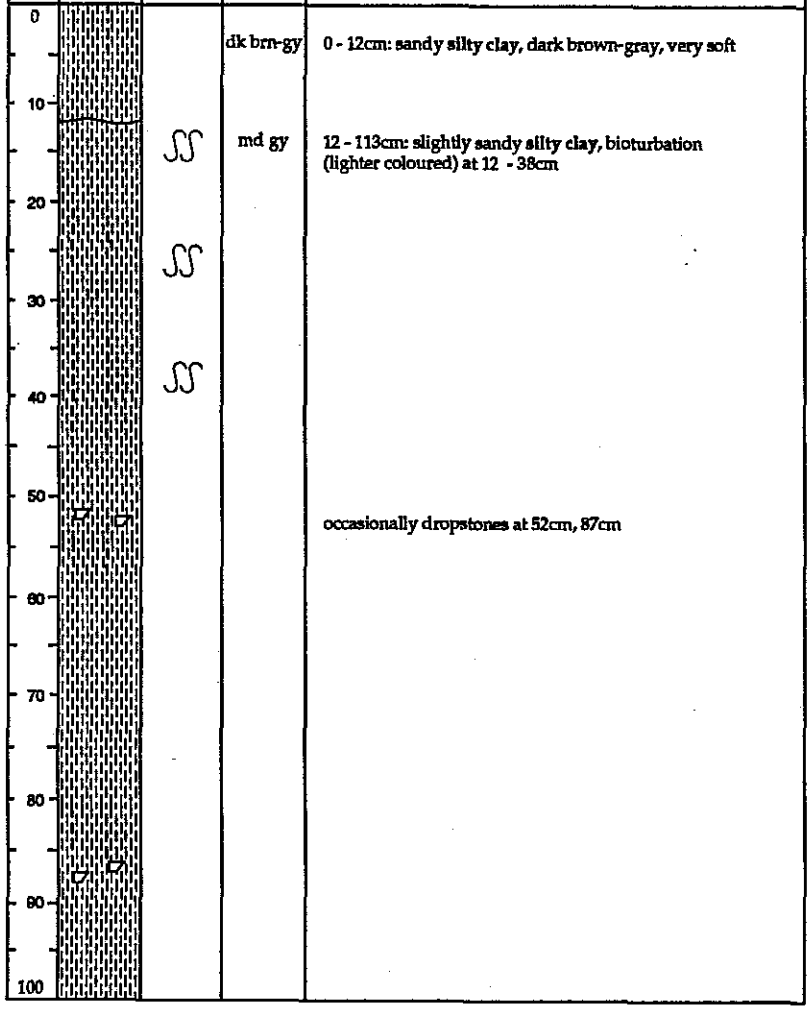

Meteor 26/3	**28.10.1993 - 26.11.1993**
Station: 501	**Date:** 29.10.1993
Position: 64° 20.732' N, 8° 23.664' E	**Water Depth:** 289 m

Core: VB 23490 - 2	**Core Recovery:** 312cm
Section: 100 - 200 cm	**Sheet:** 2/4

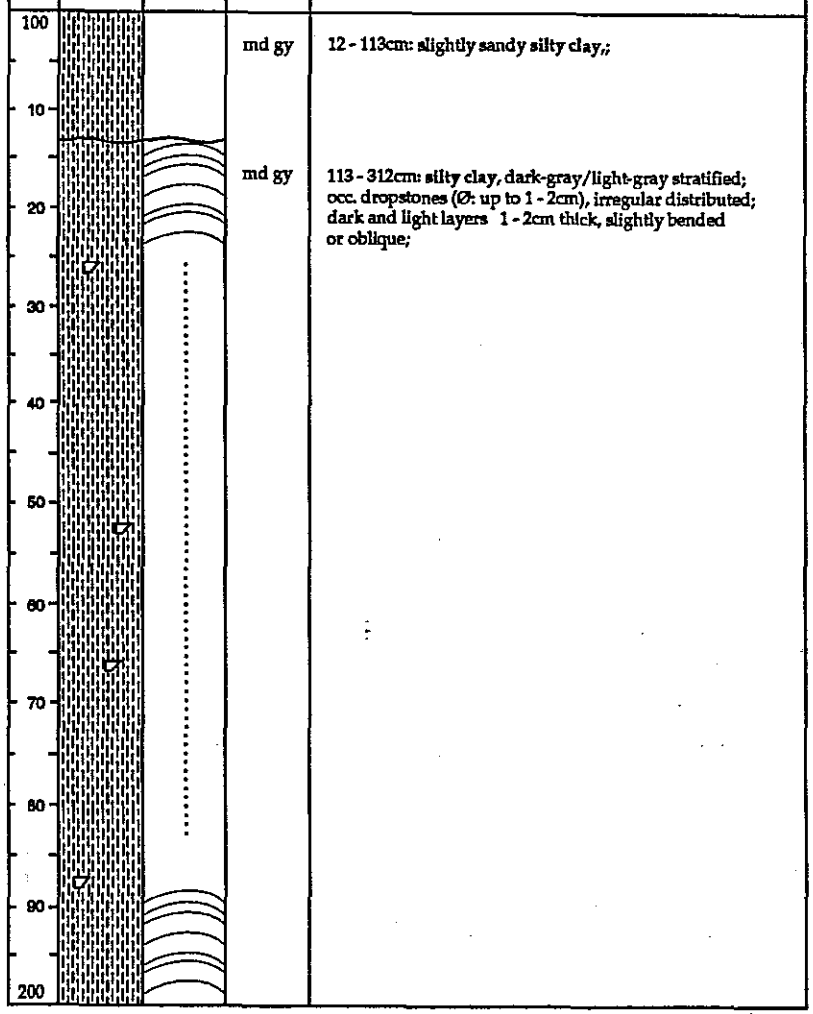

Meteor 26/3	**28.10.1993 - 26.11.1993**
Station: 501	**Date:** 29.10.1993
Position: 64° 20.732' N, 8° 23.664' E	**Water Depth:** 289 m

Core: VB 23490 - 2	**Core Recovery:** 312cm
Section: 200 - 300 cm	**Sheet:** 3/4

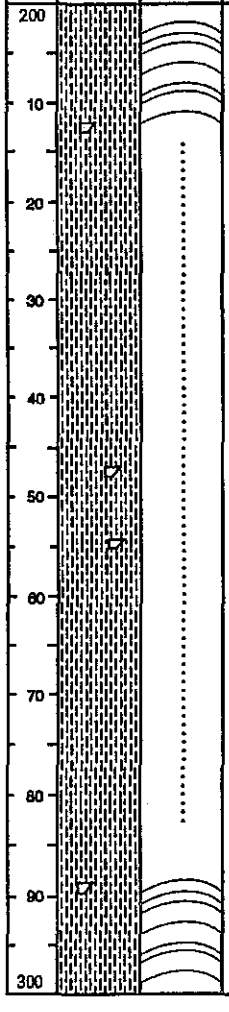

Colour	Description
md gy	113 - 312cm: silty clay, dark-gray/light-gray stratified; occ. dropstones (Ø: up to 1 - 2cm), irregular distributed; dark and light layers: 1 - 2cm thick, slightly bended or oblique;

Meteor 26/3	**28.10.1993 - 26.11.1993**
Station: 501	**Date:** 29.10.1993
Position: 64° 20.732' N, 8° 23.664' E	**Water Depth:** 289 m

Core: VB 23490 - 2	**Core Recovery:** 312cm
Section: 300 - 400 cm	**Sheet:** 4/4

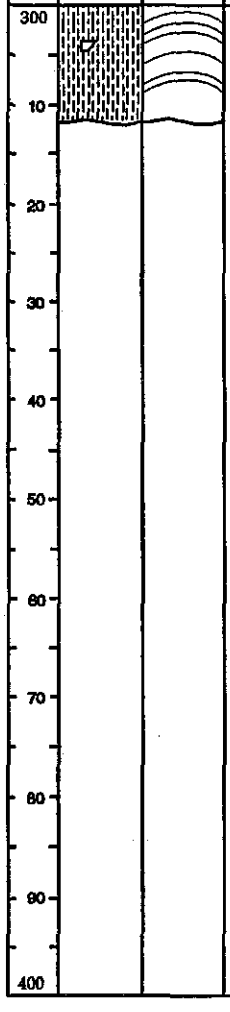

Colour	Description
md gy	113 - 312cm: silty clay, dark-gray/light-gray stratified; occ. dropstones (Ø: up to 1 - 2cm), irregular distributed; dark and light layers 1 - 2cm thick, slightly bended or oblique; 312cm: base of core

Meteor 26/3	**28.10.1993 - 26.11.1993**
Station: 502	**Date:** 29.10.1993
Position: 64° 21.634' N, 8° 21.378' E	**Water Depth:** 277 m

Core: VB 23491 - 1	**Core Recovery:** 477cm
Section: 0-100 cm	**Sheet:** 1/5

Depth [cm]	Lithology	Structure	Colour	Description
0			brn - gy	0 - 4cm: sandy silty clay, brownish-gray, foraminifers, semi-liquid;
			brn - gy	4 - 9cm: sandy silty clay, brownish-gray, foraminifers, occasionally gastropods;
10		SS		9 - 31cm: slightly sandy silty clay, bioturbation (darker);
20				
30			dk-gy, (brn)	31 - 224cm: dark gray, slightly brownish silty clay with black spots, occasionally gastropods; horizontal, homogeneous brown layers at 200 - 210cm;
40				
50				
60				
70		S		
80		S		
90				
100				

Meteor 26/3	**28.10.1993 - 26.11.1993**
Station: 502	**Date:** 29.10.1993
Position: 64° 21.634' N, 8° 21.378' E	**Water Depth:** 277 m

Core: VB 23491 - 1	**Core Recovery:** 477cm
Section: 100 - 200 cm	**Sheet:** 2/5

Depth [cm]	Lithology	Structure	Colour	Description
100			dk-gy, (brn)	31 - 224cm: dark gray, slightly brownish silty clay with black spots, very homogeneous, occasionally gastropods; horizontal;
10				
20				
30				
40				
50				
60				
70				
80				
90				
200				

Meteor 26/3	**28.10.1993 - 26.11.1993**
Station: 502	**Date:** 29.10.1993
Position: 64° 21.634' N, 8° 21.378' E	**Water Depth:** 277 m

Core: VB 23491 - 1	**Core Recovery:** 477cm
Section: 200 - 300 cm	**Sheet:** 3/5

Depth [cm]	Lithology	Structure	Colour	Description
200		∫∫	dk-gy, (brn)	31 - 224cm: dark gray, slightly brownish silty clay with black spots, very homogeneous, occationally gastropods; horizontal, homogeneous brown layers at 200 - 210cm;
10				
20				
30				224 - 477cm: gray, slightly brownish silty clay, frequent dropstones and mudclasts, bioturbation at 240 - 250cm: dark-gray in lighter coloured matrix; abundant IRD at 270cm, 290 - 310cm, 360cm, 430cm and 455cm: Ø up to 4 - 5cm;
40				
50		∫∫		
60				
70				
80				
90				
200				

Meteor 26/3	**28.10.1993 - 26.11.1993**
Station: 502	**Date:** 29.10.1993
Position: 64° 21.634' N, 8° 21.378' E	**Water Depth:** 277 m

Core: VB 23491 - 1	**Core Recovery:** 477cm
Section: 300 - 400 cm	**Sheet:** 4/5

Depth [cm]	Lithology	Structure	Colour	Description
300			dk-gy, (brn)	224 - 477cm: gray, slightly brownish silty clay, frequent dropstones and mudclasts, bioturbation at 240 - 250cm: dark-gray in lighter coloured matrix; abundant IRD at 270cm, 290 - 310cm, 360cm, 430cm and 455cm: Ø up to 4 - 5cm;
10				
20				
30				
40				
50				
60				364 - 386cm: frequently mudclasts and dropstones (Ø 1mm);
70				
80				
90				
400				

Meteor 26/3 — **28.10.1993 - 26.11.1993**
Station: 502 — **Date:** 29.10.1993
Position: 64° 21.634' N, 8° 21.378' E — **Water Depth:** 277 m

Core: VB 23491 - 1 — **Core Recovery:** 477cm
Section: 400 - 500 cm — **Sheet:** 5/5

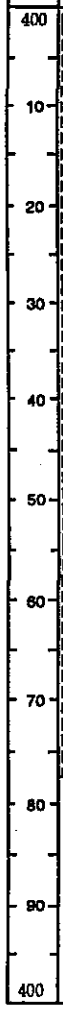

Lithology	Structure	Colour	Description
		dk-gy, (brn)	224 - 477cm: gray, slightly brownish silty clay, frequent dropstones and mudclasts, bioturbation at 240 - 250cm: dark-gray in lighter coloured matrix; abundant IRD at 270cm, 290 - 310cm, 360cm, 430cm and 455cm: Ø up to 4 - 5cm;
			477cm: base of core

Meteor 26/3 — **28.10.1993 - 26.11.1993**
Station: 503 - 3 — **Date:** 29.10.1993
Position: 64° 18.023 N, 8° 09.575' E — **Water Depth:** 284 m

Core: VB 23492 - 3 — **Core Recovery:** 234 cm
Section: 0 - 100cm — **Sheet:** 1/3

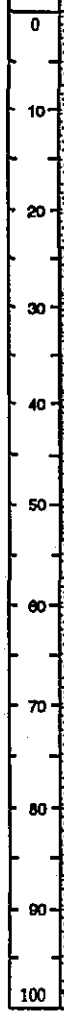

Lithology	Structure	Colour	Description
		dk gn	0 - 24cm: dark greenish, almost clay-free glauconitic sand, foraminifers and sporadic moluscs, high water content, running off
		gy - gn	24 - 50cm: gray-greenish, clayey and sandy silt, lower boundary oblique: 46 - 55cm, with occasionally big molluscs
		blk - gn	50 - 84cm: blackish - greenish glauconitic sand, lower boundary oblique: 83 - 87cm
		gy - gn	84 - 99cm: slightly finer-grained, grayish-greenish glauconitic sand, bioturbated (darker) at the basis, lower boundary horizontal

Meteor 26/3	**28.10.1993 - 26.11.1993**
Station: 503 - 3	**Date:** 29.10.1993
Position: 64° 18.023 N, 8° 09.575' E	**Water Depth:** 284 m

Core: VB 23492 - 3	**Core Recovery:** 234 cm
Section: 100 - 200cm	**Sheet:** 2/3

Depth [cm]	Lithology	Structure	Colour	Description
100		none (homog.)	dk gn	99 - 178cm: dark-green, coarse-grained glauconitic sand, vaguely horizontally stratified, no graded bedding visible, distinct basis
			blk - gn	178 - 192cm: blackish-greenish, firm, clayey glauconitic sand, more sandy intercalation at 183 - 186cm
200				

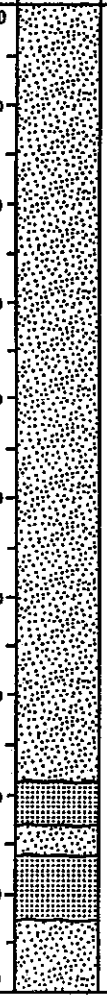

Meteor 26/3	**28.10.1993 - 26.11.1993**
Station: 503 - 3	**Date:** 29.10.1993
Position: 64° 18.023 N, 8° 09.575' E	**Water Depth:** 284 m

Core: VB 23492 - 3	**Core Recovery:** 234 cm
Section: 200 - 300cm	**Sheet:** 3/3

Depth [cm]	Lithology	Structure	Colour	Description
200			dk yel - gn	192cm - basis: dark-yellowish-greenish, coarse-grained glauconitic sand, with sub-horizontal bioturbation (lighter)
				from 205cm downwards: inner part of core missing (ran off)
				234cm: base of core
300				

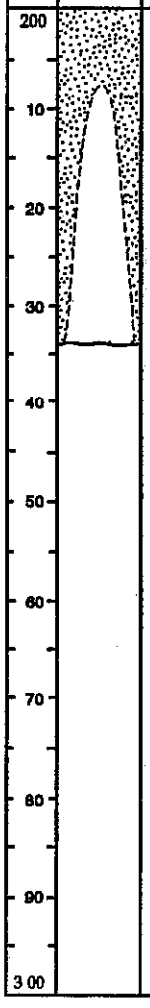

Meteor 26/3 — **28.10.1993 - 26.11.1993**
Station: 504 — **Date:** 29.10.1993
Position: 64° 18.356 N, 8° 09.244 E — **Water Depth:** 283.8 m

Core: VB 23495 - 1 — **Core Recovery:** 382 cm
Section: 0 - 100cm — **Sheet:** 1/4

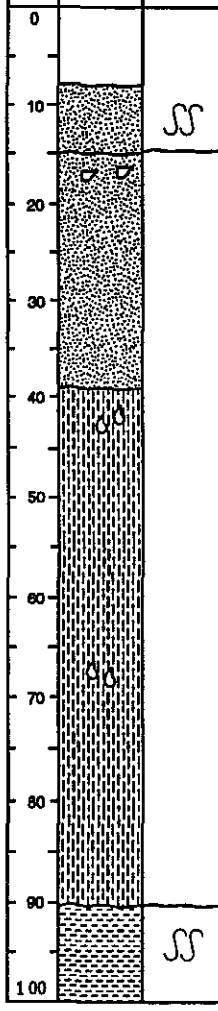

Lithology	Structure	Colour	Description
			0 - 8cm: ran off
		lt olv-gy	8 - 39cm: slightly sandy silt, light olive-gray, bioturbated to 15cm; below: enrichment of fine-grained micaceous dropstones
		lt olv-gy	39 - 90cm: clayey silt, light olive-gray, mollusc-shells at 42cm and 68cm
		gy	90 - 100cm: gray clay with some sand grains, bioturbated

Meteor 26/3 — **28.10.1993 - 26.11.1993**
Station: 504 — **Date:** 29.10.1993
Position: 64° 18.356 N, 8° 09.244 E — **Water Depth:** 283.8 m

Core: VB 23495 - 1 — **Core Recovery:** 382 cm
Section: 100 - 200cm — **Sheet:** 2/4

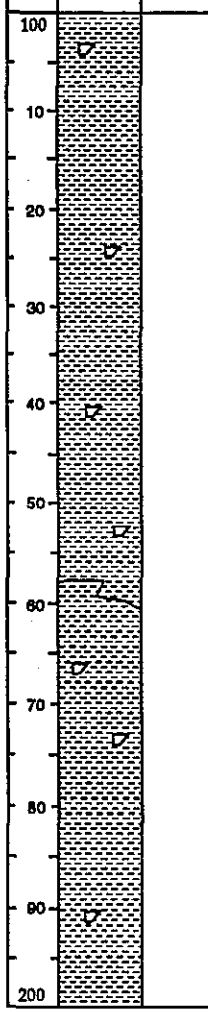

Lithology	Structure	Colour	Description
		md gy	100 - 158cm: gray clay, almost free of silt; occasionally dropstones (Ø: ~3cm); lower boundary wavy deflected, distinct change in colour from darker to lighter gray;
		olv-gy	
		lt gy	158 - 285cm: : light-gray clay, clean; occasionally dropstones (Ø: ~2mm);

Meteor 26/3	**28.10.1993 - 26.11.1993**
Station: 504	**Date:** 29.10.1993
Position: 64° 18.356 N, 8° 09.244 E	**Water Depth:** 283.8 m

Core: VB 23495 - 1	**Core Recovery:** 382 cm
Section: 200 - 300cm	**Sheet:** 3/4

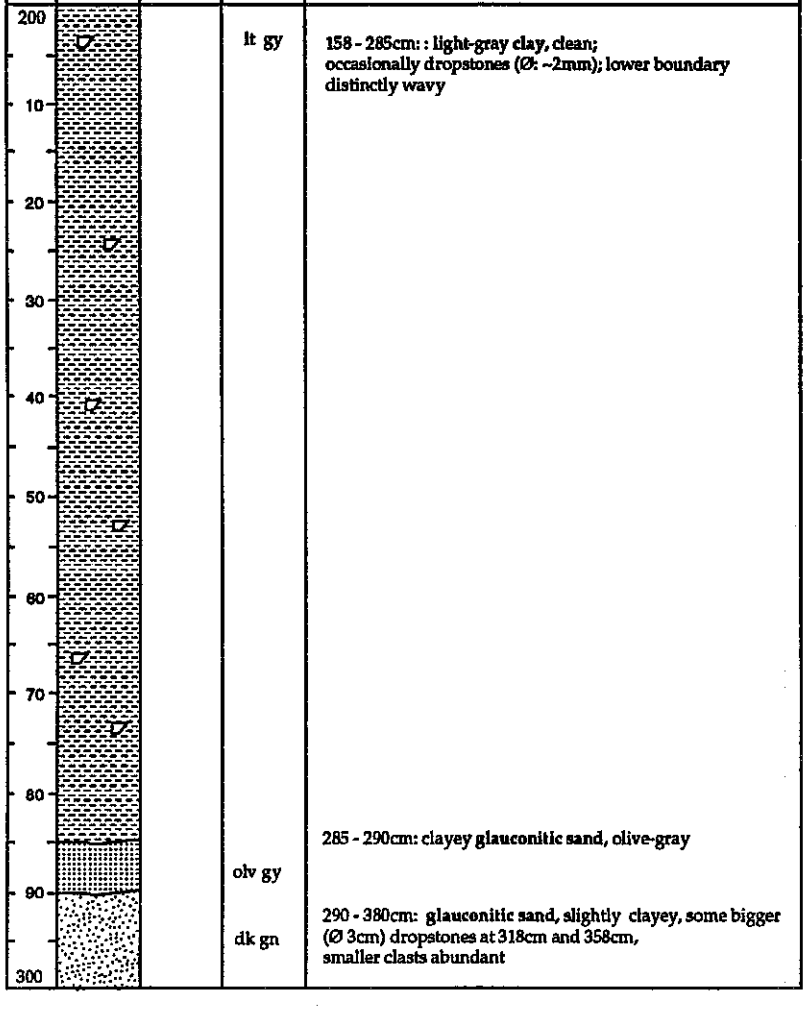

Meteor 26/3	**28.10.1993 - 26.11.1993**
Station: 504	**Date:** 29.10.1993
Position: 64° 18.356 N, 8° 09.244 E	**Water Depth:** 283.8 m

Core: VB 23495 - 1	**Core Recovery:** 382 cm
Section: 300 - 400cm	**Sheet:** 4/4

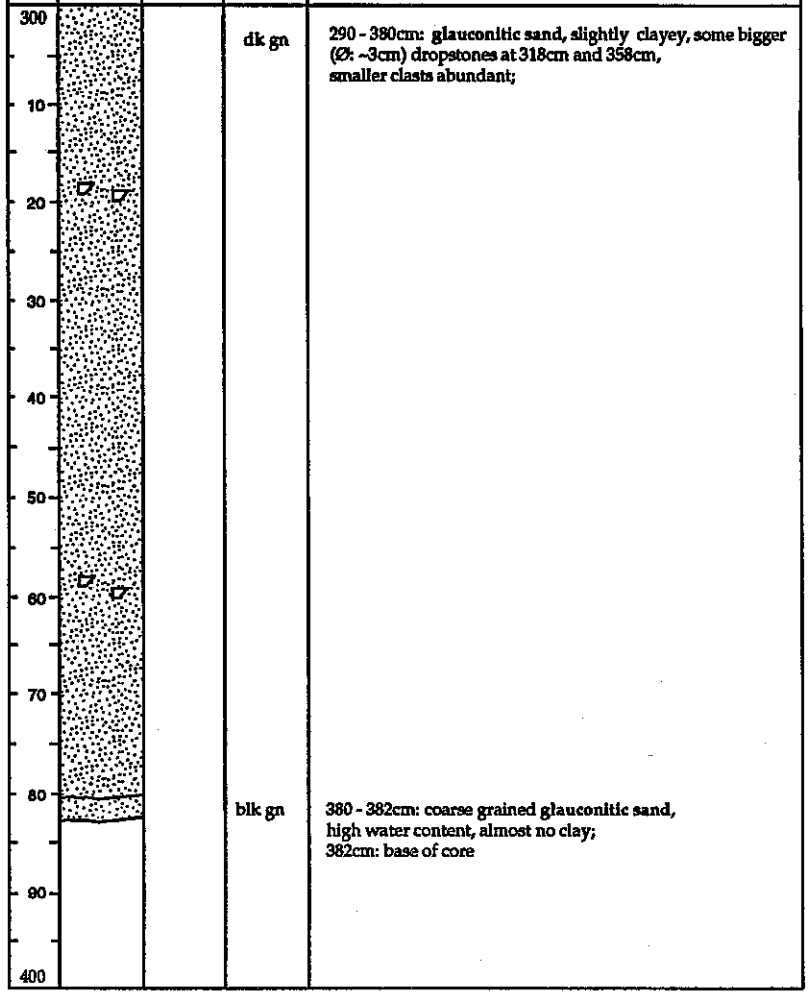

Meteor 26/3 | **28.10.1993 - 26.11.1993**
Station: 505 | **Date:** 29.10.1993
Position: 64° 17.333' N, 8° 12.418' E | **Water Depth:** 334 m

Core: VB 23496 - 1 | **Core Recovery:** 482 cm
Section: 0-100 cm | **Sheet:** 1/5

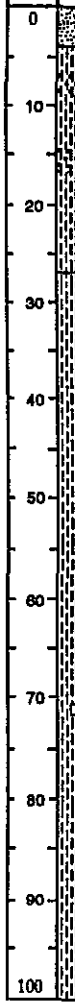

Lithology	Structure	Colour	Description
			0 - 4cm: silty clayey sand;
			4 - 27cm: silty clay with some sand and gravel, bioturbated;
		gy - gn	27 - 139cm: gray-brown silty clay with some dropstones;

Meteor 26/3 | **28.10.1993 - 26.11.1993**
Station: 505 | **Date:** 29.10.1993
Position: 64° 17.333' N, 8° 12.418' E | **Water Depth:** 334 m

Core: VB 23496 - 1 | **Core Recovery:** 482 cm
Section: 100 - 200 cm | **Sheet:** 2/5

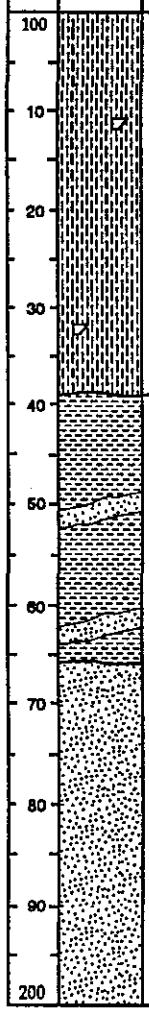

Lithology	Structure	Colour	Description
		gy - brn	27 - 139cm: gray-brown silty clay with some dropstones;
		dk gy	139 - 166cm: dark-gray layered clay, irregular sand layers, clay pellets directly below upper boundary;
		dk gy-gn	166 - 200cm: dark grayish-greenish glauconitic sand;

Meteor 26/3	**28.10.1993 - 26.11.1993**
Station: 505	**Date:** 29.10.1993
Position: 64° 17.333' N, 8° 12.418' E	**Water Depth:** 334 m

Core: VB 23496 - 1	**Core Recovery:** 482 cm
Section: 200 - 300 cm	**Sheet:** 3/5

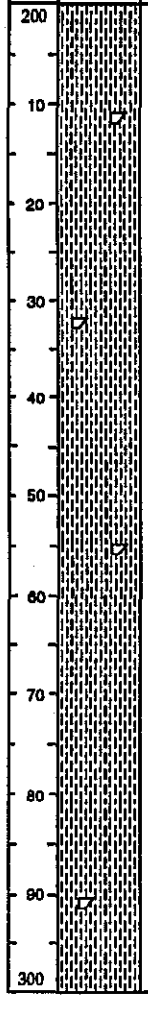

Meteor 26/3	**28.10.1993 - 26.11.1993**
Station: 505	**Date:** 29.10.1993
Position: 64° 17.333' N, 8° 12.418' E	**Water Depth:** 334 m

Core: VB 23496 - 1	**Core Recovery:** 482 cm
Section: 300 - 400 cm	**Sheet:** 4/5

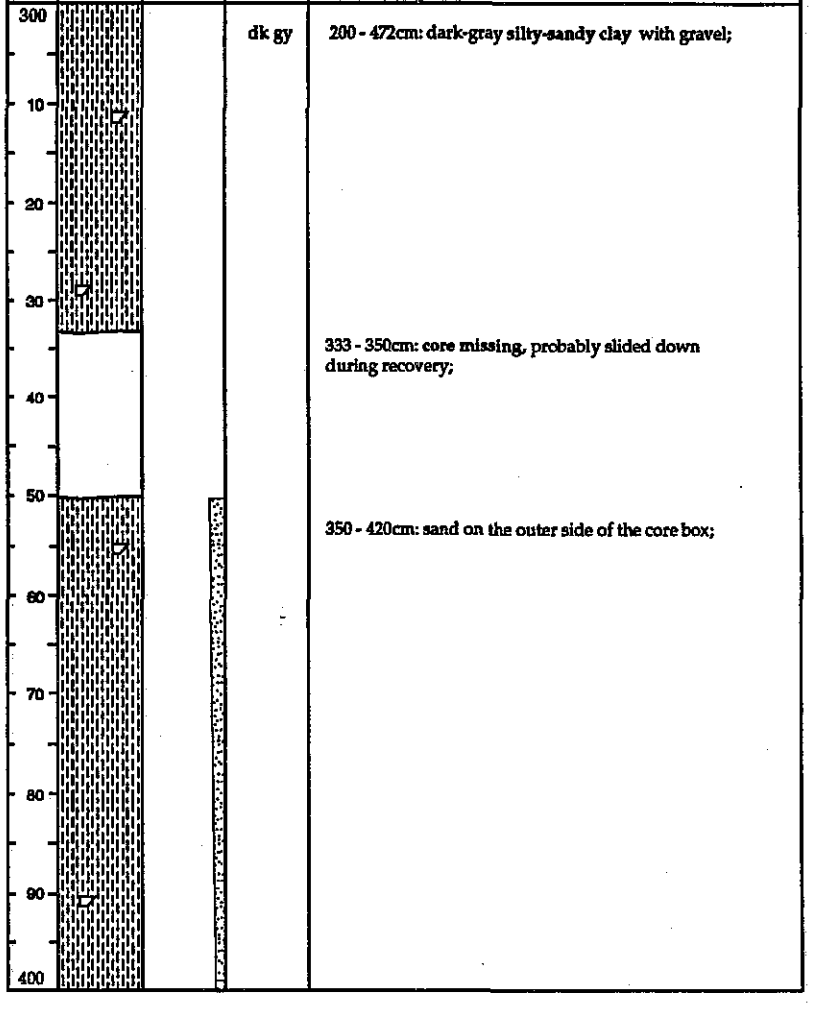

Meteor 26/3	**28.10.1993 - 26.11.1993**
Station: 505	**Date:** 29.10.1993
Position: 64° 17.333' N, 8° 12.418' E	**Water Depth:** 334 m

Core: VB 23496 - 1	**Core Recovery:** 482 cm
Section: 400 - 500 cm	**Sheet:** 5/5

Depth [cm]	Lithology	Structure	Colour	Description
400			dk gy	200 - 472cm: dark-gray silty-sandy clay with gravel;
10				350 - 420cm: sand on the outer side of the core box;
20				
30				
40				
50				
60				
70				
80				
90				
500				

Clay/Claystone (T1)

Silty Clay/Clayey Silt (T8)

Sand/Sandstone (T6)

Sandy Clay/Clayey Sand (T9)

Silty Sand/Sandy Silt (T7)

Gravel (SR1)

Erratic Clasts (Dropstones)

Shells (-Fragments)

Bioturbation

Clay Pellets

dk: dark
md: middle
lt: light
brn: brown/-ish
gy: gray/-ey
gn: green/-ish
blk: black/-ish
yel: yellow/-ish

8 Concluding Remarks and Acknowledgements (E. Suess)

The 26th voyage of RV METEOR served a multidisciplinary group of projects and hence required a great deal of coordination. This was made easy by all involved. In general the sampling programs and surveys were sufficiently completed in order to be considered a success. However, sample recovery, with the exception of work south of 50°N, was adversely affected by unfavorable weather throughout.

In addition, the work at sea during M 26 exemplified the changing scientific approach which is typical for the modern marine geological and biogeochemical sciences and which also determines successful sample recovery. Sediment coring, rock dredging, hydrocasting, acoustic profiling are still indispensable methods to obtain the necessary data. But these conventional methods are increasingly supplemented and more closely tied to *in situ* measurements, long-term observations, and *in situ* tests. The targets for studies are becoming smaller and more selective as well. In a concluding assessment it is interesting to take a look at the future in order to ascertain continued success and high standing of marine research.

The continuous chemical profiling of the ocean surface layers employing the "Kiel Pumping System" and the recovery and re-deployment of the JGOFS long-term sediment traps and those of the SFB 313 are examples of the indispensable modern tools. The continuous pumping system and the wealth of data it generated have already proven to be a cornerstone for all of the associated JGOFS-programs. The general availability of such a system should be assured.

The *in situ* and continuous methane detection system MEDUSA and the Geomar-VESP for measuring vent activities are other modern tools with potential for enormous scientific success. Currently both are prototypes and need improvements. The PUPPI (pop-up pore pressure instrument), MG-Brest (module geotechnique) and HF-OHS (high frequency ocean bottom hydrophone) are also three modern tools, one of them a prototype, which were important to the success of Leg M 26. The deployment of these tools require special shipboard routines. For examples, the small size of the targets such as vents, craters, sub-surface acoustic anomalies, plumes or special substrates and the complexity of modern instrumentation proved to be a challenge in attaining the scientific goals. Re-occupying active vent locations, presumably a few tens of square meters in size only, require exceptional navigational and nautical capabilities. In the Skagerrak, where active vents have been known for years, the side-scan sonar-, Parasound-, and video-surveys conducted during M 26/2 failed to image any of them. In spite of this, good samples were obtained by gravity coring, but through sheer serendipity. In the future, accurate sampling over a small target might be accomplished by dynamic positioning or remotely operated vehicles (ROVs) which could deployed from board the RV METEOR.

The overall success of M 26, inspite of adverse weather, was in large part due to the dedication of everybody aboard. We wish to thank in particular Cpt. Bruns, the officers and crew for their unwavering support and ingenuity to help the scientific work along. The üs Leitstelle METEOR at the University of Hamburg, as always, ensured smooth and speedy port calls and exchange of scientific crew and equipment. Special thanks are due to the Deutsche Forschungsgemeinschaft for making available generous shiptime and funding for coordinating the cruise M 26. Other funding agencies which supported the numerous projects as part of M 26, are equally acknowledged.

The preparation of individual contributions to this report and their high quality reflect the cooperative spirit of all scientists involved. However, the timely completion of the cruise report would not have been possible without the exceptional effort by Dr. P. Linke and Ms. S. Laube at GEOMAR; to both the chief scientists and editors express their appreciation and thanks.

9 References

ARCHER, D., S. EMERSON and C. REIMERS (1989): Dissolution of calcite in deep-sea sediments: pH and O_2 microelectrode results. Geochim. Cosmochim Acta, **53**, 2831-2845.

BALZER, W. (1989): Chemische Reaktionen und Transportprozesse in oberflächennahen Sedimenten borealer und polarer Meeresgebiete. Unveröff. Habil. Schr., Univ. Kiel, 312 S.

BEFRING, S. (1984): Submarine massebevegelser nordvest av Storegga utenfor More og Romsdal: en genetisk klassifikasjon av og en regional overskit over de ovre deler av sedimente i rasomradet. Unpublished Cand. Scient thesis, University of Bergen.

BENDER, M.L., K.A. FANNING, P.N. FROELICH, G. HEATH, and V. MAYNARD (1977): Interstitial nitrate profiles and oxidation of sedimentary organic matter in the eastern equatorial Atlantic. Science, **198**, 605-609.

BERGER, W.H., K. FISCHER, C. LAI and G. WU (1987): Ocean productivity and organic carbon flux. I. Overview and maps of primary production and export production. Univ. California, San Diego, SIO Reference 87-30, 67 pp.

BERGER, W.H. (1989): Appendix global maps of Ocean Productivity. In: W.H. BERGER, V. SMETACEK and G. WEFER (eds.), S. BERNHARD, Dahlem Konferenzen 1989. Productivity of the ocean: Present and past.

BERNER, R.A. (1980): Early diagenesis. A Theoretical approach. Princeton University Press, 241 pp.

BOUDREAU, B.P. (1987): A steady-state diagenetic model for dissolved carbonate species and pH in the porewater of oxic and suboxic sediments. Geochim. Cosmochim. Acta, **51**, 1985-1996.

BUGGE, T. (1983): Submarine slides on the Norwegian Continental Margin, with special emphasis on the Storegga area. IKU Publication No. **110**, 152 pp.

BUGGE, T., S. BEFRING, R.H. BELDERSON, T. EIDVIN, E. JANSEN, N.H. KENYON, H. HOLTEDAHL, and H.P. SEJRUP (1987): A giant three-stage submarine slide off Norway. Geo-Marine Letters, **7**, 191-198.

BUGGE, T., R. H. BELDERSON, and N.H. KENYON (1988): The Storegga Slide. Phil. Trans. R. Soc. Lond., A, **325**, 357-388.

COCHONAT, P., G. DAMY, J. MEUNIER, F. HARMEGNIES, and L. FLOURY (1991): Deep water geotechnical testing. Colloque ISM, **90**, 245-257.

DAWSON, A.G., D. LONG, and D. SMITH (1988): The Storegga Slide; evidence from eastern Scotland for a possible tsunami. Mar. Geol., **82**, 271-276.

EMERSON, S., R. JAHNKE, M. BENDER, P. FROELICH, G. KLINKHAMMER, C. BOWSER and B. HARTMANN (1980): Early diagenesis in sediments from eastern equatorial Pacific. I. Pore water nutrient and carbonate results. Earth Planet. Sci. Lett., **49**, 57-80.

EMERSON, S. (1985): Organic carbon preservation in marine sediments. In: E.T. SUNDQUIST and W.S. BROECKER (eds.). The carbon cycle and atmospheric CO_2: Natural variations archean to present. Geophysical Monograph, **32**, Amer. Geophys. Union, 18-87.

FANG, W.W., M.G. LANGSETH, and P.J. SCHULTHEISS (1993): Analysis and application of in situ pore pressure measurements in marine sediments. J. of Geophysical Research, **98/B5**, 7921-7938.

FROELICH, P.N., G.P. KLINKHAMMER, M.L. BENDER, N.A. LUEDTKI, G.P. HEATH, D. CULLEN, P. DAUPHIN, D. HAMMOND and B. HARTMANN (1979): Early oxidation of organic matter in pelagic sediments of the eastern equatorial Atlantic: suboxic diagenesis. Geochim. Cosmochim Acta, **43**, 1075-1090.

GERLACH, S.A. and G. GRAF (1991): EUROPÄISCHES NORDMEER, Reise Nr. 13, 6. Juli - 24. August 1990. METEOR-Bericht, Universität Hamburg, 91-2, 217 S.

HOVLAND, M. and A.G. JUDD (1988): Seabed pockmarks and seepages; Impact on geology, biology and marine environment. Graham and Trottman, London, 293 pp.

HURLEY, M.T. and P.J. SCHULTHEISS (1990): Sea-bed shear moduli from measurements of tidally induced pore pressures, In: J. Hovem, M. Richardson and R. Stoll (Eds.), Shear Waves in Marine Sediments, 411-418.

JAHNKE, R.A., S.R. EMERSON and J.W. MURRAY (1982a): A model of oxygen reduction, denitrification and organic matter mineralization in marine sediments. Limnol. Oceanogr., **27**, 610-623.

JAHNKE, R.A., D. HEGGIE, S.R. EMERSON and V. GRUNDMANIS (1982b): Pore waters of the central Pacific Ocean: nutrient results. Earth Planet. Sci. Lett., **61**, 233-256.

JAHNKE, R.A., S.R. EMERSON, C.E. REIMERS, J. SCHUFFERT, K. RUTTENBERG and D. ARCHER (1989): Benthic recycling of biogenic debris in the eastern tropical Atlantic Ocean. Geochim. Cosmochim. Acta, **53**, 2947-2960.

JANSEN, E., S. BEFRING, T. BUGGE, T. EIDVIN, H. HOLTEDAHL and H.P. SEJRUP, (1987): Large submarine slides on the Norwegian Continental Margin: sediments, transport and timing. Mar. Geol., **78**, 77-107.

LAMMERS, S. and E. SUESS (1994): Improved headspace analysis for methane in seawater reveals sources and sinks for atmospheric methane in the eastern Equatorial Pacific. Marine Chemistry (subm.).

LAMMERS, S., E. SUESS and M. HOVLAND (1994): A large methane plume east of Bear Island (Barents Sea): Implications for the marine methane cycle. Continental Shelf Research (subm.).

LANGSETH, M.G., K. BECKER, R.P. von HERZEN, and P.J. SCHULTHEISS, (1992) Heat and fluid flux through sediment on the western flank of the mid-Atlantic ridge: A hydrogeological study of North pond. Geophysical Research Letters, **19**, 517-520.

LINKE, P., E. SUESS, M. TORRES, V. MARTENS, W.D. RUGH, W. ZIEBIS and L.D. KULM (1994): In situ measurements of fluid flow from cold seeps at active continental margins. Deep-Sea Research (in press).

MIENERT, J., N.H. KENYON, J. THIEDE, and F.J. HOLLENDER (1993): Polar continental margins: studies off East Greenland. Eos, Transactions, American Geophysical Union, **74**, 225, 231, 234, 236.

MINTROP, L. (1990): Aminosäuren im Sediment - Analytische Methodik und Ergebnisse aus der Norwegischen See, Dissertation, Berichte aus dem SFB 313, Nr. 20, Kiel University, 217 pp.

OLLIER, G., J.F. ROLLIN, TOULARASTEL, and J.Y. LANDURE (1992): 1992 Annual GISP Report , EEC, 14 pp.

OTTENS, J.J. (1991): Planktic foraminifera as North Atlantic watermass indicators. Oceanologica Acta, **14**, 123-140.

PFLAUMANN, U., J. DUPRAT, C. PUJOL, and L. LABEYRIE (1994): SIMMAX, a transfer technique to deduce sea surface temperatures from planktonic foraminifera. Paleoceanography (subm.).

REDFIELD, A. (1958): The biological control of chemical factors in the environment. AM. Sci., **46**, 906-909.

SARNTHEIN, M. and K. WINN (1988): Global variations of surface ocean productivity in low and mid latitudes: Influence on CO_2 reservoirs of the deep ocean and atmosphere during the last 21,000 years. Paleooceanography, **3**, 361-399.

SCHMITT, M., E. FABER, R. BOTZ and P. STOFFERS (1991): Extraction of methane from seawater using ultrasonic vacuum degassing. Anal. Chem., **63** (5), 529-531.

SCHULTHEISS, P.J. and S.D. MCPHAIL (1986): Direct indication of pore water advection from pore pressure measurements, in Madeira abyssal plain sediments. Nature, **320**, 348-350.

SCHULTHEISS, P.J. and M.S. NOEL (1987): Evidence for pore water advection in the Madeira abyssal plain from pore pressure and temperature measurements. In: P.P.E. Weaver and J. Thomson (Eds.), Geology and Geochemistry of abyssal plains. Geological Society Special Publication, **31**, 113-129.

SCHULTHEISS, P.J. (1990a): In situ pore pressure measurements for a detailed assessment of marine sediments: state of the art. In: K. Demars and R. Chaney (Eds.), Geotechnical Engineering of Ocean Waste Disposal, ASTM STP 1087, Philadelphia, 190-205.

SCHULTHEISS, P.J. (1990b): Pore Pressures in marine sediments: An overview of measurement techniques and some geological engineering applications. Marine Geophysical Researches, **12**, 153-168.

SEIDOV, D., M. SARNTHEIM (1994): North Atlantic Ocean Circulation during the last 18,000 years-Data Interpretation and Nummerical Modelling, EGS 19th January Essembly, (in prep.).

SOLHEIM, A. and A. ELVERHOI (1985): A pockmark field in the Central Barents Sea; gas from a petrogenic source? Polar Research, **3**, 11-19.

SOLHEIM, A., A. ELVERHOI (1993): Gas-related sea floor craters in the Barents Sea. Geo-Marine Letters, **13**, 235-243.

SPENCER, C.P. (1983): Marine Biogeochemistry of Silicon. In: S.R. ASTON (ed.) Silicon Geochemistry and Biogeochemistry, Academic Press, London, 101-141.

STOKER, M.S. (1989): Judd, 60°N/06°W, Seabed Sediments 1:250,000 map series. HMSO for the British Geological Survey.

STOKER, M.S. et al. (1994): A record of the late Cenozoic stratigraphy, sedimentation and climate change from the Hebrides Slope, NE Atlantic. Journal of the Geological Society of London, **151**, 1994, 235-249.

SUESS, E. and A.V. ALTENBACH (1992): EUROPÄISCHES NORDMEER, Reise Nr. 17, 15. Juli - 25. August 1991. METEOR-Berichte, Universität Hamburg, 92-3,164 S.

SUESS, E. and M. WHITICAR (1989): Methane-derived CO_2 in pore fluids expelled from the Oregon subduction zone. Palaeogeogr. Palaeoclimatol. Palaeoecol., **71**, 119-136.

WENCK, A., L. MINTROP and J.C. DUINKER (1991): Automated determination of amino acids in seawater. Marine Chemistry, **33**, 1-7.

WESTBROOK, G.K. and M.J. SMITH (1983): Long decollements and mud volcanoes: Evidence from the Barbados ridge complex for the role of high pore water pressures in the development of an accretionary complex. Geology, **11**, 279-283.

WIESENBURG, D.A. and N.L. GUINASSO (1979): Equilibrium solubilities of methane, carbon monoxide and hydrogen in water and sea water. J. Chem. Eng. Data, **24** (4), 356-360.

ZABEL, M., A. DAHMKE and H.D. SCHULZ (1993): Regional distribution of phosphate and silicon fluxes across the sediment water interface in the eastern South Atlantic (in prep).

ZIELINSKI, G.W., T. GUNLEIKSRUD, J. SAETTEM, H.M. ZUIDBERG and J.M. GEISE (1986): Deep heatflow measurements in Quaternary sediments on the Norwegian Continental Shelf. Paper OTC 5183, Offshore Technology Conference 1986, Houston, Texas, 277-282.

Publications from METEOR expeditions
in other reports

Gerlach, S.A., J. Thiede, G. Graf und F. Werner (1986): Forschungsschiff Meteor, Reise 2 vom 19. Juni bis 16. Juli 1986. Forschungsschiff Poseidon, Reise 128 vom 7. Mai bis 8. Juni 1986. Ber. Sonderforschungsbereich 313, Univ. Kiel, 4, 140 S.

Siedler, G., H. Schmickler, T.J. Müller, H.-W. Schenke und W. Zenk (1987): Forschungsschiff Meteor, Reise Nr. 4, Kapverden - Expedition, Oktober - Dezember 1986. Ber. Inst. f. Meeresk., 173, Kiel, 123 S.

Wefer, G., G.F. Lutze, T.J. Müller, O. Pfannkuche, W. Schenke, G. Siedler und W. Zenk (1988): Kurzbericht über die Meteor - Expedition Nr. 6, Hamburg - Hamburg, 28. Oktober 1987 - 19. Mai 1988. Berichte, Fachbereich Geowissenschaften, Universität Bremen, 4, 29 S.

Müller, T.J., G. Siedler und W. Zenk (1988): Forschungsschiff Meteor, Reise Nr. 6, Atlantik 87/88, Fahrtabschnitte Nr. 1 - 3, Oktober-Dezember 1987. Ber. Inst. f. Meeresk., 184, Kiel, 77 S.

Lutze, G.F., C.O.C. Agwu, A. Altenbach, U. Henken-Mellies, C. Kothe, N. Mühlhan, U. Pflaumann, C. Samtleben, M. Sarnthein, M. Segl, Th. Soltwedel, U. Stute, R. Tiedemann und P. Weinholz (1988): Bericht über die "Meteor"-Fahrt 6-5, Dakar - Libreville, 15.1.-16.2.1988. Berichte - Reports, Geol. Paläont. Inst., Univ. Kiel, 22, 60 S.

Wefer, G., U. Bleil, P.J. Müller, H.D. Schulz, W.H. Berger, U. Brathauer, L. Brück, A. Dahmke, K. Dehning, M.L. Duarte-Morais, F. Fürsich, S. Hinrichs, K. Klockgeter, A. Kölling, C. Kothe, J.F. Makaya, H. Oberhänsli, W. Oschmann, J. Posny, F. Rostek, H. Schmidt, R. Schneider, M. Segl, M. Sobiesiak, T. Soltwedel und V. Spieß (1988): Bericht über die Meteor - Fahrt M 6-6, Libreville - Las Palmas, 18.2.1988 - 23.2.1988. Berichte, Fachbereich Geowissenschaften, Universität Bremen, 3, 97 S.

Hirschleber, H., F. Theilen, W. Balzer, B. v. Bodungen und J. Thiede (1988): Forschungsschiff Meteor, Reise 7, vom 1. Juni bis 28. September 1988, Ber. Sonderforschungsbereich 313, Univ. Kiel, 10, 358 S.

METEOR-Berichte
List of publications

89-1	(1989) Meincke, J., Quadfasel, D.	GRÖNLANDSEE 1988-Expedition, Reise Nr. 8, 27. Oktober 1988 - 18. Dezember 1988. Universität Hamburg, 40 S.
89-2	(1989) Zenk, W., Müller, T.J. Wefer, G.	BARLAVENTO-Expedition, Reise Nr. 9, 29. Dezember 1988 - 17. März 1989. Universität Hamburg, 238 S.
90-1	(1990) Zeitzschel, B., Lenz, J., Thiel, H., Boje, R., Stuhr, A., Passow, U.	PLANKTON '89 - BENTHOS '89, Reise Nr. 10, 19. März - 31. August 1989. Universität Hamburg, 216 S.
90-2	(1990) Roether, W., Sarnthein, M., Müller, T.J. Nellen, W. Sahrhage, D.	SÜDATLANTIK-ZIRKUMPOLARSTROM, Reise Nr. 11, 3. Oktober 1989 - 11. März 1990 Universität Hamburg, 169 S.
91-1	(1991) Wefer, G. Weigel, W. Pfannkuche, O.	OSTATLANTIK 90 - EXPEDITION, Reise Nr. 12, 13. März - 30. Juni 1990. Universität Hamburg, 166 S.
91-2	(1991) Gerlach, S.A. Graf, G.	EUROPÄISCHES NORDMEER, Reise Nr. 13, 6. Juli - 24. August 1990. Universität Hamburg, 217 S.
91-3	(1991) Hinz, K. Hasse, L. Schott, F.	SUBTROPISCHER & TROPISCHER ATLANTIK, Reise Nr. 14/1-3, Maritime Meteorologie und Physikalische Ozeanographie, 17. September - 30. Dezember 1990. Universität Hamburg, 58 S.
91-4	(1991) Hinz, K.	SUBTROPISCHER & TROPISCHER ATLANTIK, Reise Nr. 14/3, Geophysik, 31. Oktober - 30. Dezember 1990. Universität Hamburg, 94 S.
92-1	(1992) Siedler, G. Zenk, W.	WOCE Südatlantik 1991, Reise Nr. 15, 30. Dezember 1990 - 23. März 1991. Universität Hamburg, 126 S.
92-2	(1992) Wefer, G. Schulz, H.D. Schott, F. Hirschleber, H.B.	ATLANTIK 91 - EXPEDITION, Reise Nr. 16, 27. März - 8. Juli 1991, Universität Hamburg, 288 S.
92-3	(1992) Suess, E. Altenbach, A.V.	EUROPÄISCHES NORDMEER, Reise Nr. 17, 15. Juli - 29. August 1991, Universität Hamburg, 164 S.

93-1	(1993)	Meincke, J. Becker, G.	WOCE-NORD, Cruise No. 18, 2 September - 26 September 1991. NORDSEE, Cruise No. 19, 30 September - 12 October 1991. Universität Hamburg, 105 pp.
93-2	(1993)	Wefer, G. Schulz, H.D.	OSTATLANTIK 91/92 - EXPEDITION, Reise Nr. 20, M 20/1 und M 20/2, 18. November 1991 - 3. Februar 1992. Universität Hamburg, 248 S.
93-3	(1993)	Wefer, G. Hinz, K. Roeser, H.A.	OSTATLANTIK 91/92 - EXPEDITION, Reise Nr. 20, M 20/3, 4. Februar 1992 - 13. März 1992. Universität Hamburg, 145 S.
93-4	(1993)	Pfannkuche, O. Duinker, J.C. Graf, G. Henrich, R. Thiel, H. Zeitzschel, B.	NORDATLANTIK 92, Reise Nr. 21, 16. März - 31. August 1992. METEOR-Berichte, Universität Hamburg, 281 S.
93-5	(1993)	Siedler, G. Balzer, W. Müller, T.J. Rhein, M. Onken, R. Zenk, W.	WOCE South Atlantic 1992, Cruise No. 22, 22 September, 1992 - 31 January, 1993. Universität Hamburg, 131 pp.
94-1	(1994)	Bleil, U. Spieß, V. Wefer, G.	Geo Bremen SOUTH ATLANTIC 1993, Cruise No. 23, 4 February - 12 April, 1993. Universität Hamburg, 261 pp.
94-2	(1994)	Schmincke, H.-U. Rihm, O.	OZEANVULKAN 1993, Cruise No. 24, 15 April - 9 May 1993. Universität Hamburg, (in prep.)
94-3	(1994)	Hieke, W. Halbach, P. Türkay, M. Weikert, H.	MITTELMEER 1993, Cruise No. 25, 12 May - 20 August 1993. Universität Hamburg, (in prep.)
94-4	(1994)	Suess, E. Kremling, K. Mienert, J.	NORDATLANTIK 1993, Cruise No. 26, 24 August - 26 November 1993. Universität Hamburg, 256 pp.